

**Filoviruses Attach to a Common Cell-Surface Molecule via Distinct
and Strongly Immunogenic Receptor-binding Regions, and
Modulate Cell Entry Through Δ -Peptides**

Inaugural-Dissertation

to Obtain the Academic Degree
Doctor Rerum Naturalium (Dr. rer. nat.)

Submitted to the
**Department of Biology, Chemistry, and Pharmacy
of Freie Universität Berlin**

by

Jens H. Kuhn
from Erlangen, Germany

November, 2008

The experiments described in this dissertation were supervised by Assoc. Prof. Michael R. Farzan, PhD, at the Partners AIDS Research Center, Brigham and Women's Hospital, Harvard Medical School, Cambridge, MA, USA (November 2003 – December 2004) and the New England Primate Research Center, Harvard Medical School, Southborough, MA, USA (January 2005 – March 2008).

1st Reviewer: Assoc. Prof. Michael R. Farzan, PhD (Southborough, MA, USA)

2nd Reviewer: Prof. Dr. rer. nat. Volker Haucke (Berlin, Germany)

Date of defense: November 12, 2008

ACKNOWLEDGMENTS

The research for this dissertation was primarily performed at Harvard Medical School's New England Primate Research Center (NEPRC) in Southborough, MA, USA, under the direct supervision of Assoc. Prof. Michael R. Farzan. I would like to express my deepest gratitude to Mike for offering me a position in his laboratory and, even more so, for his willingness to divert from his specialty, HIV-1 cell entry, to support me in my endeavor of characterizing the cell entry processes of more exotic viruses. I very much appreciated the creative freedom in his laboratory and his support of all my ideas, strategies, and interests, even when obstacles seemed insurmountable for many months at a time or required considerable financial support. Next to Mike's wife, Assistant Prof. Hyeryun Choe (Children's Hospital, Harvard Medical School, Boston, MA, USA), many members of Mike's laboratory supported me with technical advice. Among them were Dr. Wenhui Li, Dr. Sweekee Wong, and, most notably, Dr. Tatyana K. Dorfman. Dr. Sheli R. Radoshitzky, at the time a graduate student in Mike's laboratory, deserves special mention here as her project, the identification of the cell-surface receptor for New World hemorrhagic fever arenaviruses, complemented mine, which allowed us to learn from each other and finish both our projects as envisioned.

I also would like to thank several students that Mike had assigned to me. Dina Uzri, a graduate student at Harvard Medical School, and Alexander C. Guth, at the time an undergraduate student at Harvard University, Cambridge, MA, USA, helped with the construction of individual plasmids, a few of which were useful for the research described here. Philip J. Kranzusch, a graduate student at Harvard Medical School, tried to develop a system for the functional assessment of ebolaviral Δ -peptides that unfortunately never came to fruition and therefore is not described here. Marc Hogenbirk from the Eijkman Graduate School for Immunology and Infectious Disease at Utrecht University, The Netherlands, created several filovirus receptor-binding region mutants for collaborations, which are mentioned in this dissertation only in passing. Dior Kingston, Andrea Kirmaier, Amy Lee, Dr. Claudia Mische, Thomas Postler, Nadine Salisch, Hannah B. Sanford, and Dr. Jingping Zhang, all friends of mine who at one time or another had worked or still work at NEPRC,

were always there when an escape from the laboratory to a coffee shop seemed unavoidable. I miss you guys.

Assoc. Prof. James M. Cunningham (Brigham and Women's Hospital, Harvard Medical School) deserves credit for repeatedly discussing my research with me, and for providing reagents. Dr. Kartik Chandran, at the time still a research fellow in Jim's laboratory, and Dr. John Misasi, a current research fellow of Jim's, provided reagents and insight. John also helped with the cathepsin assays.

Dr. Gerald A. Beltz (New England Regional Center of Excellence/Biodefense and Infectious Diseases (NERCE/BEID)), Boston, MA, USA, critically read the submitted publications and offered advice.

At the United States Army Medical Research Institute of Infectious Diseases (USAMRIID) at Fort Detrick, Frederick, MD, USA, one of the US's premier maximum-containment facilities, I would like to acknowledge the fantastic support of my research by the excellent researchers in Dr. Sina Bavari's and Dr. M. Javad Aman's groups, most notably Dr. Kelly L. Warfield and Dr. Dana Swenson. Kelly and Dana performed all experiments that required biosafety-level 4 containment, including the mouse inoculations with infectious filoviruses. Dr. Gordon Ruthel, Dr. Gene G. Olinger, and Dr. Jason Paragas, at the time also at USAMRIID, analyzed samples with the Discovery-1 microscope, performed filovirus spike-protein T-cell epitope analyses, and provided the eGFP-expressing Zaire ebolavirus isolate Mayinga cDNA clone, respectively. All work performed at USAMRIID was supported by a grant from the US Defense Threat Reduction Agency (DTO CB.63).

At the Centers for Disease Control and Prevention (CDC), Atlanta, GA, USA, another maximum-containment facility, I would like to thank Darcy Bawiec, Bobbie Rae Erickson, Marina Khristova, Dr. Jonathan S. Towner, Dr. Stuart T. Nichol, and Dr. Martin J. Vincent for providing the spike-protein amino-acid sequence of the Lake Victoria marburgvirus Angola isolate months before it was published, and for providing the spike-protein nucleotide sequence of the novel 'Uganda ebolavirus,' which has not yet been reported.

NERCE/BEID awarded a Career Development Fellowship to me (grant No. AI057159), which I very much appreciate.

I also want to thank my parents and brother for all their support. Most importantly, though, I owe my girlfriend Sheli. Without you I'd be lost.

1 TABLE OF CONTENTS

1	TABLE OF CONTENTS	6
2	LIST OF TABLES	11
3	LIST OF FIGURES	12
4	LIST OF ABBREVIATIONS	17
5	INTRODUCTION	21
5.1	Filoviruses	21
5.1.1	Background	21
5.1.2	Filovirus taxonomy and phylogeny	22
5.1.3	Filovirus epidemiology	26
5.1.4	Ecology of filoviruses	32
5.1.5	Clinical and pathological presentation of filovirus infections	34
5.1.6	Treatment of filovirus infections	38
5.1.7	Diagnosis of filovirus infections	39
5.1.8	Molecular biology of filoviruses	39
5.1.8.1	Filoviral particles	39
5.1.8.2	Filoviral genomes	41
5.1.8.3	<i>NP</i> gene	42
5.1.8.4	<i>VP35</i> gene	42
5.1.8.5	<i>VP40</i> gene	42
5.1.8.6	<i>GP</i> gene	42
5.1.8.7	<i>VP30</i> gene	43
5.1.8.8	<i>VP24</i> gene	43
5.1.8.9	<i>L</i> gene	44
5.1.8.10	Filovirus life cycle	45
5.2	Filoviral glycoproteins	47
5.2.1	Ebolaviral secreted glycoprotein	47
5.2.2	Filoviral spike protein	49
5.2.3	Ebolaviral secondary secreted glycoprotein	53
5.3	Filovirus cell entry	54
5.4	Filovirus-vaccine development	57

5.5	Objective of this dissertation	60
6	MATERIALS AND METHODS	62
6.1	Cells and culture conditions	62
6.2	Construction of filovirus glycoprotein-encoding genes and variants	63
6.2.1	General Procedures	63
6.2.2	Construction of Lake Victoria marburgvirus isolate Musoke GP ₁ -Fc	65
6.2.3	Construction of Lake Victoria marburgvirus isolate Musoke spike protein GP _{1,2} -C9	69
6.2.4	Construction of Lake Victoria marburgvirus isolate Musoke GP ₁ -Fc truncation variants	71
6.2.5	Construction of Lake Victoria marburgvirus isolate Musoke spike protein GP _{1,2} -C9 containing GP ₁ -internal deletions	76
6.2.6	Construction of Lake Victoria marburgvirus isolate Angola GP ₁ -Fc truncation variants	77
6.2.7	Construction of Lake Victoria marburgvirus isolate Musoke receptor-binding region mutants	78
6.2.8	Construction of mucin-like domain-deleted Zaire ebolavirus isolate Mayinga GP ₁	79
6.2.9	Construction of Zaire ebolavirus isolate Mayinga GP ₁ -Fc truncation variants	81
6.2.10	Construction of Zaire ebolavirus isolate Mayinga receptor-binding region mutants	83
6.2.11	Construction of Côte d'Ivoire, Reston, and Sudan ebolavirus receptor-binding regions	85
6.2.12	Construction of Zaire ebolavirus isolate Mayinga sGP-Fc	86
6.2.13	Construction of Zaire ebolavirus isolate Mayinga ssGP-Fc	87
6.2.14	Construction of ebolaviral Δ -peptides	88
6.2.15	Construction of Sudan ebolavirus Δ -peptide truncation variants	90
6.2.16	Construction of Sudan ebolavirus Δ -peptide mutants	92
6.2.17	Construction of the Reston-Sudan ebolavirus Δ -peptide chimera	94
6.2.18	Construction of the Sudan-Reston ebolavirus Δ -peptide chimera	96
6.2.19	Construction of plasmids encoding proteins fused to the Fc region	

	of murine IgG _{2A}	98
6.2.20	Construction and origin of plasmids encoding control proteins	99
6.3	Evaluation of expression of filoviral glycoprotein variants and control proteins	100
6.4	Expression of filoviral glycoprotein variants and control proteins	102
6.5	Cell binding assays	103
6.6	Cell-binding competition assay	104
6.7	Transduction assay with pseudotyped gammaretroviruses	105
6.8	Infection assay with recombinant infectious Zaire ebolavirus	108
6.9	HIV-1 neutralization assay	108
6.10	Cathepsin assay	109
6.11	Immunization and vaccination protocol	110
6.11.1	Animals	110
6.11.2	Preparation of immunogen	110
6.11.3	Immunization protocol	110
6.11.4	Determination of antibody titers	110
6.11.5	Determination of cytotoxic T-lymphocyte responses	111
6.11.6	Viral challenge	112
7	RESULTS	113
7.1	Filoviruses attach to a common cell-surface receptor	113
7.1.1	Lake Victoria marburgvirus isolate Musoke GP ₁ truncation variant 38-188-Fc binds to filovirus-permissive cells more efficiently than full-length GP ₁	113
7.1.2	Zaire ebolavirus isolate Mayinga GP ₁ truncation variant 54-201-Fc binds to filovirus-permissive cells more efficiently than mucin-like domain-deleted GP ₁	119
7.1.3	Lake Victoria marburgvirus isolate Angola and Musoke GP ₁ truncation variants bind to filovirus-permissive cells with comparable efficiency	125
7.1.4	Both Lake Victoria marburgvirus isolate Musoke GP ₁ truncation variant 38-188-Fc and Zaire ebolavirus isolate Mayinga GP ₁ truncation variant 54-201-Fc specifically inhibit entry of gammaretroviruses pseudotyped with functional spike proteins	

	of either filovirus	128
7.1.5	Both Lake Victoria marburgvirus isolate Musoke and isolate Angola 38-188 Fc inhibit entry of gammaretrovirus particles pseudotyped with Lake Victoria marburgvirus isolate Musoke GP _{1,2} more efficiently than other GP ₁ truncation variants	132
7.1.6	Lake Victoria marburgvirus isolate Musoke 38-188-Fc and Zaire ebolavirus isolate Mayinga 54-201-Fc inhibit the replication of infectious Zaire ebolavirus	134
7.1.7	All filoviruses use a common cell-entry factor	135
7.2	Identification of ebolaviral Δ -peptides as potent filovirus cell-entry modulators	142
7.2.1	Zaire ebolavirus Δ -peptide-Fc, but not secreted glycoprotein or secondary secreted glycoprotein, binds to filovirus-permissive cells	142
7.2.2	Zaire ebolavirus Δ -peptide-Fc, but not secreted glycoprotein or secondary secreted glycoprotein, inhibits entry of gammaretroviruses pseudotyped with filoviral spike protein	147
7.2.3	Côte d'Ivoire, Sudan, and Zaire, and to much lesser extent Reston, ebolaviral Δ -peptide Fc fusion proteins inhibit filoviral GP _{1,2} -mediated entry in a dose-dependent manner	150
7.2.4	Côte d'Ivoire, Sudan, and Zaire, but not Reston, ebolaviral Δ -peptide Fc fusion proteins inhibit replication of infectious Zaire ebolavirus	157
7.2.5	Ebolaviral Δ -peptides inhibit filoviral GP _{1,2} -mediated entry specifically	159
7.2.6	Mutational analysis of Sudan ebolavirus Δ -peptide	163
7.2.7	Sudan ebolavirus Δ -Fc and Lake Victoria marburgvirus isolate Musoke 38-188-Fc may compete for the same cell-surface binding factor	170
7.2.8	Ebolaviral Δ -peptides do not inhibit cathepsin B activity	172
7.3	Filoviral Fc-conjugated receptor-binding regions are strongly immunogenic filovirus candidate vaccines	174
7.3.1	C57/BL6 mice inoculated with Lake Victoria marburgvirus isolate Musoke 38-188-Fc or Zaire ebolavirus isolate Mayinga 54-201-Fc develop strong humoral and cytotoxic T-lymphocyte immune responses	174
7.3.2	Sera from C57/BL6 mice inoculated with Lake Victoria	

	marburgvirus 38-188-Fc or Zaire ebolavirus isolate Mayinga 54-201-Fc neutralize infectious Zaire ebolavirus <i>in vitro</i>	178
7.3.3	C57/BL6 mice inoculated with Lake Victoria isolate Musoke 38-188-Fc or Zaire ebolavirus isolate Mayinga 54-201-Fc are partially and fully protected against challenge with infectious Zaire ebolavirus, respectively	180
8	DISCUSSION	181
9	SUMMARY	212
10	REFERENCES	216
11	PUBLICATIONS AND PRESENTATIONS	242
12	DECLARATION	252
13	CURRICULUM VITAE	253

2 LIST OF TABLES

Table 5-1. Current organization of the viral order <i>Mononegavirales</i>	23
Table 5-2. Differentiation of marburgviruses and ebolaviruses	24
Table 5-3. Current filovirus taxonomy	25
Table 5-4. Chronology of filovirus-disease outbreaks	28
Table 5-5. Symptoms of 22 survivors of marburgvirus disease and 107 fatally infected patients, Democratic Republic of the Congo, 1998-2000	35
Table 5-6. Symptoms of 19 survivors of Zaire ebolavirus disease and 84 fatally infected patients, Zaire, 1995	36

3 LIST OF FIGURES

Figure 5-1. Maximum-containment laboratory	22
Figure 5-2. Phylogenetic analysis of filovirus isolates using the filoviral RNA-dependent RNA polymerase genes	27
Figure 5-3. Filovirus-disease outbreaks	32
Figure 5-4. Transmission electron micrograph of a Zaire ebolavirus particle	40
Figure 5-5. Schematic of a filovirus particle	40
Figure 5-6. Schematic organization of filoviral genomes	41
Figure 5-7. Filovirus life cycle	46
Figure 5-8. Expression pathway of ebolaviral secreted glycoprotein	48
Figure 5-9. Expression pathway of filoviral spike proteins	50
Figure 5-10. Schematic of filoviral spike proteins	52
Figure 5-11. Expression pathway of ebolaviral secondary secreted glycoprotein	53
Figure 6-1. Principle of recursive polymerase-chain reaction for the in vitro synthesis of open reading frames or genes	68
Figure 6-2. Principle of inverse polymerase-chain reaction for the creation of genes encoding C-terminal truncation variants of filoviral Fc fusion proteins	74
Figure 6-3. Principle of inverse polymerase-chain reaction for the creation of genes encoding N-terminal truncation variants of filoviral Fc fusion proteins	75
Figure 6-4. Production of Moloney murine leukemia virus particles pseudotyped with filoviral spike proteins	106
Figure 6-5. Principle of the Moloney murine leukemia pseudotype-inhibition assay	107
Figure 7-1. Lake Victoria marburgvirus isolate Musoke GP ₁ and GP ₁ truncation variants	114
Figure 7-2. Expression of Lake Victoria marburgvirus isolate Musoke GP ₁ and GP ₁ truncation variants	115
Figure 7-3. Binding of Lake Victoria marburgvirus isolate Musoke GP ₁ -Fc (17-432-Fc) and GP ₁ -Fc truncation variants to the surface of filovirus-permissive nonhuman primate cells	117
Figure 7-4. Binding of Lake Victoria marburgvirus isolate Musoke GP ₁ -Fc (17-432-Fc) and GP ₁ -Fc truncation variants to the surface of filovirus-permissive human cells	118

Figure 7-5. Binding of Lake Victoria marburgvirus isolate Musoke GP ₁ -Fc (17-432-Fc) and GP ₁ -Fc truncation variants to the surface of filovirus-resistant human cells	119
Figure 7-6. Zaire ebolavirus isolate Mayinga GP ₁ and GP ₁ truncation variants	120
Figure 7-7. Expression of Zaire ebolavirus isolate Mayinga GP ₁ and GP ₁ truncation variants	121
Figure 7-8. Binding of Zaire ebolavirus isolate Mayinga mucin-like domain-deleted GP ₁ -Fc (33-308-Fc) and GP ₁ -Fc truncation variants to the surface of filovirus-permissive nonhuman primate cells	122
Figure 7-9. Binding of Zaire ebolavirus isolate Mayinga mucin-like domain-deleted GP ₁ -Fc (33-308-Fc) and GP ₁ -Fc truncation variants to the surface of filovirus-permissive human cells	123
Figure 7-10. Binding of Zaire ebolavirus isolate Mayinga mucin-like domain-deleted GP ₁ -Fc (33-308-Fc) and GP ₁ -Fc truncation variants to the surface of filovirus-resistant human cells	124
Figure 7-11. Expression of Lake Victoria marburgvirus isolate Musoke and isolate Angola GP ₁ -Fc truncation variants	126
Figure 7-12. Comparison of the cell surface-binding affinities of Lake Victoria marburgvirus isolate Musoke and isolate Angola GP ₁ -Fc truncation variants	127
Figure 7-13. Lake Victoria marburgvirus isolate Musoke GP ₁ truncation variant 38-188-Fc and Zaire ebolavirus isolate Mayinga GP ₁ truncation variant 54-201-Fc inhibit Lake Victoria marburgvirus isolate Musoke GP _{1,2} -mediated entry of gammaretrovirus particles	129
Figure 7-14. Lake Victoria marburgvirus isolate Musoke GP ₁ truncation variant 38-188-Fc and Zaire ebolavirus isolate Mayinga GP ₁ truncation variant 54-201-Fc inhibit Zaire ebolavirus isolate Mayinga GP _{1,2Δ309-489} -mediated entry of gammaretrovirus particles	130
Figure 7-15. Lake Victoria marburgvirus isolate Musoke GP ₁ truncation variant 38-188-Fc and Zaire ebolavirus isolate Mayinga GP ₁ truncation variant 54-201-Fc do not inhibit vesicular stomatitis Indiana virus G-mediated entry of gammaretrovirus particles	131
Figure 7-16. Comparison of the inhibitory effects of Lake Victoria marburgvirus isolate Musoke and Angola GP ₁ -Fc truncation variants on cell-entry of gammaretrovirus	

particles pseudotyped with Lake Victoria marburgvirus isolate Musoke GP _{1,2}	133
Figure 7-17. Lake Victoria marburgvirus isolate Musoke GP ₁ truncation variant 38-188-Fc and Zaire ebolavirus isolate Mayinga GP ₁ truncation variant 54-201-Fc inhibit replication of infectious Zaire ebolavirus isolate Mayinga	135
Figure 7-18. Expression of Côte d'Ivoire ebolavirus isolate Côte d'Ivoire 54-201-Fc, Reston ebolavirus isolate Pennsylvania 55-202-Fc, and Sudan ebolavirus isolate Gulu 54-201-Fc	136
Figure 7-19. Binding of Côte d'Ivoire ebolavirus isolate Côte d'Ivoire 54-201-Fc, Reston ebolavirus isolate Pennsylvania 55-202-Fc, and Sudan ebolavirus isolate Gulu 54-201-Fc to the surface of filovirus-permissive nonhuman primate cells	138
Figure 7-20. Binding of Côte d'Ivoire ebolavirus isolate Côte d'Ivoire 54-201-Fc, Reston ebolavirus isolate Pennsylvania 55-202-Fc, and Sudan ebolavirus isolate Gulu 54-201-Fc to the surface of filovirus-permissive human cells	139
Figure 7-21. Binding of Côte d'Ivoire ebolavirus isolate Côte d'Ivoire 54-201-Fc, Reston ebolavirus isolate Pennsylvania 55-202-Fc, and Sudan ebolavirus isolate Gulu 54-201-Fc to the surface of filovirus-resistant human cells	140
Figure 7-22. Côte d'Ivoire ebolavirus isolate Côte d'Ivoire 54-201-Fc, Reston ebolavirus isolate Pennsylvania 55-202-Fc, and Sudan ebolavirus isolate Gulu 54-201-Fc inhibit cell-entry of gammaretrovirus particles pseudotyped with Lake Victoria marburgvirus isolate Musoke GP _{1,2}	141
Figure 7-23. Expression of Zaire ebolavirus isolate Mayinga secreted glycoprotein, secondary secreted glycoprotein, and Δ -peptide	143
Figure 7-24. Binding of Zaire ebolavirus isolate Mayinga secreted glycoprotein, secondary secreted glycoprotein, and Δ -peptide to the surface of filovirus-permissive nonhuman primate cells	145
Figure 7-25. Binding of Zaire ebolavirus isolate Mayinga secreted glycoprotein, secondary secreted glycoprotein, and Δ -peptide to the surface of filovirus-permissive human cells	146
Figure 7-26. Binding of Zaire ebolavirus isolate Mayinga secreted glycoprotein, secondary secreted glycoprotein, and Δ -peptide to the surface of filovirus-resistant human cells	147
Figure 7-27. Zaire ebolavirus isolate Mayinga Δ -peptide-Fc, but not secreted	

glycoprotein or secondary secreted glycoprotein, inhibits entry of gammaretrovirus particles pseudotyped with Lake Victoria marburgvirus isolate Musoke GP _{1,2}	149
Figure 7-28. Expression of Côte d'Ivoire, Sudan, Reston, and Zaire ebolaviral Δ -peptides	150
Figure 7-29. Binding of Côte d'Ivoire, Sudan, Reston, and Zaire ebolaviral Δ -peptides to the surface of filovirus-permissive nonhuman primate cells	152
Figure 7-30. Binding of Côte d'Ivoire, Sudan, Reston, and Zaire ebolaviral Δ -peptides to the surface of filovirus-permissive human cells	153
Figure 7-31. Binding of Côte d'Ivoire, Sudan, Reston, and Zaire ebolaviral Δ -peptides to the surface of filovirus-resistant human cells	154
Figure 7-32. Côte d'Ivoire, Sudan, and Zaire, and to lesser extent Reston, ebolaviral Δ -peptide Fc fusion proteins inhibit entry of gammaretrovirus particles pseudotyped with Lake Victoria marburgvirus isolate Musoke GP _{1,2} in a dose-dependent manner	156
Figure 7-33. Côte d'Ivoire, Sudan, and Zaire, but not Reston, ebolaviral Δ -peptide Fc fusion proteins inhibit replication of infectious Zaire ebolavirus isolate Mayinga	158
Figure 7-34. Sudan ebolaviral Δ -peptide inhibits filoviral GP _{1,2} -mediated entry specifically	160
Figure 7-35. Sudan ebolaviral Δ -peptide does not inhibit cell entry of infectious human immunodeficiency virus type 1	161
Figure 7-36. Overview of Sudan ebolavirus Δ -peptide mutants	163
Figure 7-37. Expression of Sudan ebolavirus Δ -peptide mutants	164
Figure 7-38. Binding of Sudan ebolavirus Δ -peptide mutants to the surface of filovirus-permissive nonhuman primate cells	166
Figure 7-39. Binding of Sudan ebolavirus Δ -peptide mutants to the surface of filovirus-resistant human cells	167
Figure 7-40. Analysis of the effect of Sudan ebolavirus Δ -peptide mutants on entry of gammaretrovirus particles pseudotyped with Lake Victoria marburgvirus isolate Musoke GP _{1,2}	169
Figure 7-41. Sudan ebolavirus Δ -Fc and Lake Victoria marburgvirus isolate Musoke 38-188-Fc may compete for the same cell-surface binding factor	171
Figure 7-42. Ebolaviral Δ -peptides do not inhibit cathepsin B activity	173
Figure 7-43. Immunization of mice with Lake Victoria marburgvirus isolate Musoke 38-188-Fc or Zaire ebolavirus isolate Mayinga 54-201-Fc	175

Figure 7-44. Mice immunized with Lake Victoria marburgvirus isolate Musoke 38-188-Fc or Zaire ebolavirus isolate Mayinga 54-201-Fc develop cross-reactive antibodies	176
Figure 7-45. Mice immunized with Lake Victoria marburgvirus isolate Musoke 38-188-Fc or Zaire ebolavirus isolate Mayinga 54-201-Fc develop splenocytes reactive to Zaire ebolavirus isolate Mayinga GP ₁ peptides	177
Figure 7-46. Sera from mice immunized with Lake Victoria marburgvirus isolate Musoke 38-188-Fc or Zaire ebolavirus isolate Mayinga 54-201-Fc inhibit replication of infectious Zaire ebolavirus	179
Figure 7-47. Mice immunized with Lake Victoria marburgvirus isolate Musoke 38-188-Fc or Zaire ebolavirus isolate Mayinga 54-201-Fc are partially and fully protected from infection with mouse-adapted Zaire ebolavirus isolate Mayinga, respectively	180
Figure 8-1. Sequence alignment of Lake Victoria marburgvirus isolate Musoke and Zaire ebolavirus isolate Mayinga receptor-binding regions	184
Figure 8-2. Location of the identified receptor-binding regions within filoviral full-length spike proteins	188
Figure 8-3. Sequence alignment of Lake Victoria marburgvirus receptor-binding regions	189
Figure 8-4. Sequence alignment of Zaire ebolavirus receptor-binding regions	190
Figure 8-5. Sequence alignment of ebolaviral receptor-binding regions	191
Figure 8-6. Hypothetical model for the role of filoviral-spike protein mucin-like domains	194
Figure 8-7. Crystal structure of trimeric mucin-like domain-deleted Zaire ebolavirus isolate Mayinga spike protein in its trimeric prefusion state	195
Figure 8-8. Principle of virus-receptor identification by coimmunoprecipitation	200
Figure 8-9. The receptor-binding sites of trimeric mucin-like domain-deleted Zaire ebolavirus isolate Mayinga spike protein in its trimeric prefusion state	203
Figure 8-10. Sequence alignment of ebolaviral Δ -peptides	206
Figure 8-11. Comparison of the C-termini of ebolaviral Δ -peptides with the receptor-binding site suggested by the crystal structure of mucin-liked domain-deleted Zaire ebolavirus isolate Mayinga GP _{1,2}	208

4 LIST OF ABBREVIATIONS

AAALAC	Association for Assessment and Accreditation of Laboratory Animal Care International
ACE2	angiotensin-converting enzyme 2
AMC	7-amino-4-methylcoumarin
ATCC	American Type Culture Collection
BHK	baby hamster kidney
bp	base pair(s)
BSA	bovine serum albumin
BSL	biosafety level
C-c ³ Ado	3-deazaadenosine/3-deazaaristeromycin
c ³ -Npc A	3-deazaneplanocin A
CD	cluster of differentiation
CDC	Centers for Disease Control and Prevention
cDNA	complementary DNA
CHO	Chinese hamster ovary
CIEBOV	Côte d'Ivoire ebolavirus
CIEBOV-CI	Côte d'Ivoire ebolavirus isolate Côte d'Ivoire
CTL	cytotoxic T-lymphocyte
DC-SIGN	dendritic cell-specific ICAM-3-grabbing non-integrin
DDM	<i>n</i> -dodecyl- β -D-maltopyranoside
dFBS	dialyzed fetal bovine serum
DMEM	Dulbecco's modified Eagle's medium
DMSO	dimethylsulfoxide
dNTP	deoxyribonucleotide triphosphate
DPBS	Dulbecco's phosphate-buffered saline
EDTA	ethylene diamine tetraacetic acid
eGFP	enhanced green fluorescent protein
ELISA	enzyme-linked immunosorbent assay
ER	endoplasmic reticulum
ESCRT	endosome-associated complex required for transport
FLUAV	influenza A virus
FP	filter and precipitation
fVLP	filovirus-like particles
G	rhabdoviral spike protein
GP	filoviral glycoprotein gene
GP _{1,2}	filoviral spike protein
ha	heat-inactivated
HA	(influenzaviral) hemagglutinin
HEPES	<i>N</i> -2-hydroxyethylpiperazine- <i>N'</i> -2-ethanesulfonic acid

HBS	HEPES-buffered saline
HBSS	Hank's buffered salt solution
HCoV	human coronavirus
HEK	human embryonic kidney
HIV-1	human immunodeficiency virus type 1
hMGL	human macrophage galactose- and <i>N</i> -acetylgalactosamine-specific C-type lectin
HPLC	high-performance liquid chromatography
ICAM	intercellular adhesion molecule
IFA	indirect immunofluorescence assay
IFN	interferon
IR	intergenic region
<i>l</i>	leader sequence
L	filoviral RNA-dependent RNA polymerase
<i>L</i>	filoviral gene encoding the RNA-dependent RNA polymerase
LASV	Lassa virus
LB	Luria Bertani
LCMV	lymphocytic choriomeningitis virus
LD ₅₀	50% lethal dose
LSECTin	liver and lymph node sinusoidal endothelial cell C-type lectin
LTR	long terminal repeat
M	paramyxoviral/mononegaviral matrix protein
M.F.I.	mean fluorescence intensity
MACV	Machupo virus
MARV	Lake Victoria marburgvirus
MARV-Ang	Lake Victoria marburgvirus isolate Angola
MARV-Ci67	Lake Victoria marburgvirus isolate Cieplik
MARV-DRC	Lake Victoria marburgvirus isolate Democratic Republic of the Congo
MARV-Mus	Lake Victoria marburgvirus isolate Musoke
MARV-Ozo	Lake Victoria marburgvirus isolate Ozolin
MARV-Pop	Lake Victoria marburgvirus isolate Poppinga
MARV-Rat	Lake Victoria marburgvirus isolate Ratayczak
MEM	modified Eagle's medium
mFc	murine Fc
MLD	filoviral spike-protein mucin-like domain
MLV	Moloney murine leukemia virus
moi	multiplicity of infection
MVB	multivesicular body
NA	(influenzaviral) neuraminidase
NEB	New England Biolabs
NEPRC	New England Primate Research Center

NERCE/BEID	New England Regional Center of Excellence/Biodefense and Infectious Diseases
NIAID	National Institute of Allergy and Infectious Diseases
NP	filoviral nucleoprotein
<i>NP</i>	filoviral nucleoprotein gene
OR	gene overlapping region
PAGE	polyacrylamide gel electrophoresis
PCR	polymerase-chain reaction
pfu	plaque-forming unit
PMO	phosphorodiamidate morpholino oligomer
PS	penicillin and streptomycin
R.F.U.	relative fluorescence units
RBD	receptor-binding domain
RBR	receptor-binding region
REBOV	Reston ebolavirus
REBOV-Pen	Reston ebolavirus isolate Pennsylvania
RNP	ribonucleoprotein
rpm	revolutions per minute
RT-PCR	reverse-transcription polymerase-chain reaction
SARS-CoV	severe acute respiratory syndrome coronavirus
SCID	severe-combined immunodeficiency
SDS	sodium dodecylsulfate
SEAP	secreted alkaline phosphatase
SEBOV	Sudan ebolavirus
SEBOV-Bon	Sudan ebolavirus isolate Boniface
SEBOV-Gul	Sudan ebolavirus isolate Gulu
sGP	ebolaviral secreted glycoprotein
SP	signal peptide
ssGP	ebolaviral secondary secreted glycoprotein
SU	(retroviral) surface unit
<i>t</i>	trailer sequence
TfR1	transferrin receptor 1
TM	(filoviral) transmembrane domain
TM	(retroviral) transmembrane unit
TPMV	Tupaia paramyxovirus
Tsg	tumor susceptibility gene
'UEBOV'	'Uganda ebolavirus'
USAMRIID	United States Army Medical Research Institute of Infectious Diseases
UV	ultraviolet
VEEV	Venezuelan equine encephalitis virus
VHF	viral hemorrhagic fever
VOPBA	virus-overlay protein-binding assay
VP24, VP30, VP35, VP40	(filo)viral proteins 24, 30, 35, 40

<i>VP24, VP30, VP35, VP40</i>	(filo)viral protein genes 24, 30, 35, 40
<i>VP40</i>	filoviral matrix protein
<i>VSIV</i>	vesicular stomatitis Indiana virus
<i>Z</i>	benzyloxycarbonyl
<i>ZEBOV</i>	Zaire ebolavirus
<i>ZEBOV-Kik</i>	Zaire ebolavirus isolate Kikwit
<i>ZEBOV-May</i>	Zaire ebolavirus isolate Mayinga

5 INTRODUCTION

5.1 Filoviruses

5.1.1 Background

Filoviruses (marburgviruses and ebolaviruses) are exotic and emerging infectious pathogens (86). In humans and various nonhuman primates, filoviruses cause viral hemorrhagic fevers (VHFs), which are severe clinical syndromes characterized by capillaropathy, fever, and a tendency towards bleeding (93, 252). Human infections occur by direct contact with infected animals or their excreta and secretions. Filoviruses are highly infectious, but not very contagious, agents. Virus spread within a human population predominantly occurs via direct body-to-body contact or via blood products and contaminated clinical utensils. This is the reason why the overall number of recorded human filovirus infections (2,731 cases and 1,884 confirmed deaths since the discovery of filoviruses in 1967) is low despite case-fatality rates of up to 90% in infected populations in larger outbreaks.

Currently, there are no licensed vaccines for the prevention and no specific antivirals for the treatment of filovirus infections. Consequently, many institutions and experts consider filoviruses a potential threat to humanity because they could be used as biological weapons (29). Filovirus public-health and biodefense research must be performed in maximum-containment laboratory facilities. In the US, filoviruses are classified as Class 4 biosafety pathogens (275), Select Agents (47) and National Institute of Allergy and Infectious Diseases (NIAID) Category A Priority Pathogens (198), and are handled under biosafety-level (BSL)-4 containment to protect laboratory workers from infection (275) (Figure 5-1). Overall, filovirus-research progress has been slow because only few such facilities exist worldwide, because maximum-containment research is tedious and complicated, and because the classification as threat agents limits the number of researchers permitted to handle them.



Figure 5-1. Maximum-containment laboratory

Two laboratorians working under a flow hood inside a biosafety-level-4 suit laboratory (courtesy of CDC/Jim Gathany, obtained from CDC's Public Health Image Library at <http://phil.cdc.gov/phil/home.asp>)

5.1.2 Filovirus taxonomy and phylogeny

Particles of marburgviruses (named after the German city of Marburg an der Lahn in Hesse (245)) and ebolaviruses (named after the Ebola River in what is now the Democratic Republic of the Congo (111)) have distinctive filamentous morphologies unique among vertebrate viruses (70, 103). These viruses were grouped together as a new taxon because they are antigenically distinct from any other virus known (1, 46, 209, 246, 277) and because they are also unique on a molecular level. Today, they are classified in their own family *Filoviridae* (from Latin *filum*: thread) (151). Sufficient molecular similarities were uncovered among viruses in the families *Bornaviridae*, *Filoviridae*, *Paramyxoviridae*, and *Rhabdoviridae* to group all of them in one order, *Mononegavirales* (214, 215) (Table 5-1). All mononegaviral particles are enveloped and contain a single copy of a negative-sense and single-stranded genomic RNA with similar genomic organization (160, 216). Conserved regions at the 3' and 5' ends of the genomes encode the core proteins and the viral polymerases. Variable regions, located between the conserved regions, encode the envelope-associated proteins (160, 216).

Table 5-1. Current organization of the viral order *Mononegavirales* (80, 214, 215)

Order	Family	Subfamily	Genus/Genera	Type species
<i>Mononegavirales</i>	<i>Bornaviridae</i>		<i>Bornavirus</i>	<i>Borna disease virus</i>
	<i>Filoviridae</i>		<i>Ebolavirus</i> <i>Marburgvirus</i>	<i>Zaire ebolavirus</i> <i>Lake Victoria marburgvirus</i>
	<i>Paramyxoviridae</i>	<i>Paramyxovirinae</i>	<i>Avulavirus</i> <i>Henipavirus</i> <i>Morbillivirus</i> <i>Respirovirus</i> <i>Rubulavirus</i> “TPMV-like viruses”	<i>Newcastle disease virus</i> <i>Hendra virus</i> <i>Measles virus</i> <i>Sendai virus</i> <i>Mumps virus</i> <i>Tupaia paramyxovirus</i>
		<i>Pneumovirinae</i>	<i>Metapneumovirus</i> <i>Pneumovirus</i>	<i>Avian metapneumovirus</i> <i>Human respiratory syncytial virus</i>
	<i>Rhabdoviridae</i>		<i>Cytorhabdovirus</i> <i>Ephemerovirus</i> <i>Lyssavirus</i> <i>Novirhabdovirus</i> <i>Nucleorhabdovirus</i> <i>Vesiculovirus</i>	<i>Lettuce necrotic yellows virus</i> <i>Bovine ephemeral fever virus</i> <i>Rabies virus</i> <i>Infectious hematopoietic necrosis virus</i> <i>Potato yellow dwarf virus</i> <i>Vesicular stomatitis Indiana virus</i>

Table 5-2. Differentiation of marburgviruses and ebolaviruses (80, 103)

	Marburgviruses	Ebolaviruses
Antigenic cross-reactivity with members of the other filoviral genus	Minimal	Minimal
Average particle length	795-828 nm	974-1,086 nm
Genome length	19.1 kb	18.9 kb
Gene overlaps	One	Several (two in the Reston ebolavirus genome, three in the Sudan and Zaire ebolavirus genomes; unknown number in the Côte d'Ivoire ebolavirus and 'Uganda ebolavirus' genomes)
Co-transcriptional <i>GP</i> mRNA editing	No	Yes
Protein profile	Seven structural proteins; homologous protein sequences among all isolates, clearly distinct from proteins expressed by ebolaviruses	Seven structural proteins and two nonstructural proteins; species-specific sequence protein differences, clearly distinct from proteins expressed by marburgviruses
Case-fatality rate in humans in larger outbreaks	≥25-90%	≥25-90% (exceptions are Côte d'Ivoire ebolavirus and Reston ebolavirus at 0%)

Table 5-3. Current filovirus taxonomy (80, 179)

Order	Family	Genus	Species	Virus (Abbreviation)
<i>Mononegavirales</i>	<i>Filoviridae</i>	<i>Ebolavirus</i>	<i>Côte d'Ivoire ebolavirus</i>	Côte d'Ivoire ebolavirus (CIEBOV)
			<i>Reston ebolavirus</i>	Reston ebolavirus (REBOV)
			<i>Sudan ebolavirus</i>	Sudan ebolavirus (SEBOV)
			<i>'Uganda ebolavirus'</i>	'Uganda ebolavirus' ('UEBOV')
			<i>Zaire ebolavirus</i>	Zaire ebolavirus (ZEBOV)
		<i>Marburgvirus</i>	<i>Lake Victoria marburgvirus</i>	Lake Victoria marburgvirus (MARV)

Progressive characterization of the filoviruses revealed substantial differences between the marburgviruses and ebolaviruses (58, 224) (Table 5-2), leading to the establishment of two genera, *Marburgvirus* and *Ebolavirus*, within the family *Filoviridae* (85, 181). The genus *Marburgvirus* contains only one species, *Lake Victoria marburgvirus*, which is represented by a single virus, Lake Victoria marburgvirus (MARV). The genus *Ebolavirus* contains five species: *Côte d'Ivoire ebolavirus* (Côte d'Ivoire ebolavirus, CIEBOV), *Reston ebolavirus* (Reston ebolavirus, REBOV), *Sudan ebolavirus* (Sudan ebolavirus, SEBOV), '*Uganda ebolavirus*' ('Uganda ebolavirus,' 'UEBOV'), and *Zaire ebolavirus* (Zaire ebolavirus, ZEBOV) (80, 179) (Table 5-3). In comparison, the genomes of members of the five ebolaviral species differ genetically by 37-41% at the nucleotide level, and all of them differ from MARV genomes by >65% (83) (Figure 5-2).

5.1.3 Filovirus epidemiology

Marburgviruses were first recognized in August of 1967, when hemorrhagic fever outbreaks were reported almost simultaneously in Marburg an der Lahn and Frankfurt am Main in Germany, and in Belgrade, Yugoslavia (245, 254, 268). The outbreaks occurred among laboratory professionals who were involved in the production and safety testing of poliomyelitis vaccines. Personnel became infected during necropsies of African green monkeys (*Chlorocebus aethiops*) or while handling their tissues or contaminated laboratory equipment. In total, 31 people fell gravely ill, and seven of them died. The three outbreaks were connected as all three laboratories had imported the African green monkeys at about the same time from the same nonhuman primate exporter in Uganda. A novel virus, today known as Lake Victoria marburgvirus (MARV) (80), was isolated from clinical materials from patients at all three locations and established as the etiological agent of the new disease, marburgvirus disease. In the following years and decades, MARV reemerged only sporadically (see Table 5-4 for a chronological listing of all confirmed filovirus-disease outbreaks), until a large marburgvirus-disease outbreak (154 cases, 128 deaths) was recorded between 1998-2000 in the Democratic Republic of the Congo among illegal gold miners (19, 21, 135). The largest outbreak was recorded in 2004-2005 in Angola, where at least 252 people came down with marburgvirus disease and of whom 227 died (135, 311, 313).

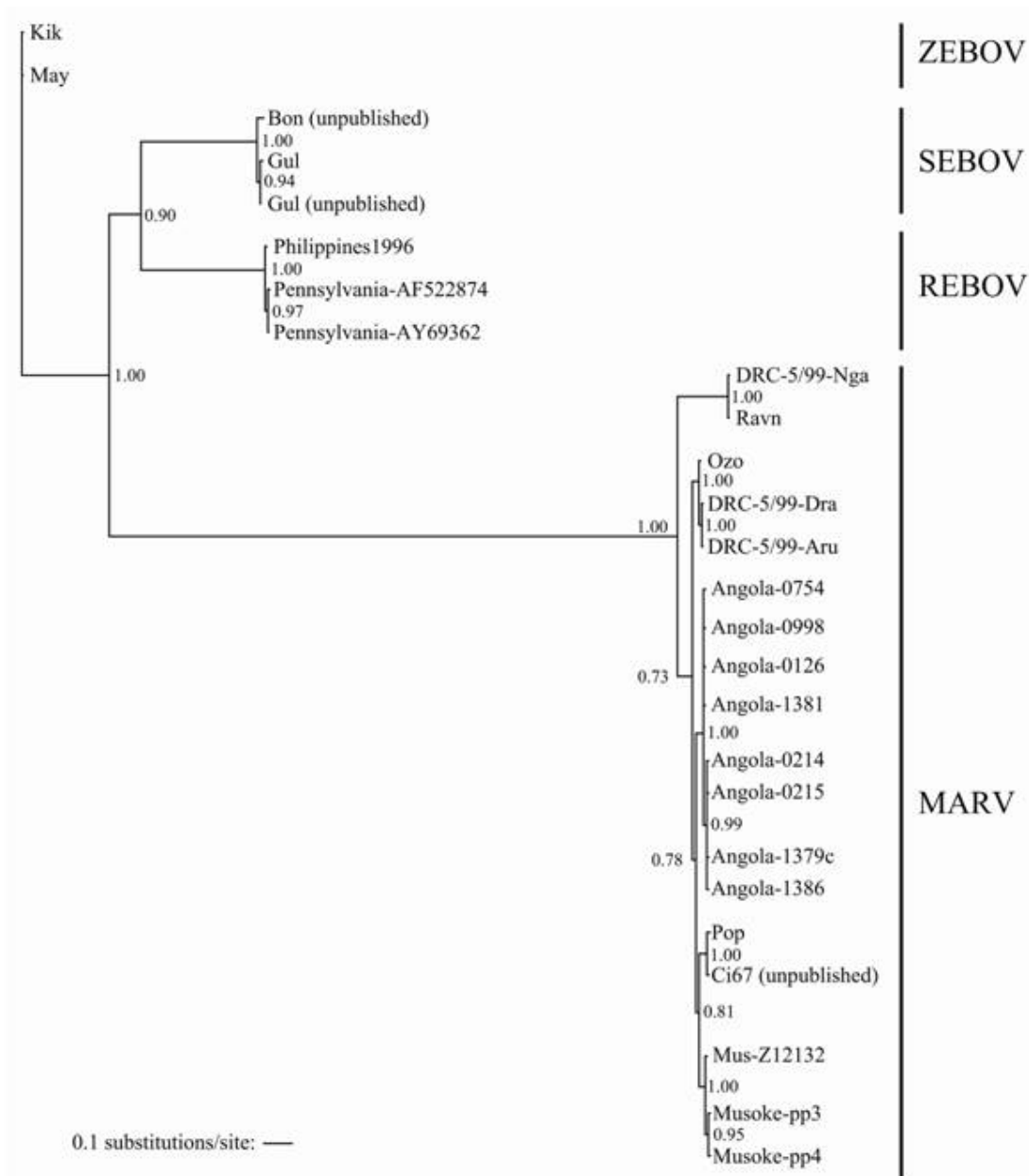


Figure 5-2. Phylogenetic analysis of filovirus isolates using the filoviral RNA-dependent RNA polymerase genes

MARV, Lake Victoria marburgvirus; REBOV, Reston ebolavirus; SEBOV, Sudan ebolavirus; ZEBOV, Zaire ebolavirus; Kik, Kikwit isolate; May, Mayinga isolate; Bon, Boniface isolate; Gul, Gulu isolate; DRC, Democratic Republic of the Congo isolate; Ozo, Ozolin isolate; Pop, Poppinga isolate; Ci67, Cieplik isolate; Mus, Musoke isolate. RNA-dependent RNA polymerase gene (*L*) gene sequences of Côte d'Ivoire ebolavirus (CIEBOV) and 'Uganda ebolavirus' ('UEBOV') have yet to be published ((157), reproduction with permission)

Table 5-4. Chronology of filovirus-disease outbreaks

Year	Location	Human cases/deaths (% case-fatality rate)	Filovirus involved	Reference(s)
1967	Germany (Marburg an der Lahn, Frankfurt am Main), Yugoslavia (Belgrade)	31/7 (22.6%)	Lake Victoria marburgvirus	(245, 254, 268)
1975	Rhodesia/South Africa (Johannesburg)	3/1 (33.3%)	Lake Victoria marburgvirus	(57, 97)
1976	Sudan (Nzara, Maridi)	284/151 (53.2%)	Sudan ebolavirus	(9, 308)
1976	Zaire (Yambuku)	318/280 (88.1%)	Zaire ebolavirus	(31, 36, 309)
1976	United Kingdom (laboratory infection, Porton Down)	1/0 (0%)	Sudan ebolavirus	(74)
1977	Zaire (Bonduni)	1/1 (100%)	Zaire ebolavirus	(125)
1979	Sudan (Nzara)	34/22 (64.7%)	Sudan ebolavirus	(15)
1980	Kenya (Mount Elgon/Nzoia)	2/1 (50%)	Lake Victoria marburgvirus	(251)
1987	Kenya (Mombassa/Mount Elgon)	1/1 (100%)	Lake Victoria marburgvirus	(144)
1988	USSR (laboratory infection, Koltsovo)	1/1 (100%)	Lake Victoria marburgvirus	(5)
1989-1990	US (Alice, Philadelphia, Reston), Philippines (Luzon)	Epizootic	Reston ebolavirus	(138)
1990	USSR (laboratory infection, Koltsovo)	1/0 (0%)	Lake Victoria marburgvirus	(201)
1992	Italy (Siena), Philippines (Luzon)	Epizootic	Reston ebolavirus	(56)
1994	Côte d'Ivoire (Guiglot)/Switzerland (Basel)	1/0 (0%)	Côte d'Ivoire ebolavirus	(89)
1994-1995	Gabon (Andok, Mékouka, Minkébé, Mayéla-Mbeza, Ovan, Etakangaye)	52/32 (61.5%)	Zaire ebolavirus	(8, 90, 106, 107)
1995	Zaire (Kikwit)	317/245 (77.3%)	Zaire ebolavirus	(135, 197, 307)
1996	Gabon (Mayibout II, Makokou)	31/21 (67.7%)	Zaire ebolavirus	(106, 107)
1996	US (Alice), Philippines (Luzon)	Epizootic	Reston ebolavirus	(227)
1996	Russia (laboratory infection, Sergiyev Posad-6)	1/1 (100%)	Zaire ebolavirus	(135)
1996-1997	Gabon (Balimba, Bouée,	62/46 (74.2%)	Zaire ebolavirus	(106, 107)

	Lastoursville, Libreville, Lolo), South Africa (Johannesburg)			
1998-2000	Democratic Republic of the Congo (Durba, Watsa)	154/128 (83.1%)	Lake Victoria marburgvirus	(19, 21, 135)
2000-2001	Uganda (Gulu, Masindi, Mbarara Districts)	425/224 (52.7%)	Sudan ebolavirus	(26, 108, 135, 205)
2001-2002	Gabon (Ekata, Etakangaye, Franceville, Grand Etoumbi, Ilahounene, Imbong, Makokou, Mékambo, Mendema, Ntolo) and Congo (Abolo, Ambomi, Entsiami, Kéllé, Olloba)	124/97 (78.2%)	Zaire ebolavirus	(165, 185, 202)
2002	Congo (Olloba)/Gabon (Ekata)	11/10 (90.9%)	Zaire ebolavirus	(135, 213)
2002-2003	Congo (Yembelengoye, Mvoula)	143/128 (89.5%)	Zaire ebolavirus	(135, 213)
2003-2004	Congo (Mbomo, Mbanza)	35/29 (82.9%)	Zaire ebolavirus	(30)
2004	Russia (laboratory infection, Koltsovo)	1/1 (100%)	Guinea pig-adapted Zaire ebolavirus	(3)
2004	Sudan (Yambio)	17/7 (41.2%)	Sudan ebolavirus	(135, 217, 264)
2004-2005	Angola (Uíge Province)	252/227 (90.1%)	Lake Victoria marburgvirus	(135, 311, 313)
2005	Congo (Etoumbi, Mbomo)	11/9 (81.9%)	Zaire ebolavirus	(310)
2007	Uganda (Kakasi Forest Reserve)	2/1 (50%)	Lake Victoria marburgvirus	(135, 312)
2007	Uganda (Kakasi Forest Reserve)	1/1 (100%)	Lake Victoria marburgvirus	(135, 312)
2007	Democratic Republic of the Congo (Kampungu, Mweka, Mwene-Ditu)	264/187 (70.8%)	Zaire ebolavirus	(135)
2007	Uganda (Bundibugyo District)	149/25 (16.8%)	‘Uganda ebolavirus’	(135, 179)
2008	Uganda (Maramagambo Forest)/The Netherlands	1/1 (100%)	Lake Victoria marburgvirus	Unpublished

The ebolaviruses were discovered in 1976, when two almost simultaneous hemorrhagic fever outbreaks occurred in Sudan and Zaire (now Democratic Republic of the Congo). The viruses isolated from patients resembled MARV in appearance as judged by electron microscopy, but proved to be antigenically distinct (9, 31, 145, 308, 309). In both countries, the outbreaks began with single index infections and were amplified nosocomially in local hospitals and then carried into neighbouring villages. In Sudan, 151 of 284 infected people died (9, 308), whereas the death toll in Zaire was 280 out of 318 infected people (31, 36, 309). Molecular studies later proved that the viruses isolated in Sudan and Zaire are not only different from MARV, but also differ considerably from each other (58, 85, 181, 224). Today, they are referred to as Sudan ebolavirus (SEBOV) and Zaire ebolavirus (ZEBOV), respectively (80), and the diseases they cause are referred to as Sudan and Zaire ebolavirus disease, respectively. SEBOV only caused one additional large outbreak. In 2004, it resurfaced around Gulu in Uganda. Again, the disease was amplified in local hospitals and spread into several Ugandan administrative districts. There were at least 425 human cases and 224 deaths (26, 108, 135, 205). As in other ebolavirus-disease outbreaks, burial rituals, and caring of and close contact with the sick had additionally contributed to the spread of the virus (92). ZEBOV repeatedly caused large outbreaks in Gabon between 1994 and 2001 (106, 107, 185, 213), in Congo between 2001 and 2005 (135, 165, 213), and in the Democratic Republic of the Congo in 1995 and 2007 (135, 197, 307). Most of these outbreaks began with people who had hunted animals in the forest or found dead animals and consumed them. Today, it is thought that especially ZEBOV is causing wandering epizootics among central chimpanzees (*Pan troglodytes troglodytes*) and western lowland gorillas (*Gorilla gorilla gorilla*), which contribute dramatically to their population decline (133, 149, 159).

Between 1989-1990, almost uniformly fatal epizootics occurred among captive cynomolgus macaques (*Macaca fascicularis*) in the US. The macaques had been imported from a supplier in the Philippines. Diagnostic tests revealed coinfection of the animals with simian hemorrhagic fever virus (an arterivirus) and a filovirus-like agent. Further tests revealed that the latter was related to, but distinct from, SEBOV and ZEBOV. The agent is

now referred to as Reston ebolavirus (REBOV) (138). REBOV and simian hemorrhagic fever virus were again isolated during epizootics among captive cynomolgus macaques in Italy in 1992 (56) and in the US in 1996 (227). In both instances, the macaques came from the same Philippine supplier implicated in the first emergence of REBOV. It remains unclear how REBOV was introduced into this facility, and the virus has not been encountered since as the facility was shut down immediately after the third REBOV disease epizootic in 1996. Interestingly, human Reston ebolavirus disease has not yet been observed, and REBOV is therefore considered apathogenic for humans by many specialists.

In 1994, a group of western chimpanzees (*Pan troglodytes verus*) was decimated by a hemorrhagic disease in Côte d'Ivoire. A filovirus was detected by electron microscopy in tissues from one of the apes. Today, it is referred to as Côte d'Ivoire ebolavirus (CIEBOV). Thus far, CIEBOV caused only one (nonfatal) human infection, which occurred during a necropsy of one of the deceased apes (89, 91). The fifth ebolavirus, 'Uganda ebolavirus' ('UEBOV'), was discovered in 2007 during an outbreak of severe gastrointestinal disease in Uganda. Data describing this outbreak have yet to be published (135, 179).

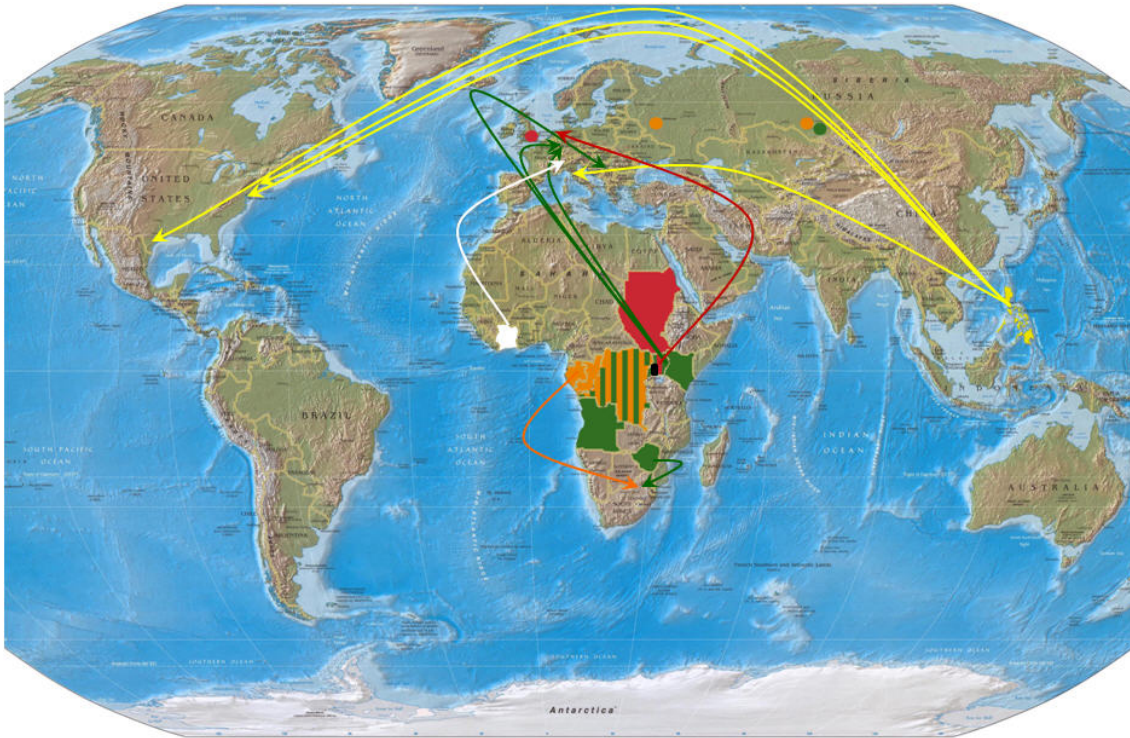


Figure 5-3. Filovirus-disease outbreaks

Countries affected by outbreaks are highlighted in color. White: Côte d'Ivoire ebolavirus disease (Côte d'Ivoire); yellow: Reston ebolavirus disease (Philippines); red: Sudan ebolavirus disease (Sudan, Uganda); black: 'Uganda ebolavirus disease' (Uganda); orange: Zaire ebolavirus disease (Congo, Democratic Republic of the Congo, Gabon); green: marburgvirus disease (Angola, Democratic Republic of the Congo, Kenya, Uganda, Zimbabwe). The location of laboratory infections is shown by colored dots. Red: Sudan ebolavirus disease (United Kingdom – Porton Down); orange: Zaire ebolavirus disease (Russia – Sergiyev Posad-6, Koltsovo); green: marburgvirus disease (Russia – Koltsovo). Arrows show exported human or animal infections (adapted from (157), reproduction with permission)

5.1.4 Ecology of filoviruses

Serological surveys were performed repeatedly among humans living in Africa and elsewhere to define the geographical distribution of filoviruses. Most of these studies were performed using indirect immunofluorescence assays (IFAs) and revealed a relatively high (5-20%) seroprevalence of anti-ebolavirus antibodies, and a relatively low (1-5%) seroprevalence of anti-marburgvirus antibodies (for a thorough overview of these studies

see (157)). However, it is commonly thought today that these results are largely artifacts, given that IFAs are prone to cross-reactions with antibodies not directed against filoviruses and because filovirus disease has so far not been recorded in many areas with allegedly high seroprevalence of anti-filovirus antibodies. Indeed, enzyme-linked immunosorbent-assay (ELISA) and western-blot studies mostly failed to confirm the presence of such antibodies in sera testing positive using IFAs (157).

The natural hosts of filoviruses still remain to be identified. If one ignores the contradictory data obtained during serological surveys and if one then analyzes disease-outbreak distribution and their particularities, one comes to the conclusion that the hosts are native to central Africa and possibly the Philippines. Several hypotheses have been brought forward as to the identity of these hosts (191). Initially, it was thought that nonhuman primates could be harboring the filoviruses, given that these animals were often associated with large human outbreaks of filovirus disease. However, it is now clear that filoviruses are even more virulent for African green monkeys, baboons, macaques, and apes than for humans, thereby excluding them as stable reservoirs, which should sustain persistent and subclinical infections (253). Consequently, the focus of the host search is now on organisms that are in contact with nonhuman primates, such as duikers (which follow chimpanzees and the fruit they leave behind) or arthropods (insects and ticks that may parasitize the animals) (163, 191, 223). Bats, which may coinhabit fruit trees occupied by nonhuman primates, are another focus of interest, especially because many of them live in caves, which were often associated with human filovirus-disease outbreaks as well. Most studies performed thus far have not even yielded traces of filoviruses (35, 109, 163, 223), but intriguing data on the reservoirs of filoviruses have been obtained from studies with bats. Experimental infections of Angolan free-tailed bats (*Mops condylurus*), little free-tailed bats (*Chaerephon pumila*), and Wahlberg's epauletted fruit bats (*Epomophorus wahlbergi*) with ZEBOV resulted in limited replication without overt signs of disease and recovery of the virus from bat feces three weeks after inoculation (259). During screening studies, IgG antibodies to ZEBOV and ZEBOV genomic fragments were detected in some Franquet's epauletted bats (*Epomops franqueti*), hammer-headed fruit bats (*Hypsignathus*

monstrosus), and little collared fruit bats (*Myonycteris torquata*), but infectious virus could not be recovered (164). IgG antibodies to MARV and MARV genomic fragments, but again not infectious virus, were detected by nested reverse-transcription polymerase-chain reaction (RT-PCR) in Egyptian fruit bats (*Rousettus aegyptiacus*) (271). Therefore, bats as reservoirs for filoviruses remains only a hypothesis at this point in time.

5.1.5 Clinical and pathological presentation of filovirus infections

Filoviruses are transmitted through direct contact. They enter humans and nonhuman primates through small skin lesions or through erosions of the mucous membranes and then infect their initial target cells, macrophages, which transport them throughout the body (230). The clinical and pathological presentation of marburgvirus and ebolavirus infections in humans is very similar (Tables 5-5 and 5-6), and occurs usually in two phases (21, 43, 273). During the early phase, after an incubation time of 3-7 days, patients present with influenza-like symptoms, such as abdominal pain, anorexia, arthralgia, asthenia, back pain, diarrhea, fever, headaches, enlarged lymph nodes, myalgia, nausea, pyrexia or vomiting. A maculopapular rash, reminiscent of the rash observed during measles, usually develops after approximately seven days on the face, buttocks, trunk, or arms, and later generalizes over almost the entire body. Patients then either recover (often with sequelae, such as alopecia, prolonged weight loss, arthralgia, conjunctivitis, loss of vision or hearing, parotitis, psychosis, orchitis, dysesthesias or pericarditis), or progress to the second phase characterized by anuria, hiccups, terminal tachypnea, and hemorrhagic manifestations, such as bleeding from the gums, hematemesis, hemoptysis, melena or hematuria. Neurological involvement is infrequent and involves confusion, convulsions, meningitis, tinnitus, hearing loss, sudden bilateral blindness or dysesthesias. Death occurs usually 8-16 days after infection in shock after multiorgan failure, often brought on by secondary bacterial infections (10, 21, 43, 91, 211).

Table 5-5. Symptoms of 22 survivors of marburgvirus disease and 107 fatally infected patients, Democratic Republic of the Congo, 1998-2000 (21, 273)

Clinical symptom	Frequency observed in survivors (%)	Frequency observed in fatal cases (%)
Abdominal pain	59	57
Anorexia	77	72
Arthralgia or myalgia	55	55
Bleeding from puncture sites	0	7
Bleeding from the gums	23	36
Bleeding from any site	59	71
Chest pain	18	4
Conjunctival injection	14	42
Cough	9	5
Diarrhea	59	56
Difficulty breathing	36	58
Epistaxis	18	34
Fever	100	92
Headaches	73	79
Hematemesis	68	76
Hematoma	0	3
Hemoptysis	9	4
Hiccups	18	44
Lumbar pain	5	8
Malaise or fatigue	86	83
Melena	41	58
Nausea and vomiting	77	76
Petechiae	9	7
Sore throat, odynophagia or dysphagia	43	43

Table 5-6. Symptoms of 19 survivors of Zaire ebolavirus disease and 84 fatally infected patients, Zaire, 1995 (43)

Clinical symptom	Frequency observed in survivors (%)	Frequency observed in fatal cases (%)
Abdominal pain	68	62
Abortion	5	2
Anorexia	47	43
Anuria	0	7
Arthralgia or myalgia	79	50
Asthenia	95	85
Bleeding from puncture sites	5	8
Bleeding from the gums	0	15
Bloody stools	5	7
Chest pain	5	10
Conjunctival injection	47	42
Convulsions	0	2
Cough	26	7
Diarrhea	84	86
Dysesthesia	5	0
Epistaxis	0	2
Fever	95	93
Headaches	74	52
Hearing loss	11	5
Hematemesis	0	13
Hematoma	0	2
Hematuria	16	7
Hemoptysis	11	0
Hepatomegaly	5	2
Hiccups	5	17
Lumbar pain	26	12
Maculopapular rash	16	14
Melena	16	8
Nausea and vomiting	68	73
Petechiae	0	8
Sore throat, odynophagia or dysphagia	58	56
Splenomegaly	5	2
Tachypnea	0	31
Tinnitus	11	1

Clinical chemistry usually reveals elevated levels of serum glutamic-oxaloacetic transaminase, serum glutamic-pyruvic transaminase, glutamate dehydrogenase, sorbitol dehydrogenase, and γ -glutamyl transpeptidase, indicating liver damage. Other typical findings are elevated levels of creatinine and urea levels prior to renal failure, and hypokalemia because of diarrhea and vomiting. Leukopenia with a left shift of the granulocytes can usually be detected during the first days of disease, accompanied by severe thrombocytopenia. During the second clinical stage, leukocytosis becomes eminent. Blood fails to clot concomitant with a decrease of clotting factors and prolonged thrombin and cephalin times, indicating disseminated intravascular coagulation (69, 91, 121, 155, 176, 211, 258).

Only very few autopsies of humans fatally infected with filoviruses have been performed. However, the pathological presentation of filoviruses is rather uniform. Focal necroses are typical findings in almost all organs in the almost complete absence of inflammatory reactions. The most severe destruction is usually seen in the liver (debris-laden Kupffer cells, destroyed parenchyma, siderosis, fatty degeneration), lymphatic system (follicle necrosis, necrosis of the red pulp of the spleen and the medulla of the lymph nodes), and kidneys (destroyed parenchyma, tubular insufficiency). Panencephalic glial nodule encephalitis is a typical finding in humans infected with MARV. Skin hemorrhages and hemorrhages into the gastrointestinal tract, as well as increased vascular permeability are also observed (22, 62, 98, 137, 196, 231).

Animal filovirus-disease models (mice, guinea pigs, hamsters, and nonhuman primates) have been developed that reproduce diseases similar, but not identical, to those observed in naturally-infected humans (101, 126, 255). Wild-type filoviruses only infect primates, whereas infections in rodents are only successful after virus adaptation through serial passage (33, 229, 290).

5.1.6 Treatment of filovirus infections

Currently, no specific antivirals are licensed for the treatment of filovirus infections. Hospital treatment must therefore rely on intensive supportive care, including oral and intravenous nutritional support, anti-microbials to treat or prevent secondary infections, and intravenous rehydration to maintain blood volume and electrolyte balance (32, 101). Whether such treatment influences the outcome of the disease remains to be demonstrated. Experimental approaches to prolong survival include the administration of interferon (IFN). For instance, recombinant IFN- α 2b decreased ZEBOV replication 100-fold in tissue culture. Unfortunately, daily administration of the drug to cynomolgus macaques only delayed viremia and death by one day (139). Similarly disappointing results were obtained with other IFN preparations or IFN inducers. Inhibitors of the tissue-factor pathway are currently evaluated as antifiloviral drugs since filoviruses induce the overexpression of the procoagulant tissue factor. In one study, subcutaneous administration of recombinant nematode anticoagulant protein c2 (rNAPc2) prolonged the survival time of rhesus macaques infected with guinea pig-adapted ZEBOV and protected individual animals from death (102). Filovirus-neutralizing antibodies are sought after for treatment, but none have yet been isolated that could ensure survival of filovirus-infected nonhuman primates. For instance, a filoviral spike protein-specific IgG₁ antibody named KZ52 protected guinea pigs against challenge with ZEBOV if administered 1 h before or 1 h after challenge (208). However, the same antibody had no effect on the survival of challenged rhesus macaques (206). Nucleoside analogs also have been evaluated for the treatment of filovirus disease, but none, including ribavirin, had any beneficial effect in nonhuman primate models of the disease. On the other hand, inhibitors of *S*-adenosylhomocysteine hydrolase, such as carbocyclic 3-deazaadenosine/3-deazaaristeromycin (C-c³Ado) and 3-deazaneplanocin A (c³-Npc A), increased the mean survival time of infected mice and African green monkeys infected with ZEBOV (132). Finally, phosphorodiamidate morpholino oligomers (PMOs), which act as antisense analogs and knock down specific filoviral mRNAs, could protect 75% of rhesus macaques challenged with ZEBOV despite the development of clinical symptoms (296).

5.1.7 Diagnosis of filovirus infections

The clinical symptoms of filovirus infections are rather unspecific, and pathognomonic markers of these diseases have not yet been uncovered. Other viral hemorrhagic fevers, in particular those caused by Rift Valley fever virus, yellow fever virus, Crimean-Congo hemorrhagic fever virus or Lassa virus, are part of the differential diagnosis, as are other African diseases, such as falciparum malaria, plague, measles, gram-negative septicemia, shigellosis, typhoid fever or platelet and vascular disorders (82, 96). Rapid diagnosis of filovirus infections is essential for the containment of ongoing outbreaks, and requires methods that can be performed in the field in the absence of sophisticated equipment. In recent years, RT-PCR has evolved to the gold-standard for filovirus diagnosis in the field and has taken the place of previously widely used IFAs and ELISAs. Confirmatory diagnosis of RT-PCR-positive samples is usually performed by virus isolation in maximum-containment facilities (113, 272).

5.1.8 Molecular biology of filoviruses

5.1.8.1 Filoviral particles

Filovirions are elongated, thread- or filamentous particles that often occur in torus-, horseshoe- or 6-shaped forms. These shapes are unique among human viruses (Figure 5-4), allowing quick and unequivocal diagnosis of tissue infection using electron microscopy. The particles have an average mass of 3.82×10^5 kD, a buoyant density in potassium tartrate of 1.14 g/cm^3 , and a sedimentation coefficient of 1,300-1,400 S (153).

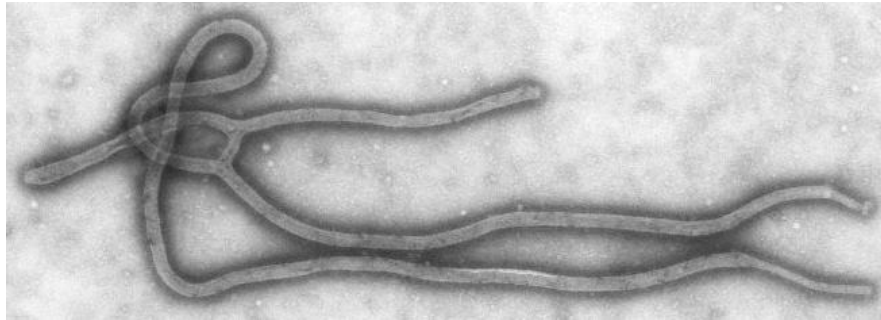


Figure 5-4. Transmission electron micrograph of a Zaire ebolavirus particle

(Courtesy of CDC/Cynthia Goldsmith, obtained from CDC's Public Health Image Library at <http://phil.cdc.gov/phil/home.asp>)

Filovirus particles are, on average, 795-828 nm (MARV), 1,026-1,086 nm (REBOV), 974-1,063 nm (SEBOV) or 990-1,086 nm (ZEBOV) long and 78-80 nm in diameter (103). The particles possess an envelope derived from the host-cell membrane. Within the filoviral envelope, ~5-10 nm-long spike proteins ($GP_{1,2}$) protrude at ~10 nm intervals. A lattice of matrix proteins (VP40 and possibly VP24) is situated beneath the membrane and wraps around the viral core, which is comprised of helically arranged nucleoproteins (NP) that bind around the viral genomic RNA. Further structural proteins (transcriptional cofactor VP30, polymerase cofactor VP35, RNA-dependent RNA polymerase L) are associated in low numbers with the genomic RNA (Figure 5-5) (153).

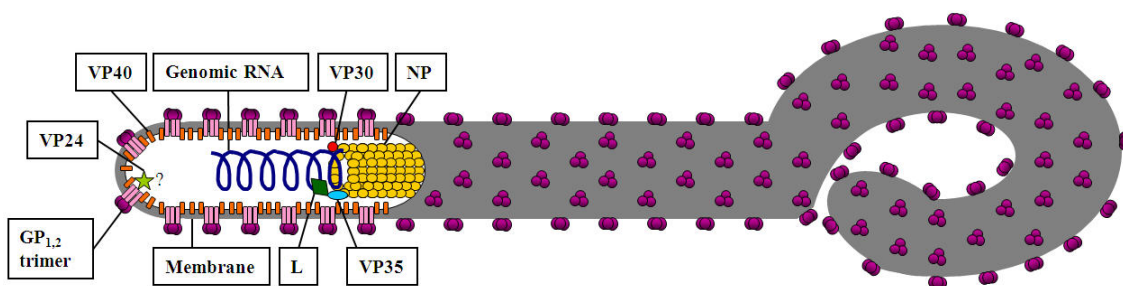


Figure 5-5. Schematic of a filovirus particle

(Adapted from (157), reproduction with permission)

5.1.8.2 Filoviral genomes

Filoviral genomes are single-stranded nonsegmented RNAs of negative polarity that have an average molecular mass of $4.0\text{-}4.2 \times 10^3$ kD. They are uncapped and not polyadenylated (72, 80, 152, 221). The genomes are ~ 19 kb in length and contain seven genes that are arranged linearly and that may be separated by intergenic regions (234) (Figure 5-6). Each filoviral gene is flanked by highly conserved transcription initiation and termination sites, but these sites differ among different filoviruses. Filoviral mRNAs are monocistronic, capped, and polyadenylated (233, 297).

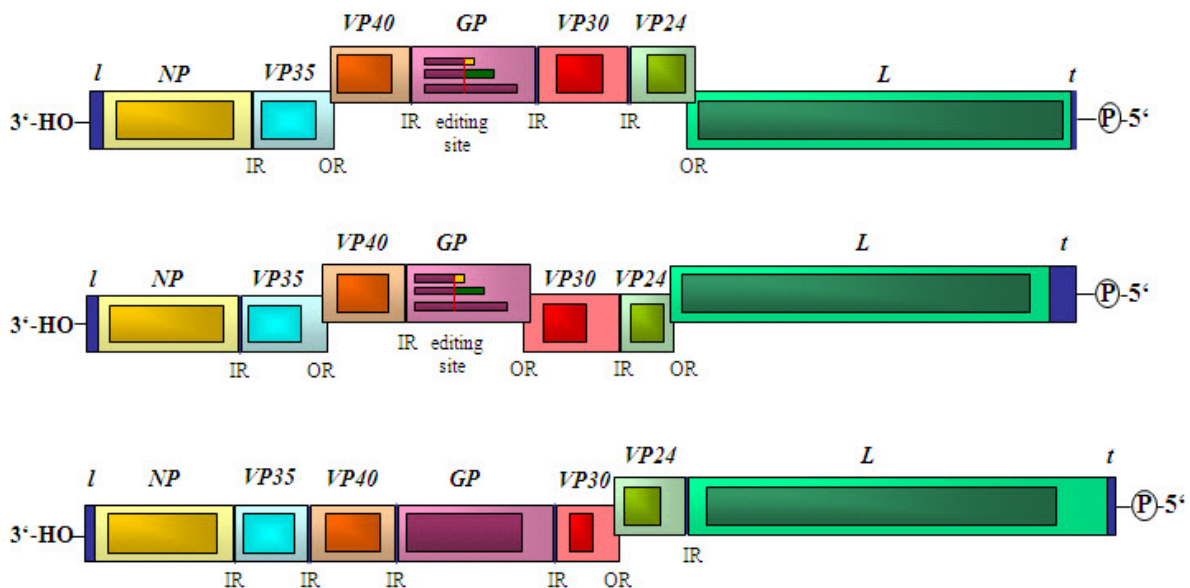


Figure 5-6. Schematic organization of filoviral genomes

Top, Reston ebolavirus; middle, Sudan and Zaire ebolaviruses; bottom, Lake Victoria marburgvirus. The complete genomic sequences of Côte d'Ivoire ebolavirus and 'Uganda ebolavirus' have yet to be determined. *l*, leader sequence; *NP*, nucleoprotein gene; *VP*, viral protein gene; *GP*, glycoprotein gene; *L*, RNA-dependent RNA polymerase gene; *t*, trailer sequence; IR, intergenic region; OR, gene overlapping region. Transcribed open reading frames are depicted as rectangles within a given gene. The *GP* gene editing site (present only in ebolaviruses) is depicted as a vertical red line spanning all three *GP* open reading frames (adapted from (157), reproduction with permission)

5.1.8.3 *NP* gene

The first (3') gene of filoviral genomes, *NP*, encodes the nucleoprotein NP (MARV: 696 amino-acid residues, 94-96 kD; ZEBOV: 739 amino-acid residues, 104 kD) (235, 236). In cells, filoviral NP is found in phosphorylated or nonphosphorylated states, but only phosphorylated NP becomes incorporated into virions (23, 72, 169) and binds to other NPs (23, 24). Similar to other mononegaviral nucleoproteins, filoviral NP mediates the formation of plus-sense (antigenome) ribonucleoprotein (RNP) complexes in the cytosol that serve as the template for filoviral genome synthesis (23). Within virions, polymerized NP encapsidates the filoviral genomic RNA and associates with VP35, VP30, and L (24).

5.1.8.4 *VP35* gene

The filoviral *VP35* gene is located immediately downstream of the *NP* gene. It encodes the VP35 protein (MARV: 329 amino-acid residues; 36 kD; ZEBOV: 321 amino-acid residues, 35 kD) (41, 84), for which no other mononegaviral analogs have yet been identified. VP35 can homooligomerize and binds to NP (190), L, and cellular and viral RNA (82, 88). VP35 is the cofactor of the filoviral RNA-dependent RNA polymerase L (195). In developing filoviral RNP complexes, VP35 confers specificity for filoviral genomic RNA (146). Furthermore, VP35 acts as an RNA-silencing suppressor, thereby counteracting the RNAi-based innate antiviral response of cells (114). VP35 and VP35-NP complexes also inhibit both dsRNA-mediated and virus-mediated induction of interferon-responsive promoters and consequently the cellular interferon innate immune response to virus infection (18, 45, 88, 119).

5.1.8.5 *VP40* gene

The filoviral *VP40* gene is located downstream of the *VP35* gene and is the most conserved of all filovirus genes. It encodes the matrix protein VP40 (MARV: 303 amino-acid residues, 34 kD; ZEBOV: 326 amino-acid residues, 35 kD) (41, 73). VP40 is a functional analog of the M proteins of other mononegaviruses, although there is no significant

sequence similarity among them (41, 73, 161). VP40 associates with cellular membranes through hydrophobic interactions (156). It occurs in monomeric and dimeric forms, but also aggregates as ring-like hexameric and octameric complexes with trimeric symmetry (241, 265). Octamers consist of four VP40 dimers, and are disc-shaped, pore-like structures that bind eight copies of single-stranded RNA (110). Hexamers are trimers of VP40 dimers, also resembling a pore (228, 241), but as is the case for octamers their function is unknown. VP40 contains short amino-acid sequences, L domains, that seem to play an important role in filovirus budding. Ebolaviral VP40 has three such domains, P(T/S)AP, PPXY, and YXXL, whereas MARV VP40 contains only a PPXY motif (7, 120, 140). Several components of the cellular protein sorting machinery bind to these L domains. For instance, the E3 ubiquitin ligase Nedd4 binds to the PPXY motif of oligomeric VP40 and probably induces multi-ubiquitinylation (266, 316). The P(T/S)AP motif of ZEBOV VP40 is a binding partner of Tsg101 (168, 174, 175, 207, 274), a component of the endosome-associated complex required for transport I (ESCRT-I). ESCRT-I, ESCRT-II, and ESCRT-III together direct multiubiquitinated proteins to late endosomes, thus creating multivesicular bodies that later fuse with lysosomes or the plasma membrane. This suggests that the ESCRT machinery is hijacked by maturing ebolavirus particles to facilitate virus release. Tsg101 is also involved in MARV budding, although MARV VP40 does not contain a P(T/S)AP motif (274).

5.1.8.6 *GP* gene

The filoviral *GP* gene and its expression product(s) are described in detail in Chapter 5.2.

5.1.8.7 *VP30* gene

The filoviral *VP30* gene, located downstream of the *GP* gene, is another unique component of filoviral genomes. It encodes a protein, VP30 (MARV: 291 amino-acid residues, 33 kD, ZEBOV: 288 amino-acid residues, 32 kD), which shares characteristics only with one other known protein, the M2-1 protein of pneumoviruses (39). VP30's phosphorylation status

determines its interaction with polymerized NP (169, 188, 189), while its homooligomerization status (monomers vs. dimers vs. hexamers) determines whether the protein is located within the cytosol or is directed into filovirions. Homooligomerization is also required for VP30's main function as a transcriptional activator (118). The N-terminus of VP30 binds directly to single-stranded RNA, and prefers filoviral RNA over unspecific RNA (143). VP30 is also a zinc-binding protein. In the absence of zinc, filovirus-genome transcription is abolished (187).

5.1.8.8 VP24 gene

The *VP24* gene is the utmost last gene in the filoviral genomes. Its expression product is VP24 (MARV: 253 amino-acid residues, 29 kD; ZEBOV: 251 amino-acid residues, 29 kD), which has no resemblance to any other protein known (39). Detergent-salt dissociation studies with filovirions and molecular characterization of the protein suggested that VP24 is a matrix protein and that VP24 and VP40 co-localize at the plasma membrane and in released filovirions (11, 72, 115). The function of VP24 remains mysterious, although it is clear that specific mutations within VP24, in conjunction with mutations in NP, are necessary for the adaptation of filoviruses to rodents (33, 54, 67, 280). Recent experiments also indicate that VP24 counteracts the interferon-response of virus-infected cells (222).

5.1.8.9 L gene

The last (5') gene of the filoviral genome is the *L* gene, which encodes the catalytic part (L protein; MARV: 2,331 amino-acid residues, 267 kD; ZEBOV: 2,212 amino-acid residues, 253 kD) of the viral RNA-dependent RNA polymerase holoenzyme, which also contains VP35 (27, 195, 283). Filoviral L proteins have a high leucine- and isoleucine-residue content, are strongly positively charged at neutral pH, and contain numerous conserved cysteine residues (269, 283). As other mononegaviral L proteins, filoviral L proteins contain three characteristic sequence motifs (A: RNA-binding element, B: RNA template-recognition element, C: nucleotide triphosphate-binding element) (194, 269). However, in

contrast to other mononegaviral L proteins, filoviral L proteins seem to be extraordinarily accurate RNA polymerases. For instance, the genomes of MARV isolates obtained in Angola (MARV-Ang) in 2004 are only 7% different from the genome of a MARV isolate obtained in Germany in 1967 (MARV-Mus) (269).

5.1.8.10 Filovirus life cycle

The filovirus life cycle resembles those of other mononegaviruses. After penetration of a host organism, filoviruses bind to a specific, yet unidentified, receptor on a target cell. The entry pathway and requirements are discussed in more detail in Chapter 5.3. The filoviral nucleocapsid is released into the cytosol subsequent to fusion of the viral and cellular membrane, and complete uncoating of the filoviral genome takes place. The polymerase holoenzyme L/VP35, brought into the cell with the nucleocapsid, then transcribes the filoviral genes in a sequential manner, synthesizes the filoviral antigenome, and uses the antigenome as a template to synthesize progeny genomes. The filoviral mRNAs are translated into the filoviral structural proteins. NP, VP30, VP35, and L assemble with the newly synthesized genomes to form RNPs complexes. These then recruit the matrix proteins VP40 and VP24 and bud from the cell's plasma membrane or are released from subcellular compartments, incorporating the spike protein GP_{1,2}. The entire filovirus life cycle occurs in the cytoplasm of the host cell (Figure 5-7).

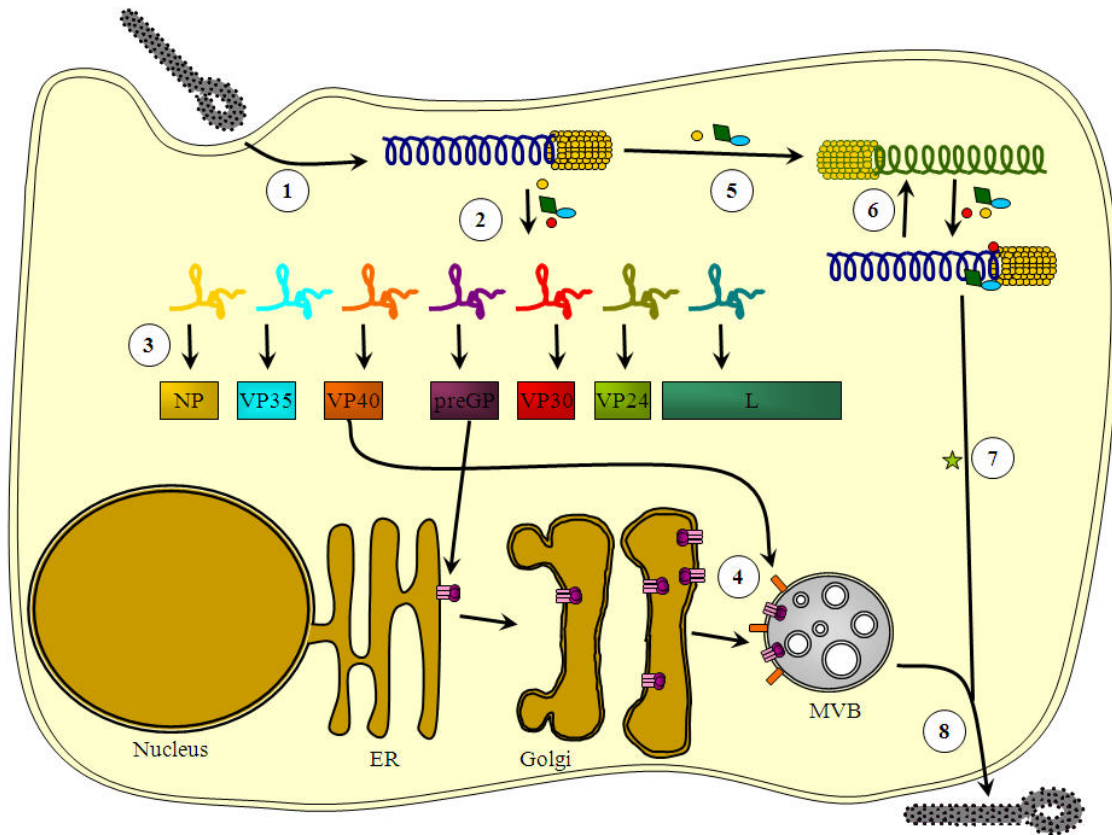


Figure 5-7. Filovirus life cycle

Filovirus particles fuse with the host cell membrane after binding to an unknown receptor with their spike proteins (GP_{1,2}, purple). Subsequently, their ribonucleocapsids are released into the cytosol (1). Uncoating releases the genome, from which the filoviral genes are transcribed into mRNAs (2) by the polymerase holoenzyme (L-VP35, green and blue) and by the transcription factor VP30 (red) in the presence of nucleoprotein NP (yellow). This step is followed by the translation of the mRNAs (3). NP controls the switch between mRNA transcription (2) and genomic replication (5, 6). GP_{1,2} is translocated into the endoplasmic reticulum (ER) and redirected by the matrix protein VP40 (orange) into multivesicular bodies (MVBs) (4). The genome is the template for antigenome synthesis (5). The antigenome is the template for progeny-genome synthesis (6). NP binds to progeny genomes and recruits VP35, VP30, and L (6). VP24 may control trafficking of the ribonucleoprotein (RNP) complexes to the MVBs (7), which then results in budding of progeny filoviral particles from the cell (8) (adapted from (157), reproduction with permission)

5.2 Filoviral glycoproteins

5.2.1 Ebolaviral secreted glycoprotein

Marburgviral and ebolaviral genomes encode one and three glycoproteins from their *GP* genes, respectively (281). Conservative transcription of the CIEBOV, REBOV, SEBOV, 'UEBOV,' and ZEBOV, but not the MARV, *GP* genes by the RNA-dependent RNA polymerases (L proteins) yields mRNAs for nonstructural glycoproteins, termed secreted glycoproteins (sGPs). ZEBOV sGP consists of 364 amino-acid residues. During its biosynthesis (Figure 5-8) it is translocated into the ER, where it becomes glycosylated and converted to a Golgi-apparatus precursor (pre-sGP, 60 kD). Pre-sGP is cleaved by furin, yielding the mature sGP monomer and a secreted small peptide, Δ -peptide (10-14 kD) (287).

The sGP monomer then dimerizes via the formation of two intermolecular disulfide bonds (involving cysteine residues 53 and 306) (16), resulting in a parallel homodimer that is secreted from the host cell (237, 279). It can be found in large amounts in the serum of acutely infected patients (237). A ZEBOV sGP monomer contains two intramolecular disulfide bonds (C₁₀₈-C₁₃₅ and C₁₂₁-C₁₄₇) that resemble the location and connection of cysteine residues in fibronectin type-II (F2) modules (287). ZEBOV sGP does not contain *O*-glycans, but five of the six predicted *N*-glycosylation sites contain complex *N*-glycans (N₄₀, N₂₀₄, N₂₂₈, N₂₅₇, N₂₆₈). The sixth site (N₂₃₈) is only infrequently glycosylated (76). Tryptophan residue 288 is C-mannosylated (Figure 5-8) (75).

The function of sGP is unknown. Both marburgviruses and ebolaviruses cause similar diseases in humans and nonhuman primates, yet marburgviruses do not express an sGP-like protein. ZEBOV sGP does not bind to primary human macrophages, the primary target cells of filoviruses, and activation of these cells does not occur upon exposure to this protein (142, 289). Since sGP shares its N-terminal 295 amino-acid residues with the actual filovirus spike protein, GP_{1,2} (237, 279), it was suggested that it might serve as an antibody decoy in the bloodstream, binding ebolavirus-neutralizing antibodies (136). However, guinea pig-adapted ZEBOV mutants that express only small amounts of sGP proved to be

as or even more virulent than unaltered guinea pig-adapted viruses (3, 134, 280). ZEBOV-like particles, which are replication-incompetent particles that assemble after coexpression of VP40 and GP_{1,2}, activated human endothelial cells and induced a decrease in barrier function. sGP induced a recovery of the barrier function. Therefore, it was suggested that sGP might play an anti-inflammatory role (288).

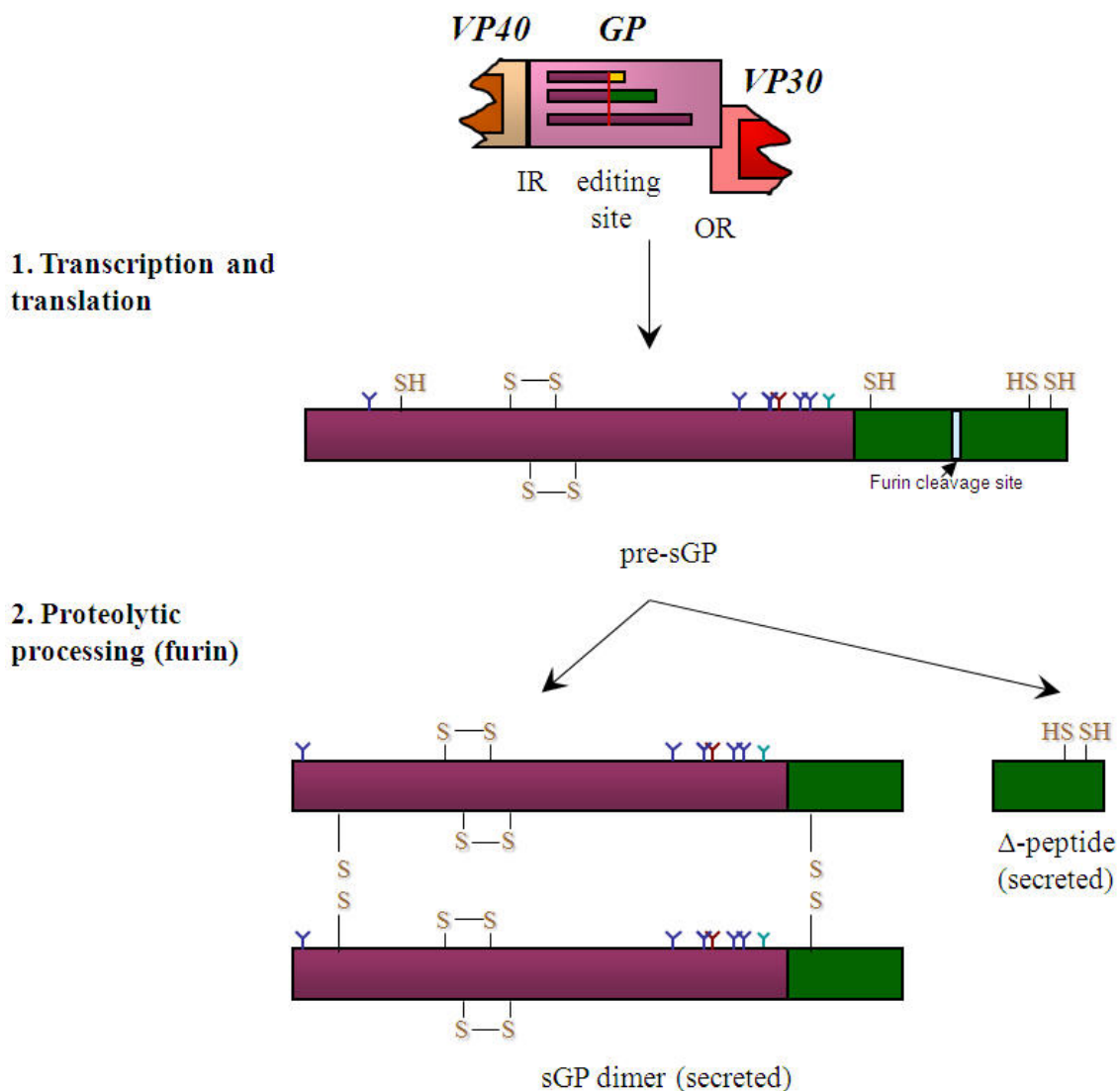


Figure 5-8. Expression pathway of ebolaviral secreted glycoprotein

Zaire ebolaviral GP gene's primary open reading frame (middle purple/green line) encodes a nonstructural protein, secreted glycoprotein (sGP), which is secreted from producer cells

as a parallel homodimer and shares its N-terminal 295 amino-acid residues with GP₁ and secondary secreted glycoprotein(ssGP) (purple), but contains a unique C-terminus (green). Proteolytic cleavage of the C-terminus of each monomer (pre-sGP) by furin yields a small, nonstructural, and secreted protein, Δ -peptide. Experimentally-proven *N*-glycan (blue and red Ys) and C-mannosylation sites (green Y) are indicated. One site (red Y) is only sometimes glycosylated (adapted from (157) with permission)

The function of ebolaviral Δ -peptides, which are *O*- but not *N*-glycosylated and sialylated, remains enigmatic (287). ZEBOV Δ -peptide does not bind or activate primary human macrophages (288), and contrary to sGP it does not reverse the decreased barrier function of endothelial cells exposed to ZEBOV-like particles (288).

5.2.2 Filoviral spike protein

Ebolaviral *GP* genes contain only one open reading frame with a start codon in Kozak-like context, which is the one encoding the secreted glycoprotein (sGP) described above. The large spike proteins that protrude from the surfaces of ebolavirions are transcribed by cotranscriptional editing (237, 279). The ebolaviral *GP* genes contain a stretch of seven consecutive uridine residues. The ebolaviral polymerase transcribes the *sGP* mRNA containing the complementary seven consecutive adenosine residues, but with a frequency of 20% stutters and adds or subtracts one or several non-template adenosine residues to the elongating transcript (237, 279). Addition of one non-template adenosine residue leads to a frame shift and to the fusion of the *sGP* open reading frame encoding its N-terminal 295 amino-acid residues to a -1 open reading frame located immediately downstream of the editing site. This fusion transcript encodes the 676 amino-acid long ebolaviral spike-protein precursor (180, 237, 279). Marburgviral *GP* genes do not contain editing sites and the 681 amino-acid long spike-protein precursors are transcribed directly (87).

The biosynthesis of filoviral spike-proteins, which are type I transmembrane proteins, follows a complex processing pathway (Figure 5-9). First, a signal peptide targets the elongating protein into the ER. The protein then becomes glycosylated with oligomannosidic *N*-glycans (preGP_{ER} or GP₀). After trafficking to the Golgi apparatus, *N*-

glycan modifications are completed, *O*-glycans are added, and phosphorylation occurs. Ebolaviral, but not marburgviral, spike proteins become sialylated (preGP, ~140-160 kD) (239, 282, 285). The glycans comprise roughly one third of the molecular mass of the mature filoviral spike proteins (85, 87).

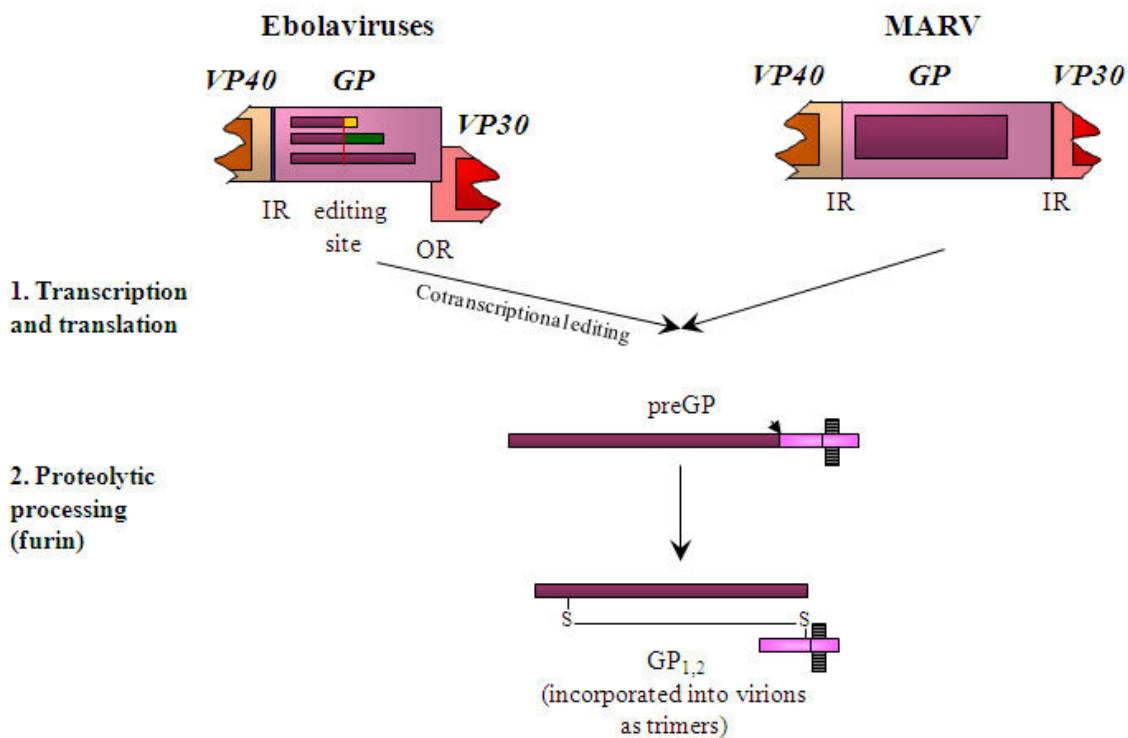


Figure 5-9. Expression pathway of filoviral spike proteins

Cotranscriptional editing (red vertical line in the ebolaviral *GP* gene) results in the spike protein (GP_{1,2}), which shares the 295 N-terminal amino-acid residues of secreted glycoprotein (sGP) and secreted glycoprotein (ssGP), but has a C-terminus consisting of 381 unique amino-acid residues. GP_{1,2} is translated as a precursor protein (preGP). Furin cleavage (arrow) separates the two subunits GP₁ and GP₂, which remain associated as a heterodimer that then trimerizes. The marburgviral *GP* gene has only one primary open reading frame, which encodes the structural spike protein (GP_{1,2}). Its expression pathway is similar to that of ebolaviral GP_{1,2} (adapted from (157) with permission)

Most of GP_{1,2}'s glycans are located in the variable central region of the spike protein (mucin-like domain, MLD) (238). These glycans are speculated to influence the antigenicity of the spike protein by masking polypeptide epitopes ("glycan shield"). The N- and C-terminal thirds of the proteins are highly conserved within a filoviral species (85), but there seems to be no antigenic cross-reactivity between marburgviral and ebolaviral spike proteins (234). The MLD is under discussion as a potential filovirus virulence factor as it exerted cytotoxic effects in tissue culture that led to cell rounding and detachment (50, 263, 315). However, these results are controversial because the MLD-containing proteins in the used systems were overexpressed (284). This could explain why cells, which were infected with a Kunjin-virus replicon continuously expressing ZEBOV GP_{1,2} to levels comparable to those seen in filovirus infections, remained healthy (4).

Filoviral preGP is proteolytically cleaved by furin and related proprotein convertases into an N-terminal subunit called GP₁ (ZEBOV: 130-140 kD, MARV: 160-170 kD) and a C-terminal subunit called GP₂ (ZEBOV: 24-26 kD, MARV: 38-45 kD), which remain attached to each other through a disulfide bond (GP_{1,2}, ZEBOV: 150 kD, MARV 170-200 kD) (282, 285). GP_{1,2} heterodimers associate as trimers that are incorporated into budding filovirions as the mature spike proteins (Figure 5-10).

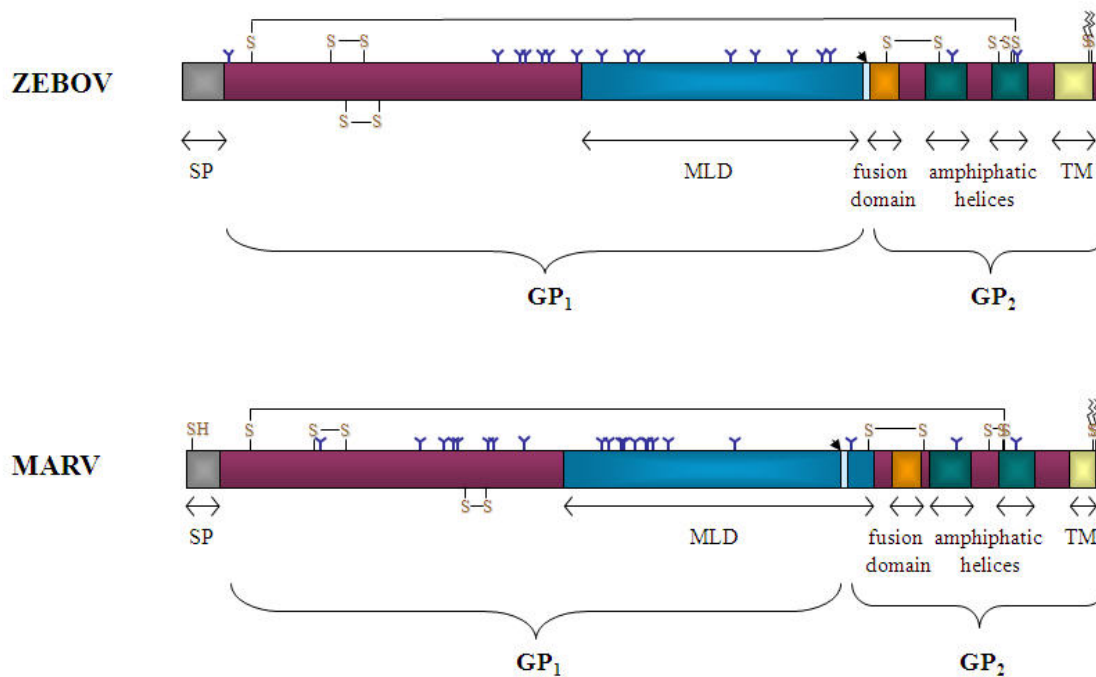


Figure 5-10. Schematic of filoviral spike proteins

preGP, the predecessor of the filoviral spike protein (GP_{1,2}), consists of two subunits, GP₁ and GP₂, which become separated during maturation by proteolytical cleavage (arrows). GP₁ and GP₂ remain attached through a disulfide bond. Trimerization of this dimer results in the mature spike protein. Ebolaviral GP₁ shares its N-terminal 295 amino-acid residues with ebolaviral sGP and ssGP (grey and purple boxes), but contains a unique C-terminus (blue box + GP₂). SP: signal peptide; MLD: mucin-like domain; TM: transmembrane domain. *N*-glycans (blue Ys) and C-terminal acylations are indicated (adapted from (157) with permission)

GP₁ is the surface-unit (SU) analog of retroviral envelope proteins (94), and therefore mediates filovirus cell entry. This notion is supported by the inhibition of filovirus cell-entry by anti-GP₁ antibodies (177, 303). However, the filovirus receptor remains unidentified and the receptor-binding region of GP₁ has not been determined, therefore leaving the function of this spike-protein subunit rather uncharacterized.

GP₂ is the transmembrane-unit (TM) analog of retroviral envelope proteins (94), and is responsible for mediating the fusion between viral and cellular membranes during cell penetration. It contains a fusion peptide, an immunosuppressive motif, α -helical heptad-

repeat regions, a conserved amino-acid loop defined by a disulfide bridge between two cysteine residues, a transmembrane domain, and a highly conserved CX₆CC motif (40, 94, 141, 238).

5.2.3 Ebolaviral secondary secreted glycoprotein

A third protein is transcribed from the ebolaviral *GP* gene by co-transcriptional mRNA editing. The addition of two non-template adenosine residues to or the subtraction of one adenosine residue from the transcript causes both a frame shift and the termination of translation immediately downstream of the editing site (279). In the case of ZEBOV, the derived secreted and possibly monomeric protein, secondary secreted glycoprotein (ssGP) consists of 297 amino acids, of which the N-terminal 295 amino-acid residues are identical to those in sGP and GP₁ (Figure 5-11) (286). The natural function of ssGP is unknown.

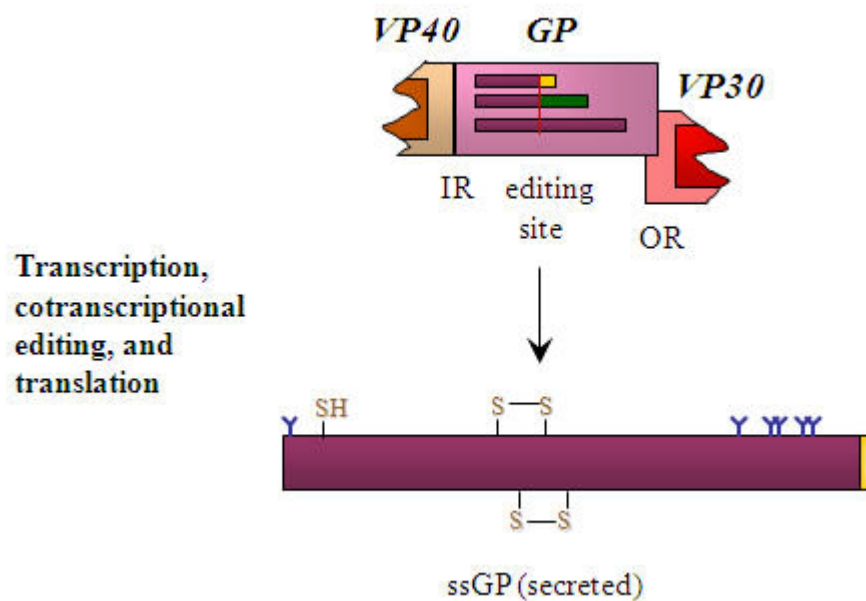


Figure 5-11. Expression pathway of ebolaviral secondary secreted glycoprotein

Zaire ebolavirus secondary secreted glycoprotein (ssGP) shares its N-terminal 295 amino-acid residues with secreted glycoprotein (sGP) and GP₁ (purple box), but contains a unique C-terminus consisting of only two amino-acid residues (yellow). Predicted *N*-glycans (blue Ys) are indicated (adapted from (157) with permission)

5.3 Filovirus cell entry

Filoviruses enter their host cells by binding to yet unidentified cell-surface receptors with their spike proteins. These receptors are present on most adherent, but generally not on suspension, cell-lines (51, 65). African green monkey kidney cells, such as CV-1 and Vero derivatives, are commonly used to grow filoviruses to high titers (71, 276). Experiments with retroviral or vesiculoviral pseudotypes carrying filoviral spike proteins demonstrated that the spike proteins alone mediate filovirus entry, and that the filovirus receptors are additionally present, for example, on human embryonic kidney (HEK) 293T cells, human and nonhuman primate macrophages, human cervical adenocarcinoma epithelial-like (HeLa) cells, baby hamster kidney (BHK) cells, and Chinese hamster ovary (CHO) cells. Many different cell lines from bats, bovids, canids, chickens, hamsters, humans, marsupials, murids, porcids, quails, simians, and turkeys can be transduced successfully (51, 262, 318). Pseudotypes, which carry filoviral spike proteins lacking the GP₁ mucin-like domain (MLD), transduce cells at least as efficiently as those carrying wild-type proteins (141, 173, 183, 315), indicating that the MLD does not play an important role in filovirus cell entry. Filoviruses do not replicate in primary human peripheral lymphocytes or suspension T (C8166, SupT1, MT-2, HUT-78, Jurkat E6-1, CEM) or B (AA-2) cells (51, 210, 250, 267), suggesting that these cells may not express the filovirus cell-surface receptors. In fact, recent data point towards the possibility that suspension cells in general are not permissive to filoviruses (65). These data are in accordance with the pathological finding that lymphocytes of humans and animals do not become infected (231). Of course, it is also possible that replication is inhibited in these cells during a step downstream of cell entry. Thus far, all cells identified as permissive to a particular filovirus are also permissive to all other filoviruses. However, the entry efficiency of different filoviruses into the same permissive cell varies (51). Consequently, it is discussed whether all filoviruses use a common receptor, different subtypes thereof, or different receptors altogether.

Filovirus-cell adsorption is slow (several hours vs. minutes) in comparison to other viruses (318), but treatment of filovirus-permissive cells with proteases abrogates pseudotype cell transduction, thereby confirming the hypothesis that the filovirus receptors are proteins (51, 262). Treatment of permissive cells with endoglycosidase H, which cleaves high-mannose-type *N*-glycosides from the cell-surface, or with tunicamycin, which inhibits *N*-glycosylation of cell-surface glycoproteins, abolished transduction by pseudotypes carrying ZEBOV, but not MARV, spike proteins (51, 262), suggesting that the receptors may be glycosylated and that ZEBOV and MARV may bind to the same protein but at different sites or to different proteins.

Several filovirus receptor candidates have been brought up for discussion. Among them are integrins, which are conserved among many species, highly glycosylated, and expressed at the cell-surface. Anti- β_1 -integrin immunoglobulins and the soluble $\alpha_5\beta_1$ -integrin complex inhibited cell transduction with vesiculoviral particles pseudotyped with ZEBOV or REBOV spike proteins (263). Unfortunately, spike proteins could not be shown to bind to β_1 -integrin directly, and filovirus-resistant cells lacking β_1 -integrin could not be rendered susceptible after transfection of β_1 -integrin-expressing plasmids (49). Other receptor candidates are C-type lectins, which bind to highly mannosylated glycoproteins. Several lectins are being discussed as potential filovirus receptors, among them dendritic cell-specific ICAM-3-grabbing non-integrin (DC-SIGN; CD209) and its homolog DC-SIGN-Related (lymph-node-specific ICAM-3-grabbing non-integrin, L-SIGN) (6, 247), the murine DC-SIGN-homolog SIGNR1 (178), LSEctin (liver and lymph node sinusoidal endothelial cell C-type lectin) (112), the human macrophage galactose- and *N*-acetylgalactosamine-specific C-type lectin (hMGL) (261), and asialoglycoprotein receptor (25). The presence of all of these molecules increases transduction rates of retroviral or vesiculoviral particles pseudotyped with filoviral spike proteins. However, these proteins 1) are not present on all cell types known to be permissive to filoviruses; 2) are present on some cell types resistant to filovirus infection; 3) cannot render resistant cells permissive; and 4) when knocked out or knocked down do not necessarily decrease filovirus infection levels. Another widely publicized filovirus receptor candidate is human folate receptor α .

This protein was identified after filovirus-resistant human acute T-cell leukemia Jurkat T lymphocytes, which had been transduced with a retroviral cDNA library derived from filovirus-permissive HeLa cells, had become permissive to infectious MARV. Antibodies to human folate receptor α or to folic acid inhibited cell entry of pseudotypes (48). However, the hypothesis of human folate receptor α being a significant filovirus receptor could not be upheld after follow-up experiments (7, 248, 249).

Expression of tyrosine-receptor tyrosine-kinases, such as Axl, Dtk, and Mer, in filovirus-resistant Jurkat T lymphocytes enhanced transduction of retroviral or vesiculoviral particles pseudotyped with filoviral spike proteins, and this increase was reversed in the presence of polyclonal antibodies against these kinases or in presence of their soluble ectodomains (243). Confusingly, there was no increase in the susceptibility of kinase-expressing Jurkat T lymphocytes to infectious filoviruses, the kinases were not detected in all known filovirus-permissive cells, anti-Axl antibody did not inhibit filovirus infection in Axl-expressing African green monkey kidney epithelial (Vero E6) cells, and Axl binding to filoviral spike proteins could not be demonstrated (242, 243).

Together, the described data suggest that all currently identified entry factors are at best virus-attachment factors or entry modulators rather than true virus receptors (see also Chapter 8 for a thorough discussion of the difference between attachment factors and receptors).

Filoviruses probably enter cells by receptor-mediated and microfilament- and microtubule-dependent endocytosis (12, 51, 103, 232, 262, 305, 318). The entry process is low-pH-dependent, as lysosomotropic agents, such as ammonium chloride or chloroquine, inhibited transduction of filovirus-permissive cells by pseudotypes carrying REBOV, ZEBOV or MARV spike proteins (12, 51, 262, 305). Furthermore, filovirus cell entry is dependent on the cysteine proteases cathepsin B and cathepsin L. Both cell transduction with vesiculoviral particles pseudotyped with ZEBOV spike protein, as well as infection with infectious ZEBOV, was almost abolished in the presence of cathepsin B/L inhibitors. Cell entry was also almost abolished in *CatB*^{-/-} *CatL*^{+/+} mouse-embryo fibroblasts, and abolished in *CatB*^{-/-} *CatL*^{-/-} cells (52, 130, 240). Together, cathepsin B and L cleave

ZEBOV GP₁ on pseudotyped vesiculoviral particles to a 17-19 kD fragment that remains attached to GP₂. Interestingly, these pseudotypes transduced target cells more efficiently than undigested control pseudotypes (52, 148, 232, 240), suggesting that large parts of GP₁ are dispensable for the mediation of cell entry.

Filoviral GP_{1,2} is a typical class I fusion-protein (298, 301) (see also Chapter 8). Its N-terminal domain (GP₁) is responsible for receptor binding, upon which the C-terminal domain, which contains an N-terminal fusion peptide, heptad repeats, and a transmembrane anchor, mediates membrane fusion. As other known class I fusion proteins, filoviral spike proproteins are proteolytically processed to these subunit domains by furin or a related protease (282, 287). However, in contrast to other class I fusion proteins, this processing is not necessary to mediate the transition from the fusion-incompetent to the fusion-competent state (136, 200, 306). Once GP₁ has bound the receptor, a complex refolding of GP_{1,2} occurs that is mainly driven by GP₂'s heptad repeats, leading to the insertion of GP₂'s fusion peptide into the host cell membrane and a subsequent pull motion that forces the host cell and viral membrane into close apposition and thereby to fusion (171, 299-301).

5.4 Filovirus-vaccine development

Filovirus vaccines could 1) prevent epizootics, and thereby limit spill-over into human populations; 2) control epidemics among humans in filovirus-endemic areas; 3) protect first responders and primary caregivers in outbreak areas; 4) protect military personnel, either deployed in endemic areas or in theater; 5) be distributed in populated areas prior to or directly following a biological attack; and 6) protect laboratory researchers working with filoviruses. However, there are currently no licensed vaccines for the prevention of filovirus infections. The immune response to filoviruses in humans and animals is only rudimentarily understood. Filovirus-vaccine development has been trial-and-error research, in part because it remains unclear whether antibody responses, cytotoxic T-lymphocyte (CTL) responses, or both are necessary to protect from filovirus infections (20, 104, 117).

The attenuation of filoviruses by repeated passaging in tissue culture and animals has not been attempted systematically thus far. However, several guinea pig-adapted and mouse-adapted filoviruses retained their virulence for nonhuman primates (34). This observation, and the possibility of reversion of an adapted virus to a wild-type virus, made attenuation a vaccine-development approach that is not considered useful.

The first filovirus candidate vaccines were based on formalin-, heat- or γ -irradiation-inactivated virus preparations, which were reported to partially protect guinea pigs, baboons, and rhesus macaques from infection with homologous virus (53, 170, 184). Today, inactivated vaccine platforms are not a research priority anymore because vaccine production would require maximum-containment facilities and because incomplete inactivation of vaccine batches would always be a safety concern independent of the efficacy of the candidate vaccine.

Replication-incompetent filovirus-like particles (fVLPs) can be synthesized in and purified from tissue culture via expression of recombinant filoviral VP40 alone or by co-expression with filoviral GP_{1,2} (140, 203, 260). Since such fVLPs resemble wild-type filoviruses in morphology and surface antigenicity, and because there would not be interference with a vector backbone, they are currently pursued as candidate vaccines (127, 293). *In vivo*, intraperitoneal immunization of Hartley guinea pigs, BALB/c mice, and C57BL/6 mice with ZEBOV fVLPs conferred 100% protection from otherwise lethal challenge with ZEBOV (291, 292). ZEBOV fVLPs also protected cynomolgus macaques from infection with ZEBOV (295). However, guinea pigs vaccinated with ZEBOV fVLPs were not protected from MARV infection, whereas guinea pigs vaccinated with MARV fVLPs were immune to MARV challenge, but succumbed to ZEBOV infection (294).

So far, there has been limited success with subunit-vaccine candidates based on purified filoviral protein preparations. Immunization of guinea pigs with MARV NP protected some animals from otherwise lethal MARV infection (2), whereas 100% protection was provided by immunization with a soluble truncation variant of MARV isolate Musoke (MARV-Mus) GP_{1,2} (amino-acid residues 17-644). However, these animals were only partially protected when viral challenge was performed with the heterologous

MARV isolate Ravn (MARV-Ravn), and they were not protected from infection with ebolaviruses (123).

Single-cycle, propagation-defective Venezuelan equine encephalitis virus (VEEV) replicons expressing MARV-Mus GP_{1,2} conferred complete protection to cynomolgus macaques challenged with homologous virus (124), but these macaques died after challenge with MARV-Ravn or ebolaviruses. Similarly, immunization with VEEV replicons expressing ZEBOV isolate Mayinga (ZEBOV-May) GP_{1,2} did not protect cynomolgus macaques from infection with ZEBOV isolate Kikwit (ZEBOV-Kik) (105).

A single intramuscular immunization with a recombinant replication-competent vesicular stomatitis Indiana virus (VSIV) expressing either ZEBOV-May or MARV-Mus GP_{1,2} completely protected cynomolgus macaques from infection after challenge with ZEBOV-Kik or MARV-Mus, respectively. Again, animals that were immunized against ZEBOV antigen were unprotected from infection with MARV and *vice versa*. Worse, only one of the animals that had survived ZEBOV challenge survived challenge with the closely related SEBOV, whereas all animals that had survived MARV-Mus challenge were protected from infection with the Popp (MARV-Pop), Ravn, and Angola (MARV-Ang) isolates (59, 147). The VSIV candidate vaccines hold promise as post-exposure prophylactics, because VSIV expressing MARV-Mus GP_{1,2} prevented the death of rhesus macaques that had been infected with homologous virus even when the immunization was performed as late as 20-30 min. after challenge (60). Similar results have been obtained with SEBOV (100) and ZEBOV (81).

Another promising candidate vaccine is based on replication-incompetent human adenovirus 5 vectors. Immunization of cynomolgus macaques with two such vectors, one expressing ZEBOV NP, and the other expressing ZEBOV GP_{1,2}, with or without previous immunization with DNA vaccines encoding the same proteins, fully protected the animals from disease and death caused by homologous, but again not by heterologous, virus (256, 257).

Last, a respirovirus-based candidate vaccine has been described recently. Rhesus macaques immunized by aerosol with recombinant replication-competent human

parainfluenzavirus 3 expressing ZEBOV GP_{1,2} were fully protected against challenge with ZEBOV (38).

It remains unclear which candidate vaccine should be pursued further. For instance, adenoviral vaccines are complicated by background immunity to adenoviruses in humans and animals, and VSIV vaccines are based on replication-competent viruses that may pose health risks for immunocompromised individuals. In any case, it has become clear that there is so far no monovalent candidate vaccine in sight that has the potential to protect against marburgviruses and ebolavirus simultaneously. Additionally, none of the currently available candidate vaccines could be easily transported, stored, and distributed among people or animals in filovirus-endemic areas.

5.5 Objective of this dissertation

The objective of this dissertation is to further the understanding of filovirus cell entry, and to develop tools and methods that could be used to identify the yet unidentified filovirus cell-surface receptors. In particular, the experiments described in this dissertation aim to answer the following questions: first, it is to be determined whether filoviral spike proteins contain discrete receptor-binding domains or regions, and if so, whether such regions exert higher affinity to the unknown filovirus receptors than the full-length spike-protein ectodomains. The answer to this question will inform us on receptor-binding requirements and therefore may allow further speculation on the identity of the receptors. Furthermore, such receptor-binding regions may turn out to be ideal bait proteins for the receptors in coimmunoprecipitation experiments. Second, to clear up the confusion in the literature, it is to be determined whether marburgviruses and ebolaviruses use a common receptor. If so, receptor-identification strategies may be developed that focus on only one particular filovirus bait protein, namely the one with the highest affinity to the receptor and the best expression properties to ensure easy production, and one particular filovirus, namely the one most easily grown and detected in tissue culture. Third, the role of the ebolaviral secreted glycoproteins (sGP, ssGP, and Δ -peptide) in filovirus entry, if any, is to be

evaluated. Finally, in the case that receptor-binding regions are identified, experiments are to be performed that answer the question whether such protein fragments could serve as the basis for a subunit filovirus candidate vaccine.

6 MATERIALS AND METHODS

6.1 Cells and culture conditions

African green monkey (*Chlorocebus aethiops*) kidney epithelial (Vero E6) cells, human cervical adenocarcinoma epithelial-like (HeLa) cells, and human acute T-cell leukemia Jurkat E6-1 T lymphocytes were obtained from the American Type Culture Collection in Manassas, VA, USA (ATCC numbers CRL-1586, CCL-2, and TIB-152, respectively). Human embryonic kidney (HEK) 293T cells, a derivative of HEK 293 cells (ATCC number CRL1573) and originally known as 293/*tsA1609*neo (66), were obtained from Joseph Sodroski, Dana Farber Cancer Institute, Harvard Medical School, Boston, MA, USA. Human MT-4 and SupT1 T lymphocytes were provided by Hyeryun Choe at Children's Hospital, Harvard Medical School, Boston, MA, USA. Human C8166-45LTR-SEAP T lymphocytes were obtained from Ronald C. Desrosiers' laboratory at the New England Primate Research Center, Harvard Medical School, Southborough, MA, USA.

Adherent (Vero E6, HeLa, and HEK 293T) cells were maintained in Dulbecco's modified Eagle's medium (DMEM, GIBCO-Invitrogen, Grand Island, NY, USA), and suspension (Jurkat E6-1, MT-4, SupT1, C8166-45LTR-SEAP cells) T lymphocytes in RPMI Medium 1640 (GIBCO-Invitrogen). All media were supplemented with 10% heat-inactivated (ha, 56 °C, 1h) fetal-bovine serum (FBS, Sigma-Aldrich, St. Louis, MO, USA), 100 IU/ml penicillin and 100 µg/ml streptomycin (PS, Cellgro, Herndon, VA, USA), and cell cultures were maintained in vented tissue-culture flasks (Nunc, Rochester, New York, USA) at 37 °C in a humidified 5% CO₂ atmosphere. All adherent cells were passaged by trypsinization after reaching 90% confluency as judged by eye using microscopy. Briefly, cells were washed in warm (37 °C) Dulbeccos's phosphate-buffered saline (DPBS, GIBCO-Invitrogen) and then detached with an appropriate volume (1 ml for a 75 cm², 2 ml for a 175 cm² flask) of Cellgro's 0.25% trypsin/2.21 mM ethylene diamine tetraacetic acid (EDTA) in Hank's buffered salt solution (HBSS). Detached cells were washed in DPBS, counted under the microscope using a manual cytometer, and divided into new flasks as

needed. Suspension cells were maintained by serial dilution. For long-term storage, cells were suspended in DMEM/haFBS/PS supplemented with 5% (vol./vol.) dimethylsulfoxide (DMSO, ATCC) into cryotubes, and frozen and stored in liquid nitrogen provided by the New England Primate Research Center, Southborough, MA, USA.

6.2 Construction of filovirus glycoprotein-encoding genes and variants

6.2.1 General Procedures

HPLC-purified (25-60 mers) or PAGE-purified (>60 mers) DNA oligomers were ordered from Integrated DNA Technologies (IDT, Coralville, IA, USA). Oligomers were reconstituted in TE buffer (QIAGEN, Valencia, CA, USA) to a final concentration of 10 pmol/ μ l, aliquoted, and stored until use at -20 °C. Polymerase-chain reactions (PCRs) were performed using cloned pfuTurbo and its corresponding 10x cloned pfuTurbo buffer (Stratagene, LaJolla, CA, USA), both of which were aliquoted and stored until use at -20 °C. dNTP stocks were ordered from GIBCO-Invitrogen, diluted in a master mix to a final concentration of 2.5 mM of each dNTP (10x dNTP master mix), aliquoted, and stored until use at -20 °C.

All DNA fragments, including PCR products, were analyzed with DNA standard ladders (New England Biolabs (NEB), Ipswich, MA, USA) on gels containing 1% (PCR products >1 kb) or 2% (PCR products <1 kb) UltraPure agarose (GIBCO-Invitrogen) in TAE buffer (GIBCO-Invitrogen) with 50 μ g/100 ml ethidium bromide (Sigma-Aldrich). DNA was visualized by brief exposure of the gels to UV light.

All DNA restriction digests were performed at 37 °C for 1-2 h using restriction endonucleases, corresponding 10x buffers, and 10x bovine serum albumin (BSA) from NEB according to NEB instructions.

All DNA ligation reactions were performed at 16 °C overnight using T4 DNA ligase and its corresponding 10x buffer from NEB according to NEB instructions.

PCR products, restriction-digest fragments or ligation products were purified from agarose gels using QIAGEN's QIAquick Gel Extraction Kit, or directly from reaction mixtures using QIAGEN's MinElute PCR Purification Kit according to the manufacturer's instructions.

pCDM8-derived vectors (77) were transformed into MC1061 *Escherichia coli* competent bacteria (Invitrogen) using the heat-shock method according to the manufacturer's instructions. Transformed bacteria were grown on Luria Bertani agar plates (LB agar plates, Sigma-Aldrich) containing 10 µg/ml tetracycline (Sigma-Aldrich) in 50% ethanol (Spectrum Chemicals, Gardena, CA, USA) and 30 µg/ml ampicillin (Sigma-Aldrich) at 37 °C for 24 h. Colonies were amplified for screening or DNA preparation by inoculating Luria Bertani broth (LB broth, Sigma-Aldrich) containing 20 µg/ml tetracycline in 50% ethanol and 30 µg/ml ampicillin, and shaking the cultures at 225 rpm overnight at 37 °C. Cultures for medium-scale, large-scale or ultra-large scale plasmid DNA preparation were then boosted with an equal volume of LB/tetracycline/ampicillin and 1/100th vol. 1 M glucose (Sigma-Aldrich), and grown for an additional 4, 6, and 10 h, respectively.

All other vectors (pCR2.1, pcDNA3.1, pCAGGS) were transformed into DH5α *Escherichia coli* competent bacteria (GIBCO-Invitrogen) using the heat-shock method according to the manufacturer's instructions. Transformed bacteria were grown on LB agar plates containing 30 µg/ml ampicillin at 37 °C overnight. Colonies were amplified for screening or DNA preparation by inoculating LB containing 30 µg/ml ampicillin and shaking the cultures at 225 rpm overnight at 37 °C.

Small-scale (< 20 µg) and medium scale (20-100 µg) plasmid DNA purification was performed with QIAGEN's QIAprep Spin Miniprep Kit and QIAfilter Plasmid Midi Kit, respectively, according to the manufacturer's instructions. Large-scale (100 µg - 2.5 mg) and ultra-large scale (2.5-10 mg) plasmid DNA purification was performed with Invitrogen's PureLink HiPure Plasmid FP (Filter and Precipitator) Maxiprep Kit and QIAGEN's QIAfilter Plasmid Giga Kit, respectively, according to the manufacturers' instructions.

DNA plasmid inserts were sequenced routinely before use by Retrogen, San Diego, CA, USA, using the company's submission instructions. For sequencing the coding sequences of pCDM8-based vectors, oligomers ϕ f (CTCACCTGCGGTGCCAGCTG) and ϕ b (TAGCCTGTGCCTGCCAGAGCCT) were sent to the company together with template DNA at the requested concentration. For sequencing the coding sequences of pCR2.1-based vectors, pcr2.1 seqfor (CAGGAAACAGCTATGAC) and pcr2.1 seqrev (TACGACTCACTATAGGGCGAATTG) were sent. Sequence analyses, oligomer and plasmid design, and sequence alignments were performed using the Lasergene Software Package (DNASar, Madison, WI, USA).

6.2.2 Construction of Lake Victoria marburgvirus isolate Musoke GP₁-Fc

The Lake Victoria marburgvirus isolate Musoke (MARV-Mus) open reading frame (ORF) encoding GP₁ lacking its signal sequence (amino-acid residues 17-432) was synthesized and amplified by *de novo* recursive PCR *in vitro* (218) (Figure 6-1). The reaction was set up using the following overlapping DNA oligomers, which are based on the MARV-Mus GP₁ protein sequence (GenBank accession number [CAA78117](#)) and which are codon-optimized for expression in mammalian cells according to a proprietary algorithm developed by Michael R. Farzan:

Forward oligomers:

mbg1 (TTCCGTGCTAGCGAAGAACCTGCCATCCTCGAGAT)
 mbg2 (CGCCAGCAACAACCAGCCGAGAACGTGGACAGCGTGTGCAGCGGCACCTTGCAGAAGACCGAGGACGT)
 mbg3 (GCACCTCATGGGCTTACCCTGTCCGGCCAGAAGGTGGCCGACAGCCCGCTGGAGGCCTCCAAGCGCTG)
 mbg4 (GGCCTTCCGGACCGGCGTGC CGCCGAAGAACGTGGAGTACACCGAGGGCGAGGAGGCCAAGACCTGCTA)
 mbg5 (CAACATCAGCGTGACCGACCCGTCGGCAAGAGCCTGCTCCTGGACCCGCCACCAACATCCGCGACTA)
 mbg6 (CCCGAAGTGCAAGACCATCCACCACATCCAGGGCCAGAACCCGCACGCCAGGGCATCGCCCTGCACCT)
 mbg7 (CTGGGGCGCCTTCTTCTCTACGACCGGATCGCCTCCACCACGATGTACCGCGGCAAGGTGTTCAACGA)
 mbg8 (GGGCAACATCGCCGCGATGATCGTGAACAAGACCGTGACACAAGATGATCTTCAGCCGCGCAGGGCCAGGG)
 mbg9 (CTACAGGCACATGAACCTGACCTCCACCAACAAGTACTGGACCAGCTCCAACGGCACCCAGACCAACGA)
 mbg10 (CACCGGTGCTTTCGGCGCCCTCCAAGAGTACAACAGCACCAAGAACCAGACCTGCGCGCCCTCCAAGAT)
 mbg11 (CCCGCCGCTCTGCCACCGCCCGGCCGAGATCAAGCTCACCAGCACGCCACCGACGCCACCAAGCT)
 mbg12 (GAACACCACGGACCCGTCAGCGACGACGAGGACCTCGCCACCTCCGGCAGCGGGTCCGGCGAGCGCGA)
 mbg13 (GCCGCACACCACGACGCGCGTGAACAAGCAGGGCCTGTCCAGCACCATGCCGCCACGCGGAGCCC)

mbg14 (GCAGCCCTCCACGCCGCAACAGGGCGGCAACAACACCAACCACAGCCAGGACGCCGTGACCGAGCTCGA)
 mbg15 (CAAGAACAACACCACCGCCAGCCAGCATGCCGCCGACAAACACCACGACCATCTCCACCAACAACAC)
 mbg16 (CAGCAAGCACAACCTTCTCCACCCTGAGCGCGCCGCTGCAGAACACCACGAACGACAACACCCAGTCCAC)
 mbg17 (CATCACCGAGAACGAGCAGACCAGCGCGCCCTCCATCACACGCTGCCGCCACCGGCAACCCGACCAC)
 mbg18 (GGCCAAGAGCACCTCCAGCAAGAAGGGCCCGGCCACCACGGCGCCCAACACCACGAACGAGCACTTAC)
 mbg19 (CTCGCCGCCGCCACGCCCTCGTCGACCGCCAGCACCTCGTGTACTTCCGCGGCGCGGATCCCGAGGG)

Reverse oligomers:

mbg20 (CCCTCGGGATCCCGCGCCGCGGAAGTACACGAGGTGC)
 mbg21 (TGGGCGGTCGACGAGGGCGTGGGCGGCGGCGAGGTGAAGTGCTCGTTCTGTTGGGCGCCGTGGTG)
 mbg22 (GCCGGGCCCTTCTTGCTGGAGGTGCTCTTGGCCGTGGTCCGGTTGCCGGTGGGCGGCAGCGTGGTGATG)
 mbg23 (GAGGGCGCGCTGGTCTGCTCGTTCTCGGTGATGGTGGACTGGGTGTTGTCGTTCTGGTGTCTTGCAGC)
 mbg24 (GGCGCGCTCAGGGTGGAGAAGTTGTGCTTGTGTTGTTGGTGGAGATGGTCTGGTGTGTTGTGCGGC)
 mbg25 (GGCATGCTGGGCTGGGCGGTGGTGTGTTCTTGTGTCAGCTCGGTCACGGCGTCCGGCTGTGGTTGGTG)
 mbg26 (TTGTTGCCGCCCTGTTGCGGCGTGGAGGGCTGCGGGCTCGGCGTGGGCGGCATGGTGTGGACAGGCCC)
 mbg27 (TGCTTGGTACGGCGTCTGCTGGTGGTGTGCGGCTCGGCTCGCCGGACCCGCTGCCGGAGGTGGCGAGG)
 mbg28 (TCCTCGTCTGCTGGACGGGTCCGTGGTGTTCAGCTTGGTGGCGTCCGTGGGCGTGTGGTGGAGCTTG)
 mbg29 (ATCTCGGGCCGGGCGGTGGGAGAGGCGGCGGGATCTTGGAGGGCGCGCAGGTCTGGTTCTTGGTGTCTG)
 mbg30 (TTGTACTCTTGGAGGGCGCCGAAGCAGCCGGTGTCTGTTGGTCTGGGTGCCGTTGGAGCTGGTCCAGTAC)
 mbg31 (TTGTTGGTGGAGGTGAGGTTTCATGTGCCTGTAGCCCTGGCCCTGCCGGCTGAAGATCATCTTGTGCAGC)
 mbg32 (GTCTTGTTCACGATCATCGCGGCGATGTTGCCCTCGGTGAACACCTTGCCGCGGTACATCGTGGTGGAG)
 mbg33 (GCGATCCGGTCTGATAGGAAGAAGGCGCCCAAGAGGTGCAGGGCGATGCCCTGGGCGTGGCGGTTCTGG)
 mbg34 (CCCTGGATGTGGTGGATGGTCTTGCACCTCGGGTAGTCCGGATGTTGGTGGGCGGTTCCAGGAGCAGG)
 mbg35 (CTCTTGGCCGACGGGTCCGTACGCTGATGTTGTAGCAGGTCTTGGCCTCCTCGCCCTCGGTGTACTCC)
 mbg36 (ACGTTCTTGGGCGGCACGCCGGTCCGGAAGGCCAGCGCTTGGAGGCCTCCAGCGGGCTGTGGCCACC)
 mbg37 (TTCTGGCCGGACAGGGTGAAGCCCATGAGGTGCACGTCTCGGTCTTCTGCAAGGTGCCGCTGCACACG)
 mbg38 (CTGTCCACGTTCTGCGGCTGGTTGTTGCTGGCGATCTCGAGGATGGGACAGGTTCTTGCTAGCACGGAA)

The inner oligomers (mbg2–mbg19, mbg21–mbg38) were diluted in a master mix (mbg master mix) to a final concentration of 0.2 pmol/μl each. The PCR was performed after mixing

36 μl water

5 μl 10x cloned pfuTurbo buffer

5 μl 10x dNTP mix

1 μl mbg master mix

1 μl oligomer_{mbg1}

1 μ l oligomer _{mbg20}

1 μ l cloned pfuTurbo

using the following cycle conditions:

3 min. 94 °C

35x (30 s 94 °C, 2 min. 70 °C) [two-step PCR]

7 min. 72 °C

The main PCR product (1,278 bp), containing unique *NheI* (GCTAGC) and *BamHI* (GGATCC) restriction sites at the 5' and 3' ends of the MARV-Mus GP₁ ORF, respectively, was detected by agarose-gel electrophoresis, excised, and purified. The product was then digested with *NheI* and *BamHI*, purified again, ligated into a previously described *NheI*- and *BamHI*-digested pCDM8-derived expression vector (77) encoding the human CD5 signal sequence (MPMGSLQPLATLYLLGMLVASVLA) upstream of the *NheI* site and the Fc region of human immunoglobulin G₁ (IgG₁) downstream of the *BamHI* site, and transformed (MARV-Mus 17-432-Fc).

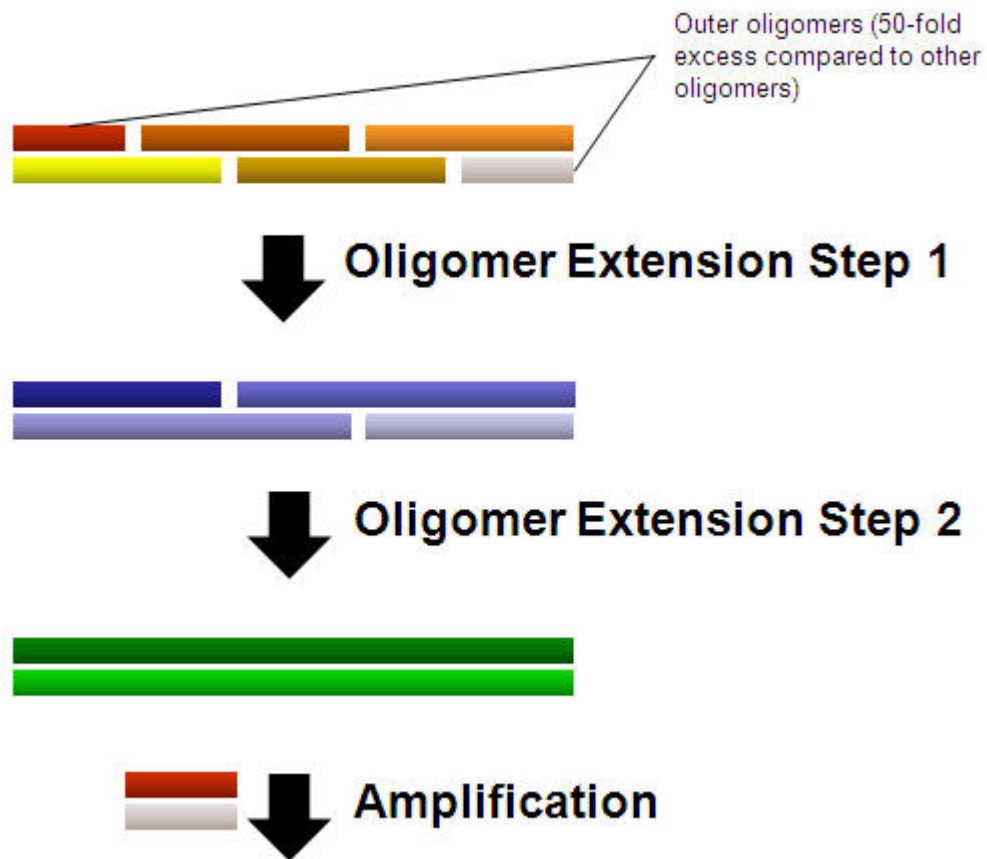


Figure 6-1. Principle of recursive polymerase-chain reaction for the *in vitro* synthesis of open reading frames or genes

Overlapping oligomers, covering the entire sequence of the desired open reading frame, are designed and synthesized. All oligomers, with the exception of the most 5' and 3' ones, are then mixed at equimolar concentrations. The 5' and 3' oligomers are added in 50-fold excess. During the polymerase-chain reaction (PCR), oligomers bind to their overlapping partners and become extended (Oligomer Extension Step 1). The resulting extended oligomers again hybridize and become extended, until the full-length open reading frame has been synthesized (Oligomer Extension Step 2). The open reading frame is then amplified using the 5' and 3' excess oligomers as primers

6.2.3 Construction of Lake Victoria marburgvirus isolate Musoke spike protein GP_{1,2}-C9

The MARV-Mus ORF encoding the spike protein GP_{1,2} lacking its N-terminal signal sequence (amino-acid residues 17-681) but containing a C-terminal C9 tag (amino-acid sequence TETSQVAPA derived from the rhodopsin C-terminus) followed by a stop codon was constructed by synthesizing and amplifying the ORF encoding GP₂ by *de novo* recursive PCR *in vitro* (218) (Figure 6-1). The reaction was set up with the following overlapping DNA oligomers, which are based on the MARV-Mus GP₂ protein sequence (GenBank accession number [CAA78117](#)) and which are codon-optimized for expression in mammalian cells according to a proprietary algorithm developed by Michael R. Farzan:

Forward oligomers:

mbg41 (ACGCCCTCGTCTGACCGCCCAGCACCTCGTGTACTT)
 mbg42 (CCGCCGGAAGCGCAGCATCCTGTGGCGGGAGGGCGACATGTTCCCGTTCCCTCGACGGCCTGATCAACGCGCCC)
 mbg43 (ATCGACTTCGACCCGGTGCCCAACACCAAGACCATCTTCGACGAGTCCAGCTCCAGCGGCGCTCCGCGGAGG)
 mbg44 (AAGACCAGCACGCCTCGCCCAACATCTCCCTCACCTGAGCTACTTCCCGAACATCAACGAGAACACCGCCTA)
 mbg45 (CTCCGGCGGAGAACGAGAACGACTGCGACGCGGAGCTCCGCATCTGGAGCGTGCAGGAGGACGATCTGGCCGCG)
 mbg46 (GGCCTCTCCTGGATTCCGTTCTTCGGCCCGGCATCGAGGGCCTGTACACCGCCGTGCTCATCAAGAACCAGA)
 mbg47 (ACAACCTGGTGTGCCGGCTCCGCGGCTGGCCAACCAGACCGCCAAGAGCCTCGAGCTGCTCCTGCGCGTGAC)
 mbg48 (CACGGAGGAGCGGACCTTCTCCCTCATCAACCGCCACGCCATCGACTTCCTGCTCACCCGGTGGGGCGGGACC)
 mbg49 (TGCAAGGTGCTGGGCCGGACTGCTGTATCGGCATCGAGGACCTCAGCAAGAACATCTCCGAGCAGATCGACC)
 mbg50 (AGATCAAGAAGGACGAGCAGAAGGAGGGCACCGCTGGGGCCTGGGCGGGAAGTGGTGGACCAGCGACTGGGG)
 mbg51 (CGTGCTCACCAACCTGGGCATCCTCTGCTCCTGTCCATCGCCGTGCTCATCGCCCTGAGCTGCATCTGCCGC)
 mbg52 (ATCTTCACCAAGTACATCGGCGGTACCGAGACCTCCAGGTGGCGCCCGCCTAGGGCGCGGATCCCGAGGGTC)

Reverse oligomers:

mbg53 (GACCCTCGGGATCCGCGCCCTAGGCGGGCGCCACC)
 mbg54 (TGGGAGGTCTCGGTACCGCCGATGTACTTGGTGAAGATGCGGCAGATGCAGCTCAGGGCGATGAGCACGGCGA)
 mbg55 (TGGACAGGAGCAGGAGGATGCCAGGTTGGTGAAGCAGCCCAAGTCCGCTGGTCCACCCTTCCCGCCAGGCC)
 mbg56 (CCAGCCGGTGCCTCTCTTCTGCTCGTCTTCTTGATCTGGTTCGATCTGCTCGGAGATGTTCTTGCTGAGGTCC)
 mbg57 (TCGATGCCGATACAGCAGTCCGGGCCAGCACCTTGCAGTCCCGCCACCGGGTGGAGCAGGAAGTCGATGG)
 mbg58 (CGTGGCGGTTGATGAGGGAGAAGGTCGCTCCTCCGTGGTTCAGCGCAGGAGCAGCTCGAGGCTCTTGGCGGT)
 mbg59 (CTGGTTGGCCAGCCGCGGAGCCGGCACACCAGGTTGTTCTGGTTCTTGATGAGCACGGCGGTGTACAGGCC)
 mbg60 (TCGATGCCCGGCCGAAGAACGGAATCCAGGAGAGGCCCGCGCCAGATCGTCTCCTGTCAGCTCCAGATGC)
 mbg61 (GGAGCTCGGCGTCGCAGTCGTTCTCGTTCGCGGAGTAGGCGGTGTTCTCGTTGATGTTCCGGGAAGTAGCT)

mbg62 (CAGGGTGAGGGAGATGTTGGGCGAGGCGTGCTGGTCTTCTCGGGCGGAGGCGCCGCTGGAGCTGGACTCGTCCG)
 mbg63 (AAGATGGTCTTGGTGTGGGCACCGGGTCGAAGTCGATGGGCGCGTTGATCAGGCCGTCGAGGAACGGGAACA)
 mbg64 (TGTCGCCCTCCCGCCACAGGATGCTGCGCTTCCGGCGGAAGTACACGAGGTGCTGGGCGGTCGACGAGGGCGT)

The inner oligomers (mbg42–mbg52, mbg54–mbg64) were diluted in a master mix (mbg master mix 2) to a final concentration of 0.2 pmol/μl each. The PCR was performed after mixing

36 μl water
 5 μl 10x cloned pfuTurbo buffer
 5 μl 10x dNTP mix
 1 μl mbg master mix 2
 1 μl oligomer mbg41
 1 μl oligomer mbg53
 1 μl cloned pfuTurbo

using the following cycle conditions:

3 min. 94 °C
 35x (30 s 94 °C, 1 min. 70 °C) [two-step PCR]
 7 min. 72 °C

The main PCR product (911 bp), containing unique *SalI* (GTCGAC) and *BamHI* restriction sites at the 5' and 3' ends of the MARV-Mus GP₂-C9 ORF, respectively, was detected by agarose-gel electrophoresis, excised, purified. The product was then digested with *SalI* and *BamHI*, purified again, ligated into the *SalI*- and *BamHI*-digested pCDM8(MARV-Mus-17-432-Fc) vector, and transformed (MARV-Mus 17-681-C9).

6.2.4 Construction of Lake Victoria marburgvirus isolate Musoke GP₁-Fc truncation variants

The plasmids encoding N-terminal or C-terminal truncation variants of MARV-Mus 17-432-Fc were created by inverse PCR (Figures 6-2 and 6-3). The plasmids encoding C-terminal truncation variants 17-308-Fc, 17-265-Fc, 17-230-Fc, 17-188-Fc, 17-167-Fc, and 17-134-Fc were created using oligomer `mucnegforward`

(CTATGTACGGATCCCGAGGGTGAGTACTAAGCT) and the following oligomers, respectively:

17-308-Fc: `mucnegrev2` (TGCAATGGATCCGCGCCGCCCTGTTGCGGCGTGGAGGGCTGCGGGCT)

17-265-Fc: `mucnegrev1` (TGCAATGGATCCGCGCCGTCCTCGTCGTCGCTGGACGGGTCCGTGGT)

17-230-Fc: `mucnegrev1plus1` (TGCAATGGATCCGCGCCCTTGAGGGCGCGCAGGTCTGGTTCTTGGT)

17-188-Fc: `mucnegrev1plus2` (TGCAATGGATCCGCGCCGTCCTGTAGCCCTGGCCCTGCCGGCTGAA)

17-167-Fc: `mucnegrev1plus3` (TGCAATGGATCCGCGCCCGCGCGATGTTGCCCTCGGTGAACACCTT)

17-134-Fc: `mucnegrev1plus4` (TGCAATGGATCCGCGCCGCCCTGGGCGTGCGGTTCTGGCCCTGGAT)

Reactions were performed after mixing

x µl water to reach a total volume of 50 µl

5 µl 10x cloned pfuTurbo buffer

5 µl 10x dNTP mix

0.1 µg template plasmid (MARV-Mus 17-432-Fc)

1 µl oligomer `mucnegforward`

1 µl oligomer `mucnegrev1`, `mucnegrev2`, `mucnegrev1plus1`, `mucnegrev1plus2`,

`mucnegrev1plus3` OR `mucnegrev1plus4`

1 µl cloned pfuTurbo

using the following cycle conditions:

3 min. 94 °C

30x (30 s 94 °C, 7 min. 70 °C) [two-step PCR]

7 min. 72 °C

To destroy template (methylated) DNA, the reaction mix was incubated with 2 µl *DpnI* (NEB) for 2 h at 37 °C. The (unmethylated) PCR product was detected by agarose-gel electrophoresis, excised, purified, digested with *BamHI*, purified again, ligated, and transformed.

The plasmids encoding N-terminal truncation variants 38-432-Fc, 61-432-Fc, and 87-432-Fc were created using oligomer *firstcrev* (CAAGTTAGCTAGCACGGAAGCGACCAGCATCCC) and the following oligomers, respectively:

38-432-Fc: *firstcmarvforward* (CTATGTACGCTAGCGAGCGGCACCTTGCAGAAGACCGAGGACGTG)

61-432-Fc: *firstcplus1marvforward* (CTATGTACGCTAGCGGACAGCCCGCTGGAGGCCTCCAAGCGCTGG)

87-432-Fc: *firstcplus2marvforward* (CTATGTACGCTAGCGGAGGAGGCCAAGACCTGCTACAACATCAGC)

Reactions were performed after mixing

x µl water to reach a total volume of 50 µl

5 µl 10x cloned pfuTurbo buffer

5 µl 10x dNTP mix

0.1 µg template plasmid (MARV-Mus 17-432-Fc)

1 µl oligomer *firstcrev*

1 µl oligomer *firstcmarvforward*, *firstcplus1marvforward* **OR** *firstcplus2marvforward*

1 µl cloned pfuTurbo

using the following cycle conditions:

3 min. 94 °C

30x (30 s 94 °C, 7 min. 70 °C) [two-step PCR]

7 min. 72 °C

To destroy (methylated) template DNA, the reaction mix was incubated with 2 μ l *DpnI* for 2 h at 37 °C. The (unmethylated) PCR product was detected by agarose-gel electrophoresis, excised, purified, digested with *NheI*, purified again, ligated, and transformed.

The plasmids encoding N- and C-terminal truncations (38-308-Fc, 38-265-Fc, 38-230-Fc, 38-188-Fc, 38-167-Fc, 38-134-Fc, 61-308-Fc, 61-265-Fc, 61-230-Fc, 61-188-Fc, 61-167-Fc, 61-134-Fc, 87-308-Fc, 87-265-Fc, 87-230-Fc, 87-188-Fc, 87-167-Fc, 87-134-Fc) were created by using the synthesized plasmids described above as templates and subjecting them to inverse PCR using the various oligomers and PCR conditions described above.

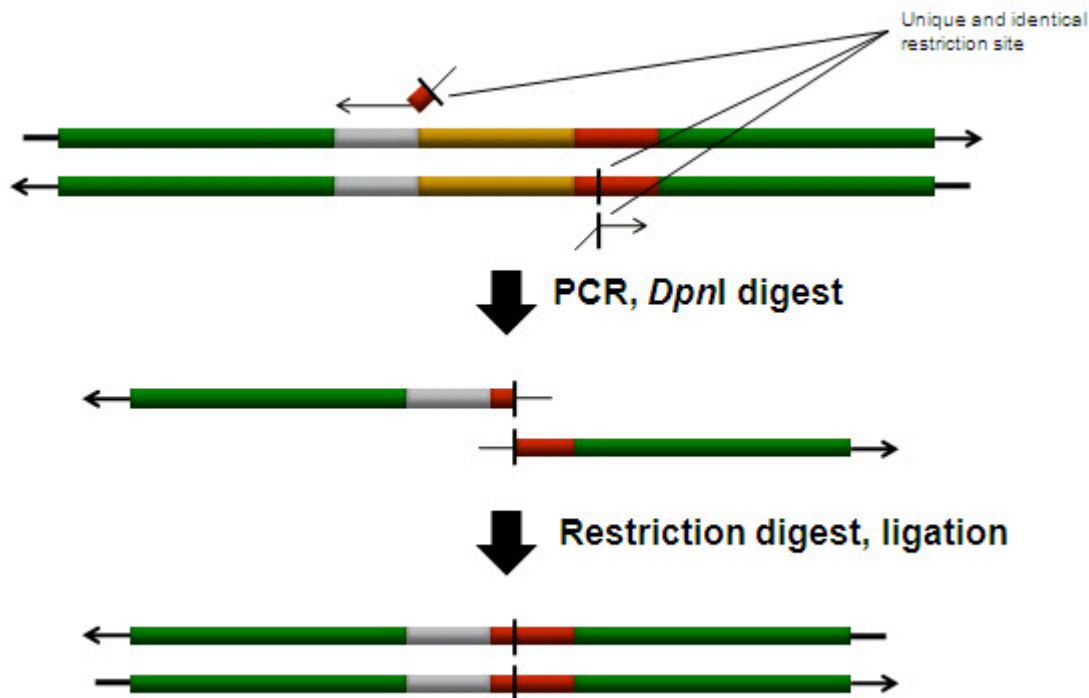


Figure 6-2. Principle of inverse polymerase-chain reaction for the creation of genes encoding C-terminal truncation variants of filoviral Fc fusion proteins

An oligomer is designed that binds to the utmost C-terminal region of the template open reading frame (red) and the downstream region of the vector (green), containing a unique restriction site (in this case *Bam*HI in oligomer *mucnegforward*). A second oligomer is designed that binds to the specific region within the open reading frame that encodes the C terminus of the envisioned truncation variant (grey), ending with a sequence that complements the restriction site-containing region of the first oligomer. After polymerase-chain reaction (PCR), template (methylated) DNA is digested with *Dpn*I, the linear fragments are digested with the restriction enzyme, and the plasmid is circularized by ligation

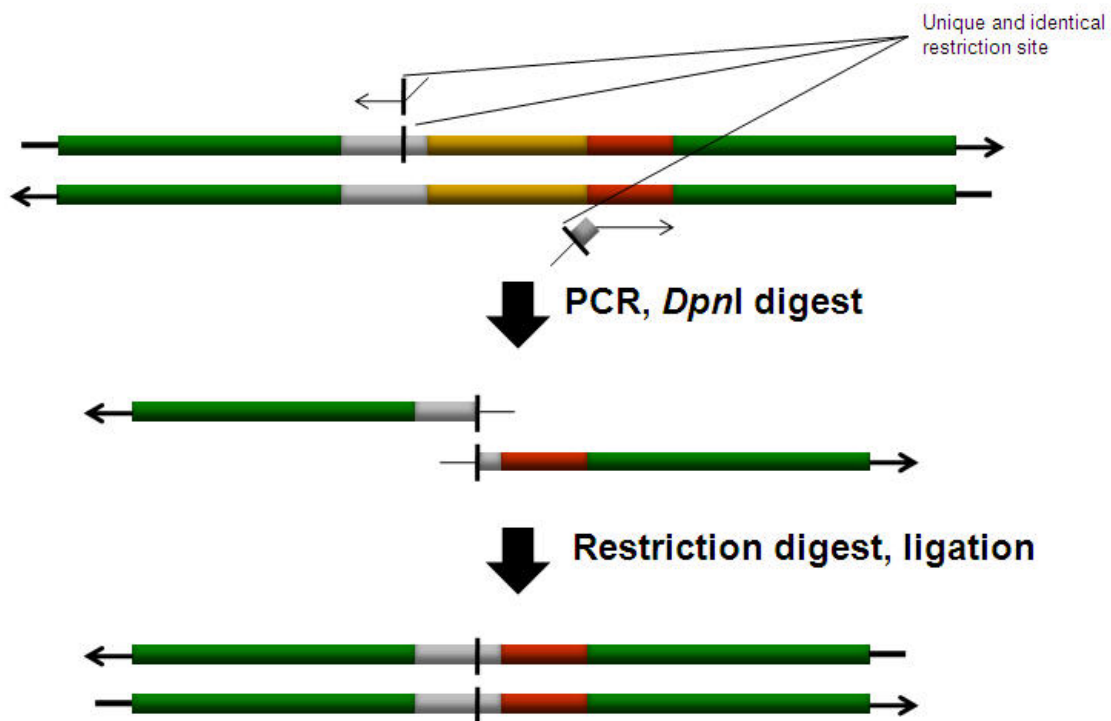


Figure 6-3. Principle of inverse polymerase-chain reaction for the creation of genes encoding N-terminal truncation variants of filoviral Fc fusion proteins

An oligomer is designed that binds to the utmost N-terminal region of the template open reading frame (white) and the upstream region of the vector (green), containing a unique restriction site (in this case *NheI* in oligomer *firstcrev*). A second oligomer is designed that binds to the specific region within the open reading frame that encodes the N-terminus of the envisioned truncation variant (red), ending with a sequence that complements the restriction site-containing region of the first oligomer. After polymerase-chain reaction (PCR), template (methylated) DNA is digested with *DpnI*, the linear fragments are digested with the restriction enzyme, and the plasmid is circularized by ligation

6.2.5 Construction of Lake Victoria marburgvirus isolate Musoke spike protein GP_{1,2}-C9 containing GP₁-internal deletions

The plasmids encoding deletions within the GP₁ region of MARV-Mus spike protein GP_{1,2}-C9 (17-681-C9) were created by inverse PCR (Figures 6-2 and 6-3) using oligomer *marvps del1* (ATGTACACATGTTCCCCTCCCTCGACGGCCTG) and the following oligomers, respectively:

MARV-Mus 17-681_{Δ266-432}-C9:

marvps265 (TGCAATACATGTCGCCCTCCCGCCACAGGATGCTGCGCTTCCGGCGGTCCTCGTCGCTGGACGGGTCCGTGGT)

MARV-Mus 17-681_{Δ231-432}-C9:

marvps230 (TGCAATACATGTCGCCCTCCCGCCACAGGATGCTGCGCTTCCGGCGGTTGGAGGGCGCGCAGGTCTGGTTCTTGGT)

MARV-Mus 17-681_{Δ189-432}-C9:

marvps188 (TGCAATACATGTCGCCCTCCCGCCACAGGATGCTGCGCTTCCGGCGGTCCTGTAGCCCTGGCCCTGCCGGCTGAA)

Reactions were performed after mixing

x μl water to reach a total volume of 50 μl

5 μl 10x cloned pfuTurbo buffer

5 μl 10x dNTP mix

0.1 μg template plasmid (MARV-Mus-17-681-C9)

1 μl oligomer *marvps265*, *marvps230* OR *marvps188*

1 μl oligomer *marvps del1*

1 μl cloned pfuTurbo

using the following cycle conditions:

3 min. 94 °C

30x (30 s 94 °C, 7 min. 70 °C) [two-step PCR]

7 min. 72 °C

To destroy template (methylated) DNA, the reaction mix was incubated with 2 μ l *DpnI* (NEB) for 2 h at 37 °C. The (unmethylated) PCR product was detected by agarose-gel electrophoresis, excised, purified, digested with *PciI* (ACATGT), purified again, ligated, and transformed.

6.2.6 Construction of Lake Victoria marburgvirus isolate Angola GP₁-Fc truncation variants

The amino-acid sequence of Lake Victoria marburgvirus isolate Angola (MARV-Ang) spike protein GP_{1,2} was provided by Dr. Stuart T. Nichol and his team at the Centers for Disease Control and Prevention (CDC) in Atlanta, GA, USA, and has since been published (269). In the GP₁ area of interest to the research described in this dissertation, this sequence differs in only one position from that of MARV-Mus (T₇₄→A). The plasmids encoding MARV-Ang 38-188-Fc, 38-167-Fc, 61-188-Fc, and 61-167-Fc were created by site-directed mutagenesis using the QuickChange method (Stratagene) to mutate the codon for threonine 74 to a codon for alanine. Briefly, reactions were performed after mixing

x μ l water to reach a total volume of 50 μ l

5 μ l 10x cloned pfuTurbo buffer

5 μ l 10x dNTP mix

0.1 μ g template plasmid (MARV-Mus-38-188-Fc, 38-167-Fc, 61-188-Fc or 61-167-Fc)

1 μ l oligomer Angola_f (CAAGCGCTGGGCCTTCCGGGCCGGCGTGCCGCCCAAGAAC)

1 μ l oligomer Angola_b (GTTCTTGGGCGGCACGCCGCCCGGAAGGCCAGCGCTTG)

1 μ l cloned pfuTurbo

using the following cycle conditions:

3 min. 94 °C

30x (30 s 94 °C, 30 s 65 °C, 7 min. 70 °C) [three-step PCR]

7 min. 72 °C

To destroy (methylated) template DNA, the reaction mixes were incubated with 2 μ l *DpnI* for 2 h at 37 °C. The (unmethylated) PCR products were detected by agarose-gel electrophoresis, excised, purified, and transformed.

6.2.7 Construction of Lake Victoria marburgvirus isolate Musoke receptor-binding region mutants

The plasmids encoding MARV-Mus 38-188N94A-Fc, and 38-188N171A-Fc were created by site-directed mutagenesis using the QuickChange method (Stratagene) to mutate the codon for asparagine 94 or asparagine 171 to codons for alanine. Briefly, reactions were performed after mixing

x μ l water to reach a total volume of 50 μ l
 5 μ l 10x cloned pfuTurbo buffer
 5 μ l 10x dNTP mix
 0.1 μ g template plasmid (MARV-Mus 38-188-Fc)
 1 μ l cloned pfuTurbo

with 1 μ l oligomer of each of the following oligomers:

MARV-Mus 38-188N94A:

38-188N94Af (GAGGCCAAGACCTGCTACGCCATCAGCGTGACCGACCCG)
 38-188N94Ab (CGGGTCGGTCACGCTGATGGCGTAGCAGGTCTTGGCCTC)

MARV-Mus 38-188N171A:

38-188N171Af (ATCGCCGCGATGATCGTGGCCAAGACCGTGACACAAGATG)
 38-188N171Ab (CATCTTGTGCACGGTCTTGGCCACGATCATCGCGGCGAT)

using the following cycle conditions:

3 min. 94 °C

30x (30 s 94 °C, 30 s 65 °C, 6 min. 70 °C) [three-step PCR]

7 min. 72 °C

To destroy template DNA, the reaction mixes were incubated with 2 μ l *DpnI* for 2 h at 37 °C. The PCR products were detected by agarose-gel electrophoresis, excised, purified, and transformed.

The plasmid encoding MARV-Mus 38-188N94A,N171A-Fc was synthesized by following the protocol above using the plasmid encoding MARV-Mus 38-188N94A-Fc as template and oligomers 38-188N171Af and 38-188N171Ab.

6.2.8 Construction of mucin-like domain-deleted Zaire ebolavirus isolate Mayinga GP₁

The Zaire ebolavirus isolate Mayinga (ZEBOV-May) ORF encoding GP₁ lacking its signal sequence and its C-terminal mucin-like domain (MLD) was synthesized (amino-acid residues 33-308) and amplified by *de novo* recursive PCR *in vitro* (218) (Figure 6-1). The reaction was set up using the following overlapping DNA oligomers, which are based on the ZEBOV-May GP₁ protein sequence (GenBank accession number [NP_066246](#)) and which are codon-optimized for expression in mammalian cells according to a proprietary algorithm developed by Michael R. Farzan:

Forward oligomers:

- Em1 (ATTTCCGTGCTAGCGCGCGACCGTTCA)
- Em2 (AGCGCACCAGCTTCTTTCTGTGGGTGATCATTCTCTCCAGCGGACCTTCTCCATCCCGCTGGGCGTGATCCACA)
- Em3 (ACAGCACCTCCAGGTGTCGAGGTGGACAAGCTGGTGTGCCGCGACAAGCTCAGCTCCACCAACCAGCTGCCGA)
- Em4 (GCGTGGGCTCAACCTGGAGGGCAACGGCGTGGCCACCGACGTGCCCTCCGCCACCAAGCGCTGGGGCTTCCGGA)
- Em5 (GCGGCGTGCCGCCCAAGGTGGTCAACTACGAGGCCGCGAGTGGGCCGAGAAGTCTACAACCTCGAGATCAAGA)
- Em6 (AACCCGACGGCTCCGAGTGCCTGCCCGCCGCGCCGACGGCATCCGCGGCTTCCCGAGGTGCCGCTACGTGCACA)
- Em7 (AAGTCAGCGGCACCGGGCCCTGCGCCGGCGACTTCGCCTTCCACAAGGAGGGCGCCTTCTTTCTCTACGACCGGC)

Em8 (TGGCCTCCACCCTGATCTACCGCGGCACCACGTTTCGCCGAGGGCGTGGTTCGCCTTCCTCATCCTGCCGCAAGCCA)
 Em9 (AGAAAGACTTCTTTAGCTCCCACCCGCTCCGGGAGCCCGTGAACGCCACCGAGGCCGAGCTCCGGCTACTATA)
 Em10 (GCACCACGATCCGCTACCAGGCCACCCGGTTCGGCACCACGAGACCAGTACCTGTTCGAGGTGGACAACCTCA)
 Em11 (CCTACGTGCAGCTGGAGTCCCAGTTCACGCCGAGTTCCTCCTGCAGCTCAACGAGACCATCTACACCAGCGGCA)
 Em12 (AGCGCTCCAACACGACCGGCAAGCTGATCTGGAAGGTGAACCCGAGATCGACACCACGATCGGCGAGTGGCCT)
 Em13 (TCTGGGAGACCAAGAAAACCTCACCCGGAAGATCCGCAGCGAAGAGCTGTCCTTCGGCGCGGATCCCGAGGTA)

Reverse oligomers:

Em14 (TACCCTCGGGATCCGCGCCGAAGGACAG)
 Em15 (CTCTTCGCTGCGGATCTTCCGGGTGAGGTTTTTCTTGGTCTCCAGAAGGCCACTCGCCGATCGTGGTGTTCGAT)
 Em16 (CTCCGGGTTACCTTCCAGATCAGCTTGCCGGTTCGTGTTGGAGCGCTTGCCGCTGGTGTAGATGGTCTCGTTGAG)
 Em17 (CTGCAGGAGAACTGCGGCGTGAACCCGGACTCCAGTGCACGTAGGTGAGGTTGTCCACCTCGAACAGGTACTC)
 Em18 (GGTCTCGTTGGTGC CGAAGCCGGTGGCCTGGTAGCGGATCGTGGTGTATAGTAGCCGGAGCTCGGGTCTCCGGT)
 Em19 (GGCGTTCACGGGCTCCCGGAGCGGGTGGGAGCTAAAGAAGTCTTCTTGGCTTGCCGAGGATGAGGAAGGCGAC)
 Em20 (CACGCCCTCGGCGAACGTGGTGCCCGGTAGATCACGGTGGAGGCCAGCCGGTTCGTAGAGAAAGAAGGCGCCCTC)
 Em21 (CTTGTGGAAGGCGAAGTCGCCGGCGCAGGGCCCGGTGCCGCTGACTTGTGTGCACGTAGCGGCACCTCGGGAAGCC)
 Em22 (GCGGATGCCGTCGGGCGCGGGCAGGCACTCGGAGCCGTCGGGTTCTTGATCTCGAGGTTGTAGCAGTTCTC)
 Em23 (GGCCACTCGCCGGCCTCGTAGTTGACCACCTTGGGCGGCACGCCGCTCCGGAAGCCCGAGCGCTTGGTGGCGGA)
 Em24 (GGGCACGTCCGGTGGCCACGCCGTTGCCCTCCAGGTTGAGGCCACGCTCCGCAGCTGGTTGGTGGAGCTGAGCTT)
 Em25 (GTCGCGGCACACCAGCTTGTCCACCTCGGACACCTGGAGGGTGTCTGTGTGGATCACGCCCGAGCGGGATGGAGAA)
 Em26 (GGTCCGCTGGAAGAGAAATGATCACCCACAGAAAGAAGCTGGTGCCTTGAACCGGTCCGCGCGCTAGCACGGAAT)

The inner oligomers (Em2-Em13, Em15-Em26) were diluted in a master mix (zebov master mix) to a final concentration of 0.2 pmol/ μ l each. The PCR was performed after mixing

36 μ l water

5 μ l 10x cloned pfuTurbo buffer

5 μ l 10x dNTP mix

1 μ l zebov master mix

1 μ l oligomer Em1

1 μ l oligomer Em14

1 μ l cloned pfuTurbo

using the following cycle conditions:

3 min. 94 °C
 35x (30 s 94 °C, 1 min. 70 °C) [two-step PCR]
 7 min. 72 °C

The main PCR product (928 bp), containing unique *NheI* and *BamHI* restriction sites at the 5' and 3' ends of the ZEBOV-May GP₁ 33-308 ORF, was detected by agarose-gel electrophoresis, excised, and purified. The product was then digested with *NheI* and *BamHI*, purified again, ligated into the *NheI*- and *BamHI*-digested pCDM8-derived expression vector (77), and transformed (ZEBOV-May 33-308-Fc).

6.2.9 Construction of Zaire ebolavirus isolate Mayinga GP₁-Fc truncation variants

Plasmids encoding N-terminal or C-terminal truncation variants of ZEBOV-May 33-308-Fc were created by inverse PCR (Figures 6-2 and 6-3). Plasmids encoding C-terminal truncation variants 33-267-Fc, 33-237-Fc, 33-201-Fc, 33-172-Fc, 33-156-Fc were created using oligomer *mucnegforward* (Chapter 6.2.4) and the following oligomers, respectively:

33-267-Fc: *mucnegplus1zebovrev* (TGCAATGGATCCGCGCCGGAGCGCTTGCCGCTGGTGTAGATGGTCTC)

33-237-Fc: *mucnegplus2zebovrev* (TGCAATGGATCCGCGCCGTCCACCTCGAACAGGTACTCGGTCTCGTT)

33-201-Fc: *maynplus1* (TGCAATGGATCCGCGCCCTCCCGGAGCGGGTGGGAGCTAAAGAAGTC)

33-172-Fc: *maynplus2* (TGCAATGGATCCGCGCCGCGGTAGATCACGGTGGAGGCCAGCCGGTC)

33-156-Fc: *maynplus3* (TGCAATGGATCCGCGCCCTCCTTGTGGAAGGCGAAGTCGCCGGCGCA)

Reactions were performed after mixing

x µl water to reach a total volume of 50 µl

5 µl 10x cloned pfuTurbo buffer

5 µl 10x dNTP mix

0.1 µg template plasmid (ZEBOV-May 33-308-Fc)

1 µl oligomer *mucnegforward*

1 μ l oligomer mucnegplus1zebovrev, mucnegplus2zebovrev, maynplus1, maynplus2 OR
maynplus3

1 μ l cloned pfuTurbo

using the following cycle conditions:

3 min. 94 °C

30x (30 s 94 °C, 6 min. 70 °C) [two-step PCR]

7 min. 72 °C

To destroy template (methylated) DNA, the reaction mix was incubated with 2 μ l *DpnI* for 2 h at 37 °C. The (unmethylated) PCR product was detected by agarose-gel electrophoresis, excised, purified, digested with *BamHI*, purified again, ligated, and transformed.

Plasmids encoding N-terminal truncation variants 54-308-Fc, 76-308-Fc, and 78-308-Fc, 100-308-Fc, and 149-308-Fc were created using oligomer *firstcrev* (Chapter 6.2.4) and the following oligomers, respectively:

54-308-Fc: *firstczebovforward* (CTATGTACGCTAGCGCGCGACAAGCTCAGCTCCACCAACCAGCTG)

76-308-Fc: *maycplus1* (CTATGTACGCTAGCGGCCACCGACGTGCCCTCCGCCACCAAGCGC)

78-308-Fc: *zebovc1plusforward* (CTATGTACGCTAGCGGACGTGCCCTCCGCCACCAAGCGCTGGGGC)

100-308-Fc: *zebovc2plusforward* (CTATGTACGCTAGCGGAGCCGGCGAGTGGGCCGAGAAGTGTCTAC)

149-308-Fc: *zebovc3plusforward* (CTATGTACGCTAGCGGGCGACTTCGCCTTCCACAAGGAGGGCGCC)

Reactions were performed after mixing

x μ l water to reach a total volume of 50 μ l

5 μ l 10x cloned pfuTurbo buffer

5 μ l 10x dNTP mix

0.1 μ g template plasmid (ZEBOV-May 33-308-Fc)

1 μ l oligomer firstczebovforward, maycplus1, zebovc1plusforward, zebovc2plusforward OR
zebovc3plusforward

1 μ l oligomer firstcrev

1 μ l cloned pfuTurbo

using the following cycle conditions:

3 min. 94 °C

30x (30 s 94 °C, 6 min. 70 °C) [two-step PCR]

7 min. 72 °C

To destroy (methylated) template DNA, the reaction mix was incubated with 2 μ l *DpnI* for 2 h at 37 °C. The (unmethylated) PCR product was detected by agarose-gel electrophoresis, excised, purified, digested with *NheI*, purified again, ligated, and transformed.

Plasmids encoding N- and C-terminal truncations (54-267-Fc, 54-237-Fc, 54-201-Fc, 54-172-Fc, 54-156-Fc, 76-201-Fc, 76-172-Fc, and 76-156-Fc) were created by using plasmids encoding the created truncation variants above as templates and subjecting them to inverse PCR using the appropriate oligomers and PCR conditions described above.

6.2.10 Construction of Zaire ebolavirus isolate Mayinga receptor-binding region mutants

Plasmids encoding ZEBOV-May 54-201F88A-Fc, 54-201F159A-Fc, 54-201G74A,V75A-Fc, and 54-201V96A,V97A-Fc were created by site-directed mutagenesis using the QuickChange method (Stratagene). Briefly, reactions were performed after mixing

x μ l water to reach a total volume of 50 μ l

5 μ l 10x cloned pfuTurbo buffer

5 μ l 10x dNTP mix

0.1 µg template plasmid (ZEBOV-May 54-201-Fc)

1 µl cloned pfuTurbo

with 1 µl oligomer of each of the following oligomers:

ZEBOV-May 54-201F88A-Fc:

54-201F88Af (ACCAAGCGCTGGGGCGCCCGAGCGGCGTGCCG)

54-201F88Ab (CGGCACGCCGCTCCGGGCGCCCGAGCGCTTGGT)

ZEBOV-May 54-201F159A-Fc:

54-201F159Af (CACAAGGAGGGCGCCGCCCTTCTCTACGACCGG)

54-201F159Ab (CCGGTCGTAGAGAAAGGCGGCCCTCCTTGTTG)

ZEBOV-May 54-201G74A,V75A-Fc:

54-201G74AV75Af (AACCTGGAGGGCAACGCCGCGCCACCGACGTGCC)

54-201G74AV75Ab (GGGCACGTCGGTGGCCGCGGCGTTGCCCTCCAGGTT)

ZEBOV-May 54-201V96A,V97A-Fc:

54-201V96AV97Af (GGCGTGCCGCCCAAGGCGGCCAACTACGAGGCCGGC)

54-201V96AV97Ab (GCCGGCCTCGTAGTTGGCCGCCTTGGGCGGCACGCC)

using the following cycle conditions:

3 min. 94 °C

30x (30 s 94 °C, 30 s 65 °C, 7 min. 70 °C) [three-step PCR]

7 min. 72 °C

To destroy template DNA, the reaction mixes were incubated with 2 µl *DpnI* for 2 h at 37 °C. The PCR products were detected by agarose-gel electrophoresis, excised, purified, and transformed.

6.2.11 Construction of Côte d'Ivoire, Reston, and Sudan ebolavirus receptor-binding regions

Non-codon-optimized ORFs encoding Côte d'Ivoire ebolavirus isolate Côte d'Ivoire (CIEBOV-CI) GP₁ residues 54-201, Reston ebolavirus isolate Pennsylvania (REBOV-Pen) GP₁ residues 55-202, and Sudan ebolavirus isolate Gulu (SEBOV-Gul) GP₁ residues 54-201 were cloned from GP_{1,2}-encoding template plasmids provided by Dr. M. Javad Aman at the United States Army Medical Research Institute of Infectious Diseases (USAMRIID), Fort Detrick, Frederick, MD, USA. The oligomers used for the reactions were designed according to deposited spike-protein gene sequences (GenBank accession numbers [Q66810](#), [NP_690583](#), and [AAU43887](#), respectively) and are listed below:

CIEBOV-CI 54-201-Fc:

CIEBOV_RBDf (CTATGTACGCTAGCGCGAGACAACTCTCTCAACT)
 CIEBOV_RBDb (TGCAATGTGGATCCGCGCCCTCATGCAATGGAGGAGACTG)

REBOV-Pen 55-202-Fc:

REBOV_RBDf (CTATGTACGCTAGCGCGGGACAACTGTCATCAACC)
 REBOV_RBDb (TGCAATGTGGATCCGCGCCTTCATGAGCTGGTGTAGCCTT)

SEBOV-Gul 54-201-Fc:

SEBOVGul_RBDf (CTATGTACGCTAGCGAAGGATCATCTTGATCTACT)
 SEBOVGul_RBDb (TGCAATGTGGATCCGCGCCCTCTCGAATGGGGGGTACTG)

The reactions were performed after mixing

x µl water to reach a total volume of 50 µl

5 µl 10x cloned pfuTurbo buffer

5 µl 10x dNTP mix

0.1 µg template plasmid (CIEBOV-CI GP_{1,2}, REBOV-Pen GP_{1,2}, or SEBOV-Gul GP_{1,2})

1 µl oligomer CIEBOV_RBDf, REBOV_RBDf OR SEBOVGul_RBDf

1 µl oligomer CIEBOV_RBDb REBOV_RBDb OR SEBOVGul_RBDb

1 µl cloned pfuTurbo

using the following cycle conditions:

3 min. 94 °C

30x (30 s 94 °C, 30 s 65 °C, 2 min. 70 °C) [three-step PCR]

7 min. 72 °C

The main PCR products, containing unique *NheI* and *BamHI* restriction sites at the 5' and 3' ends, respectively, were detected by agarose-gel electrophoresis, excised, and purified. The product was then digested with *NheI* and *BamHI*, ligated into the *NheI*- and *BamHI*-digested pCDM8-derived expression vector (77), and transformed (CIEBOV-CI 54-201-Fc, REBOV-Pen 55-202-Fc, and SEBOV-Gul 54-201-Fc).

6.2.12 Construction of Zaire ebolavirus isolate Mayinga sGP-Fc

The ZEBOV-May secreted glycoprotein sGP shares the N-terminal 295 amino-acid residues with GP₁ and ssGP. To construct ZEBOV-May sGP-Fc, an ORF encoding the unique sGP C-terminus without Δ-peptide (amino-acid residues 296-324) and with a defective furin-cleavage site (R₃₂₁VRS instead of R₃₂₁VRR) was synthesized and amplified by *de novo* recursive PCR *in vitro* (218) (Figure 6-1). The reaction was set up using the following overlapping DNA oligomers, which are based on the ZEBOV-May sGP protein sequence (GenBank accession numbers [NP_066247](#)) and which are codon-optimized for expression in mammalian cells according to a proprietary algorithm developed by Michael R. Farzan:

sGP forward oligomers:

sgpfc1 (ATCAGT **CGATCG**GCGAGTGGGCCTTCTGGGA)

sgpfc2 (GACCAAGAAAACCAGCCTGGAGAAGTTCGCCGTGAAGTCCTGCCTCAGCCAGCTGTA)

sgpfc3 (CCAGACCGAGCCCAAGACCTCCGTGGTCCGCGTCCGAGCGCGC **GGATCC**CGAGGG)

sGP reverse oligomers:

sgpfc4 (CCCTCGGGATCCGCGCCGCTCCGCACGCGGA)

sgpfc5 (CCACGGAGGTCTTGGGCTCGGTCTGGTACAGCTGGCTGAGGCAGGACTTCACGGCGA)

sgpfc6 (ACTTCTCCAGGCTGGTTTTCTTGGTCTCCAGAAAGGCCACTCGCCGATCGACTGAT)

The PCR was performed as described in Chapter 6.2.2 with a shorter elongation time (30 s). The main PCR product (290 bp), containing unique *PvuI* (CGATCG) and *BamHI* restriction sites at the 5' and 3' ends, respectively, was detected by agarose-gel electrophoresis, excised, and purified. The product was then digested with *PvuI* and *BamHI*, purified again, ligated into the *PvuI*- and *BamHI*-digested pCDM8(ZEBOV-May 33-308-Fc) vector backbone (see Chapter 6.2.8), and transformed (ZEBOV-May sGP-Fc).

6.2.13 Construction of Zaire ebolavirus isolate Mayinga ssGP-Fc

The ZEBOV-May secondary secreted glycoprotein ssGP shares the N-terminal 295 amino-acid residues with GP₁ and sGP and contains only two unique C-terminal amino acids (P₂₉₆H, see GenBank accession number [NP_066248](#)). ZEBOV-May ssGP-Fc was synthesized by modified inverse PCR (Figures 6-2 and 6-3) using oligomers `mucnegforward` (Chapter 6.2.4) and `ssgpfc` (TGCAATGGATCCGCGCCGTGCGGTTTTCTTGGTCTCCAGAAAGGCCACTCGCC).

The reaction was performed after mixing

- x µl water to reach a total volume of 50 µl
- 5 µl 10x cloned pfuTurbo buffer
- 5 µl 10x dNTP mix
- 0.1 µg template plasmid (ZEBOV-May 33-308-Fc)
- 1 µl oligomer `ssgpfc`
- 1 µl oligomer `mucnegforward`
- 1 µl cloned pfuTurbo

using the following cycle conditions:

3 min. 94 °C
 30x (30 s 94 °C, 6 min. 70 °C) [two-step PCR]
 7 min. 72 °C

To destroy template (methylated) DNA, the reaction mix was incubated with 2 μ l *DpnI* for 2 h at 37 °C. The (unmethylated) PCR product was detected by agarose-gel electrophoresis, excised, purified, digested with *BamHI*, purified again, ligated, and transformed.

6.2.14 Construction of ebolaviral Δ -peptides

Codon-optimized ORFs encoding Δ -peptides of CIEBOV (sGP amino-acid residues 325-365, renumbered as Δ -peptide amino-acid residues 1-41), REBOV (sGP amino-acid residues 326-367, renumbered as Δ -peptide amino-acid residues 1-42), SEBOV (sGP amino-acid residues 325-372, renumbered as Δ -peptide amino-acid residues 1-48), and ZEBOV (sGP amino-acid residues 325-364, renumbered as Δ -peptide amino-acid residues 1-40) were synthesized and amplified by *de novo* recursive PCR *in vitro* (218) (Figure 6-1). The reactions were set up using the following overlapping DNA oligomers, which are based on the CIEBOV, REBOV, SEBOV, and ZEBOV sGP protein sequences (GenBank accession numbers [AAB37092](#), [NP_690584](#), [AAU43886](#), [NP_066247](#), respectively) and which are codon-optimized for expression in mammalian cells according to a proprietary algorithm developed by Michael R. Farzan:

CIEBOV Δ -peptide forward oligomers:

cdelpepfc1 (TTCCGT**GCTAGC**GTCCCTCCTGCCCAGCCCG)
 cdelpepfc2 (CCCACCACGACCCAGGCCAAGACCACGAAGAACTGGTTCCAGCGCATCCCCGTGCAGTGGT)
 cdelpepfc3 (TCGGTGCAAGACCTCCCGCGAGCGGACCCAGTGCCAGCCGAGGGCGC**GGATCC**CGAGGG)

CIEBOV Δ -peptide reverse oligomers:

cdelpepfc4 (CCCTCG**GGATCC**GCGCCCTGCGGCTGGCACT)

cdelpepfc5 (GGGTCCGCTCGCGGGAGGTCTTGACCCGGAACCACTGCAGCGGGATGCGCTGGAACCAGTT)
 cdelpepfc6 (CTTCGTGGTCTTGGCCTGGGTCTGGTGGGCGGGCTGGGCAGGAGGGACGCTAGCACGGAA)

REBOV Δ -peptide forward oligomers:

rdelpepfc1 (TTCCGTGCTAGCGGAGCTGTCCAAGGAGAAGC)
 rdelpepfc2 (TCGCCACCACGCACCCGCCACCAGCCAGCTGGTTCCAGCGCATCCCGCTGCAGTGGTTC)
 rdelpepfc3 (CAGTGCTCCCTCCAGGACGGCCAGCGCAAGTGCCGGCCCAAGGTGGGCGCGGATCCCGAGGG)

REBOV Δ -peptide reverse oligomers:

rdelpepfc4 (CCCTCGGGATCCGCGCCACCTTGGGCCGGCA)
 rdelpepfc5 (CTTGCGCTGGCCCTCCTGGAGGAGCACTGGAACCACTGCAGCGGGATGCGCTGGAACCAGC)
 rdelpepfc6 (TGGGCGTGGTGGGCGGGTGCCTGGTGGCGAGCTTCTCCTTGGACAGCTCCGCTAGCACGGAA)

SEBOV Δ -peptide forward oligomers:

sdelpepfc1 (TTCCGTGCTAGCGGAGCTGCAGCGGAGGAATCT)
 sdelpepfc2 (CCCACCGCCCGCCCGCAGCATCCGGACCTGGTTCCAGCGCATCCCGCTCGGCTGGTCCACTGCACCT)
 sdelpepfc3 (ACCAGAAGGGCAAGCAGCACTGCCGGCTGCGCATCCGCCAGAAGGTGGAGGAAGGCGCGGATCCCGAGGG)

SEBOV Δ -peptide reverse oligomers:

sdelpepfc4 (CCCTCGGGATCCGCGCCTTCTCCACCTTCTGGC)
 sdelpepfc5 (GGATGCGCAGCCGGCAGTGCTGCTTGCCTTCTGGTAGGTGCAGTGAACAGCCGAGCGGGATGCGCTG)
 sdelpepfc6 (GAACCAGTCCGGATGCTGCCGGGCGGGCGGTGGAGATTCTCGCTGCAGCTCCGCTAGCACGGAA)

ZEBOV Δ -peptide forward oligomers:

delpepfc1 (TTCCGTGCTAGCGGAGCTGCTCCCGACCCA)
 delpepfc2 (GGGCCGACCCAGCAACTGAAGACCACGAAGTCTGGCTCCAGAAGATCCCGTTGCAGTG)
 delpepfc3 (GTTCAAGTGCACCGTGAAGGAGGGCAAGCTGCAGTGCCGCATCGGCGCGGATCCCGAGGG)

ZEBOV Δ -peptide reverse oligomers:

delpepfc4 (CCCTCGGGATCCGCGCCGATGCGGCACTGC)
 delpepfc5 (AGCTTGCCCTCCTTACGGTGCACCTGAACCACTGCAACGGGATCTTCTGGAGCCAGGAC)
 delpepfc6 (TTCGTGGTCTTCAAGTGGTGGGCGGGTGGGAGCAGCTCCGCTAGCACGGAA)

The PCRs were performed as described in Chapter 6.2.2 with shorter elongation times (30 s). The main PCR products, containing unique *NheI* and *BamHI* restriction sites at the 5' and 3' ends, respectively, were detected by agarose-gel electrophoresis, excised, and purified. The products were then digested with *NheI* and *BamHI*, ligated into the *NheI*- and *BamHI*-digested pCDM8-derived expression vector (77), and transformed (CIEBOV, REBOV, SEBOV, and ZEBOV Δ -Fc).

6.2.15 Construction of Sudan ebolavirus Δ -peptide truncation variants

Plasmids encoding N-terminal or C-terminal truncation variants of SEBOV Δ -Fc (Δ 1-48-Fc) were created by inverse PCR (Figures 6-2 and 6-3). Plasmids encoding C-terminal truncation variants Δ 1-39-Fc, Δ 1-33-Fc, Δ 1-28-Fc, and Δ 1-17-Fc were created using oligomer *mucnegforward* (Chapter 6.2.4) and the following oligomers, respectively:

Δ 1-39-Fc: *sebovcde11* (TGCAATGGATCCGCGCCCCGGCAGTGCTGCTTGCCCTTCTGGTAGGT)

Δ 1-33-Fc: *sebovcde12* (TGCAATGGATCCGCGCCCTTCTGGTAGGTGCAGTGGAACCA)

Δ 1-28-Fc: *sebovcde13* (TGCAATGGATCCGCGCCGTGGAACCAGCCGAGCGGGATGCG)

Δ 1-17-Fc: *sebovcde14* (TGCAATGGATCCGCGCCGGTCCGGATGCTGCCGGCGGGCC)

Reactions were performed after mixing

x μ l water to reach a total volume of 50 μ l

5 μ l 10x cloned pfuTurbo buffer

5 μ l 10x dNTP mix

0.1 μ g template plasmid (SEBOV Δ -Fc)

1 μ l oligomer *sebovcde11*, *sebovcde12*, *sebovcde13* OR *sebovcde14*

1 μ l oligomer *mucnegforward*

1 μ l cloned pfuTurbo

using the following cycle conditions:

3 min. 94 °C

30x (30 s 94 °C, 5 min. 70 °C) [two-step PCR]

7 min. 72 °C

To destroy template (methylated) DNA, the reaction mix was incubated with 2 µl *DpnI* for 2 h at 37 °C. The (unmethylated) PCR product was detected by agarose-gel electrophoresis, excised, purified, digested with *BamHI*, purified again, ligated, and transformed.

Plasmids encoding N-terminal truncation variants Δ7-48-Fc, Δ13-48-Fc, Δ18-48-Fc, and Δ28-48-Fc were created using oligomer *firstcrev* (Chapter 6.2.4) and the following oligomers, respectively:

Δ7-48-Fc: sebovnde13 (CTATGTACGCTAGCGTCTCCCACCGGCCCGCCCGGCAGC)

Δ13-48-Fc: sebovnde11 (CTATGTACGCTAGCGGGCAGCATCCGGACCTGGTTCCAGCGCATC)

Δ18-48-Fc: sebovnde12 (CTATGTACGCTAGCGACCTGGTTCCAGCGCATCCCGCTC)

Δ28-48-Fc: sebovnde14 (CTATGTACGCTAGCGGAGGAGGCCAAGACCTGCTACAACATCAGC)

Reactions were performed after mixing

x µl water to reach a total volume of 50 µl

5 µl 10x cloned pfuTurbo buffer

5 µl 10x dNTP mix

0.1 µg template plasmid (SEBOV Δ-Fc)

1 µl oligomer sebovnde11, sebovnde12, sebovnde13 OR sebovnde14

1 µl oligomer *firstcrev*

1 µl cloned pfuTurbo

using the following cycle conditions:

3 min. 94 °C

30x (30 s 94 °C, 5 min. 70 °C) [two-step PCR]
7 min. 72 °C

To destroy (methylated) template DNA, the reaction mix was incubated with 2 μ l *DpnI* for 2 h at 37 °C. The (unmethylated) PCR product was detected by agarose-gel electrophoresis, excised, purified, digested with *NheI*, purified again, ligated, and transformed.

The plasmid encoding Sudan ebolavirus Δ -peptide-1-39-Fc T₉→A (SEBOV Δ 1-39T9A-Fc) was synthesized as described for SEBOV Δ 1-39-Fc above but with the plasmid encoding SEBOV Δ T9A-Fc (see Chapter 6.2.16) as template.

6.2.16 Construction of Sudan ebolavirus Δ -peptide mutants

Plasmids encoding SEBOV Δ -peptide-Fc mutants were created by site-directed mutagenesis using the QuickChange method (Stratagene). Reactions were performed after mixing

x μ l water to reach a total volume of 50 μ l
5 μ l 10x cloned pfuTurbo buffer
5 μ l 10x dNTP mix
0.1 μ g template plasmid (SEBOV Δ -Fc)
1 μ l cloned pfuTurbo

with 1 μ l oligomer of each of the following oligomers:

Sudan ebolavirus Δ -peptide-Fc S₁₄→A (SEBOV Δ S14A-Fc):

Forward oligomer: S Δ eltaS14Af (GGCCCGCCCGGCCCATCCGGACCTG)

Reverse oligomer: S Δ eltaS14Ar (CAGGTCCGGATGGCGCCGGGCGGGCC)

Sudan ebolavirus Δ -peptide-Fc W₁₈→A (SEBOV Δ W18A-Fc):

Forward oligomer: *sdeltaW18Af* (GGCAGCATCCGGACCGCATTCCAGCGCATCCCGCTC)

Reverse oligomer: *sdeltaW18Ar* (GAGCGGGATGCGCTGGAATGCGGTCCGGATGCTGCC)

Sudan ebolavirus Δ -peptide-Fc W₂₆→A (SEBOV Δ W26A-Fc):

Forward oligomer: *sdeltaW26Af2* (CAGCGCATCCCGCTCGGCGCATTCCACTGCACCTACCAG)

Reverse oligomer: *sdeltaW26Ar2* (CTGGTAGGTGCGAGTGAATGCGCCGAGCGGGATGCGCTG)

using the following cycle conditions:

3 min. 94 °C

30x (30 s 94 °C, 5 min. 70 °C) [two-step PCR]

7 min. 72 °C

To destroy (methylated) template DNA, the reaction mixes were incubated with 2 μ l *DpnI* for 2 h at 37 °C. The (unmethylated) PCR products were detected by agarose-gel electrophoresis, excised, purified, and transformed.

The plasmid encoding Sudan ebolavirus Δ -peptide-Fc T₉→A (SEBOV Δ T9A-Fc) was synthesized *in vitro* by recursive PCR as described in Chapter 6.2.11 by replacing oligomers *sdelpepfc2* and *sdelpepfc6* with *sdelpepfc2TtoA* (CCC GCCGCCCCCGGCAGCATCCGGACCTGGTTCCAGCGCATCCCGCTCGGCTGGTTCCACTGCACCT) and *sdelpepfc6TtoA* (GAACCAGGTCCGGATGCTGCCGGGGCGGCGGGAGATTCTCGCGCTGCAGCTCCGGATCCACGGAA), respectively.

The plasmid encoding Sudan ebolavirus Δ -peptide-Fc R₂₁→A (SEBOV Δ R21A-Fc) was synthesized *in vitro* by recursive PCR as described in Chapter 6.2.11 by replacing oligomers *sdelpepfc2* and *sdelpepfc5* with *sdelpepfc2RtoA* (CCCACCGGCCCGCCCGGCAGCATCCGGACCTGGTTCCAGGCCATCCCGCTCGGCTGGTTCCACTGCACCT) and *sdelpepfc5RtoA* (GGATGCGCAGCCGGCAGTGCTGCTTCCCTTCTGGTAGGTGCGAGTGAACCAGCCGAGCGGGATGGCCTG), respectively.

The plasmid encoding Sudan ebolavirus Δ -peptide-Fc C₂₉→A,C₃₈→A (SEBOV Δ C29A,C38A-Fc) was synthesized *in vitro* by recursive PCR as described in Chapter 6.2.11 by replacing oligomers *sdelpepfc2*, *sdelpepfc3*, and *sdelpepfc5* with *sdelpepfc2CtoA* (CCCACCGGCCCGCCCGCAGCATCCGACCTGGTTCCAGCGCATCCCGCTCGGCTGGTTCCACGCCACCT), *sdelpepfc3CtoA* (ACCAGAAGGGCAAGCAGCACGCTCGGCTGCGCATCCGCCAGAAGGTGGAGGAAGGCGCGGATCCCGAGGG), and *sdelpepfc5CtoA* (GGATGCGCAGCCGAGCGTGCTGCTTCCCTTCTGGTAGGTGGCGTGAACCCAGCCGAGCGGGATGCGCTG), respectively.

6.2.17 Construction of the Reston-Sudan ebolavirus Δ -peptide chimera

The plasmid encoding Reston-Sudan chimeric Δ -peptide-Fc (REBOV Δ -peptide N-terminal amino-acid residues 1-24 fused to SEBOV Δ -peptide C-terminal amino-acid residues 25-48) was synthesized by three consecutive polymerase-chain reactions.

In PCR 1, the ORF encoding REBOV Δ -peptide amino-acid residues 1-24 was amplified by mixing

x μ l water to reach a total volume of 50 μ l

5 μ l 10x cloned pfuTurbo buffer

5 μ l 10x dNTP mix

0.1 μ g template plasmid (REBOV Δ -Fc)

1 μ l oligomer *chimf* (GCCTCAATAAAGCTTCTAGAG)

1 μ l oligomer *RSchim1b* (GCAGTGAACCCAGCCGAGCGGGATGCGCTGGAAC)

1 μ l cloned pfuTurbo

In PCR 2, the ORF encoding SEBOV Δ -peptide amino-acid residues 25-48 was amplified by mixing

x μ l water to reach a total volume of 50 μ l

5 μ l 10x cloned pfuTurbo buffer

5 μ l 10x dNTP mix

0.1 µg template plasmid (SEBOV Δ-Fc)

1 µl oligomer_{RSchim1f} (GTTCCAGCGCATCCCGCTCGGCTGGTTCCACTGC)

1 µl oligomer_{chimb} (CCAGAAGACCCTCTCCCTG)

1 µl cloned pfuTurbo

Both reactions were performed using the following cycle conditions:

3 min. 94 °C

30x (30 s 94 °C, 30s 70 °C) [two-step PCR]

7 min. 72 °C

PCR products 1 (286 bp) and 2 (249 bp), which overlap (grey highlighted complimentary oligomers), were each detected by agarose-gel electrophoresis, excised, purified, and dissolved in 20 µl TE buffer.

In PCR 3, the ORF encoding the REBOV-SEBOV Δ-peptide chimera was amplified by mixing

x µl water to reach a total volume of 50 µl

5 µl 10x cloned pfuTurbo buffer

5 µl 10x dNTP mix

10 µl PCR product 1

10 µl PCR product 2

1 µl oligomer_{chimf}

1 µl oligomer_{chimb}

1 µl cloned pfuTurbo

using the following cycle conditions:

3 min. 94 °C

30x (30 s 94 °C, 30s 70 °C) [two-step PCR]

7 min. 72 °C

The main PCR product (501 bp), containing unique *NheI* and *BamHI* restriction sites at the 5' and 3' ends of the chimera ORF, respectively, was detected by agarose-gel electrophoresis, excised, and purified. The product was then digested with *NheI* and *BamHI*, purified again, ligated into the *NheI*- and *BamHI*-digested pCDM8-derived expression vector (77), and transformed (RSΔ-Fc).

6.2.18 Construction of the Sudan-Reston ebolavirus Δ-peptide chimera

The plasmid encoding Sudan-Reston chimeric Δ-peptide-Fc (SEBOV Δ-peptide N-terminal amino-acid residues 1-24 fused to REBOV Δ-peptide C-terminal amino-acid residues 25-42) was synthesized by three consecutive polymerase-chain reactions.

In PCR 1, the ORF encoding SEBOV Δ-peptide amino-acid residues 1-24 was amplified by mixing

x μl water to reach a total volume of 50 μl

5 μl 10x cloned pfuTurbo buffer

5 μl 10x dNTP mix

0.1 μg template plasmid (SEBOV Δ-Fc)

1 μl oligomer *chimf* (Chapter 6.2.17)

1 μl oligomer *SRchim2b* (CACTGGAACCACTGCAGCGGGATGCGCTGGAACCAG)

1 μl cloned pfuTurbo

In PCR 2, the ORF encoding REBOV Δ-peptide amino-acid residues 25-42 was amplified by mixing

x μl water to reach a total volume of 50 μl

5 μl 10x cloned pfuTurbo buffer

5 μl 10x dNTP mix

0.1 μg template plasmid (REBOV Δ-Fc)

1 μ l oligomer *SRchim2f* (CTGGTTCCAGCGCATCCCCTGCAGTGGTTCCAGTG)

1 μ l oligomer *chimb* (Chapter 6.2.17)

1 μ l cloned *pfuTurbo*

Both reactions were performed using the following cycle conditions:

3 min. 94 °C

30x (30 s 94 °C, 30s 70 °C) [two-step PCR]

7 min. 72 °C

PCR products 1 (285 bp) and 2 (234 bp), which overlap (grey highlighted complimentary oligomers), were each detected by agarose-gel electrophoresis, excised, and purified and dissolved in 20 μ l TE buffer.

In PCR 3, the ORF encoding the SEBOV-REBOV Δ -peptide chimera was amplified by mixing

x μ l water to reach a total volume of 50 μ l

5 μ l 10x cloned *pfuTurbo* buffer

5 μ l 10x dNTP mix

10 μ l PCR product 1

10 μ l PCR product 2

1 μ l oligomer *chimf*

1 μ l oligomer *chimb*

1 μ l cloned *pfuTurbo*

using the following cycle conditions:

3 min. 94 °C

30x (30 s 94 °C, 30s 70 °C) [two-step PCR]

7 min. 72 °C

The main PCR product (483 bp), containing unique *NheI* and *BamHI* restriction sites at the 5' and 3' ends of the chimera ORF, respectively, was detected by agarose-gel electrophoresis, excised, and purified. The product was then digested with *NheI* and *BamHI*, purified again, ligated into the *NheI*- and *BamHI*-digested pCDM8-derived expression vector (77), and transformed (SRΔ-Fc).

6.2.19 Construction of plasmids encoding proteins fused to the Fc region of murine IgG_{2A}

The plasmid encoding SEBOV Δ-peptide fused to the Fc region of murine IgG_{2A} (mFc) was synthesized by PCR using the plasmid encoding SEBOV Δ-Fc as template and oligomers SEBOVdelta mFcf (TACGCCAAGCTTAGGCCAGAAACCATGCCCATGG) and SEBOVdelta mFcr (ACCCTCGGGATCCGCGCCTTCCTC). The forward oligomer was designed to contain a unique *HinDIII* restriction site, shared by the multicloning site of the target vector, followed by a Kozak sequence and beginning of the CD5 signal sequence encoded in the template plasmid. The reverse oligomer was designed to contain a unique *BamHI* restriction site, shared by the template and target vectors. Reactions were performed after mixing

x μl water to reach a total volume of 50 μl
 5 μl 10x cloned pfuTurbo buffer
 5 μl 10x dNTP mix
 0.1 μg template plasmid (SEBOV Δ-Fc)
 1 μl oligomer SEBOVdelta mFcf
 1 μl oligomer SEBOVdelta mFcr
 1 μl cloned pfuTurbo

using the following cycle conditions:

3 min. 94 °C
 30x (30 s 94 °C, 30 s 70 °C) [two-step PCR]

7 min. 72 °C

The main PCR product (264 bp) consisted, in 5' to 3' order, of the *HinDIII* restriction site, followed by sequence encoding the CD5 signal sequence (containing the unique *NheI* restriction site described above) and SEBOV Δ -peptide. The fragment ended with sequence encoding the N-terminal amino-acid residues of human IgG₁ Fc, which are identical to the N-terminal amino-acid residues of murine IgG_{2A} Fc, containing the unique *BamHI* restriction site. The fragment was detected by agarose-gel electrophoresis, excised, and purified. The product was then digested with *HinDIII* and *BamHI*, purified again, ligated into the *HinDIII*- and *BamHI*-digested, murine IgG_{2A} Fc-encoding vector pCR2.1 previously created in the laboratory (provided by Hyeryun Choe), and transformed (SEBOV Δ -mFc).

6.2.20 Construction and origin of plasmids encoding control proteins

The plasmid encoding only the Fc region of human IgG₁ was created by inverse PCR (Figures 6-2 and 6-3) using oligomer *mucnegforward* (Chapter 6.2.4) and oligomer *fc* (TGCAATGGATCCGCGCCCGCTAGCACGGAAGCGACCAGCAT). Reactions were performed after mixing

x μ l water to reach a total volume of 50 μ l

5 μ l 10x cloned pfuTurbo buffer

5 μ l 10x dNTP mix

0.1 μ g template plasmid (MARV-Mus 17-432-Fc)

1 μ l oligomer *mucnegforward*

1 μ l oligomer *fc*

1 μ l cloned pfuTurbo

using the following cycle conditions:

3 min. 94 °C

30x (30 s 94 °C, 5 min. 70 °C) [two-step PCR]
7 min. 72 °C

To destroy template (methylated) DNA, the reaction mix was incubated with 2 μ l *DpnI* for 2 h at 37 °C. The (unmethylated) PCR product was detected by agarose-gel electrophoresis, excised, purified, digested with *BamHI*, purified again, ligated, and transformed.

The pcDM8-based expression plasmids encoding 1) the severe acute respiratory syndrome coronavirus (SARS-CoV) receptor-binding domain (SARS-CoV S protein amino-acid residues 318-510), 2) human immunodeficiency virus type 1 strain ADA (HIV-1_{ADA}) gp120, and 3) Machupo virus (MACV) strain Carvallo receptor-binding domain (MACV GPC amino-acid residues 79-258), all fused N-terminally to the signal sequence of human CD5 and C-terminally to the Fc region of human IgG₁ (SARS-CoV RBD-Fc, HIV-1 gp120-Fc, MACV GP1 Δ -Fc), have been developed in the laboratory and were reported previously (55, 219, 304). Likewise, full-length spike proteins of human influenza A virus (FLUAV) strain A/FPV/Rostock/34 H7N1, Lassa virus (LASV) strain Josiah, Machupo virus (MACV) strain Carvallo, and lymphocytic choriomeningitis virus (LCMV) strain Armstrong have been created in the laboratory for the creation of retroviral pseudotypes and were reported previously (131, 219).

6.3 Evaluation of expression of filoviral glycoprotein variants and control proteins

Expression of filoviral glycoproteins, mutants thereof, deletion variants or control proteins from plasmids was evaluated using transfection followed by radiolabeling/autoradiography. For each plasmid, human embryonic kidney (HEK) 293T cells were grown in a 25 cm² flask to 40% confluency. Transfection was performed using the calcium-phosphate method. Briefly, two polystyrene tubes were prepared containing

- 1) x μ l water for a total volume of 250 μ l, 10 μ g expression plasmid, and 25 μ l 2.5 M CaCl_2
- 2) 250 μ l 2x HEPES-buffered saline (2x HBS; 80 mM NaCl, 1.5 mM Na_2HPO_4 , 50 mM HEPES pH 7.1, adjusted to pH 7.5)

The content of tube 1 was added dropwise to that of tube 2, and incubated at room temperature for 10 min. to allow for the formation of calcium-phosphate crystals. The reaction mix was then added drop-by-drop to the medium and the cells in the tissue-culture flask, mixed cautiously, and incubated at 37 °C in a humidified 5% CO_2 atmosphere for 6 h. Transfected cells were then washed twice with warm (37 °C) DPBS and incubated for 36-48 h at 37 °C in a humidified 5% CO_2 atmosphere in 3 ml of L-methionine- and L-cystine-free DMEM (GIBCO-Invitrogen) containing 10% heat-inactivated (56 °C, 1 h) dialyzed FBS (dFBS, GIBCO-Invitrogen), 4 mM L-glutamine (Sigma-Aldrich), and 50 μ Ci/ml EasyTag EXPRESS Protein Labeling Mix ^{35}S (PerkinElmer, Waltham, MA, USA).

In the case of secreted, soluble proteins (filoviral and control Fc fusion proteins), media were harvested, cell debris removed by centrifugation and filtration through a 0.22 μ m-pore size filter (Corning, Lowell, MA, USA), and proteins were immunoprecipitated under constant rocking with ~10 μ l packed protein A-sepharose Fast Flow beads (GE Healthcare, Piscataway, NJ, USA) at 4 °C for 16 h in the presence of 1 tablet/50 ml Complete Protease Inhibitor (Roche, Mannheim, Germany). Beads were washed twice with cold (4 °C) wash buffer 1 (0.5 M NaCl, 1% Nonidet P-40, and 0.1% SDS in PBS) and once in cold (4 °C) PBS, and proteins were eluted into denaturing SDS-containing reducing PAGE sample buffer (GIBCO-Invitrogen) by boiling in a water bath for 4 min. Proteins were evaluated by size on precast 10% Tris-glycine polyacrylamide gels (Invitrogen) with Precision Plus Protein Dual Color Standards (BioRad, Hercules, CA, USA). Gels were fixed for 20 min. in 50% methanol/10% acetic acid (vol./vol.) at room temperature, dried at 80 °C for 1 h in a vacuum gel dryer, and exposed to Kodak BioMax film (Sigma-Aldrich) at -70 °C for appropriate time spans. Films were developed in the dark using an automated system.

In the case of membrane-bound proteins (C9-tagged constructs), media were discarded, and cells were lysed by exposure to 3 ml of cold (4 °C) 0.3% (weight/vol.) *n*-dodecyl- β -D-maltopyranoside (DDM; Anatrace, Maumee, OH, USA) in PBS. Debris (membrane fragments) was removed by centrifugation (14,000 x *g*, 4 °C, 20 min.), and proteins were immunoprecipitated under constant rocking with ~0.5 μ g of an antibody to the C9 tag (1D4, provided by Hyeryun Choe, Harvard Medical School, Boston, MA, USA) together with ~10 μ l packed protein A-sepharose Fast Flow beads at 4 °C for 16 h in the presence of 1 tablet/30 ml Complete Protease Inhibitor. Beads were washed twice with cold (4 °C) wash buffer 2 (0.1 M NaCl, and 0.025% SDS in PBS) and once in cold (4 °C) PBS, and proteins analyzed as described above.

6.4 Expression of filoviral glycoprotein variants and control proteins

For large-scale protein purification, human embryonic kidney (HEK) 293T cells were transfected with plasmids encoding filoviral or control Fc fusion proteins using the calcium-phosphate method. For each plasmid, HEK 293T cells were grown in multiple (20-40) 175 cm² flasks to 40% confluency. Transfection was performed by preparing two polystyrene tubes per flask containing

- 1) x μ l water for a total volume of 1000 μ l, 80 μ g expression plasmid, and 100 μ l 2.5 M CaCl₂
- 2) 1000 μ l 2x HBS

The content of tube 1 was added dropwise to that of tube 2, and incubated at room temperature for 10 min. to allow for the formation of calcium-phosphate crystals. The reaction mix was then added drop-by-drop to the to the medium and the cells in the tissue-culture flask, mixed cautiously, and incubated at 37 °C in a humidified 5% CO₂ atmosphere for 6 h. Transfected cells were then washed twice with warm (37 °C) DPBS and incubated at 37 °C in a humidified 5% CO₂ atmosphere in 293 SFM II medium (GIBCO-Invitrogen)

supplemented with PS, 100 μ M MEM non-essential amino-acids solution (GIBCO-Invitrogen), 2 mM sodium butyrate (Sigma-Aldrich), and 4 mM L-glutamine. Media were harvested after 36-48 h, and cell debris was removed by centrifugation (3,000 \times g, 4 °C, 20 min.) and sequential filtration through 0.45 and 0.22 μ m-pore size filters (Corning). Proteins were immunoprecipitated under constant rocking with ~1 ml packed protein A-sepharose Fast Flow beads at 4 °C for 16 h in the presence of 1 tablet/50 ml Complete Protease Inhibitor. Beads were collected in columns, washed once with 30 bed volumes of cold (4 °C) 0.5 M NaCl in PBS (NaCl: Fisher Scientific, Fair Lawn, NJ, USA) and washed once with 10 bed volumes of cold (4 °C) PBS. Proteins were eluted with cold (4 °C) 50 mM sodium citrate/50 mM glycine pH 2 (sodium citrate: Fisher Scientific; glycine: BIO-RAD, Hercules, CA, USA), and neutralized with sodium hydroxide (Fisher Scientific). The proteins were dialyzed three times (1.5 h, 1.5 h, 12 h) in cold (4 °C) PBS using commercial Slide-A-Lyzer dialysis cassettes (Pierce, Rockford, IL, USA) with the appropriate molecular weight cut-off, and concentrated with Centricon centrifugal filter units (Millipore, Billerica, MA, USA) with the appropriate molecular weight cut-off. Purified proteins were assayed for size and concentration by comparison to BSA standards (Sigma-Aldrich) by using SDS-PAGE, followed by Bio-Safe Coomassie (BIO-RAD) staining (1 h at room temperature) and by destaining in water (overnight at room temperature). Estimated protein quantities were confirmed by using the Micro BCA protein assay kit (Pierce) according to the manufacturer's instructions.

6.5 Cell binding assays

90% confluent adherent cells were detached with PBS/5mM EDTA (GIBCO-Invitrogen) 48 h after plating, resuspended in an equal volume of PBS/5mM MgCl₂ (Sigma-Aldrich), and washed twice in cold (4 °C) PBS/2% heat-inactivated (56 °C, 1h) goat serum (Sigma-Aldrich). Suspension cells were harvested and washed twice in cold (4 °C) PBS/2% goat serum. Filoviral Fc fusion constructs or control proteins were added to 3 \times 10⁵ or 5 \times 10⁵ cells (experiments described in Chapters 7.1 and 7.2, respectively) to a final concentration of

100-200 nM, and incubated on ice for 1-1.5 h. Cells with bound proteins were washed twice in cold (4 °C) PBS/2% goat serum, and incubated for 45 min. on ice with a 1:40 dilution of goat Fc-specific fluorescein isothiocyanate (FITC) conjugated anti-human antibody in cold (4 °C) PBS/2% goat serum. Cells were washed three times with cold (4 °C) PBS/2% goat serum, once in cold (4 °C) PBS, and fixed with PBS/2% formaldehyde (Sigma-Aldrich) overnight. Cell-surface binding of constructs was detected by flow cytometry with 10,000 events counted per sample using a FACSCalibur flow cytometer (BD Biosciences, San Jose, CA, USA) and analyzed with FlowJo software (Tree Star, Ashland, OR, USA). Baseline fluorescence was determined by measuring cells treated only with goat Fc-specific FITC-conjugate anti-human IgG antibody, which was then subtracted from binding values of the tested constructs and control proteins.

6.6 Cell-binding competition assay

Cell-binding competition assays were performed following the procedures described in Chapter 6.5 with the following modifications: for the first incubation step, human IgG₁ Fc-conjugated MARV-Mus 38-188 (MARV-Mus 38-188-Fc) or murine IgG_{2A} Fc-conjugated SEBOV Δ (SEBOV Δ -mFc) constructs were added to 3×10^5 cells to a final concentration of 200 nM, and incubated on ice for 1-1.5 h. Cells with bound proteins were washed twice in cold (4 °C) PBS/2% goat serum. Cells with bound Fc construct were exposed to 800 nM of mFc construct or 800 nM BSA, and cells with bound mFc construct were exposed to 800 nM of Fc construct or 800 nM BSA. Both sets of cells were incubated on ice for 1-1.5 h. Cells were washed twice in cold (4 °C) PBS/2% goat serum, and incubated for 45 min. on ice with a 1:40 dilution of goat Fc-specific FITC conjugated anti-human Fc (hAb) or anti-murine Fc (mAb) antibody (Sigma-Aldrich) in cold (4 °C) PBS/2% goat serum.

6.7 Transduction assay with pseudotyped gammaretroviruses

To generate gammaretroviral pseudotypes, human embryonic kidney (HEK) 293T cells were transfected by the calcium-phosphate method as described in Chapter 6.3 with plasmid encoding 1) influenza A virus (FLUAV) strain A/FPV/Rostock/34 H7N1 hemagglutinin 7 (HA7) and neuraminidase (NA1) proteins, Lassa virus strain Josiah (LASV) GPC protein, lymphocytic choriomeningitis virus strain Armstrong (LCMV) GPC protein, Machupo virus strain Carvallo (MACV) GPC protein, MARV-Mus GP_{1,2} 17-681-C9, vesicular stomatitis Indiana virus (VSIV) G protein (provided by Hyeryun Choe, Children's Hospital, Harvard Medical School, Boston, MA, USA) or mucin-like domain-deleted ZEBOV-May GP_{1,2Δ309-489} (described and provided by James Cunningham, Harvard Medical School, Boston, MA, USA (52)), together with 2) the pQCXIX vector (BD Biosciences) expressing enhanced green fluorescent protein (eGFP) flanked by the MLV long terminal repeats (LTRs), and 3) plasmid encoding the Moloney murine leukemia virus (MLV) *gag/pol* genes (192) (Figure 6-4).

Plasmid quantities used per 75 cm² tissue-culture flask were:

- 1) 3 μg FLUAV HA7, 12 μg FLUAV NA1, 8 μg eGFP, 8 μg *gag/pol*
- 2) 8 μg LASV GPC, 8 μg eGFP, 8 μg *gag/pol*
- 3) 8 μg LCMV GPC, 8 μg eGFP, 8 μg *gag/pol*
- 4) 8 μg MACV GPC, 8 μg eGFP, 8 μg *gag/pol*
- 5) 8 μg MARV-Mus GP_{1,2} 17-681-C9, 8 μg eGFP, 8 μg *gag/pol*
- 6) 0.8 μg VSIV G, 8 μg eGFP, 8 μg *gag/pol*
- 7) 20 μg ZEBOV-May GP_{1,2Δ309-489}, 8 μg eGFP, 8 μg *gag/pol*

Cell supernatants were harvested 36-48 h post transfection, cleared of cellular debris by centrifugation (3,000 x g, 4 °C, 20 min.) and filtration through 0.45 μm-pore size filters, and stored at 4 °C for short-term storage or aliquoted at -70 °C for long-term storage.

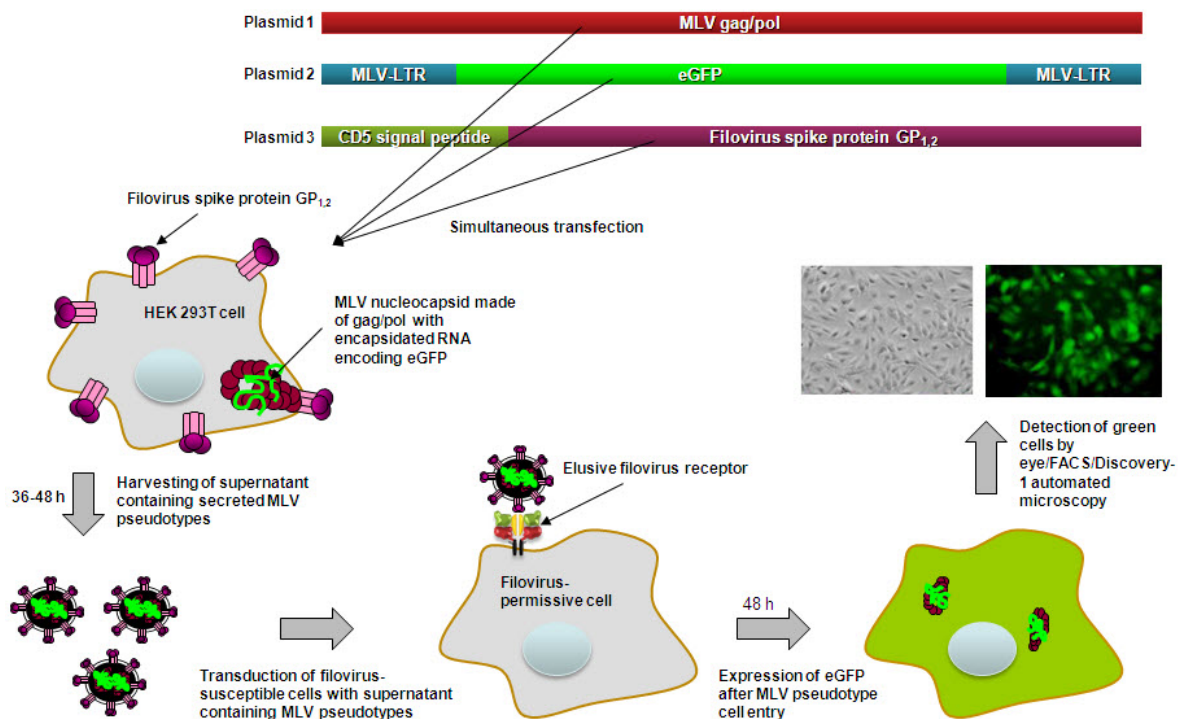


Figure 6-4. Production of Moloney murine leukemia virus particles pseudotyped with filoviral spike proteins

Human embryonic kidney (HEK) 293T cells are transfected with plasmids encoding 1) the Moloney murine leukemia virus (MLV) capsid proteins gag/pol, 2) enhanced green fluorescent protein (eGFP) RNA flanked by the MLV long-terminal repeats (LTR), and 3) a functional filoviral spike protein (GP_{1,2}). After expression, MLV gag/pol encapsidates the RNA encoding eGFP. The particles become enveloped during budding from the cell surface by taking with them part of the cell membrane, which contains the expressed filoviral GP_{1,2}. The resulting spherical particles resemble MLV (and not filoviruses) in shape, but can only enter cells expressing the filovirus receptor. Subsequent to entry, eGFP is expressed and the green fluorescence can be detected by fluorescent microscopy. Further transmission of the particles is impossible because the particles do not bring with them the genetic material to express further gag/pol or spike proteins. Therefore, these particles can be used at biosafety level 2 as a surrogate system for infectious filoviruses, which must be handled at biosafety level 4. Pseudotypes carrying nonfiloviral spike proteins can be produced in a similar manner.

Supernatants containing pseudotyped viruses were added to permissive cells in the presence or absence of the indicated concentrations of filovirus Fc fusion proteins or

control proteins (Figure 6-5) in 24-well plate wells. After 5 h, cells were washed once in warm (37 °C) PBS, and replenished with fresh warm (37 °C) media containing PS and haFBS. After 36-48 h, cells were imaged by fluorescent microscopy, and then detached with 200 µl trypsin. Cells were washed twice in cold (4 °C) PBS, and fixed with PBS/2% formaldehyde overnight. eGFP expression was detected by flow cytometry with 10,000 events counted per sample. Baseline fluorescence was determined by measuring cells exposed to mock control (media), which was then subtracted from measured values of cells exposed to pseudotypes.

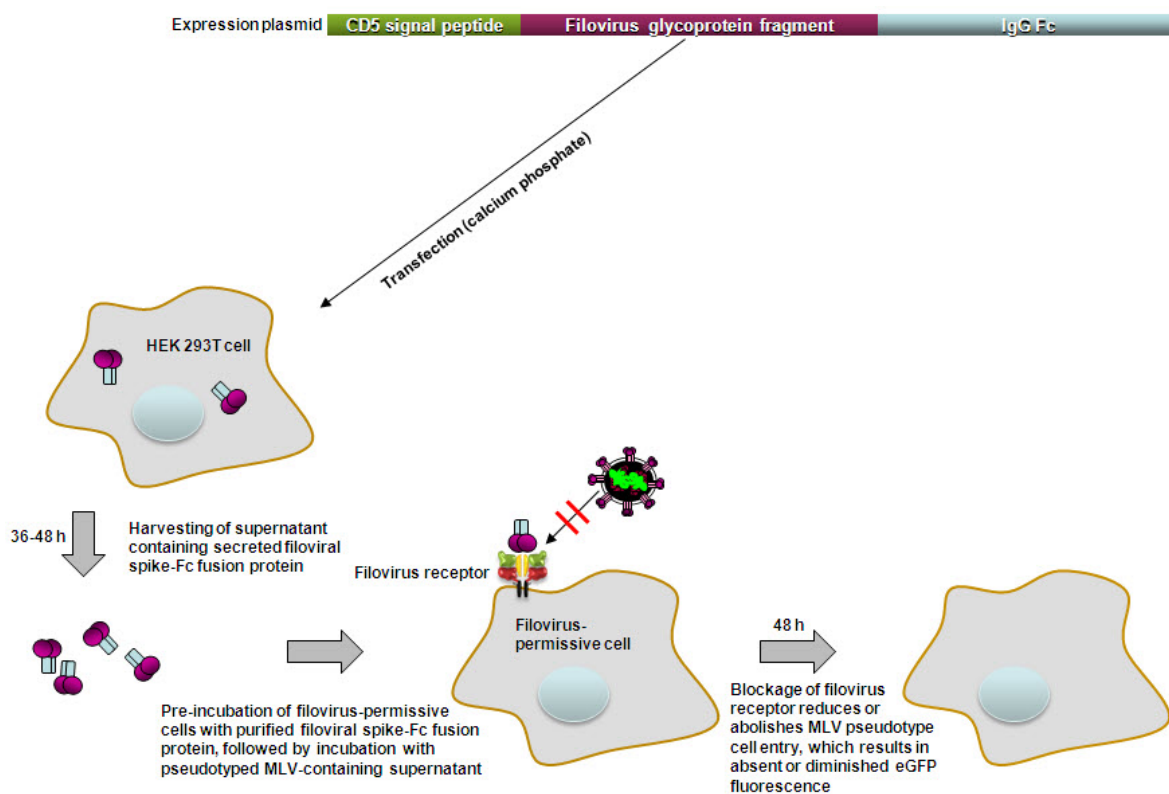


Figure 6-5. Principle of the Moloney murine leukemia pseudotype-inhibition assay

Filovirus glycoprotein-Fc fusion proteins, fused N-terminally to the signal sequence of human CD5 and C-terminally to the Fc region of IgG, are expressed from plasmids by transfection of human embryonic kidney (HEK) 293T cells, purified, and quantified. Moloney murine leukemia virus (MLV) particles expressing enhanced green-fluorescent protein (eGFP) and pseudotyped with filoviral spike proteins compete with Fc fusion

proteins that bind to the receptor (diminished or abolished eGFP expression), but not with those that do not or those that are misfolded (unchanged eGFP expression compared to cells exposed only to pseudotypes)

6.8 Infection assay with recombinant infectious Zaire ebolavirus

All experiments with infectious filovirus were performed under BSL-4 conditions by Dr. Sina Bavari's and Dr. M. Javad Aman's team members at the United States Army Medical Research Institute of Infectious Diseases (USAMRIID), Fort Detrick, Frederick, MD, USA. African green monkey kidney epithelial (Vero E6) cells were preincubated with or without the indicated concentrations of filoviral Fc or control proteins for 1 h at 4 °C. After removal of the media, cells were infected with eGFP-expressing ZEBOV-May created by reverse genetics (270). Cells were incubated with virus at a multiplicity of infection (moi) equal to 1 for 1 h at 37 °C. Virus-containing medium was removed, cells were washed in warm (37 °C) PBS, and media were replenished. After 48 h, cells were fixed in 10% neutral-buffered formalin. After 3 days of fixation, cells were removed from the BSL-4 suite and the percent of eGFP-expressing cells was measured with a Discovery-1 automated microscope (Molecular Devices Corp., Sunnyvale, CA, USA) by measuring 9 individual spots per well.

6.9 HIV-1 neutralization assay

The effect of Sudan ebolavirus Δ -peptide on cell entry of human immunodeficiency virus type 1 (HIV-1) was measured using a previously described assay (182). Briefly, HIV-1_{NL4.3} (obtained from Ronald C. Desrosiers' laboratory at the New England Primate Research Center, Harvard Medical School, Southborough, MA, USA) was incubated with human C8166-45 T lymphocytes stably transfected with plasmid encoding a secreted alkaline phosphatase (SEAP) reporter gene under the control of a *tat*-responsive promoter derived from HIV-1_{NL4.3} (C8166-45LTR-SEAP cells). SEAP activity is upregulated upon HIV-1_{NL4.3} infection and correlates directly with the amount of input virus. Consequently, to measure the effect of SEBOV Δ -Fc on HIV-1 entry, HIV-1_{NL4.3} – amounting to the

equivalent of 2 ng p24 (measured using the Lentivirus p24 ELISA Kit from Cell Biolabs, San Diego, CA, USA) – was incubated for 1 h with varying amounts of SEBOV Δ -Fc or CD4-Fc control at 37°C in a humidified 5% CO₂ atmosphere in a total volume of 100 μ l RPMI 1640 media supplemented with 10% ha FBS. Then, 80,000 C8166-45LTR-SEAP cells were added to each sample, reaching a total volume of 200 μ l per sample. After 72 h of incubation at 37°C in a humidified 5% CO₂ atmosphere, infection levels were measured by detecting SEAP activity in harvested cell-culture supernatant with the Phospha-Light™ SEAP Reporter Gene Assay System (Applied Biosystems, Foster City, CA, USA) and a Victor³ V plate reader (Perkin-Elmer, Waltham, MA, USA) according to the instructions of the respective manufacturers.

6.10 Cathepsin assay

1 μ g/ml of human cathepsin B, purified from liver (Calbiochem, La Jolla, CA, USA), was incubated in 96-well fluorimeter plates for 20 min. at room temperature in assay buffer (100 mM sodium acetate (Sigma-Aldrich), 50 mM NaCl, 1 mM EDTA, 5 mM dithiothreitol (DTT, Sigma-Aldrich), and 2 μ g/ml aprotinin (Sigma-Aldrich)) with either 1% DMSO, 30 μ M cathepsin-B inhibitor CA074 (Sigma-Aldrich), 30 nM ebolaviral Δ -Fc variant, 30 nM Fc or assay buffer. Dilutions of Fc proteins were made with assay buffer. After incubation, fluorescent substrate Z-Arg-Arg-AMC (Sigma-Aldrich) was added in serial 2-fold dilutions to give final concentrations of substrate from 0-427 μ M. Fluorescent signal was determined every 3 min. for 1 h on a Fluoroskan Ascent FL plate reader (Thermo Scientific, Waltham, MA, USA) using an excitation setting of 485 nm and an emission setting of 538 nm. Background signal was determined by adding Z-Arg-Arg-AMC to assay buffer at reaction concentrations in the absence of cathepsin B. Background signal was subtracted from the appropriate corresponding well. All data points were obtained in duplicate. The mean values for V₀ (measured in relative fluorescent units (R.F.U.)) were plotted against the corresponding concentrations of Z-Arg-Arg-AMC.

6.11 Immunization and vaccination protocol

6.11.1 Animals

Eight to ten week-old wild-type male and female C57BL/6 house mice (*Mus musculus*) were obtained from the National Cancer Institute (NCI), Frederick Cancer Research and Development Center, Fort Detrick, Frederick, MD, USA, and randomly divided into treatment groups. The mice were held in microisolator cages and provided autoclaved water and chow *ad libitum*. Research was performed in compliance with the US Animal Welfare Act and other federal statutes and regulations relating to animal experimentation, and adhered to principles stated in the US National Research Council's 1996 Guide for the Care and Use of Laboratory Animals (Washington, DC, USA). The facilities used for the research described in this dissertation are fully accredited by the Association for Assessment and Accreditation of Laboratory Animal Care International (AAALAC).

6.11.2 Preparation of immunogen

MARV-Mus 38-188-Fc and ZEBOV-May 54-201-Fc proteins were produced, purified, and quantified as described in Chapter 6.4.

6.11.3 Immunization protocol

Three groups of 13 mice each were immunized intramuscularly on days 0, 14, and 28 with 20 µg (60 µg total) of either MARV-Mus 38-188-Fc or ZEBOV-May 54-201-Fc in 200 µl RIBI adjuvant (Corixa, Hamilton, MT) or with 200 µl RIBI adjuvant alone.

6.11.4 Determination of antibody titers

Blood samples were obtained from mice of all three immunization groups on days 14, 28, and 42 from the retroorbital sinus under combination anesthesia (ketamine, acepromazine, and xylanine) given intramuscularly, and serum was collected and stored at -70 °C. Levels

of ZEBOV-specific antibodies were determined as previously described (123). Briefly, ZEBOV-Kik (a ZEBOV isolate obtained in 1995 that is closely related to ZEBOV-May) was grown by Dr. Sina Bavari's and Dr. M Javad Aman's team members in a BSL-4 laboratory in African green monkey kidney epithelial (Vero E6) cells, purified through a sucrose cushion, and inactivated by γ -irradiation with 10^7 rad. Wells of a 96-well plate were coated with the virus preparation and serial 3-fold dilutions of individual serum samples were added to the wells. Antibodies were detected by ELISA using a horseradish peroxidase-conjugated secondary antibody (Sigma-Aldrich) and tetramethylbenzidine substrate (Sigma-Aldrich) according to the instructions of the manufacturer. Antibody titers were defined as the reciprocal of the highest dilution showing a net optical density (OD) ≥ 0.2 .

6.11.5 Determination of cytotoxic T-lymphocyte responses

On day 35, three mice of each of the three groups were euthanized using carbon dioxide inhalation followed by cervical dislocation, dissected, and splenocytes were collected and pooled for the analysis of cytotoxic T-lymphocyte (CTL) responses as previously described (302). Briefly, splenocytes were placed in RPMI 1640 medium supplemented with 10% haFBS, 2 mM glutamine, 1 mM HEPES (Gibco), and 0.1 mM MEM nonessential amino acids. Contaminating erythrocytes were lysed with ACK lysing buffer (Invitrogen), and the remaining splenocytes were washed twice in RPMI1640 medium. 2×10^6 splenocytes were then incubated with 1-5 μg overlapping peptides of ZEBOV-May GP₁ (15-mers overlapping the down- and upstream peptides by five residues; purchased as pin-synthesized PepSets in DMSO from Mimotopes, Clayton, Victoria, Australia) or with phorbol myristate acetate (PMA; 25 ng/ml; Sigma-Aldrich) and ionomycin (1.25 $\mu\text{g}/\text{ml}$; Sigma-Aldrich) as a positive control for activation/cytokine secretion in 100 μl of RPMI 1640 supplemented with 10% haFBS, 2 mM glutamine, 10 $\mu\text{g}/\text{ml}$ gentamicin (GIBCO-Invitrogen), 10 $\mu\text{g}/\text{ml}$ of brefeldin A (Epicenter Technologies, Madison, WI, USA), 5 mM HEPES, and 0.05 mM β -mercaptoethanol (GIBCO-Invitrogen) for 5 h at 37°C in a

humidified 5% CO₂ atmosphere. Splenocytes were blocked with a monoclonal antibody to the FcRIII/II receptor (CD16/32, BD Biosciences) and stained with anti-CD44 FITC and either anti-CD8 or anti-CD4 Cy-Chrome (Pharmingen, San Diego, CA, USA) in staining wash buffer (PBS, 2% FBS, 0.01% sodium azide (Sigma-Aldrich)), with brefeldin A (10 µg/ml). The cells were fixed in 1% formaldehyde (Ted Pella, Redding, CA, USA) made permeable with staining wash buffer containing 0.5% saponin (Sigma-Aldrich), and stained with anti-IFN-phycoerythrin (Pharmingen, San Diego, CA, USA). Data were acquired by flow cytometry using a FACSCalibur flow cytometer and analyzed with FlowJo software. Samples were considered positive if the percentage of CD8⁺, CD44⁺, IFN⁺-cells was greater than 2-fold above background. Background was determined by staining a sample without any peptides, but with an equivalent amount of DMSO.

6.11.6 Viral challenge

On day 56, mice were challenged by intraperitoneal injection with 1,000 pfu (~30,000 LD₅₀) of mouse-adapted ZEBOV-May diluted in PBS (33). Mice were observed at least twice daily for clinical symptoms, such as reduced grooming, ruffled fur, hunched posture, subdued response to stimulation, nasal discharge or bleeding, for a total period of 28 days.

7 RESULTS

7.1 Filoviruses attach to a common cell-surface receptor

7.1.1 Lake Victoria marburgvirus isolate Musoke GP₁ truncation variant 38-188-Fc binds to filovirus-permissive cells more efficiently than full-length GP₁

The ectodomains of spike proteins of some enveloped viruses, such as severe acute respiratory syndrome coronavirus (SARS-CoV), include discrete, independently folded domains that bind viral cell-surface receptors as efficiently as, or even more efficiently than, their full-length ectodomains (304). One goal of the research described in this dissertation was to evaluate whether the Lake Victoria marburgvirus (MARV) spike-protein ectodomain GP₁ also contains such a distinct similar receptor-binding region (RBR), and if so, whether this RBR binds with higher efficiency to the still unidentified MARV receptor as compared to full-length GP₁. To determine the location of the MARV GP₁ RBR, a codon-optimized gene was synthesized *in vitro* that encodes the full-length mature GP₁ protein of the type isolate of MARV, Musoke (MARV-Mus), fused to the Fc region of human immunoglobulin G₁ at the C-terminus (17-432-Fc). Four sets of seven truncation variants were created, starting at N-terminal residues 17, 38, 61 or 87, and ending at C-terminal residues 432, 308, 265, 230, 188, 167 or 134 (Figure 7-1). All 28 constructs expressed sufficiently in human embryonic kidney (HEK) 293T cells as Fc-fusion proteins (Figure 7-2), and were purified and quantified.

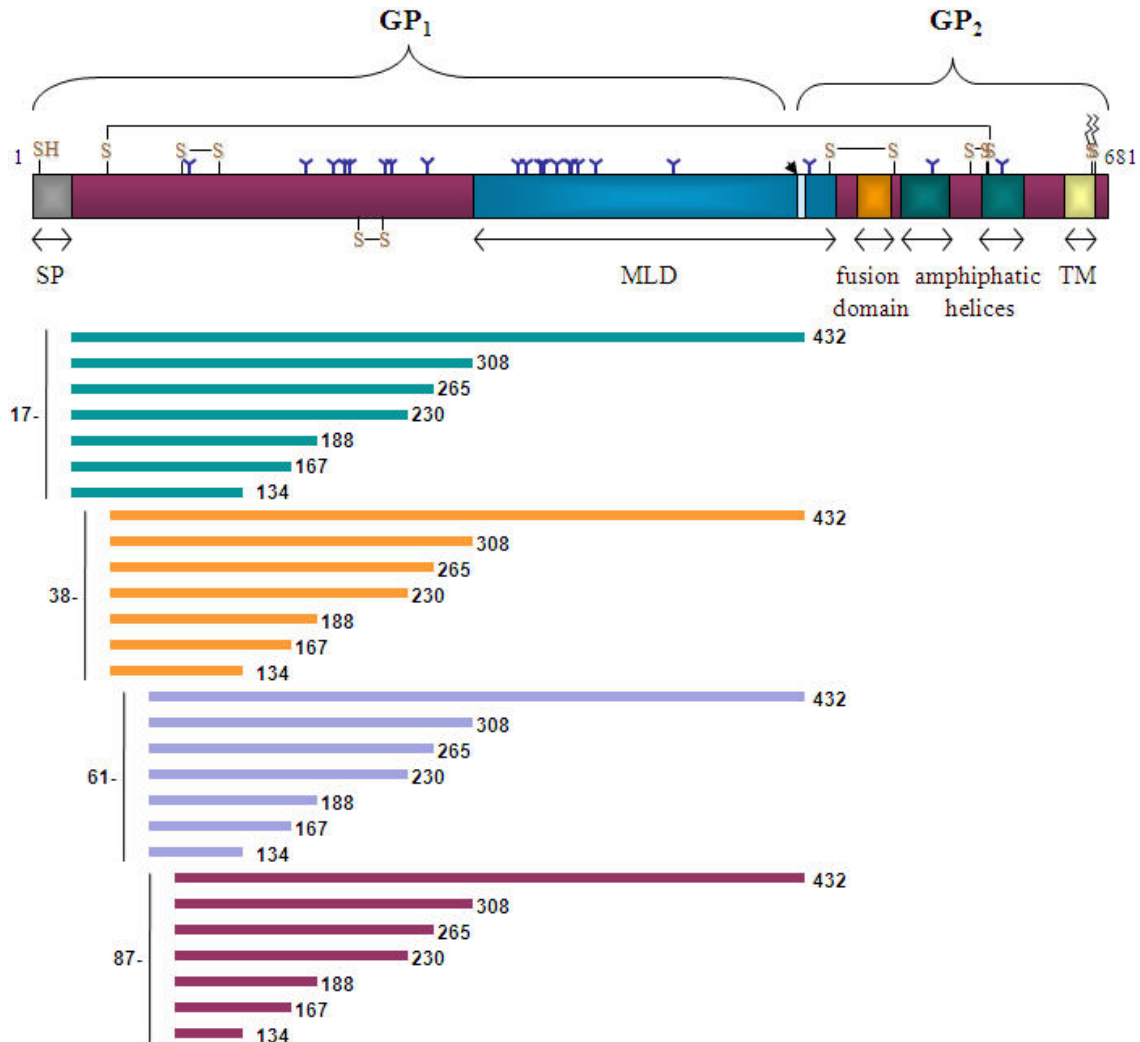


Figure 7-1. Lake Victoria marburgvirus isolate Musoke GP₁ and GP₁ truncation variants

Representation of Lake Victoria marburgvirus isolate Musoke (MARV-Mus) GP₁ truncation variants in relation to the full-length MARV-Mus GP_{1,2} envelope spike protein (amino-acid residues 1-681). SP, signal peptide; MLD, mucin-like domain; TM, transmembrane domain. Cysteine residues (-SH), predicted or experimentally confirmed disulfide bonds (-S-S-), potential N-glycosylation sites (blue Ys), and the furin cleavage site (arrow) (141, 278) are indicated

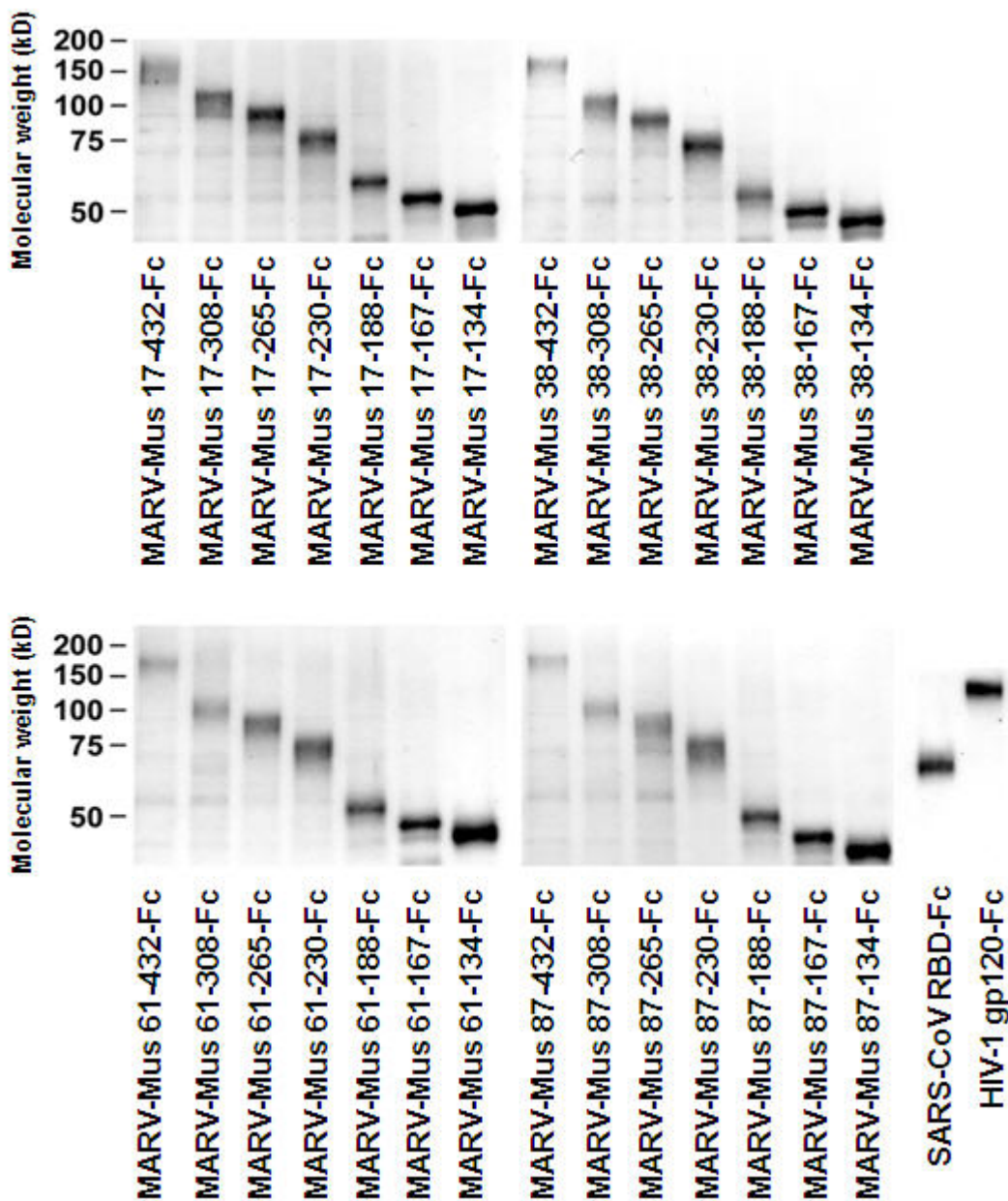


Figure 7-2. Expression of Lake Victoria marburgvirus isolate Musoke GP₁ and GP₁ truncation variants

Lake Victoria marburgvirus isolate Musoke (MARV-Mus) GP₁-Fc, containing GP₁ residues 17-432 fused to the Fc region of human IgG₁ (17-432-Fc), truncation variants of 17-432-Fc containing the indicated GP₁ residues or control proteins severe acute respiratory syndrome coronavirus (SARS-CoV) RBD-Fc and human immunodeficiency virus type 1 (HIV-1) gp120-Fc were purified from supernatants of transfected human embryonic kidney (HEK)

293T cells. 17-432-Fc, truncation variants, and control proteins were quantified, normalized for expression, and visualized by Coomassie staining

Equivalent concentrations of each truncation variant (100 nM) were incubated with filovirus-permissive African green monkey kidney epithelial (Vero E6) and HEK 293T cells, and with filovirus-resistant human acute T-cell leukemia Jurkat E6-1 lymphocytes (51). Cell-surface association of each variant was determined by flow cytometry. The receptor-binding domain (RBD) of the SARS-CoV S protein (residues 318-510) and human immunodeficiency virus type 1 (HIV-1) gp120, expressed as Fc-fusion proteins (SARS-CoV RBD-Fc, HIV-1 gp120-Fc), were used as controls (55, 304). As previously reported, SARS-CoV RBD-Fc efficiently bound SARS-CoV-permissive Vero E6 cells, which naturally express the SARS-CoV receptor, angiotensin-converting enzyme 2 (ACE2) (167). Moreover, SARS-CoV RBD-Fc did not bind to HEK 293T cells or Jurkat E6-1 lymphocytes, which express only minute amounts of ACE2, if any (167). Also expectedly, HIV-1 gp120-Fc bound Jurkat E6-1 lymphocytes, which naturally express the principle HIV-1 receptor CD4, but not to Vero E6 or HEK 293T cells, which do not (61, 154). All 28 MARV-Mus GP₁ truncation variants bound to Vero E6 and HEK 293T cells with varying efficiencies (Figures 7-3 and 7-4), whereas little or no association was observed with Jurkat E6-1 lymphocytes in most cases (Figure 7-5). Successive truncation of the C-termini of MARV-Mus GP₁ variants initiated with residues 17, 38, 61 or 87 led to successively increased cell-surface binding to Vero E6 cells, up through the C-terminal truncation at residue 188 (Figure 7-3). Further truncation beyond residue 188 decreased cell association. A single exception to this trend was observed with variant 87-432-Fc, which bound Vero E6 cells with higher affinity than 87-308-Fc and 87-265-Fc. In general, variants initiated with residues 38, 61, and 87 bound more efficiently than those initiated with residues 17, with MARV-Mus 38-188-Fc consistently binding most efficiently to Vero E6 and 293T cells (Figures 7-3 and 7-4). These data identify a cell surface-binding region of MARV-Mus GP₁, located between residues 38 and 188.

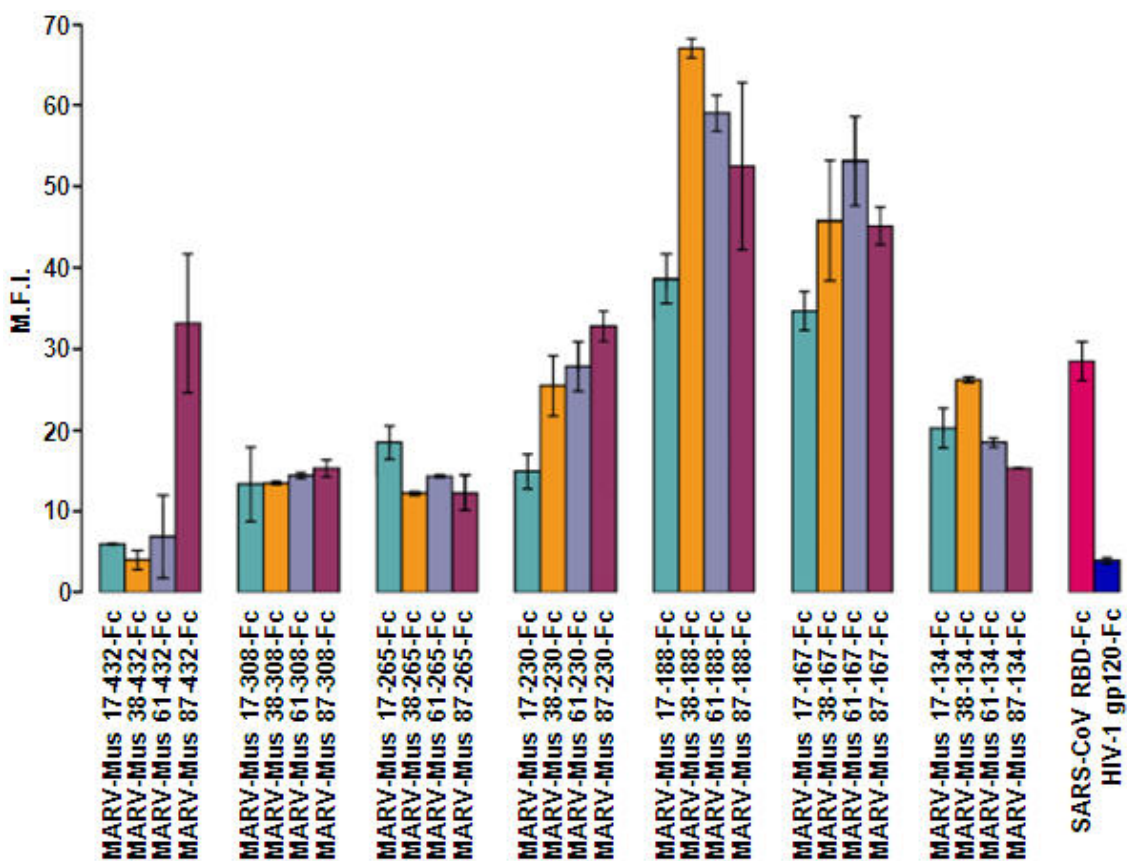


Figure 7-3. Binding of Lake Victoria marburgvirus isolate Musoke GP₁-Fc (17-432-Fc) and GP₁-Fc truncation variants to the surface of filovirus-permissive nonhuman primate cells

100 nM of the indicated Lake Victoria marburgvirus isolate Musoke (MARV-Mus) GP₁-Fc constructs and control proteins were incubated on ice with filovirus-permissive African green monkey kidney epithelial (Vero E6) cells. Fc-construct binding to the cell surface was analyzed by flow cytometry using an Fc-specific fluorescein isothiocyanate-conjugated secondary antibody. Bars indicate mean fluorescence intensity (M.F.I.) averages of two or more experiments. Error bars indicate standard deviations

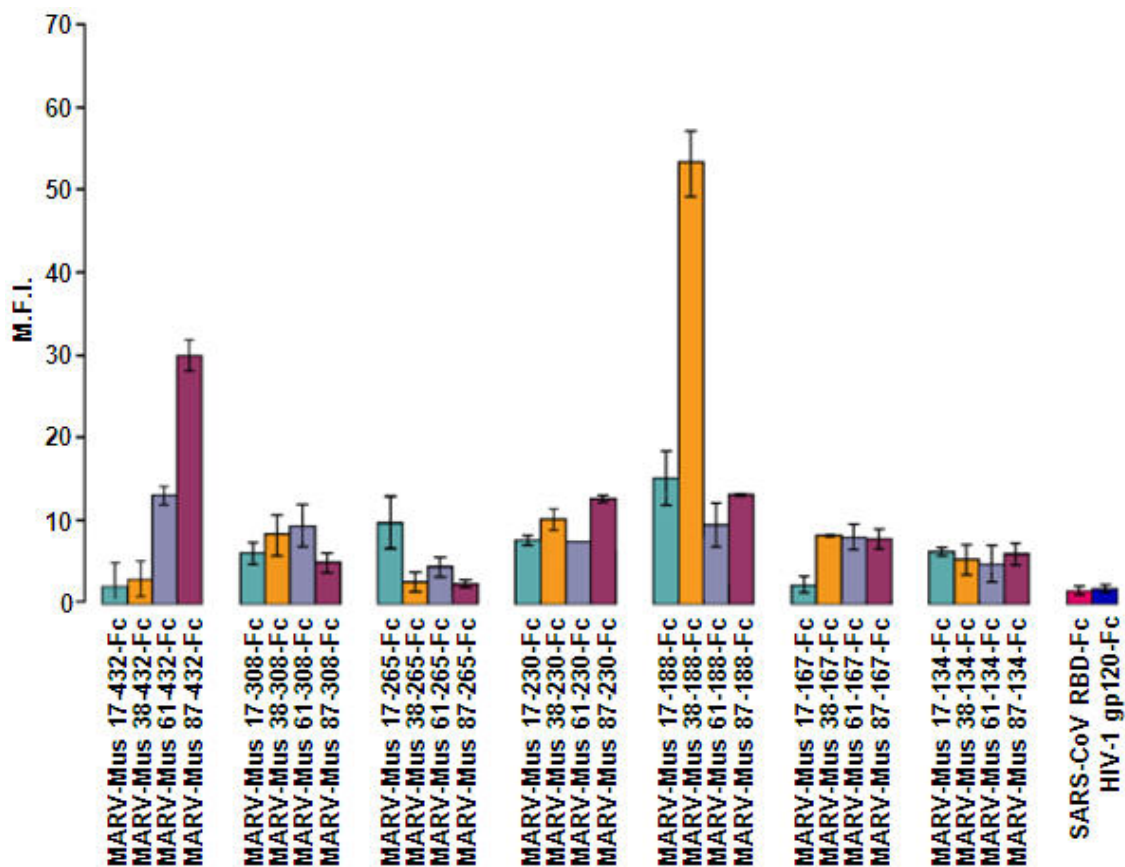


Figure 7-4. Binding of Lake Victoria marburgvirus isolate Musoke GP₁-Fc (17-432-Fc) and GP₁-Fc truncation variants to the surface of filovirus-permissive human cells

100 nM of the indicated Lake Victoria marburgvirus isolate Musoke (MARV-Mus) GP₁-Fc constructs and control proteins were incubated on ice with filovirus-permissive human embryonic kidney (HEK) 293T cells. Fc construct binding to the cell surface was analyzed by flow cytometry using an Fc-specific fluorescein isothiocyanate-conjugated secondary antibody. Bars indicate mean fluorescence intensity (M.F.I.) averages of two or more experiments. Error bars indicate standard deviations. Similar results were also obtained with filovirus-permissive human cervical adenocarcinoma epithelial-like (HeLa) cells (data not shown)

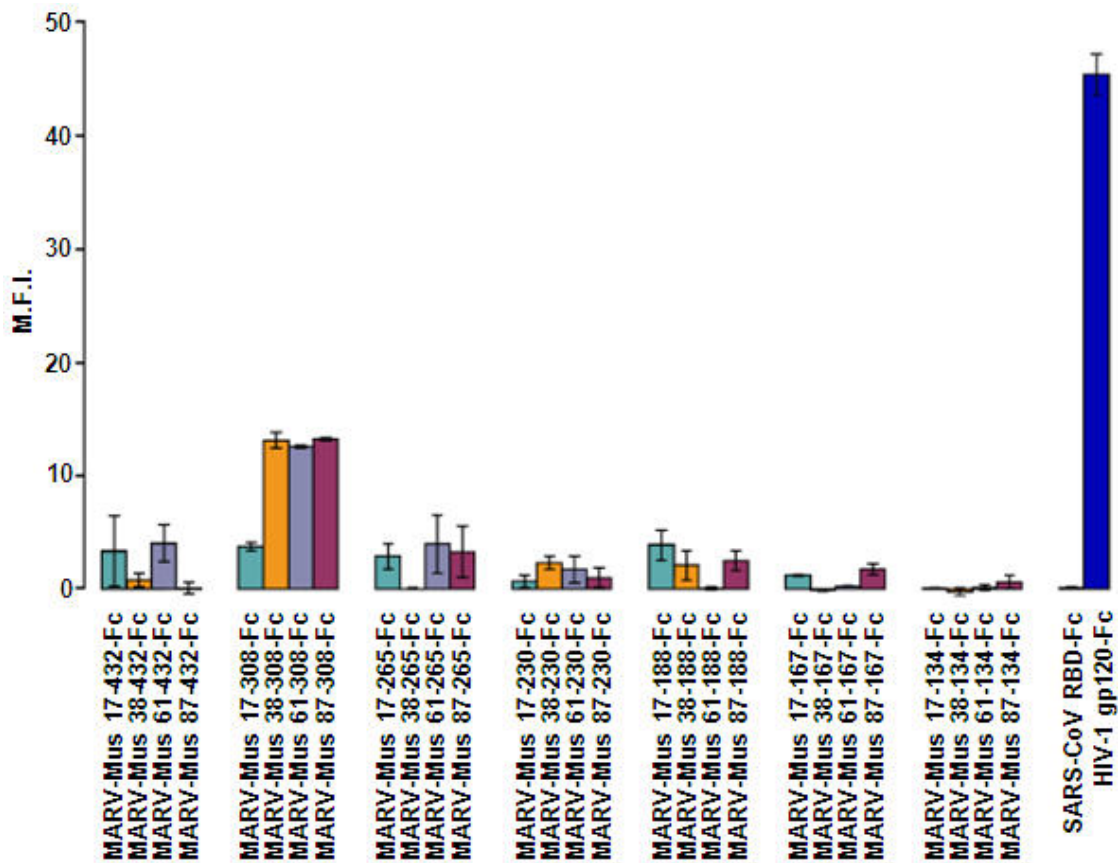


Figure 7-5. Binding of Lake Victoria marburgvirus isolate Musoke GP₁-Fc (17-432-Fc) and GP₁-Fc truncation variants to the surface of filovirus-resistant human cells

100 nM of the indicated Lake Victoria marburgvirus isolate Musoke (MARV-Mus) GP₁-Fc constructs and control proteins were incubated on ice with filovirus-resistant human acute T-cell leukemia Jurkat E6-1 lymphocytes. Fc construct binding to the cell surface was analyzed by flow cytometry using an Fc-specific fluorescein isothiocyanate-conjugated secondary antibody. Bars indicate mean fluorescence intensity (M.F.I.) averages of two or more experiments. Error bars indicate standard deviations. Similar results were also obtained with filovirus-resistant human MT-4 and SupT1 lymphocytes (data not shown)

7.1.2 Zaire ebolavirus isolate Mayinga GP₁ truncation variant 54-201-Fc binds to filovirus-permissive cells more efficiently than mucin-like domain-deleted GP₁

Another goal of the research described in this dissertation was to evaluate whether the Zaire ebolavirus spike-protein ectodomain GP₁ contains a cell-binding region comparable to that

identified for MARV-Mus. To determine the location of the Zaire ebolavirus isolate Mayinga (ZEBOV-May) GP₁ cell-binding region, a codon-optimized gene was synthesized *in vitro* that encodes the mature ZEBOV GP₁ protein, lacking its mucin-like domain (residues 309-497) that has been determined as unnecessary for ZEBOV cell entry (141, 173, 183, 315), and fused to the IgG₁ Fc region (33-308-Fc). Three sets of four truncation variants, starting at N-terminal residues 33, 54 or 76, and ending at C-terminal residues 308, 201, 172 or 156, were created (Figure 7-6). Variant 76-172-Fc, as well as five additionally created variants (33-267-Fc, 33-237-Fc, 78-308-Fc, 100-308-Fc, and 149-308-Fc), could not be expressed in sufficient quantities for follow-up experiments. All other truncation variants expressed sufficiently (Figure 7-7).

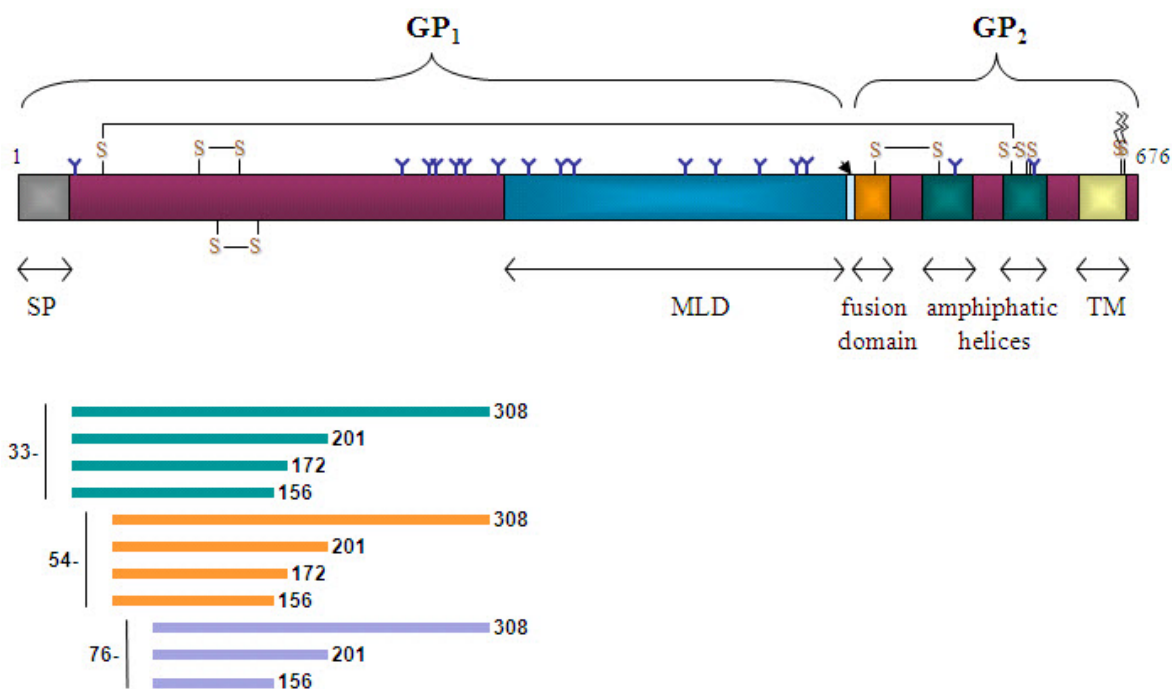


Figure 7-6. Zaire ebolavirus isolate Mayinga GP₁ and GP₁ truncation variants

Representation of Zaire ebolavirus isolate Mayinga (ZEBOV-May) GP₁ truncation variants in relation to the full-length ZEBOV-May GP_{1,2} envelope spike protein (amino-acid residues 1-676). SP, signal peptide; MLD, mucin-like domain; TM, transmembrane domain. Cysteine residues (-SH), predicted or experimentally confirmed disulfide bonds (-

S-S-), potential *N*-glycosylation sites (blue Ys), and the furin cleavage site (141, 278) are indicated. Truncation variants 76-172-Fc, 33-276-Fc, 33-237-Fc, 78-308-Fc, 100-308-Fc, and 149-308-Fc did not express to sufficient levels for further experiments and therefore are not illustrated in this figure

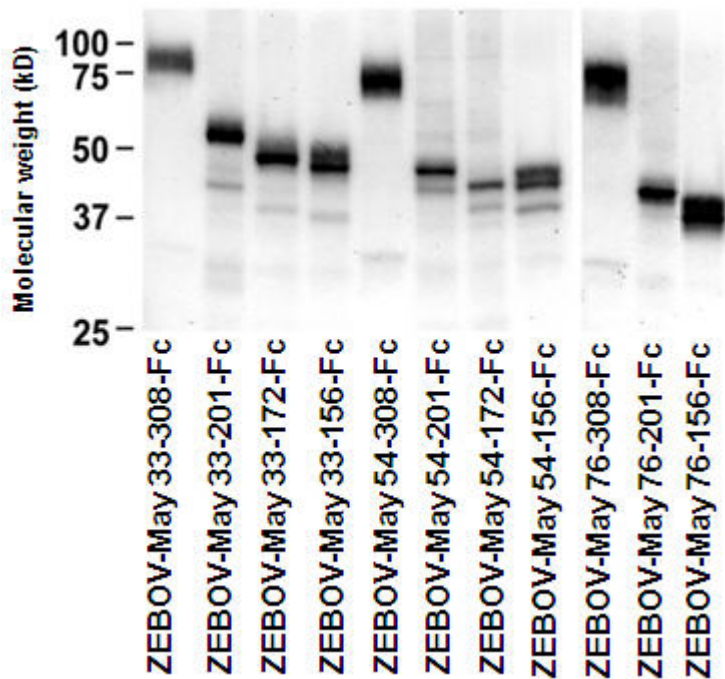


Figure 7-7. Expression of Zaire ebolavirus isolate Mayinga GP₁ and GP₁ truncation variants

Mucin-like domain-deleted Zaire ebolavirus isolate Mayinga (ZEBOV-May) GP₁-Fc, containing GP₁ residues 33-308 fused to the Fc region of human IgG₁ (33-308-Fc) or truncation variants of 33-308-Fc containing the indicated GP₁ residues were purified from supernatants of transfected human embryonic kidney (HEK) 293T cells. 33-308-Fc and truncation variants were quantified, normalized for expression, and visualized by Coomassie staining

As with the MARV-Mus GP₁ truncation variants, equivalent concentrations of each ZEBOV GP₁ truncation variant (100 nM) were incubated with filovirus-permissive Vero E6 and HEK 293T cells, and with filovirus-resistant Jurkat E6-1 lymphocytes (51), and cell association was assayed by flow cytometry. All eleven expressed ZEBOV-May GP₁

variants bound to Vero E6 (Figure 7-8) and HEK 293T cells (Figure 7-9), whereas binding to Jurkat E6-1 lymphocytes was negligible in all cases (Figure 7-10). The ZEBOV-May GP₁ truncation variants showed a pattern of association to Vero E6 and HEK 293T cells similar to that observed with MARV-Mus GP₁ variants. In particular, ZEBOV-May 54-201-Fc and 76-201-Fc bound filovirus-permissive cells more efficiently than all other ZEBOV-May GP₁ variants assayed, with 54-201-Fc binding slightly but consistently better than 76-201-Fc. These data identify a cell-binding region of ZEBOV-May, located between GP₁ residues 54 and 201.

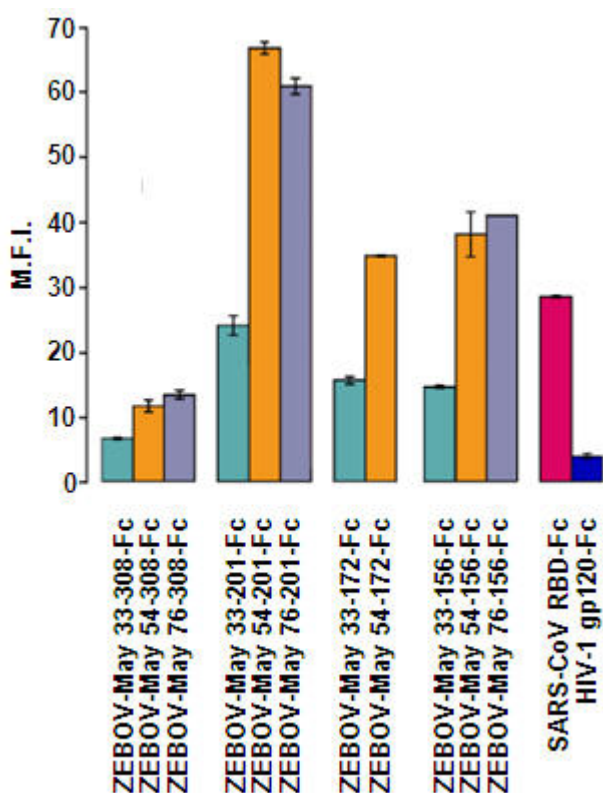


Figure 7-8. Binding of Zaire ebolavirus isolate Mayinga mucin-like domain-deleted GP₁-Fc (33-308-Fc) and GP₁-Fc truncation variants to the surface of filovirus-permissive nonhuman primate cells

100 nM of the indicated Zaire ebolavirus isolate Mayinga (ZEBOV-May) GP₁-Fc constructs and control proteins were incubated on ice with filovirus-permissive African green monkey kidney epithelial (Vero E6) cells. Fc construct binding to the cell surface

was analyzed by flow cytometry using an Fc-specific fluorescein isothiocyanate-conjugated secondary antibody. Bars indicate mean fluorescence intensity (M.F.I.) averages of two or more experiments. Error bars indicate standard deviations

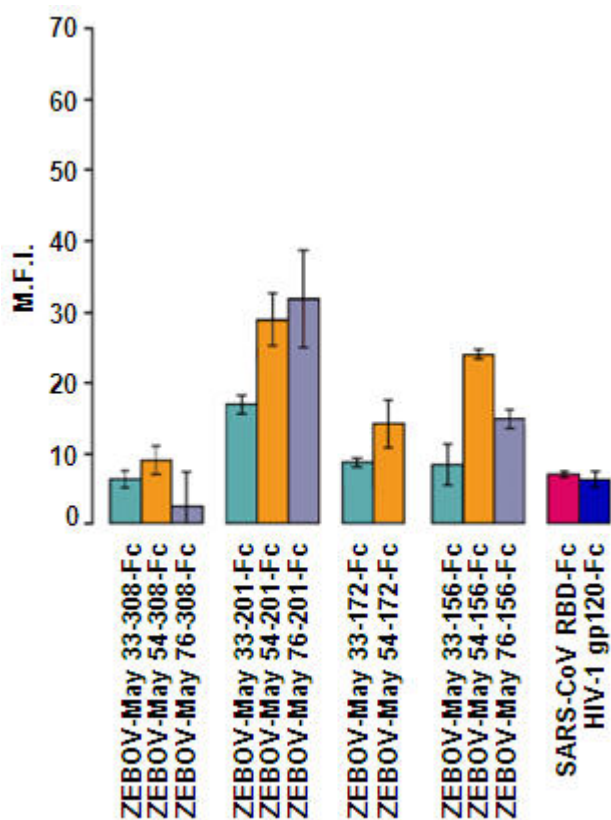


Figure 7-9. Binding of Zaire ebolavirus isolate Mayinga mucin-like domain-deleted GP₁-Fc (33-308-Fc) and GP₁-Fc truncation variants to the surface of filovirus-permissive human cells

100 nM of the indicated Zaire ebolavirus isolate Mayinga (ZEBOV-May) GP₁-Fc constructs and control proteins were incubated on ice with filovirus-permissive human embryonic kidney (HEK) 293T cells. Fc construct binding to the cell surface was analyzed by flow cytometry using an Fc-specific fluorescein isothiocyanate-conjugated secondary antibody. Bars indicate mean fluorescence intensity (M.F.I.) averages of two or more experiments. Error bars indicate standard deviations. Similar results were also obtained with filovirus permissive human cervical adenocarcinoma epithelial-like (HeLa) cells (data not shown)

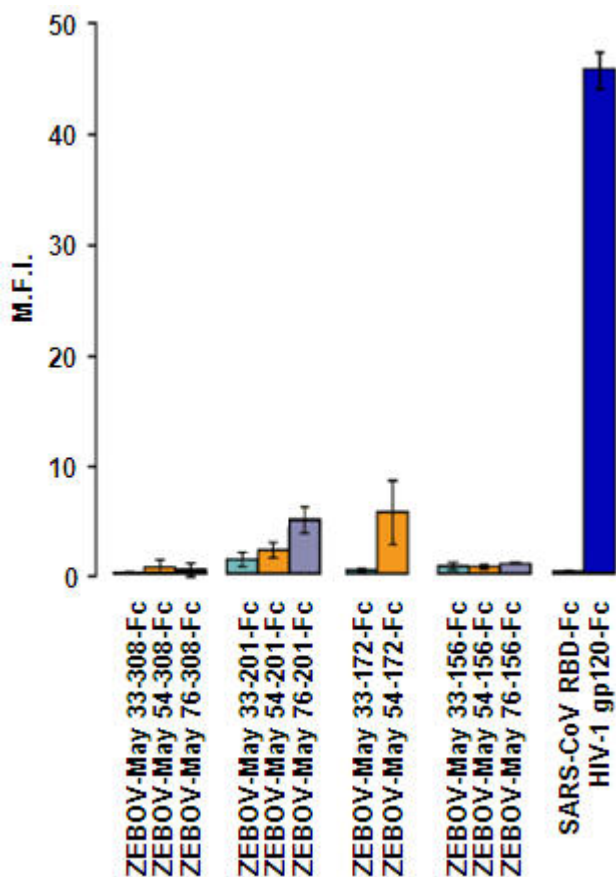


Figure 7-10. Binding of Zaire ebolavirus isolate Mayinga mucin-like domain-deleted GP₁-Fc (33-308-Fc) and GP₁-Fc truncation variants to the surface of filovirus-resistant human cells

100 nM of the indicated Zaire ebolavirus isolate Mayinga (ZEBOV-May) GP₁-Fc constructs and control proteins were incubated on ice with filovirus-resistant human acute T-cell leukemia Jurkat E6-1 lymphocytes. Fc construct binding to the cell surface was analyzed by flow cytometry using an Fc-specific fluorescein isothiocyanate-conjugated secondary antibody. Bars indicate mean fluorescence intensity (M.F.I.) averages of two or more experiments. Error bars indicate standard deviations. Similar results were also obtained with filovirus-resistant human MT-4 and SupT1 lymphocytes (data not shown)

7.1.3 Lake Victoria marburgvirus isolate Angola and Musoke GP₁ truncation variants bind to filovirus-permissive cells with comparable efficiency

The largest and most severe MARV disease outbreak to date occurred in Angola in early 2005 (129, 135, 311, 313). Studies revealed that the MARV Angola isolate (MARV-Ang) is more virulent than the Musoke isolate (MARV-Mus) in nonhuman primate models (99), but the molecular basis for this observation remains unclear. The spike-protein amino-acid sequence of the MARV-Ang isolate is very similar to that of the MARV-Mus isolate (269). In particular, a comparison between the MARV-Mus GP₁ cell-binding region (residues 38-188) with the corresponding region of MARV-Ang yielded only one amino-acid change, at position 74 (T₇₄→A). Using site-directed mutagenesis, plasmids encoding MARV-Mus 38-188-Fc, 38-167-Fc, 61-188-Fc, and 61-167-Fc were altered to express the corresponding Angola proteins (MARV-Ang 38-188-Fc, 38-167-Fc, 61-188-Fc, and 61-167-Fc; Figure 7-11). Cell association of each of these variants was compared with those of MARV-Mus in assays similar to those described above. Each MARV-Ang variant bound Vero E6 cells slightly less efficiently than its MARV-Mus counterpart (Figure 7-12). These data exclude the possibility that more efficient cellular association of the MARV-Ang cell-binding region contributes to increased severity of disease.

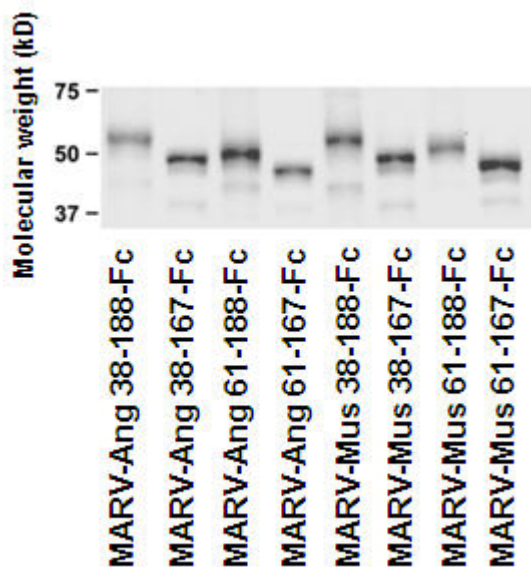


Figure 7-11. Expression of Lake Victoria marburgvirus isolate Musoke and isolate Angola GP₁-Fc truncation variants

Lake Victoria marburgvirus isolate Angola (MARV-Ang) GP₁-Fc truncation variants, differing from corresponding isolate Musoke (MARV-Mus) GP₁-Fc truncation variants at residue 74 (threonine for MARV-Mus; alanine for MARV-Ang), were quantified, normalized for expression, and visualized by Coomassie staining

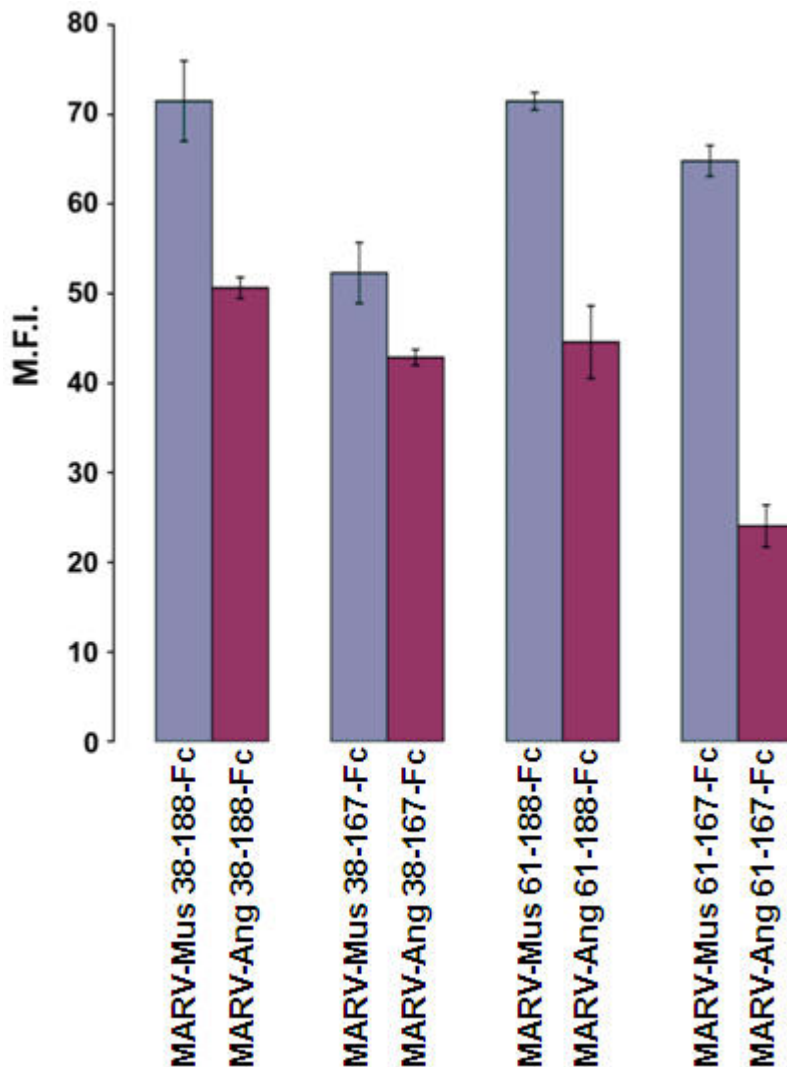


Figure 7-12. Comparison of the cell surface-binding affinities of Lake Victoria marburgvirus isolate Musoke and isolate Angola GP₁-Fc truncation variants

100 nM of the indicated Lake Victoria marburgvirus isolate Musoke (MARV-Mus) and isolate Angola (MARV-Ang) GP₁-Fc constructs were incubated with filovirus-permissive African green monkey kidney epithelial (Vero E6) cells and analyzed by flow cytometry using an Fc-specific fluorescein isothiocyanate-conjugated secondary antibody. Bars indicate mean fluorescence intensity (M.F.I.) averages of two or more experiments. Error bars indicate standard deviations

7.1.4 Both Lake Victoria marburgvirus isolate Musoke GP₁ truncation variant 38-188-Fc and Zaire ebolavirus isolate Mayinga GP₁ truncation variant 54-201-Fc specifically inhibit entry of gammaretroviruses pseudotyped with functional spike proteins of either filovirus

The ability of the MARV-Mus 38-188-Fc and ZEBOV-May 54-201-Fc proteins to inhibit entry of pseudotyped gammaretrovirus particles was assayed to determine if the identified GP₁ cell-binding regions of MARV-Mus (Chapter 7.1.1) and ZEBOV-May (Chapter 7.1.2) associate specifically with cell-surface factors necessary for infection. A Moloney murine leukemia virus (MLV) vector expressing enhanced green fluorescent protein (eGFP) (192) was pseudotyped with GP_{1,2} of MARV-Mus (MARV/MLV), with mucin-like domain-deleted GP_{1,2Δ309-489} of ZEBOV-May (ZEBOV/MLV) or with the G protein of vesicular stomatitis Indiana virus (VSIV/MLV control). Vero E6 cells, which are permissive to infection with MARV (unknown receptor), ZEBOV (unknown receptor), and VSIV (cell-membrane lipid receptor) were incubated with varying concentrations of MARV-Mus 38-188-Fc (unknown cell-surface binding partner), ZEBOV-May 54-201-Fc (unknown cell-surface binding partner) or SARS-CoV RBD-Fc control (binds to angiotensin-converting enzyme 2, ACE2) and the different pseudotyped gammaretrovirus particles. As expected, no Fc fusion protein inhibited VSIV/MLV cell entry (Figure 7-15). However, both MARV-Mus 38-188-Fc and ZEBOV-May 54-201-Fc efficiently inhibited both MARV/MLV (Figure 7-13) and ZEBOV/MLV cell entry (Figure 7-14) in a dose-dependent manner. Also as expected, SARS-CoV RBD-Fc did not inhibit infection of either pseudotyped virus (Figures 7-13, 7-14, and 7-15), thereby excluding a role of ACE2 in filovirus cell entry. MARV-Mus 38-188-Fc was the more potent of the two cell-binding regions, inhibiting MARV/MLV and ZEBOV/MLV with an apparent 50% inhibitory concentration (IC₅₀) of ~40 nM and ~120 nM in this assay, respectively (Figures 7-13 and 7-14). These data indicate that MARV-Mus 38-188-Fc and ZEBOV-May 54-201-Fc bind specifically to a common cell-surface factor critical to filovirus entry. Accordingly, and by analogy with

other viral entry proteins, these cell-binding regions of MARV-Mus and ZEBOV-May GP₁ can be referred to as receptor-binding regions (RBRs).

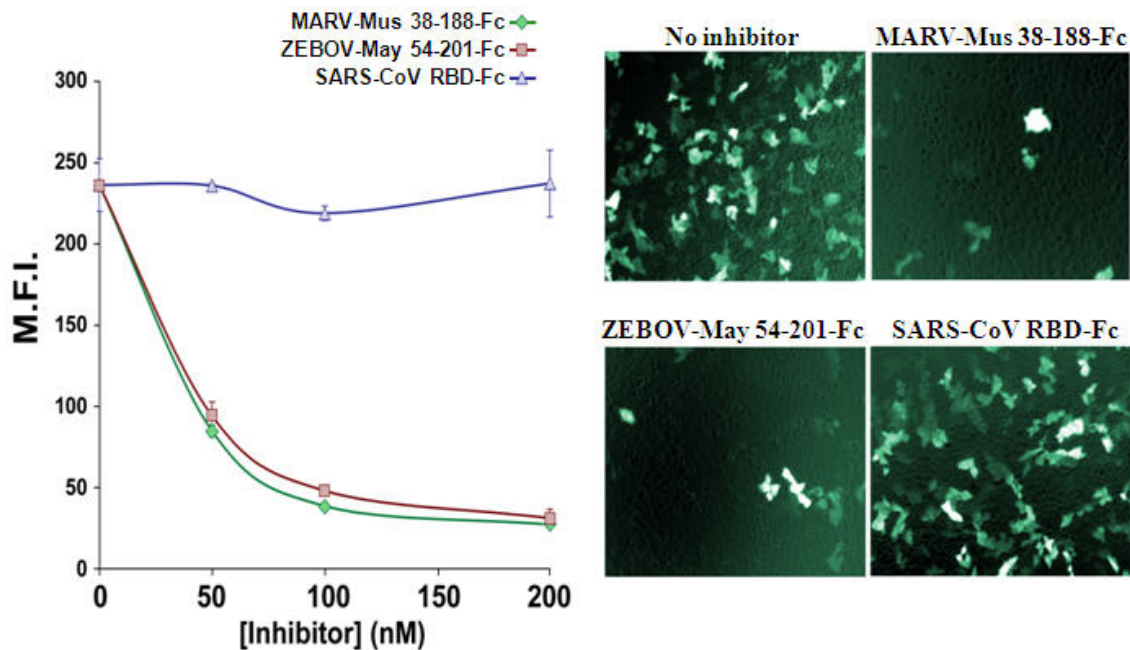


Figure 7-13. Lake Victoria marburgvirus isolate Musoke GP₁ truncation variant 38-188-Fc and Zaire ebolavirus isolate Mayinga GP₁ truncation variant 54-201-Fc inhibit Lake Victoria marburgvirus isolate Musoke GP_{1,2}-mediated entry of gammaretrovirus particles

The indicated concentrations of Lake Victoria marburgvirus isolate Musoke (MARV-Mus) GP₁ truncation variant 38-188-Fc, Zaire ebolavirus isolate Mayinga (ZEBOV-May) GP₁ truncation variant 54-201-Fc, and severe acute respiratory syndrome coronavirus (SARS-CoV) RBD-Fc protein were incubated with filovirus-permissive African green monkey kidney epithelial (Vero E6) cells together with enhanced green fluorescent protein-expressing Moloney murine leukemia virus (MLV) particles pseudotyped with MARV-Mus GP_{1,2}. Entry of pseudotyped MLV was quantified by measuring green fluorescence using flow cytometry. Bars indicate mean fluorescence intensity (M.F.I.) averages of two or more experiments. Error bars indicate standard deviations

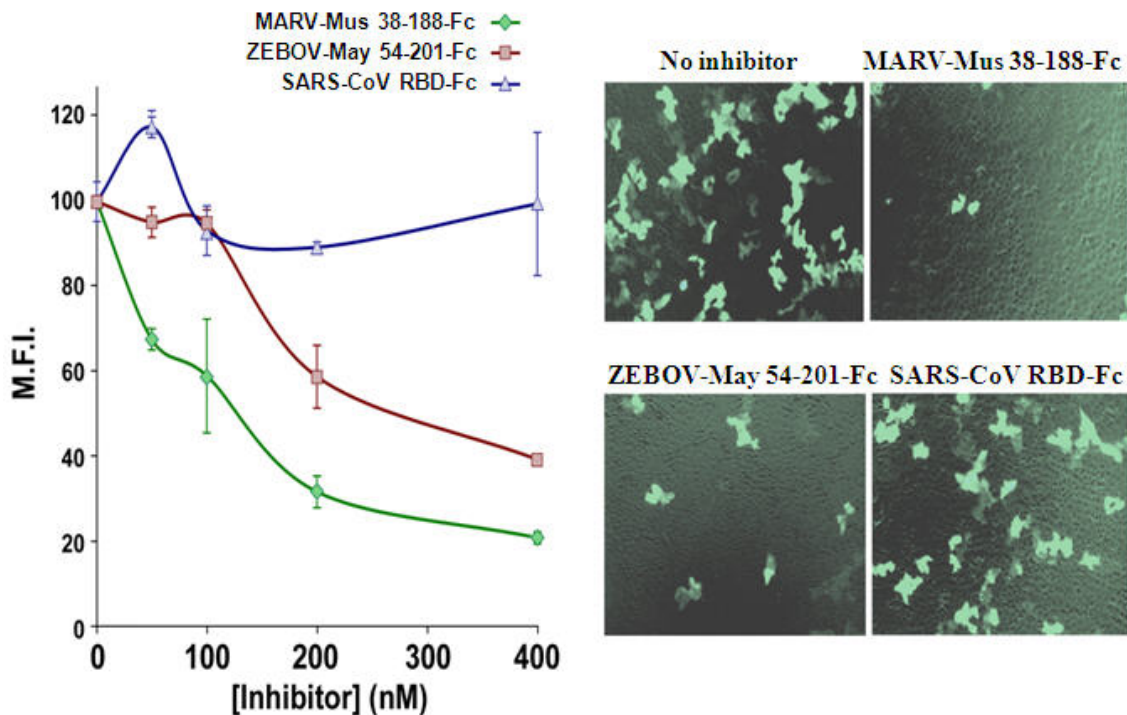


Figure 7-14. Lake Victoria marburgvirus isolate Musoke GP₁ truncation variant 38-188-Fc and Zaire ebolavirus isolate Mayinga GP₁ truncation variant 54-201-Fc inhibit Zaire ebolavirus isolate Mayinga GP_{1,2Δ309-489}-mediated entry of gammaretrovirus particles

The indicated concentrations of Lake Victoria marburgvirus isolate Musoke (MARV-Mus) GP₁ truncation variant 38-188-Fc, Zaire ebolavirus isolate Mayinga (ZEBOV-May) GP₁ truncation variant 54-201-Fc, and severe acute respiratory syndrome coronavirus (SARS-CoV) RBD-Fc protein were incubated with filovirus-permissive African green monkey kidney epithelial (Vero E6) cells together with enhanced green fluorescent protein-expressing Moloney murine leukemia virus (MLV) particles pseudotyped with ZEBOV-May GP_{1,2Δ309-489}. Entry of pseudotyped MLV was quantified by measuring green fluorescence using flow cytometry. Bars indicate mean fluorescence intensity (M.F.I.) averages of two or more experiments. Error bars indicate standard deviations

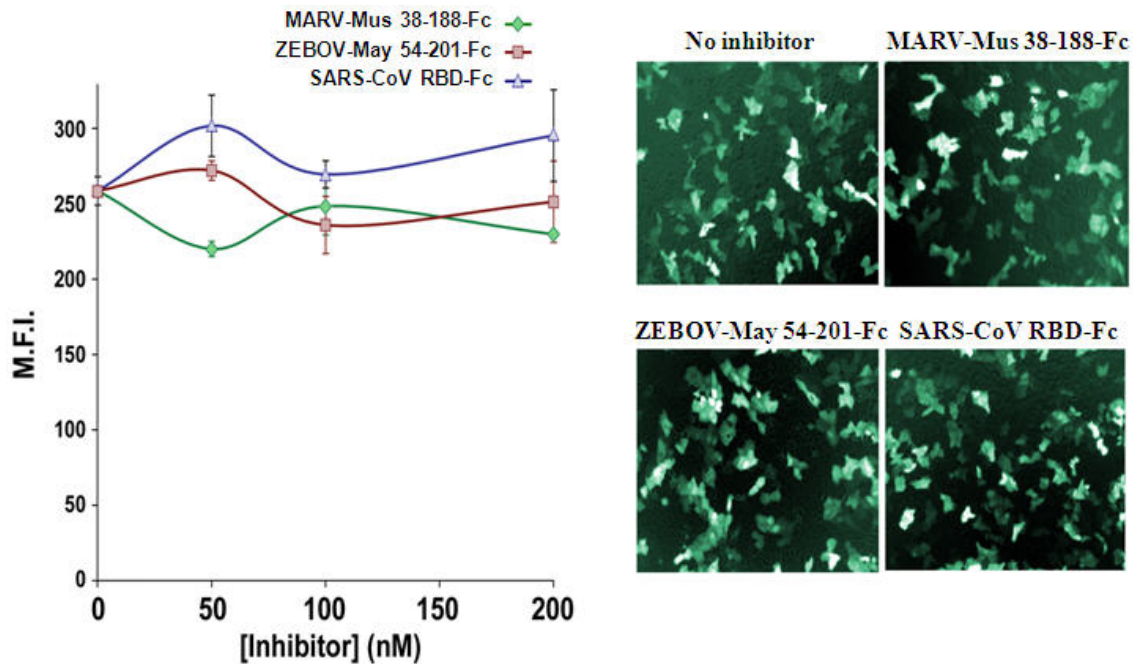


Figure 7-15. Lake Victoria marburgvirus isolate Musoke GP₁ truncation variant 38-188-Fc and Zaire ebolavirus isolate Mayinga GP₁ truncation variant 54-201-Fc do not inhibit vesicular stomatitis Indiana virus G-mediated entry of gammaretrovirus particles

The indicated concentrations of Lake Victoria marburgvirus isolate Musoke (MARV-Mus) GP₁ truncation variant 38-188-Fc, Zaire ebolavirus isolate Mayinga (ZEBOV-May) GP₁ truncation variant 54-201-Fc, and severe acute respiratory coronavirus (SARS-CoV) RBD-Fc protein were incubated with filovirus-permissive African green monkey kidney epithelial (Vero E6) cells together with enhanced green fluorescent protein-expressing Moloney murine leukemia virus (MLV) particles pseudotyped with vesicular stomatitis Indiana virus (VSIV) G. Entry of pseudotyped MLV was quantified by measuring green fluorescence using flow cytometry. Bars indicate mean fluorescence intensity (M.F.I.) averages of two or more experiments. Error bars indicate standard deviations

7.1.5 Both Lake Victoria marburgvirus isolate Musoke and isolate Angola 38-188 Fc inhibit entry of gammaretrovirus particles pseudotyped with Lake Victoria marburgvirus isolate Musoke GP_{1,2} more efficiently than other GP₁ truncation variants

One question arising from the results described above was whether the cell-binding efficiency of MARV-Mus and MARV-Ang GP₁ truncation variants correlated with their ability to inhibit entry of pseudotyped gammaretrovirus particles. Vero E6 cells were incubated with the GP₁-Fc truncation variants and with MARV/MLV or VSIV/MLV. None of the GP₁-Fc truncation variants inhibited VSIV/MLV cell entry, whereas most of the MARV-Mus GP₁ variants assayed inhibited cell entry of MARV/MLV, albeit to different degrees (Figure 7-16). In some cases, there was no correlation between entry inhibition and cell-binding. Notably, full-length MARV-Mus GP₁ (17-432-Fc) inhibited MARV/MLV entry as efficiently as the defined receptor-binding regions of MARV-Mus and MARV-Ang (38-188-Fc), although almost no cell surface-binding of 17-432-Fc was observed (Figures 7-3 and 7-4). Apart from this interesting exception, the MARV-Mus RBR-Fc inhibited entry more efficiently than any other GP₁ variant assayed. Importantly, the MARV-Ang and MARV-Mus RBR-Fcs inhibited transduction to comparable levels. Together, these data show that variants of the MARV-Mus RBR that are slightly longer or shorter inhibit MARV/MLV less efficiently, consistent with their relatively lower affinity for filovirus-permissive cell lines.

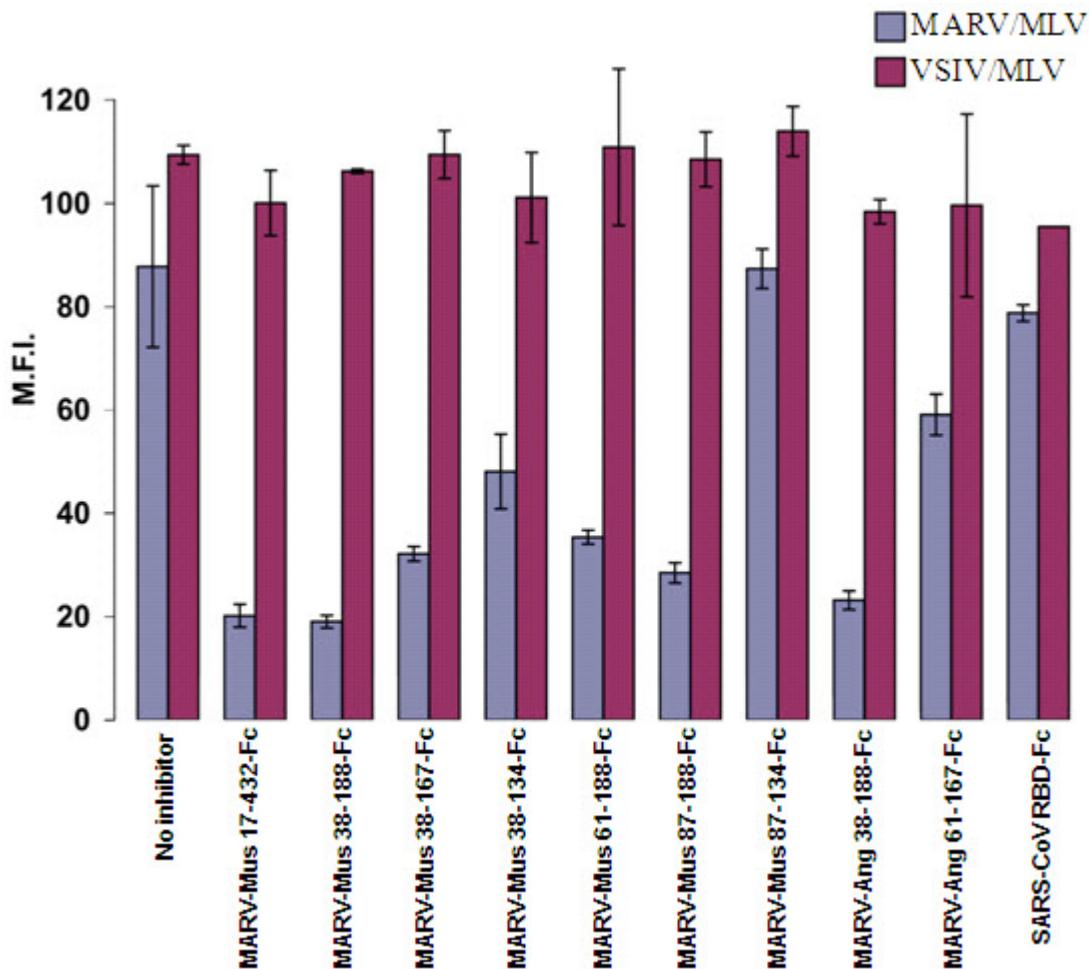


Figure 7-16. Comparison of the inhibitory effects of Lake Victoria marburgvirus isolate Musoke and Angola GP₁-Fc truncation variants on cell-entry of gammaretrovirus particles pseudotyped with Lake Victoria marburgvirus isolate Musoke GP_{1,2}

100 nM of the indicated Lake Victoria marburgvirus isolate Musoke (MARV-Mus) or isolate Angola (MARV-Ang) GP₁-Fc truncation variants or severe acute respiratory syndrome coronavirus (SARS-CoV) RBD-Fc were incubated with filovirus-permissive African green monkey kidney epithelial (Vero E6) cells together with enhanced green fluorescent protein-expressing Moloney murine leukemia virus (MLV) particles pseudotyped with MARV-Mus GP_{1,2} or VSIV G. Entry of pseudotyped MLV was quantified by measuring green fluorescence using flow cytometry. Bars indicate mean fluorescence intensity (M.F.I.) averages of two or more experiments. Error bars indicate standard deviations

7.1.6 Lake Victoria marburgvirus isolate Musoke 38-188-Fc and Zaire ebolavirus isolate Mayinga 54-201-Fc inhibit the replication of infectious Zaire ebolavirus

To determine whether the identified MARV and ZEBOV RBR-Fc proteins also inhibit infectious filoviruses, Vero E6 cells were preincubated with MARV-Mus 38-188-Fc, ZEBOV-May 54-201-Fc or SARS-CoV RBD-Fc. After washing, cells were infected with infectious Zaire ebolavirus isolate Mayinga, modified to express eGFP (270), at a multiplicity of infection (moi) of 1. Viral replication, measured as percentage of infected cells, was specifically inhibited by both filovirus RBRs, but not by SARS-CoV RBD-Fc (Figure 7-17). As observed with pseudotyped gammaretrovirus particles, MARV-Mus 38-188-Fc inhibited infectious ZEBOV-May more efficiently than ZEBOV-May 54-201-Fc. Similar inhibition of ZEBOV-May replication was observed in primary monocyte-derived human dendritic cells treated with ZEBOV-May 54-201-Fc or MARV-Mus 38-188-Fc (experiment performed by Sina Bavari's and M. Javad Aman's teams, data not shown). The efficiency with which MARV-Mus 38-188-Fc inhibited ZEBOV-May replication is consistent with the utilization of a common entry factor by marburgviruses and ebolaviruses.

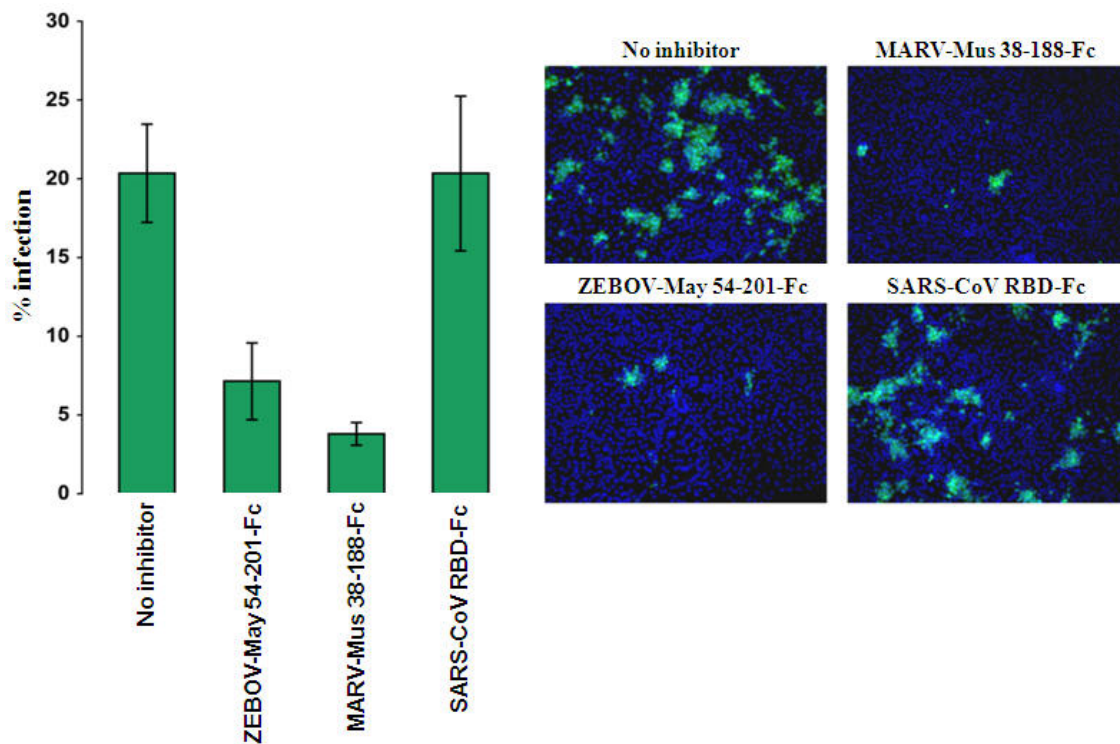


Figure 7-17. Lake Victoria marburgvirus isolate Musoke GP₁ truncation variant 38-188-Fc and Zaire ebolavirus isolate Mayinga GP₁ truncation variant 54-201-Fc inhibit replication of infectious Zaire ebolavirus isolate Mayinga

800 nM of Lake Victoria marburgvirus isolate Musoke (MARV-Mus) GP₁ truncation variant 38-188-Fc, Zaire ebolavirus isolate Mayinga (ZEBOV-May) GP₁ truncation variant 54-201-Fc or severe acute respiratory syndrome coronavirus (SARS-CoV) RBD-Fc were incubated with recombinant, enhanced green fluorescent protein-expressing Zaire ebolavirus isolate Mayinga. Infection was quantified by measuring green fluorescence using Discovery-1 automated microscopy. Bars indicate percentage of infected cells, averaged over three experiments. Error bars indicate standard deviations

7.1.7 All filoviruses use a common cell-entry factor

The results above suggested that all filoviruses may use a common-cell entry factor. To test this hypothesis, open reading frames were cloned that encode Côte d'Ivoire ebolavirus isolate Côte d'Ivoire, Reston ebolavirus isolate Pennsylvania, and Sudan ebolavirus isolate Gulu GP₁ residues analogous to ZEBOV-May GP₁ residues 54-201-Fc (CIEBOV-CI 54-

201-Fc, REBOV-Pen 55-202-Fc, and SEBOV-Gul 54-201-Fc). The constructs were expressed and purified from mammalian cells (Figure 7-18).

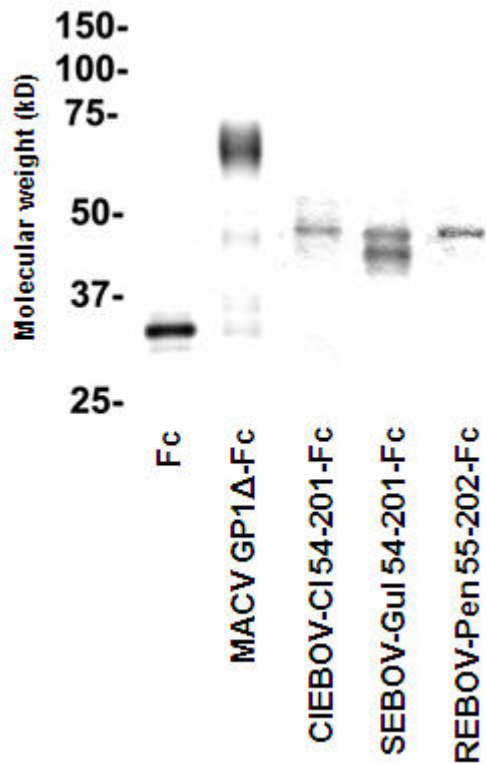


Figure 7-18. Expression of Côte d’Ivoire ebolavirus isolate Côte d’Ivoire 54-201-Fc, Reston ebolavirus isolate Pennsylvania 55-202-Fc, and Sudan ebolavirus isolate Gulu 54-201-Fc

Côte d’Ivoire ebolavirus isolate Côte d’Ivoire (CIEBOV-CI) 54-201-Fc, Reston ebolavirus isolate Pennsylvania (REBOV-Pen) 55-202-Fc, Sudan ebolavirus isolate Gulu (SEBOV-Gul) 54-201-Fc, and control proteins Fc and Machupo virus (MACV) GP1 Δ -Fc were purified from supernatants of transfected human embryonic kidney (HEK) 293T cells, quantified, normalized for expression, and visualized by Coomassie staining

Equivalent concentrations of each protein (100 nM) were incubated with Vero E6 cells, HeLa cells or Jurkat E6-1 lymphocytes, and cell-surface association of each protein was determined by flow cytometry (Figures 7-19, 7-20, and 7-21). SARS-CoV RBD-Fc and HIV-1 gp120-Fc, described in Chapter 7.1.1, as well as Fc alone, the Machupo virus

RBD (MACV GP1 Δ -Fc) (219), MARV-Mus 38-188-Fc, and ZEBOV-May 54-201-Fc were used as controls. SARS-CoV RBD-Fc, HIV-1 gp120-Fc, MARV-Mus 38-188-Fc, and ZEBOV-May 54-201-Fc behaved as expected (Figures 7-19, 7-20, and 7-21). Fc did not bind to either cell type (Figures 7-19, 7-20, and 7-21). MACV GP1 Δ -Fc bound to Vero E6 and HeLa cells (Figures 7-19 and 7-20), which express the MACV receptor, transferrin receptor 1 (TfR1), but not to Jurkat E6-1 lymphocytes, which do not (219) (Figure 7-21). CIEBOV-CI 54-201-Fc, REBOV-Pen 55-202-Fc, and SEBOV-Gul 54-201-Fc did not bind to filovirus-resistant cells (Figure 7-21), but all bound to filovirus-permissive Vero E6 and HeLa cells (Figures 7-19 and 7-20). REBOV 55-202-Fc bound these cells with higher affinity than CIEBOV-CI and SEBOV-Gul, yet all three Fc fusion proteins bound less efficiently than ZEBOV-May 54-201-Fc.

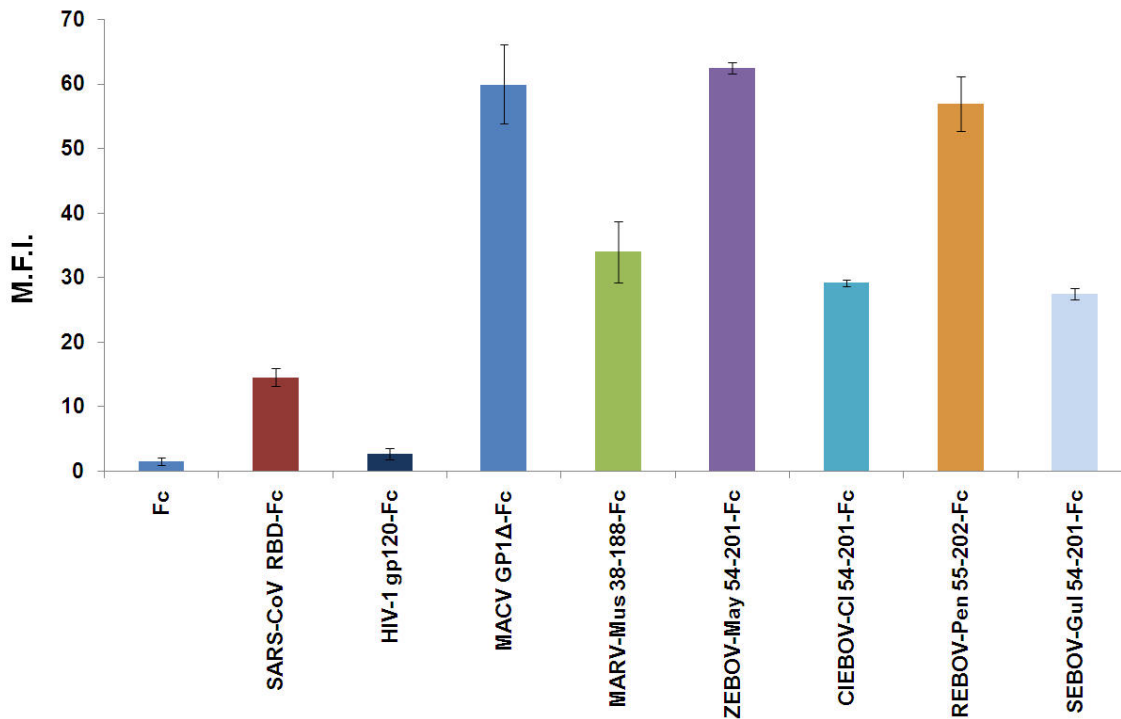


Figure 7-19. Binding of Côte d’Ivoire ebolavirus isolate Côte d’Ivoire 54-201-Fc, Reston ebolavirus isolate Pennsylvania 55-202-Fc, and Sudan ebolavirus isolate Gulu 54-201-Fc to the surface of filovirus-permissive nonhuman primate cells

100 nM of Côte d’Ivoire ebolavirus isolate Côte d’Ivoire (CIEBOV-CI) 54-201-Fc, Reston ebolavirus isolate Pennsylvania (REBOV-Pen) 55-202-Fc or Sudan ebolavirus isolate Gulu (SEBOV-Gul) 54-201-Fc, and control proteins Fc, Lake Victoria marburgvirus isolate Musoke (MARV-Mus) 38-188-Fc, Zaire ebolavirus isolate Mayinga (ZEBOV-May) 54-201-Fc, severe acute respiratory syndrome coronavirus (SARS-CoV) RBD-Fc, human immunodeficiency virus type 1 (HIV-1) gp120-Fc or Machupo virus (MACV) GP1Δ-Fc were incubated with filovirus-permissive African green monkey kidney epithelial (Vero E6) cells and analyzed by flow cytometry using an Fc-specific fluorescein isothiocyanate-conjugated secondary antibody. Bars indicate mean fluorescence intensity (M.F.I.) averages of two or more experiments. Error bars indicate standard deviations

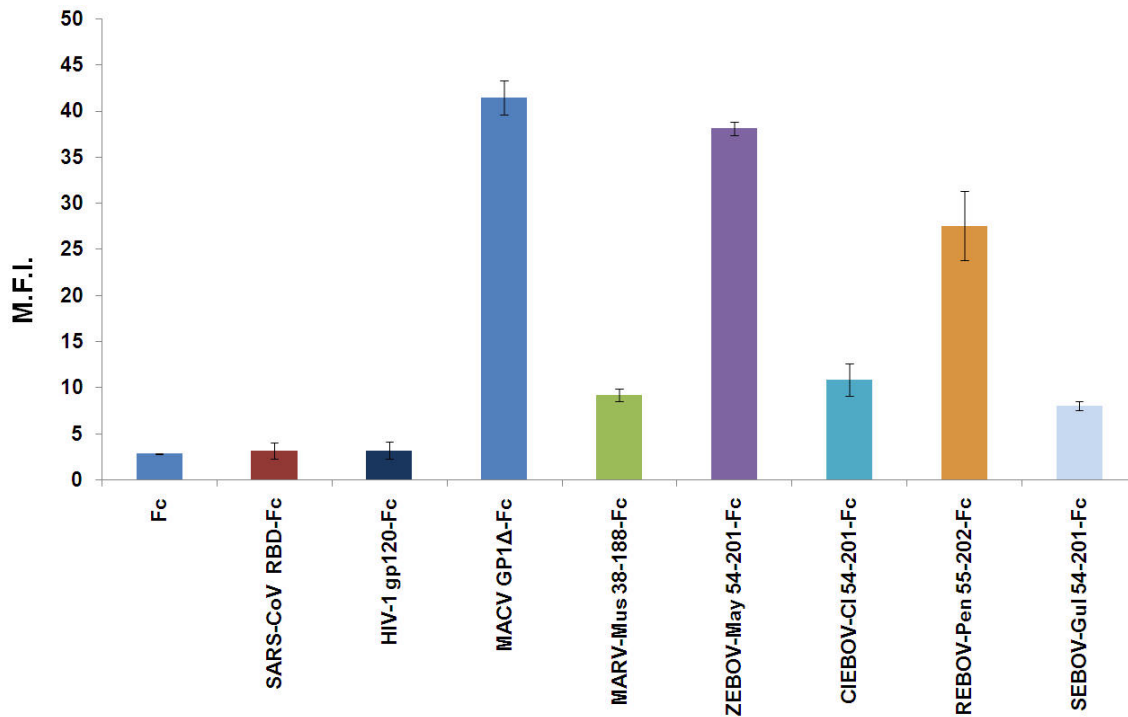


Figure 7-20. Binding of Côte d'Ivoire ebolavirus isolate Côte d'Ivoire 54-201-Fc, Reston ebolavirus isolate Pennsylvania 55-202-Fc, and Sudan ebolavirus isolate Gulu 54-201-Fc to the surface of filovirus-permissive human cells

100 nM of Côte d'Ivoire ebolavirus isolate Côte d'Ivoire (CIEBOV-CI) 54-201-Fc, Reston ebolavirus isolate Pennsylvania (REBOV-Pen) 55-202-Fc or Sudan ebolavirus isolate Gulu (SEBOV-Gul) 54-201-Fc, and control proteins Fc, Lake Victoria marburgvirus isolate Musoke (MARV-Mus) 38-188-Fc, Zaire ebolavirus isolate Mayinga (ZEBOV-May) 54-201-Fc, severe acute respiratory syndrome coronavirus (SARS-CoV) RBD-Fc, human immunodeficiency virus type 1 (HIV-1) gp120-Fc or Machupo virus (MACV) GP1Δ-Fc were incubated with filovirus-permissive cervical adenocarcinoma epithelial-like (HeLa) cells at a concentration of 100 nM, and analyzed by flow cytometry using an Fc-specific fluorescein isothiocyanate-conjugated secondary antibody. Bars indicate mean fluorescence intensity (M.F.I.) averages of two or more experiments. Error bars indicate standard deviations

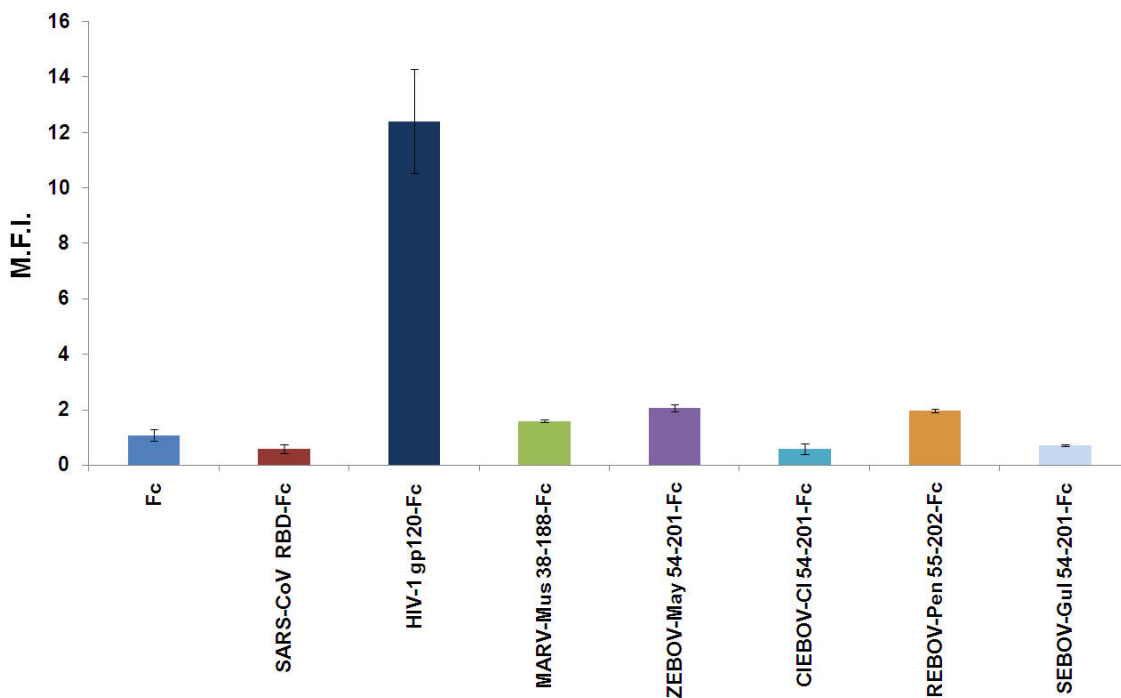


Figure 7-21. Binding of Côte d'Ivoire ebolavirus isolate Côte d'Ivoire 54-201-Fc, Reston ebolavirus isolate Pennsylvania 55-202-Fc, and Sudan ebolavirus isolate Gulu 54-201-Fc to the surface of filovirus-resistant human cells

100 nM of Côte d'Ivoire ebolavirus isolate Côte d'Ivoire (CIEBOV-CI) 54-201-Fc, Reston ebolavirus isolate Pennsylvania (REBOV-Pen) 55-202-Fc or Sudan ebolavirus isolate Gulu (SEBOV-Gul) 54-201-Fc, and control proteins Fc, Lake Victoria marburgvirus isolate Musoke (MARV-Mus) 38-188-Fc, Zaire ebolavirus isolate Mayinga (ZEBOV-May) 54-201-Fc, severe acute respiratory syndrome coronavirus (SARS-CoV) RBD-Fc, human immunodeficiency virus type 1 (HIV-1) gp120-Fc or Machupo virus (MACV) GP1 Δ -Fc were incubated with filovirus-resistant human acute T-cell leukemia Jurkat E6-1 lymphocytes at a concentration of 100 nM, and analyzed by flow cytometry using an Fc-specific fluorescein isothiocyanate-conjugated secondary antibody. Bars indicate mean fluorescence intensity (M.F.I.) averages of two or more experiments. Error bars indicate standard deviations

Next, Vero E6 cells were incubated with CIEBOV-CI 54-201-Fc, REBOV-Pen 55-202-Fc, SEBOV-Gul 54-201-Fc or controls and with MARV/MLV. All three filoviral proteins inhibited cell transduction by MARV/MLV (Figure 7-22). Interestingly, CIEBOV-CI 54-201-Fc and REBOV-Pen 55-202-Fc inhibited transduction as efficiently as MARV-

Mus 38-188-Fc, whereas SEBOV-Gul 54-201-Fc was the least efficient inhibitor. Together, these data indicate that all filoviruses can utilize at least one common cell-entry factor.

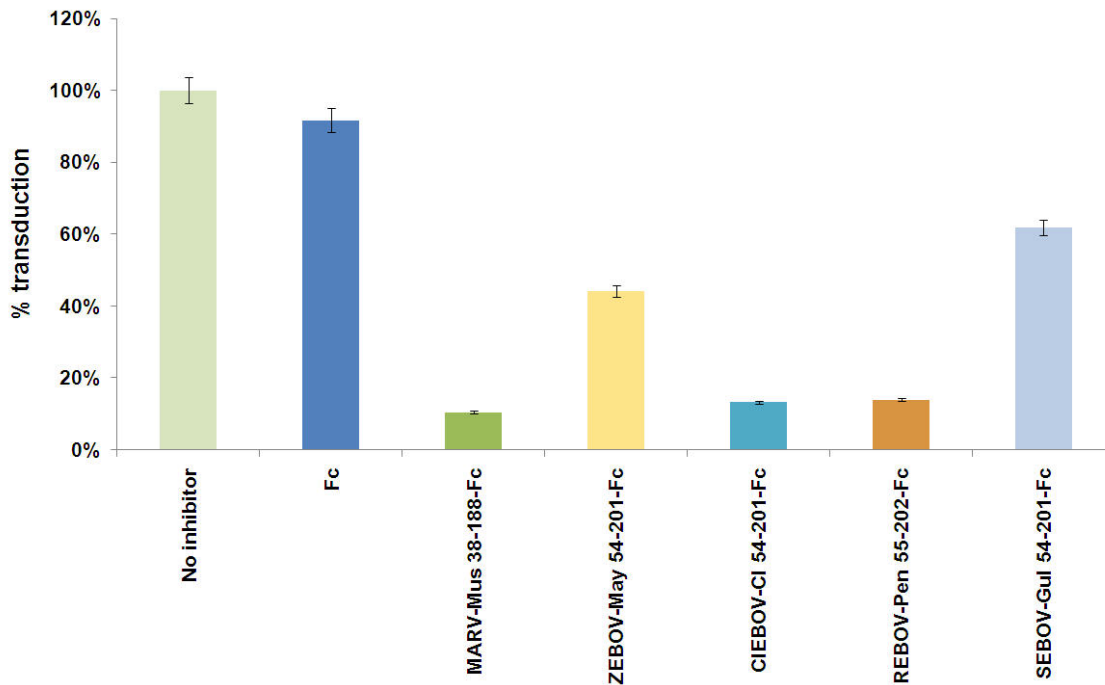


Figure 7-22. Côte d'Ivoire ebolavirus isolate Côte d'Ivoire 54-201-Fc, Reston ebolavirus isolate Pennsylvania 55-202-Fc, and Sudan ebolavirus isolate Gulu 54-201-Fc inhibit cell-entry of gammaretrovirus particles pseudotyped with Lake Victoria marburgvirus isolate Musoke GP_{1,2}

200 nM of Côte d'Ivoire ebolavirus isolate Côte d'Ivoire (CIEBOV-CI) 54-201-Fc, Reston ebolavirus isolate Pennsylvania (REBOV-Pen) 55-202-Fc or Sudan ebolavirus isolate Gulu (SEBOV-Gul) 54-201-Fc, and control proteins Fc, Lake Victoria marburgvirus isolate Musoke (MARV-Mus) 38-188-Fc or Zaire ebolavirus isolate Mayinga (ZEBOV-May) 54-201-Fc were incubated with filovirus-permissive African green monkey kidney epithelial (Vero E6) cells together with enhanced green fluorescent protein-expressing Moloney murine leukemia virus (MLV) particles pseudotyped with MARV-Mus GP_{1,2}. Entry of pseudotyped MLV was quantified by measuring green fluorescence using flow cytometry. Bars are normalized to show relative cell entry percentages compared to mock-inhibited control (defined as 100%) and indicate averages of two or more experiments. Error bars indicate standard deviations

7.2 Identification of ebolaviral Δ -peptides as potent filovirus cell-entry modulators

7.2.1 Zaire ebolavirus Δ -peptide-Fc, but not secreted glycoprotein or secondary secreted glycoprotein, binds to filovirus-permissive cells

The ebolaviral *GP* gene encodes two additional glycoproteins next to the spike protein GP_{1,2}, secreted glycoprotein (sGP) and secondary secreted glycoprotein (ssGP), which are produced by cotranscriptional editing (237, 279). In the case of Zaire ebolavirus (ZEBOV), GP₁, sGP, and ssGP contain an identical N-terminus of 295 amino-acid residues (see Chapter 5.2). The identified ZEBOV receptor-binding region (RBR) is located between residues 54 and 201 (Chapter 7.1), which suggests that all three proteins may contain a functional RBR. To evaluate this hypothesis, codon-optimized genes were synthesized *in vitro* that encode the full-length mature Zaire ebolavirus isolate Mayinga (ZEBOV-May) sGP or ssGP, fused to the Fc region of human immunoglobulin G₁ at the C-terminus (sGP-Fc, ssGP-Fc). As a control, a gene encoding ZEBOV-May Δ -peptide, a C-terminal proteolytic cleavage product of sGP that is generated during sGP maturation (287) (see also Chapter 5.2.1), was synthesized in a similar manner (Δ -Fc). The three constructs expressed efficiently in human embryonic kidney (HEK) 293T cells as Fc-fusion proteins (Figure 7-23), and were purified and quantified.

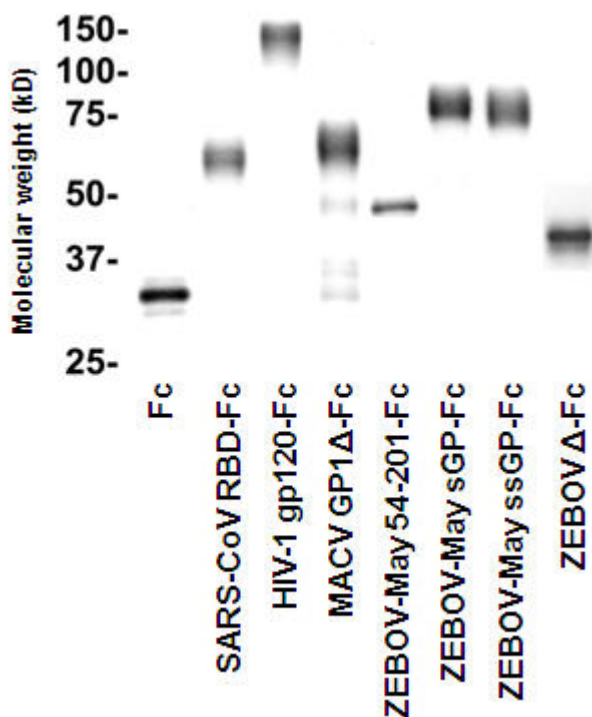


Figure 7-23. Expression of Zaire ebolavirus isolate Mayinga secreted glycoprotein, secondary secreted glycoprotein, and Δ -peptide

Zaire ebolavirus isolate Mayinga (ZEBOV-May) secreted glycoprotein (sGP-Fc), secondary secreted glycoprotein (ssGP-Fc), Δ -peptide (Δ -Fc), and control proteins Fc, severe acute respiratory syndrome coronavirus (SARS-CoV) RBD-Fc, human immunodeficiency virus type 1 (HIV-1) gp120-Fc, Machupo virus (MACV) GP1 Δ -Fc, and ZEBOV-May 54-201-Fc were purified from supernatants of transfected human embryonic kidney (HEK) 293T cells, quantified, normalized for expression, and visualized by Coomassie staining

Equivalent concentrations of each protein (100 nM) were incubated with filovirus-permissive African green monkey kidney epithelial (Vero E6) cells, filovirus-permissive human cervical adenocarcinoma epithelial-like (HeLa) cells or with filovirus-resistant human acute T-cell leukemia Jurkat E6-1 lymphocytes, and cell-surface association of each protein was determined by flow cytometry. SARS-CoV RBD-Fc and HIV-1 gp120-Fc, described in Chapter 7.1.1, as well as Fc alone, the Machupo virus RBD (MACV GP1 Δ -Fc) (219), and ZEBOV-May 54-201-Fc were used as controls. SARS-CoV RBD-Fc bound

SARS-CoV-permissive Vero E6 cells (Figure 7-24), which naturally express the SARS-CoV receptor, angiotensin-converting enzyme 2 (ACE2) (167). SARS-CoV RBD-Fc did not bind to Jurkat E6-1 lymphocytes or HeLa cells, which express only minute amounts of ACE2, if any (167) (Figures 7-25 and 7-26). HIV-1 gp120-Fc bound Jurkat E6-1 lymphocytes, which naturally express the principle HIV-1 receptor CD4 (Figure 7-26), but not to Vero E6 or HeLa cells, which do not (61, 154) (Figures 7-24 and 7-25). Fc did not bind to either cell type (Figures 7-24, 7-25, and 7-26), whereas MACV GP1 Δ -Fc bound to Vero E6 cells (Figure 7-24), which express the MACV receptor, transferrin receptor 1 (TfR1), but not to Jurkat E6-1 lymphocytes, which do not (219) (Figure 7-26). Surprisingly, little to no Vero E6 or HeLa cell-association was measured with ZEBOV-May sGP-Fc and ssGP-Fc, whereas Δ -Fc bound these cells with high affinity (Figures 7-24 and 7-25). None of the three proteins associated with Jurkat E6-1 lymphocytes (Figure 7-26). These data suggest that ebolaviral sGP and ssGP do not associate with the yet unidentified filovirus receptor despite them containing the ZEBOV RBR, and that Δ -peptide, which bears no resemblance in sequence to that of the ZEBOV RBR and whose function is enigmatic (see discussion in Chapter 8), may play a previously unknown role in filovirus cell entry.

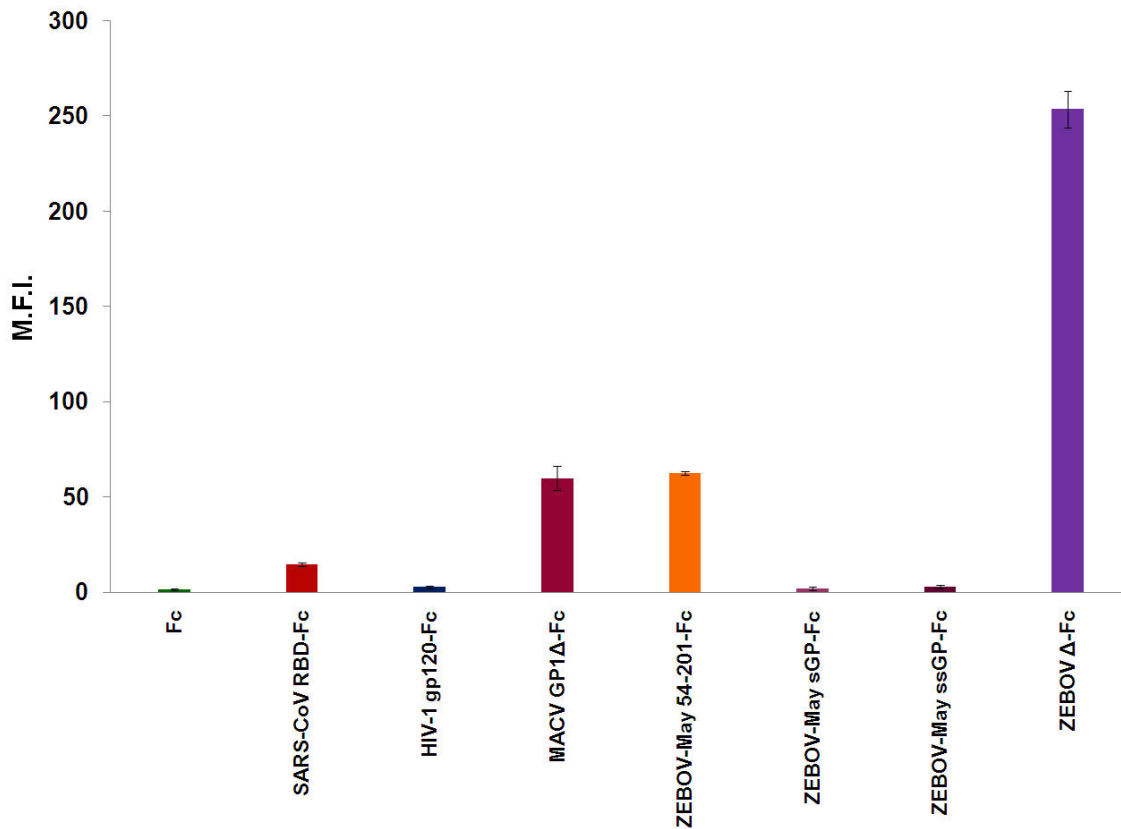


Figure 7-24. Binding of Zaire ebolavirus isolate Mayinga secreted glycoprotein, secondary secreted glycoprotein, and Δ -peptide to the surface of filovirus-permissive nonhuman primate cells

Zaire ebolavirus isolate Mayinga (ZEBOV-May) secreted glycoprotein (sGP-Fc), secondary secreted glycoprotein (ssGP-Fc) or Δ -peptide (Δ -Fc), and control proteins Fc, severe acute respiratory syndrome coronavirus (SARS-CoV) RBD-Fc, human immunodeficiency virus type 1 (HIV-1) gp120-Fc, Machupo virus (MACV) GP1 Δ -Fc or ZEBOV-May 54-201-Fc were incubated with filovirus-permissive African green monkey kidney epithelial (Vero E6) cells at a concentration of 100 nM, and analyzed by flow cytometry using an Fc-specific fluorescein isothiocyanate-conjugated secondary antibody. Bars indicate mean fluorescence intensity (M.F.I.) averages of two or more experiments. Error bars indicate standard deviations

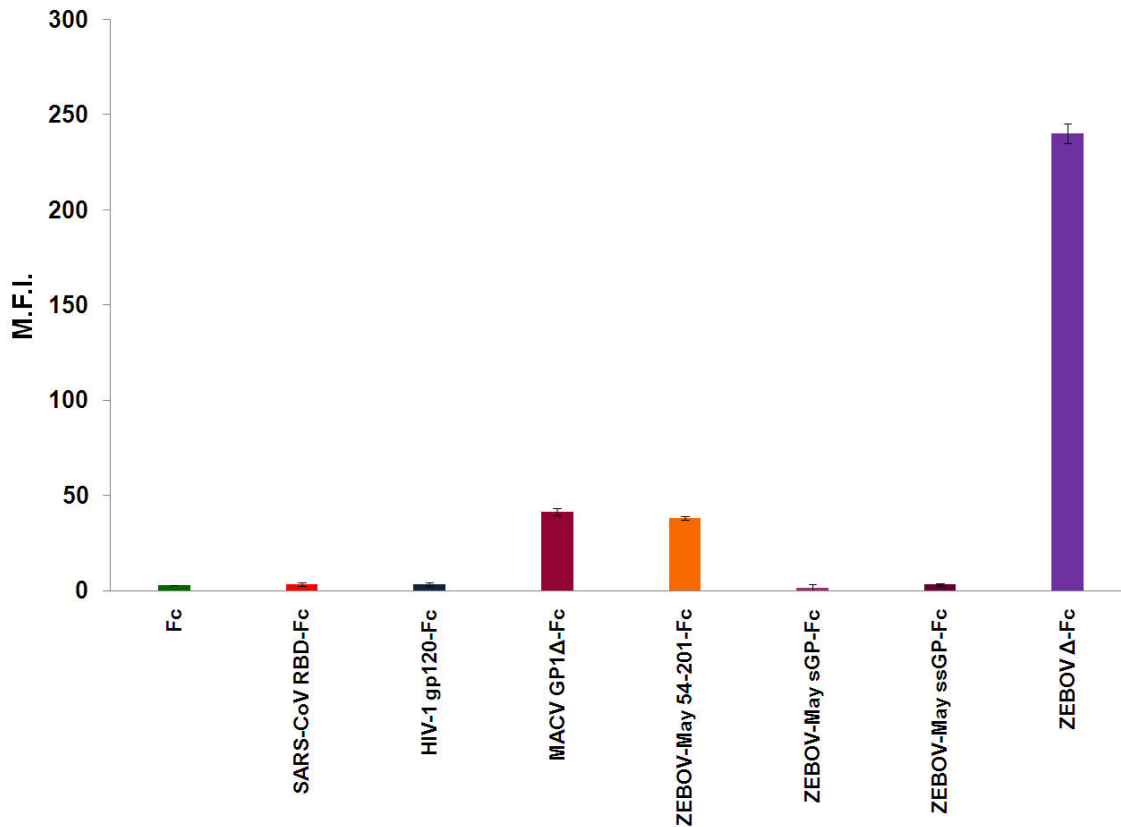


Figure 7-25. Binding of Zaire ebolavirus isolate Mayinga secreted glycoprotein, secondary secreted glycoprotein, and Δ -peptide to the surface of filovirus-permissive human cells

Zaire ebolavirus isolate Mayinga (ZEBOV-May) secreted glycoprotein (sGP-Fc), secondary secreted glycoprotein (ssGP-Fc) or Δ -peptide (Δ -Fc), and control proteins Fc, severe acute respiratory syndrome coronavirus (SARS-CoV) RBD-Fc, human immunodeficiency virus type 1 (HIV-1) gp120-Fc, Machupo virus (MACV) GP1 Δ -Fc or ZEBOV-May 54-201-Fc were incubated with filovirus-permissive human cervical adenocarcinoma epithelial-like (HeLa) cells at a concentration of 100 nM, and analyzed by flow cytometry using an Fc-specific fluorescein isothiocyanate-conjugated secondary antibody. Bars indicate mean fluorescence intensity (M.F.I.) averages of two or more experiments. Error bars indicate standard deviations

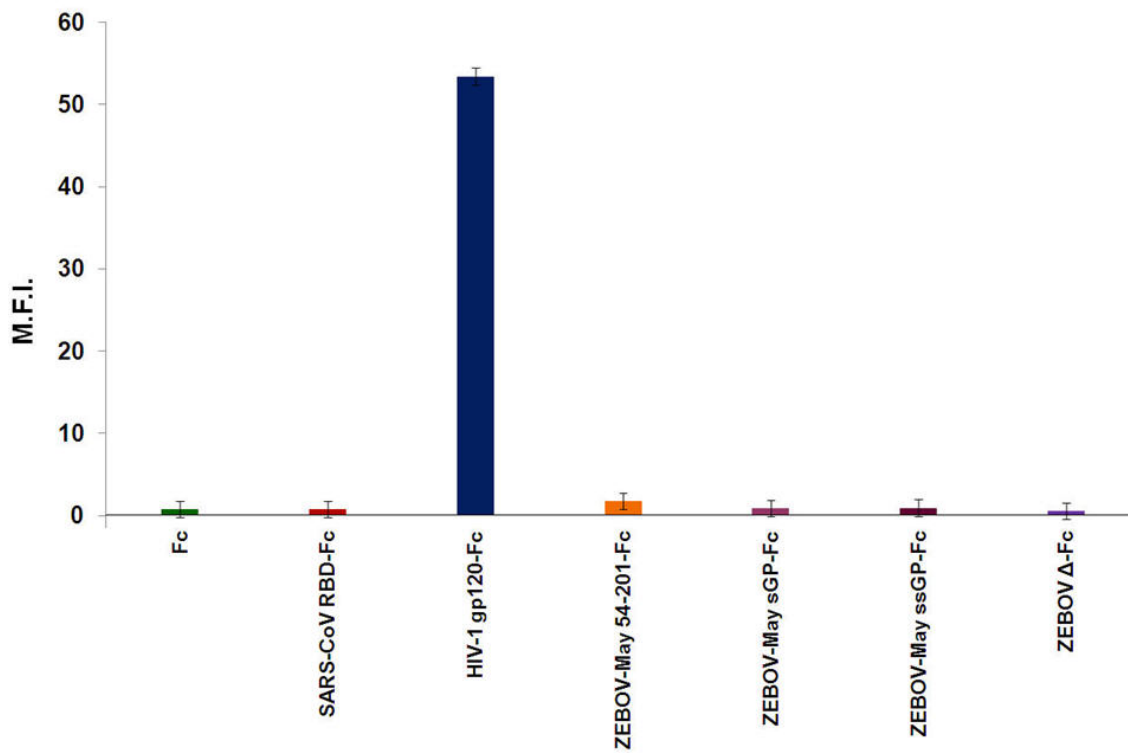


Figure 7-26. Binding of Zaire ebolavirus isolate Mayinga secreted glycoprotein, secondary secreted glycoprotein, and Δ -peptide to the surface of filovirus-resistant human cells

Zaire ebolavirus isolate Mayinga (ZEBOV-May) secreted glycoprotein (sGP-Fc), secondary secreted glycoprotein (ssGP-Fc) or Δ -peptide (Δ -Fc), and control proteins Fc, severe acute respiratory syndrome coronavirus (SARS-CoV) RBD-Fc, human immunodeficiency virus type 1 (HIV-1) gp120-Fc or ZEBOV-May 54-201-Fc were incubated with filovirus-resistant human acute T-cell leukemia Jurkat E6-1 lymphocytes at a concentration of 100 nM, and analyzed by flow cytometry using an Fc-specific fluorescein isothiocyanate-conjugated secondary antibody. Bars indicate mean fluorescence intensity (M.F.I.) averages of two or more experiments. Error bars indicate standard deviations

7.2.2 Zaire ebolavirus Δ -peptide-Fc, but not secreted glycoprotein or secondary secreted glycoprotein, inhibits entry of gammaretroviruses pseudotyped with filoviral spike protein

The ability of ZEBOV Δ -Fc to inhibit entry of pseudotyped retrovirus particles was assayed to evaluate the hypothesis that this peptide may be involved in modulating filovirus cell

entry by binding to the common filovirus receptor. As described in Chapter 7.1.4, a Moloney murine leukemia virus (MLV) vector expressing enhanced green fluorescent protein (eGFP) was pseudotyped with the spike protein (GP_{1,2}) of Lake Victoria marburgvirus isolate Musoke (MARV-Mus; MARV/MLV). MARV/MLV was chosen because it already had been demonstrated that both marburgviral and ebolaviral RBRs could inhibit either MARV/MLV or ZEBOV/MLV (Chapter 7.1.4) and because MARV/MLV was easier to produce in large quantities and behaved more consistently in transduction assays than ZEBOV/MLV (data not shown). Vero E6 cells were incubated with MARV/MLV and 200 nM of ZEBOV-May Δ -Fc, sGP-Fc, ssGP-Fc or control proteins. In accordance with the cell-binding data, ZEBOV-May sGP-Fc and ssGP-Fc inhibited cell transduction by MARV/MLV only minimally, whereas ZEBOV-May Δ -Fc inhibited MARV/MLV transduction even more efficiently than ZEBOV-May 54-201-Fc (Figure 7-27). These data indicate that ZEBOV Δ -peptide, for which there is no equivalent in the MARV proteome, can interfere with MARV GP_{1,2}-mediated entry and therefore suggest that this interference may involve the common filovirus receptor.

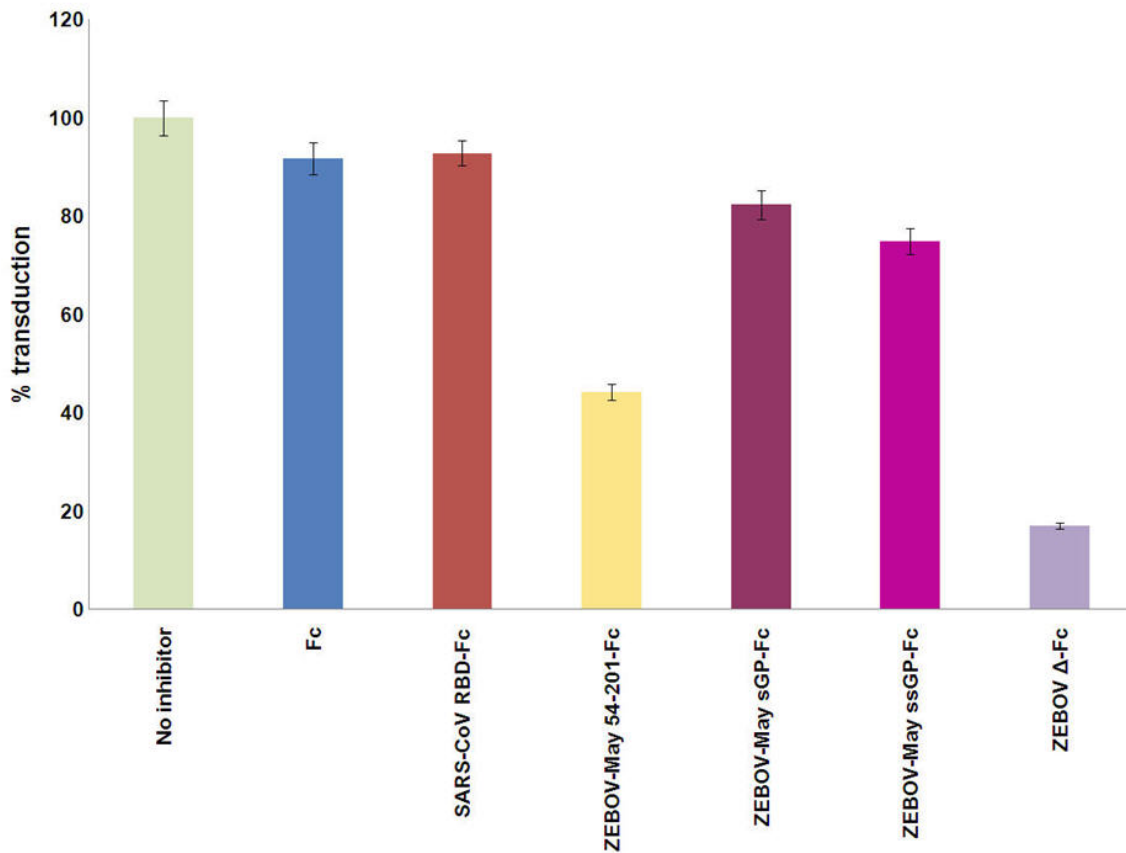


Figure 7-27. Zaire ebolavirus isolate Mayinga Δ -peptide-Fc, but not secreted glycoprotein or secondary secreted glycoprotein, inhibits entry of gammaretrovirus particles pseudotyped with Lake Victoria marburgvirus isolate Musoke GP_{1,2}

200 nM of Zaire ebolavirus isolate Mayinga (ZEBOV-May) secreted glycoprotein (sGP-Fc), secondary secreted glycoprotein (ssGP-Fc) or Δ -peptide (Δ -Fc), and control proteins Fc, severe acute respiratory syndrome coronavirus (SARS-CoV) RBD-Fc or ZEBOV-May 54-201-Fc were incubated with filovirus-permissive African green monkey kidney epithelial (Vero E6) cells and enhanced green fluorescent protein-expressing Moloney murine leukemia virus (MLV) particles pseudotyped with MARV-Mus GP_{1,2}. Entry of pseudotyped MLV was quantified by measuring green fluorescence using flow cytometry. Bars are normalized to show relative cell entry percentages compared to mock-inhibited control (defined as 100%) and indicate averages of two or more experiments. Error bars indicate standard deviations

7.2.3 Côte d'Ivoire, Sudan, and Zaire, and to much lesser extent Reston, ebolaviral Δ -peptide Fc fusion proteins inhibit filoviral GP_{1,2}-mediated entry in a dose-dependent manner

The obtained data raised the question whether all ebolaviral Δ -peptides have a common function. To answer this question, open reading frames encoding the Δ -peptides of three other ebolaviruses, Côte d'Ivoire ebolavirus (CIEBOV), Reston ebolavirus (REBOV), and Sudan ebolavirus (SEBOV), were cloned from sGP expression plasmids obtained from collaborators and introduced into the Fc fusion-protein expression vector. All three proteins were expressed in HEK 293T cells as Fc-fusion proteins (Figure 7-28), purified and quantified. While REBOV and SEBOV Δ -Fc expressed very efficiently, CIEBOV Δ -Fc expressed only to low levels. SEBOV Δ -Fc migrated lower during polyacrylamide gel electrophoresis (PAGE) than all other Δ -Fc, despite being the longest peptide (48 amino-acid residues, compared to 41 (CIEBOV), 42 (REBOV), and 40 (ZEBOV)). This observation suggests that the ebolaviral Δ -peptides may be posttranslationally modified to different extent.

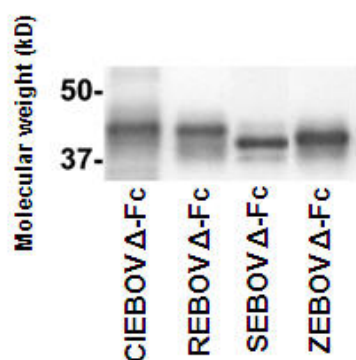


Figure 7-28. Expression of Côte d'Ivoire, Sudan, Reston, and Zaire ebolaviral Δ -peptides

Côte d'Ivoire ebolavirus (CIEBOV), Reston ebolavirus (REBOV), Sudan ebolavirus (SEBOV), and Zaire ebolavirus (ZEBOV) Δ -peptides (Δ -Fc) were purified from supernatants of transfected human embryonic kidney (HEK) 293T cells, quantified, normalized for expression, and visualized by Coomassie staining

Equivalent concentrations of each Δ -Fc (100 nM) were incubated with Vero E6 cells, HeLa cells, and Jurkat E6-1 lymphocytes, and cell-surface association of each protein was determined by flow cytometry. SARS-CoV RBD-Fc, gp120-Fc, Fc, and MACV GP1 Δ -Fc were used as controls as described and behaved as expected (Chapter 7.2.1). Fc did not bind to either cell type (Figures 7-29, 7-30, and 7-31), whereas MACV GP1 Δ -Fc bound to Vero E6 and HeLa cells (Figures 7-29 and 7-30). None of the ebolaviral Δ -peptide bound to filovirus-resistant Jurkat E6-1 lymphocytes (Figure 7-31). In contrast, all of them associated with the cell surface of filovirus-permissive Vero E6 and HeLa cells, albeit to varying degree. ZEBOV Δ -Fc bound to the surface of these cells with much higher affinity than CIEBOV and SEBOV Δ -Fc, whereas REBOV Δ -Fc exhibited the least efficient binding phenotype (Figures 7-29 and 7-30).

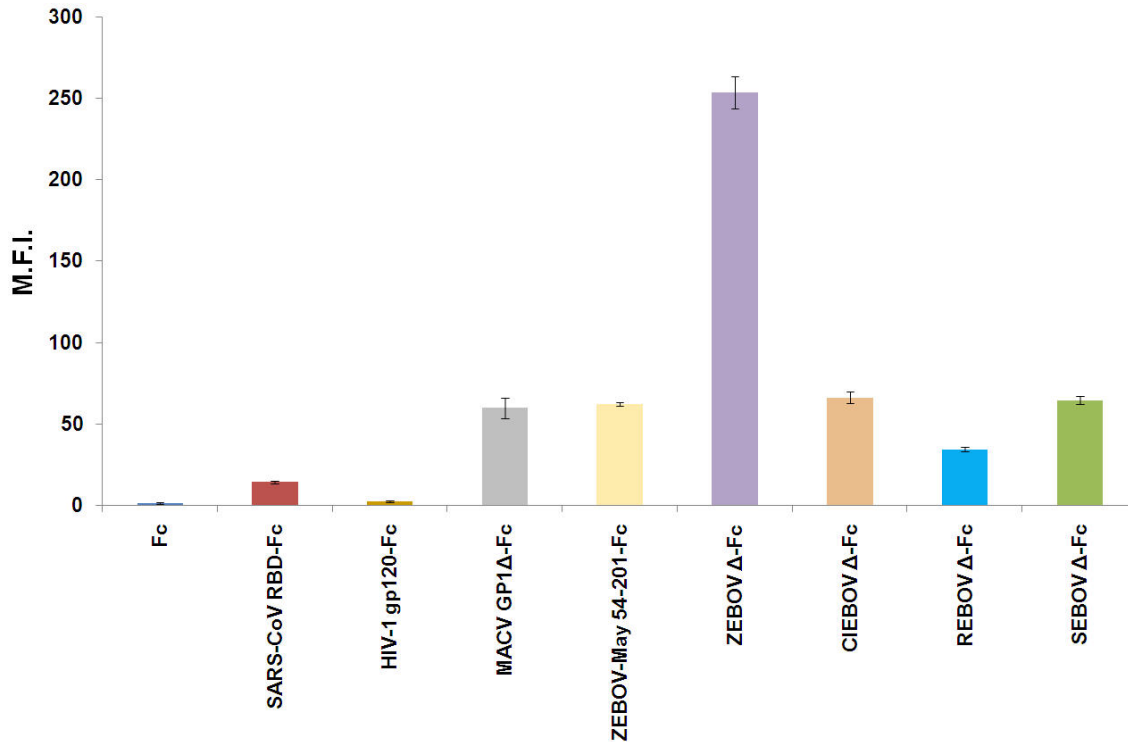


Figure 7-29. Binding of Côte d’Ivoire, Sudan, Reston, and Zaire ebolaviral Δ -peptides to the surface of filovirus-permissive nonhuman primate cells

Côte d’Ivoire ebolavirus (CIEBOV), Reston ebolavirus (REBOV), Sudan ebolavirus (SEBOV) or Zaire ebolavirus (ZEBOV) Δ -peptides (Δ -Fc), and control proteins Fc, severe acute respiratory syndrome coronavirus (SARS-CoV) RBD-Fc, human immunodeficiency virus type 1 (HIV-1) gp120-Fc, Machupo virus (MACV) GP1 Δ -Fc or Zaire ebolavirus isolate Mayinga (ZEBOV-May) 54-201-Fc were incubated with filovirus-permissive African green monkey kidney epithelial (Vero E6) cells at a concentration of 100 nM, and analyzed by flow cytometry using an Fc-specific fluorescein isothiocyanate-conjugated secondary antibody. Bars indicate mean fluorescence intensity (M.F.I.) averages of two or more experiments. Error bars indicate standard deviations

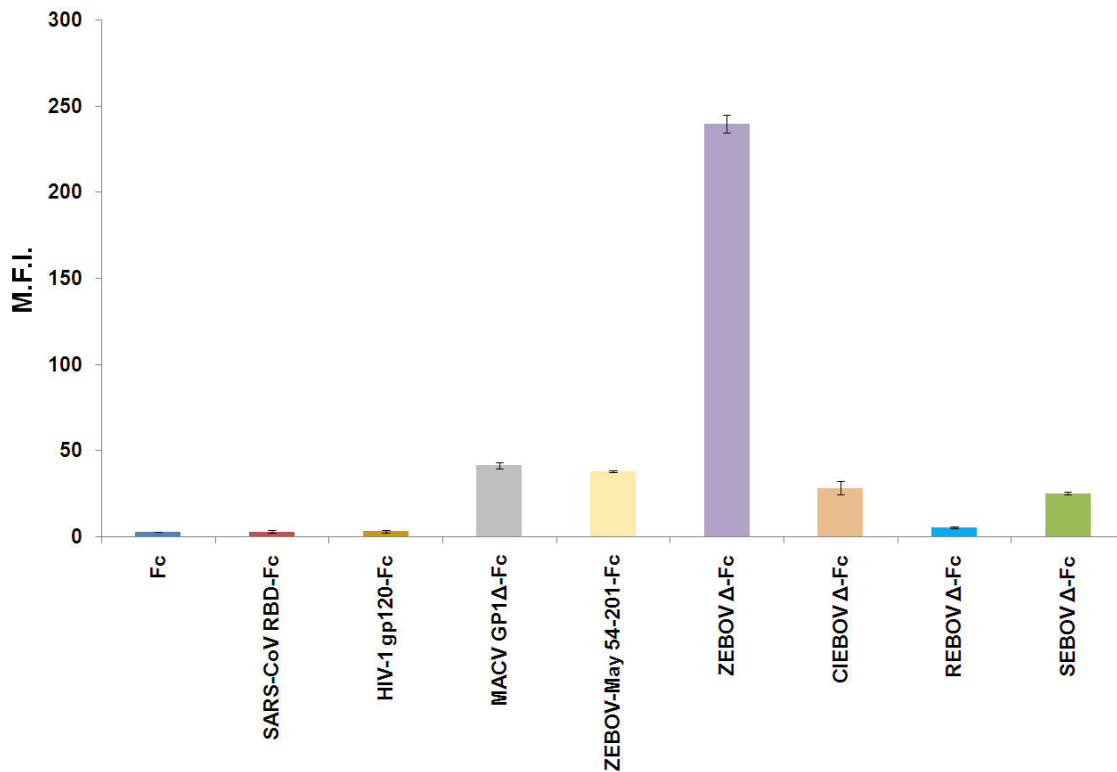


Figure 7-30. Binding of Côte d’Ivoire, Sudan, Reston, and Zaire ebolaviral Δ -peptides to the surface of filovirus-permissive human cells

Côte d’Ivoire ebolavirus (CIEBOV), Reston ebolavirus (REBOV), Sudan ebolavirus (SEBOV) or Zaire ebolavirus (ZEBOV) Δ -peptides (Δ -Fc), and control proteins Fc, severe acute respiratory syndrome coronavirus (SARS-CoV) RBD-Fc, human immunodeficiency virus type 1 (HIV-1) gp120-Fc, Machupo virus (MACV) GP1 Δ -Fc or Zaire ebolavirus isolate Mayinga (ZEBOV-May) 54-201-Fc were incubated with filovirus-permissive cervical adenocarcinoma epithelial-like (HeLa) cells at a concentration of 100 nM, and analyzed by flow cytometry using an Fc-specific fluorescein isothiocyanate-conjugated secondary antibody. Bars indicate mean fluorescence intensity (M.F.I.) averages of two or more experiments. Error bars indicate standard deviations

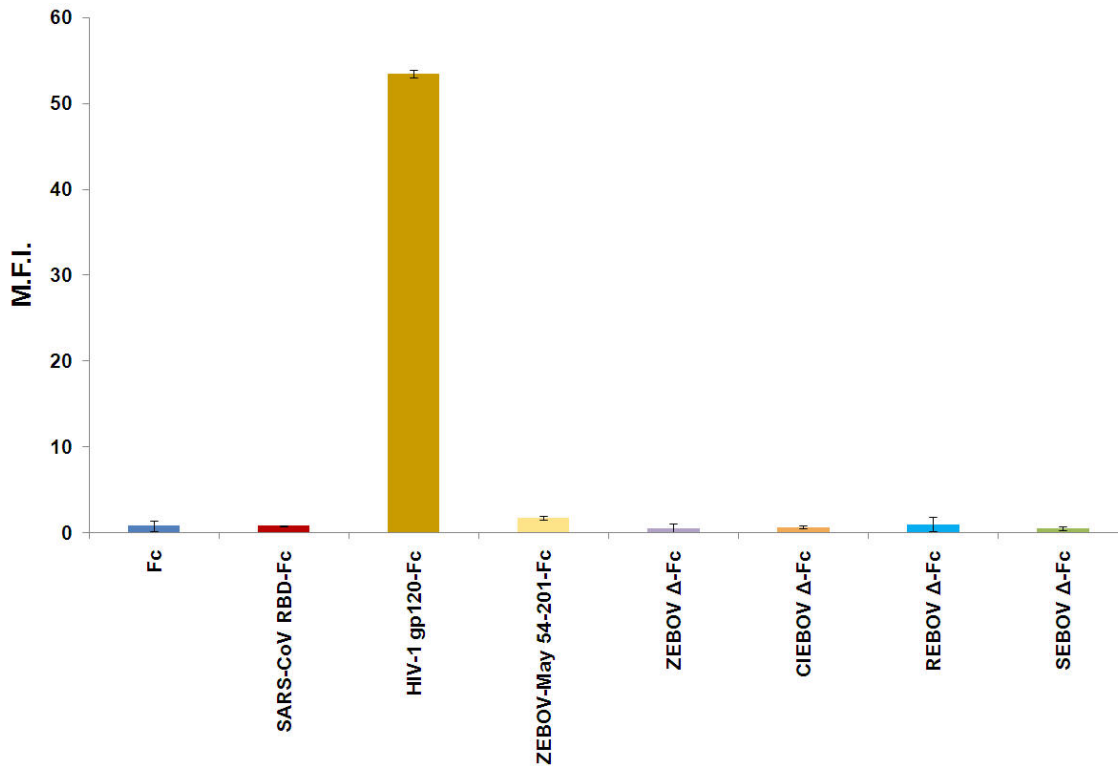


Figure 7-31. Binding of Côte d’Ivoire, Sudan, Reston, and Zaire ebolaviral Δ -peptides to the surface of filovirus-resistant human cells

Côte d’Ivoire ebolavirus (CIEBOV), Reston ebolavirus (REBOV), Sudan ebolavirus (SEBOV) or Zaire ebolavirus (ZEBOV) Δ -peptides (Δ -Fc), and control proteins Fc, severe acute respiratory syndrome coronavirus (SARS-CoV) RBD-Fc, human immunodeficiency virus type 1 (HIV-1) gp120-Fc or Zaire ebolavirus isolate Mayinga (ZEBOV-May) 54-201-Fc were incubated with filovirus-resistant human acute T-cell leukemia Jurkat E6-1 lymphocytes at a concentration of 100 nM, and analyzed by flow cytometry using an Fc-specific fluorescein isothiocyanate-conjugated secondary antibody. Bars indicate mean fluorescence intensity (M.F.I.) averages of two or more experiments. Error bars indicate standard deviations

The ability of the four ebolaviral Δ -Fc_s to inhibit entry of pseudotyped gammaretrovirus particles was assayed as described above, using eGFP-expressing MARV/MLV. Vero E6 cells were incubated with increasing concentrations of CIEBOV Δ -Fc, REBOV Δ -Fc, SEBOV Δ -Fc, ZEBOV Δ -Fc or control proteins and pseudotyped gammaretrovirus particles (Figure 7-32). Δ -Fc_s of CIEBOV, SEBOV, and ZEBOV efficiently inhibited Vero E6 cell transduction by MARV/MLV. SEBOV Δ -Fc and CIEBOV Δ -Fc were even more efficient inhibitors than ZEBOV Δ -Fc and MARV-Mus 38-188-Fc. Surprisingly, Δ -Fc derived from REBOV, the only filovirus thought to be apathogenic for humans, inhibited transduction much less efficiently than the other Δ -peptides (Figure 7-32). This minimal inhibitory effect correlates with its minimal binding to the surface of these cells (Figure 7-29). Finally, Fc and SARS-CoV RBD-Fc fusion control proteins did not inhibit cell transduction (Figure 7-32), thereby emphasizing the specificity of the inhibitory effect of ebolaviral Δ -peptides. Together, these data indicate that ebolaviral Δ -peptides generally modulate filovirus cell entry and suggest that they may be important virulence factors.

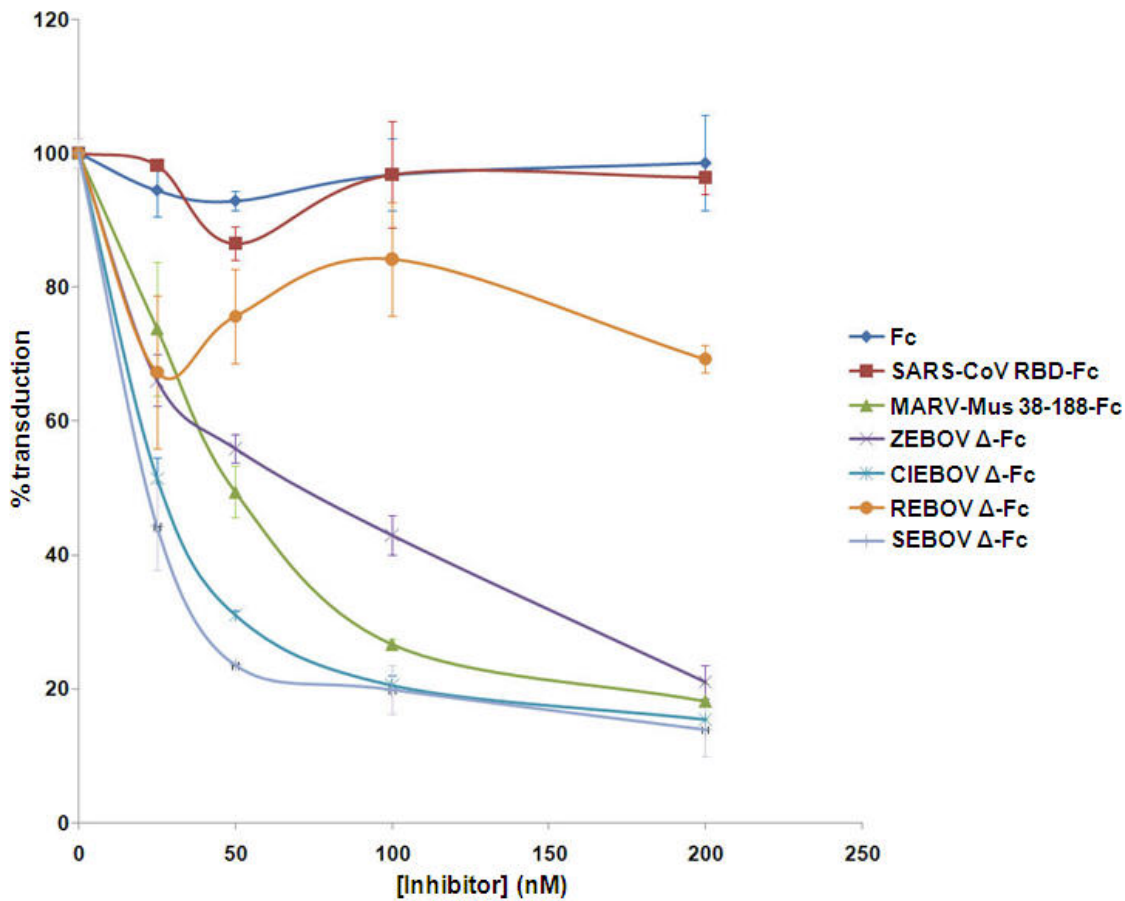


Figure 7-32. Côte d'Ivoire, Sudan, and Zaire, and to lesser extent Reston, ebolaviral Δ -peptide Fc fusion proteins inhibit entry of gammaretrovirus particles pseudotyped with Lake Victoria marburgvirus isolate Musoke GP_{1,2} in a dose-dependent manner

Côte d'Ivoire ebolavirus (CIEBOV), Reston ebolavirus (REBOV), Sudan ebolavirus (SEBOV) or Zaire ebolavirus (ZEBOV) Δ -peptides (Δ -Fc), and control proteins Fc, severe acute respiratory syndrome coronavirus (SARS-CoV) RBD-Fc or Lake Victoria marburgvirus isolate Musoke (MARV-Mus) 38-188-Fc were incubated at increasing concentrations with filovirus-permissive African green monkey kidney epithelial (Vero E6) cells and enhanced green fluorescent protein-expressing Moloney murine leukemia virus (MLV) pseudotyped with MARV-Mus GP_{1,2}. Entry of pseudotyped MLV was quantified by measuring green fluorescence using flow cytometry. Individual measure points show relative cell entry percentages compared to mock-inhibited control (defined as 100%) and indicate averages of two or more experiments. Error bars indicate standard deviations

7.2.4 Côte d'Ivoire, Sudan, and Zaire, but not Reston, ebolaviral Δ -peptide Fc fusion proteins inhibit replication of infectious Zaire ebolavirus

To determine whether ebolaviral Δ -Fc fusion proteins also inhibit infectious filoviruses, Vero E6 cells were preincubated with increasing concentrations of CIEBOV Δ -Fc, REBOV Δ -Fc, SEBOV Δ -Fc, ZEBOV Δ -Fc or control protein SARS-CoV RBD-Fc. Cells were washed and exposed to infectious ZEBOV-May modified to express eGFP (270), at a multiplicity of infection (moi) of 1. In accordance with experiments with pseudotyped MLV particles, viral replication, measured as percentage of infected cells, was specifically inhibited by CIEBOV, SEBOV, and ZEBOV Δ -Fc. SEBOV Δ -Fc was again the most efficient inhibitor, whereas REBOV Δ -Fc did not inhibit ZEBOV-May replication at all and behaved like the SARS-CoV RBD-Fc negative control (Figure 7-33). These data demonstrate that CIEBOV, SEBOV, and ZEBOV Δ -peptides, in addition to their inhibitory effect on MARV GP_{1,2}-mediated entry, also inhibit ZEBOV entry. This supports the notion that Δ -peptides may modulate the cell entry of all filoviruses.

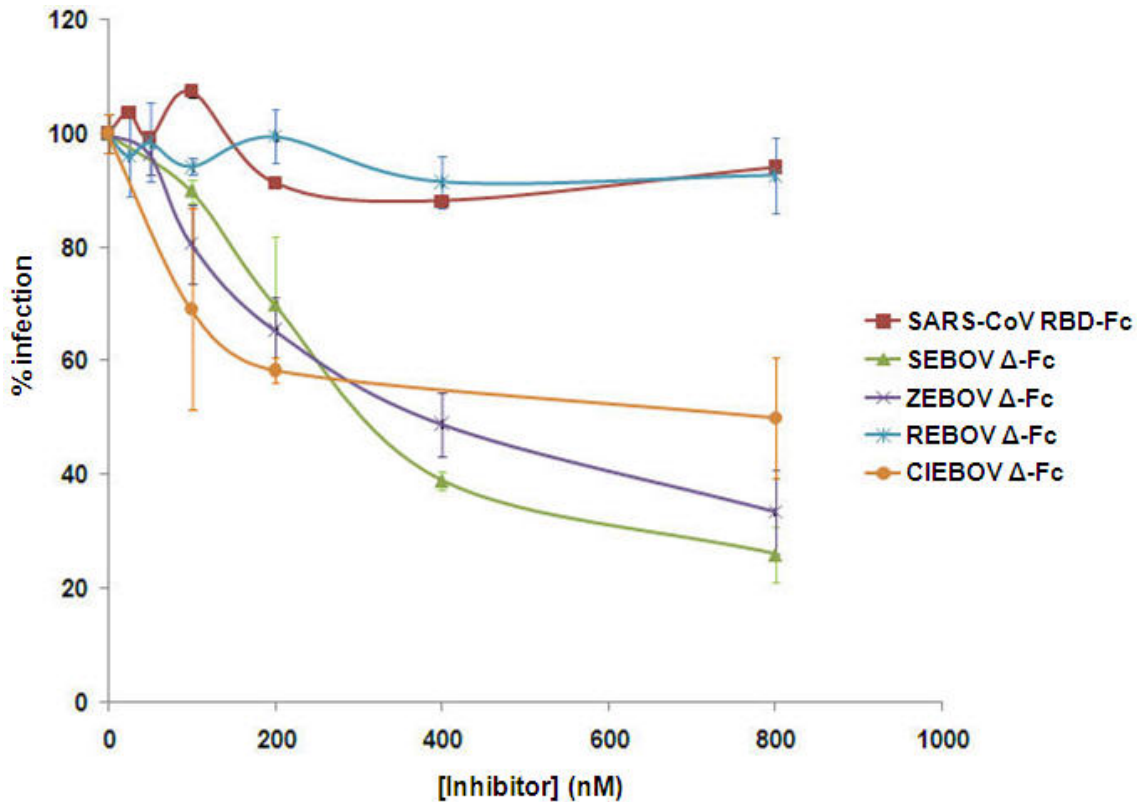


Figure 7-33. Côte d'Ivoire, Sudan, and Zaire, but not Reston, ebolaviral Δ -peptide Fc fusion proteins inhibit replication of infectious Zaire ebolavirus isolate Mayinga

Increasing concentrations of Côte d'Ivoire ebolavirus (CIEBOV), Reston ebolavirus (REBOV), Sudan ebolavirus (SEBOV) or Zaire ebolavirus (ZEBOV) Δ -peptides (Δ -Fc) or control protein severe acute respiratory syndrome coronavirus (SARS-CoV) RBD-Fc were incubated with recombinant, enhanced green fluorescent protein-expressing Zaire ebolavirus isolate Mayinga (ZEBOV-May). Infection was quantified by measuring green fluorescence using Discovery-1 automated microscopy. Individual measure points show relative cell entry percentages compared to mock-inhibited control (defined as 100%) and indicate averages of three or more experiments. Error bars indicate standard deviations

7.2.5 Ebolaviral Δ -peptides inhibit filoviral GP_{1,2}-mediated entry specifically

In the previously described experiments (Chapters 7.2.3 and 7.2.4), it was shown that SEBOV Δ -Fc inhibited MARV-Mus GP_{1,2}-mediated entry and ZEBOV-May replication more efficiently than all other tested Δ -peptides. Consequently, all follow-up experiments were performed with SEBOV Δ -Fc or derivatives thereof. To evaluate whether ebolaviral Δ -peptide Fc-fusion proteins specifically inhibit filovirus cell entry, Vero E6 cells were incubated with 100 nM of SEBOV Δ -Fc or SARS-CoV RBD-Fc control, as well as with MLV pseudotyped with the spike proteins of human influenza A virus (FLUAV/MLV), Lassa virus (LASV/MLV), lymphocytic choriomeningitis virus (LCMV/MLV), Machupo virus (MACV/MLV), MARV (MARV/MLV), or VSIV (VSIV/MLV) (Figure 7-34). The results demonstrate that SEBOV Δ -Fc does not inhibit the transduction of Vero E6 cells by MLV pseudotyped with non-filoviral spike proteins, indicating that ebolaviral Δ -peptide Fc-fusion proteins modulate filovirus cell-entry processes specifically.

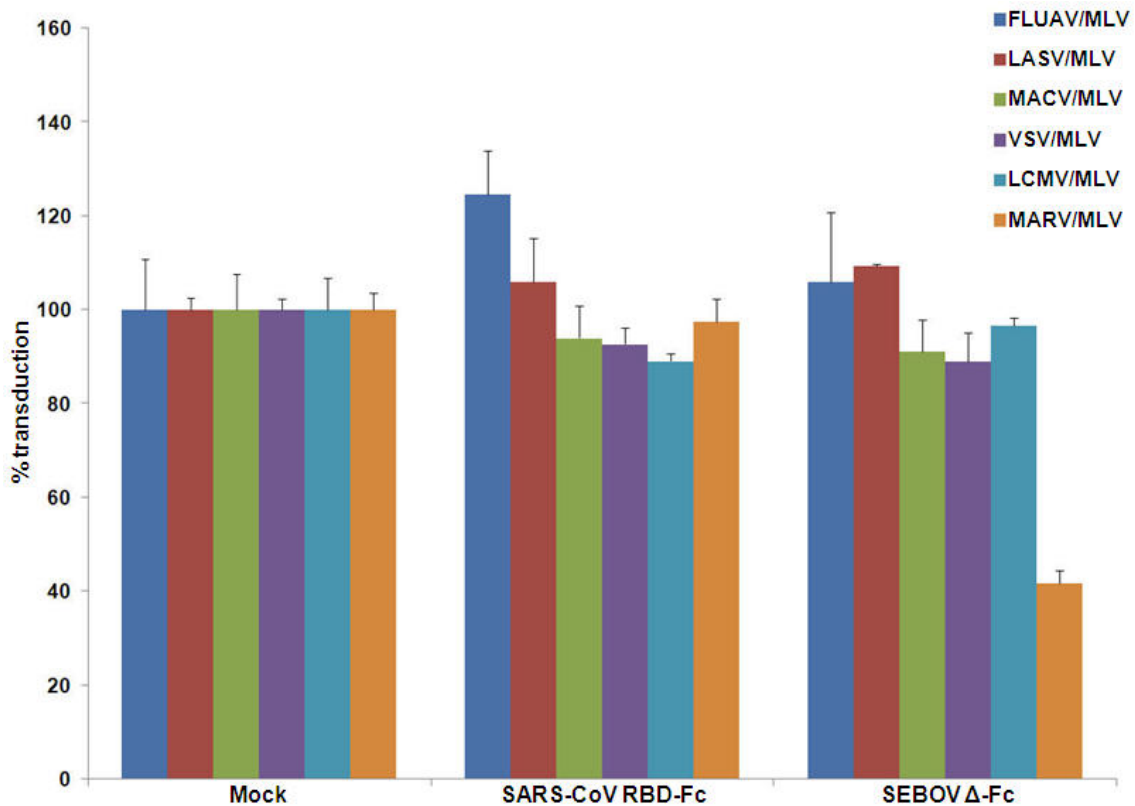


Figure 7-34. Sudan ebolaviral Δ -peptide inhibits filoviral GP_{1,2}-mediated entry specifically

100 nM of Sudan ebolavirus (SEBOV) Δ -Fc fusion protein were incubated with filovirus-permissive African green monkey kidney epithelial (Vero E6) cells together with enhanced green fluorescent protein-expressing Moloney murine leukemia virus (MLV) particles pseudotyped with the spike proteins of either influenza A virus (FLUAV), Lassa virus (LASV), Machupo virus (MACV), vesicular stomatitis Indiana virus (VSIV), lymphocytic choriomeningitis virus (LCMV) or Lake Victoria marburgvirus (MARV). Entry of pseudotyped MLV was quantified by measuring green fluorescence using flow cytometry. Bars show relative cell entry percentages compared to mock-inhibited control (defined as 100%) and indicate averages of two or more experiments. Error bars indicate standard deviations

To further emphasize this result, SEBOV Δ -Fc was evaluated in a human immunodeficiency virus type 1 (HIV-1) secreted alkaline phosphatase (SEAP) reporter neutralization assay (182). Briefly, infectious HIV-1 was incubated in the presence of increasing concentrations of SEBOV Δ -Fc. As a control, HIV-1 was incubated with the same concentrations of CD4-Fc, a soluble version of the principle HIV-1 receptor, CD4, which previously has been shown to inhibit HIV-1 cell entry efficiently (64). As expected, CD4-Fc inhibited HIV-1 entry in this assay, whereas SEBOV Δ -Fc had no effect (Figure 7-35). These data further support the notion that ebolaviral Δ -peptides interfere specifically with filovirus cell entry.

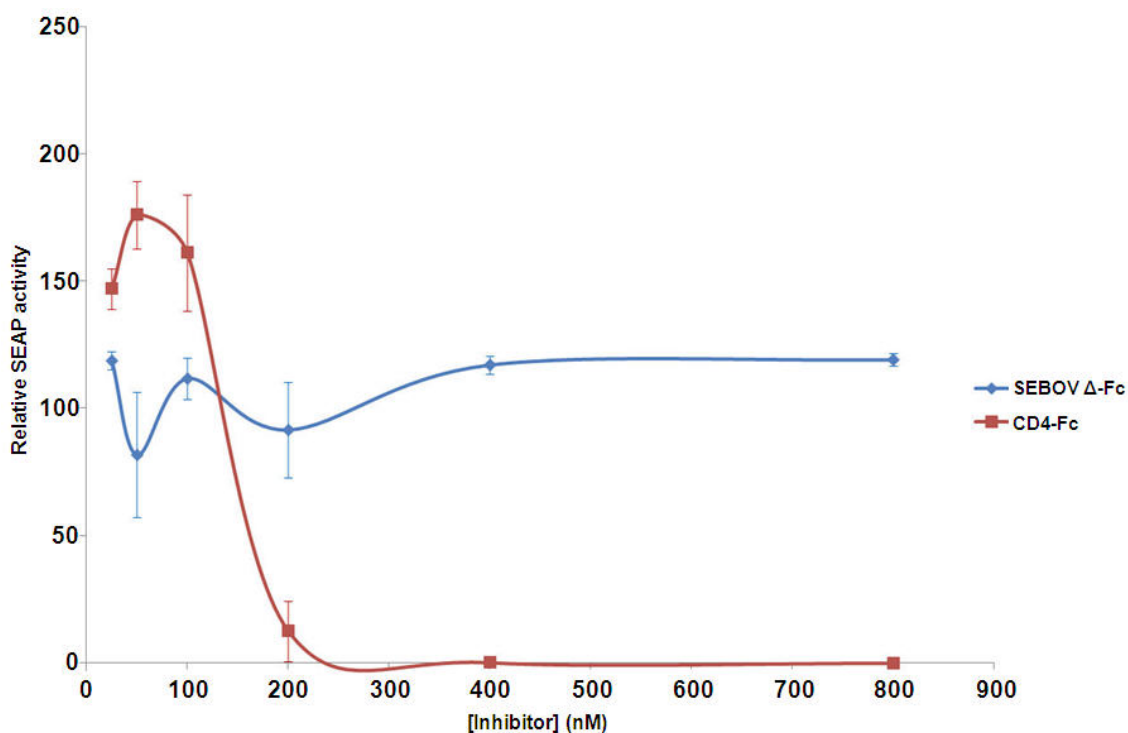


Figure 7-35. Sudan ebolaviral Δ -peptide does not inhibit cell entry of infectious human immunodeficiency virus type 1

Infectious human immunodeficiency virus type 1 (HIV-1) and the indicated concentrations of SEBOV Δ -Fc or control protein CD4-Fc were incubated with cells stably transfected with plasmid encoding a secreted alkaline phosphatase (SEAP) reporter gene under the

control of a *tat*-responsive promoter derived from HIV-1. SEAP activity correlates directly with the amount of HIV-1 entering the cell and was measured as relative light units.

7.2.6 Mutational analysis of Sudan ebolavirus Δ -peptide

Mutants of SEBOV Δ -Fc were created to further define how ebolaviral Δ -peptides exert their effect on filovirus cell entry. Individual SEBOV Δ -peptide amino-acid residues, suspected to play a role in binding to filovirus-permissive cells, were mutated to alanine by subjecting a plasmid encoding SEBOV Δ -Fc (Δ 1-48-Fc) to site-directed mutagenesis. Alternatively, mutants were created by *de novo* recursive PCR. N- and C-terminal truncations of SEBOV Δ -peptide were created by inverse PCR to evaluate which parts of the peptide are mandatory for its function. Last, chimeras of SEBOV Δ -peptide and REBOV Δ -peptide were synthesized by sequential PCRs to understand why REBOV Δ -Fc is the only ebolaviral Δ -peptide that does not inhibit replication of infectious filoviruses (Chapters 7.2.3 and 7.2.4). N-terminal truncation mutants SEBOV Δ 7-48-Fc, SEBOV Δ 13-48-Fc, and SEBOV Δ 18-48-Fc did not express. All other constructs (see Figure 7-36 for a list of all created mutants) expressed efficiently or at least sufficiently in HEK 293T cells as Fc-fusion proteins (Figure 7-37), and were purified and quantified.

SEBOV Δ -Fc	<u>ELQREESPTGPPGSIRTWFQRIPLGWFHCTYQKGKQHCLRLRIRQKVEE</u>
SEBOV Δ 1-17-Fc	ELQREESPTGPPGSIRT
SEBOV Δ 1-28-Fc	ELQREESPTGPPGSIRTWFQRIPLGWFH
SEBOV Δ 1-33-Fc	ELQREESPTGPPGSIRTWFQRIPLGWFHCTYQK
SEBOV Δ 1-39-Fc	ELQREESPTGPPGSIRTWFQRIPLGWFHCTYQKGKQHCR
SEBOV Δ 7-48-Fc	SPTGPPGSIRTWFQRIPLGWFHCTYQKGKQHCLRLRIRQKVEE
SEBOV Δ 13-48-Fc	GSIRTWFQRIPLGWFHCTYQKGKQHCLRLRIRQKVEE
SEBOV Δ 18-48-Fc	WFQRIPLGWFHCTYQKGKQHCLRLRIRQKVEE
SEBOV Δ 28-48-Fc	HCTYQKGKQHCLRLRIRQKVEE
SEBOV Δ T9A-Fc	ELQREESPTGPPGSIRTWFQRIPLGWFHCTYQKGKQHCLRLRIRQKVEE
SEBOV Δ 1-39T9A-Fc	ELQREESPTGPPGSIRTWFQRIPLGWFHCTYQKGKQHCR
SEBOV Δ S14A-Fc	ELQREESPTGPPGSAIRTWFQRIPLGWFHCTYQKGKQHCLRLRIRQKVEE
SEBOV Δ W18A-Fc	ELQREESPTGPPGSIRTAFQRIPLGWFHCTYQKGKQHCLRLRIRQKVEE
SEBOV Δ R21A-Fc	ELQREESPTGPPGSIRTWFQAIPLGWFHCTYQKGKQHCLRLRIRQKVEE
SEBOV Δ W26A-Fc	ELQREESPTGPPGSIRTWFQRIPLGAFHCTYQKGKQHCLRLRIRQKVEE
SEBOV Δ C29A, C38A-Fc	ELQREESPTGPPGSIRTWFQRIPLGWFHATYQKGKQHARLRLRIRQKVEE
SEBOV Δ -Fc	ELQREESPTGPPGSIRTWFQRIPLGWFHCTYQKGKQHCLRLRIRQKVEE
REBOV Δ -Fc	ELSKKLATTHPPTTPSWFQRIPLGWFQCSLQDGQRKCRPKV
SR Δ -Fc	ELQREESPTGPPGSIRTWFQRIPLGWFQCSLQDGQRKCRPKV
RS Δ -Fc	ELSKKLATTHPPTTPSWFQRIPLGWFHCTYQKGKQHCLRLRIRQKVEE

Figure 7-36. Overview of Sudan ebolavirus Δ -peptide mutants

Mutants were created by recursive polymerase-chain reaction (PCR) and site-directed mutagenesis (alanine-scanning), and/or inverse PCR (N- and C-terminal truncation variants) using a plasmid encoding Sudan ebolavirus (SEBOV) Δ -Fc (top panel). Mutated residues are printed in red color. Sudan-Reston Δ -Fc chimeras (SR Δ -Fc) and Reston-Sudan Δ -Fc chimeras (RS Δ -Fc) were created by sequential PCRs using plasmids encoding SEBOV Δ -Fc and Reston ebolavirus (REBOV) Δ -Fc (lower panel). Residues shared by both SEBOV Δ - and REBOV Δ -peptides are highlighted green. Residues unique to SEBOV and REBOV are highlighted yellow and red, respectively

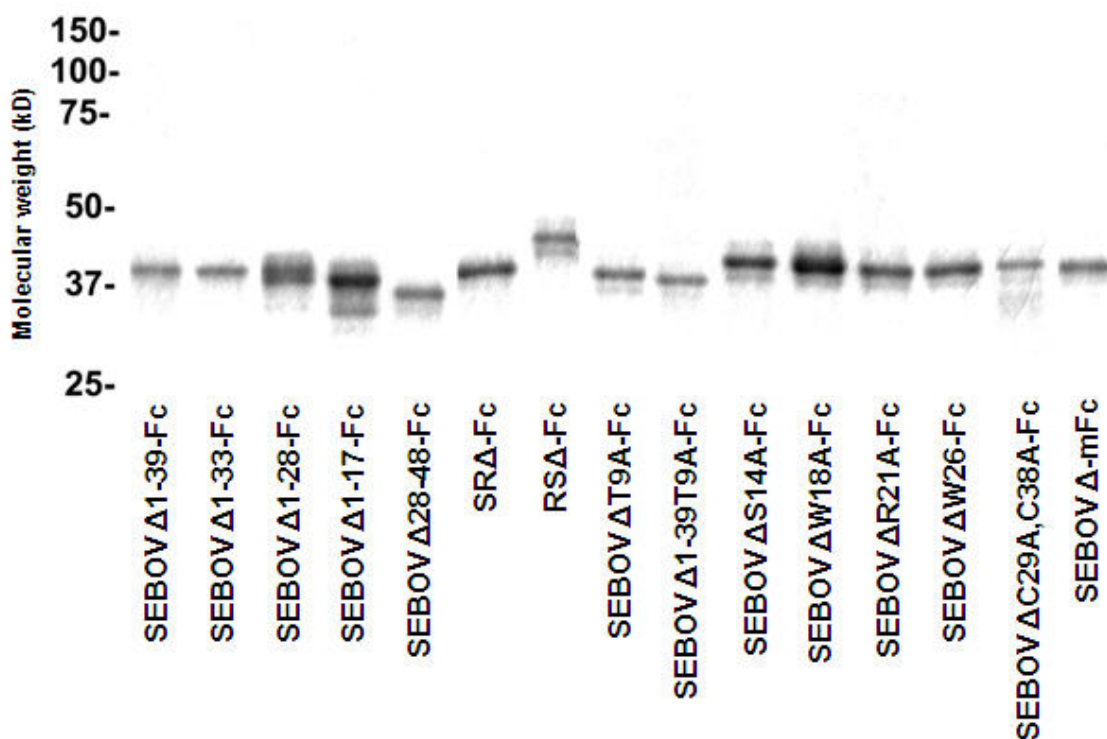


Figure 7-37. Expression of Sudan ebolavirus Δ -peptide mutants

Sudan ebolavirus (SEBOV) Δ -peptide (Δ -Fc) mutants were purified from supernatants of transfected human embryonic kidney (HEK) 293T cells, quantified, normalized for expression, and visualized by Coomassie staining. SR, Sudan-Reston Δ -peptide chimera; RS, Reston-Sudan Δ -peptide chimera; mFc, murine Fc

Equivalent concentrations of some of these proteins (100 nM) were incubated with Vero E6 cells or with Jurkat E6-1 lymphocytes, and cell-surface association of each protein was determined by flow cytometry. SARS-CoV RBD-Fc and HIV-1 gp120-Fc were used as controls as described and behaved as expected. None of the created SEBOV Δ -peptide mutants bound to filovirus-resistant Jurkat E6-1 lymphocytes (Figure 7-39) but all of them, with the exception of SEBOV Δ 1-28-Fc, associated with the cell surface of filovirus-permissive Vero E6 cells (Figure 7-38). As can be seen in Figure 7-38, N-terminal truncation variant SEBOV Δ 1-39-Fc bound as efficiently to Vero E6 cells as wild-type SEBOV Δ -Fc (SEBOV Δ 1-48-Fc), while further N-terminal truncation reduced (SEBOV

Δ 1-33-Fc) or abolished (SEBOV Δ 1-28-Fc) cell-surface association. Mutant SEBOV Δ T9A-Fc was created to evaluate whether a computationally predicted *O*-glycosylation site within SEBOV Δ -peptide plays an important role in Δ -peptide-mediated inhibition. Exchanging residue T₉ for an alanine did lead to a migration shift during PAGE analysis (data not shown), suggesting that this residue is indeed glycosylated. Surprisingly, SEBOV Δ T9A-Fc bound to Vero E6 cells with increased affinity compared to SEBOV Δ -Fc (Figure 7-38). The exchange of SEBOV Δ -Fc residue R₂₁ for alanine did not have an effect on cell association, whereas simultaneous exchange of C₂₉ and C₃₈, which are 100% conserved among all ebolaviral Δ -peptides, for alanines increased cell binding.

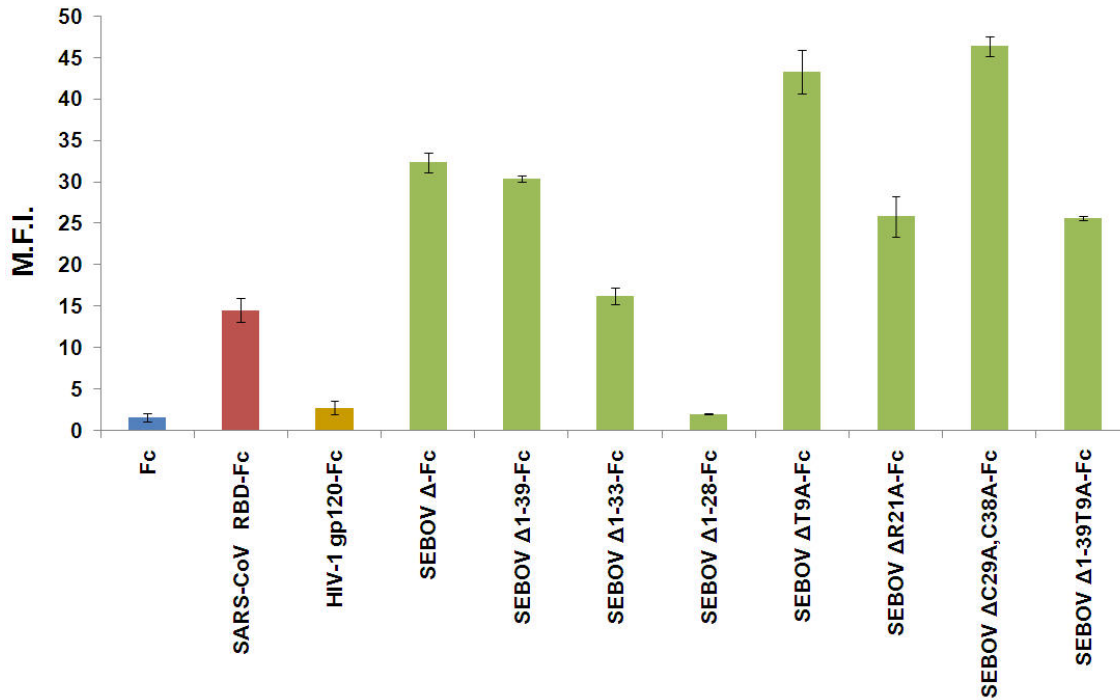


Figure 7-38. Binding of Sudan ebolavirus Δ -peptide mutants to the surface of filovirus-permissive nonhuman primate cells

Sudan ebolavirus (SEBOV) Δ -peptide (Δ -Fc) mutants, and control proteins Fc, severe acute respiratory syndrome coronavirus (SARS-CoV) RBD-Fc, human immunodeficiency virus type 1 (HIV-1) gp120-Fc or SEBOV Δ -Fc were incubated with filovirus-permissive African green monkey kidney epithelial (Vero E6) cells at a concentration of 100 nM, and analyzed by flow cytometry using an Fc-specific fluorescein isothiocyanate-conjugated secondary antibody. Bars indicate mean fluorescence intensity (M.F.I.) averages of two or more experiments. Error bars indicate standard deviations

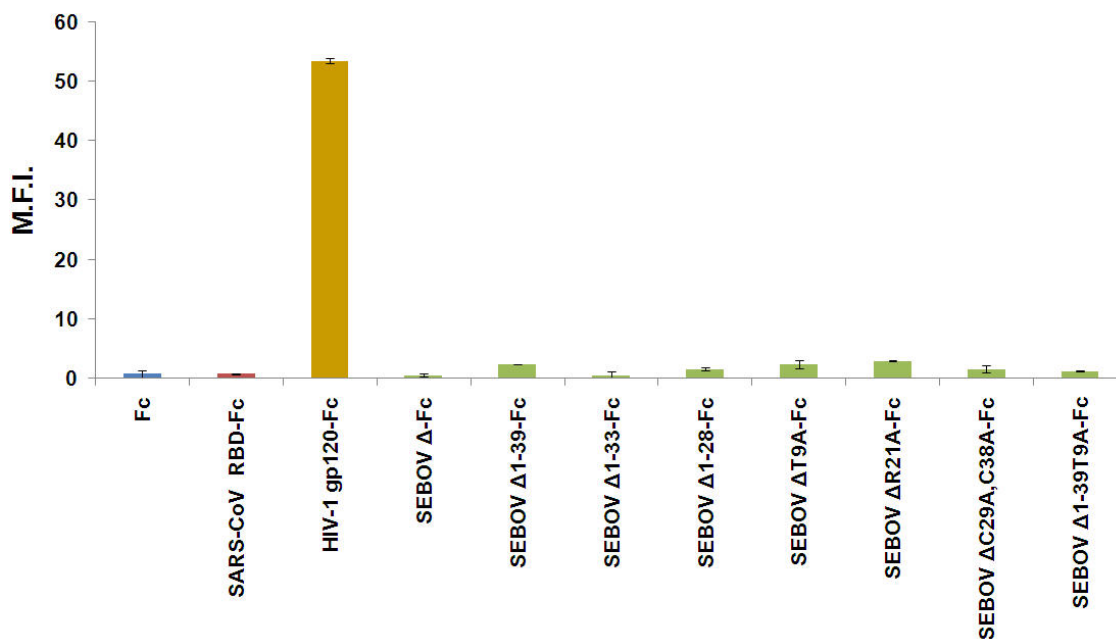


Figure 7-39. Binding of Sudan ebolavirus Δ -peptide mutants to the surface of filovirus-resistant human cells

Sudan ebolavirus (SEBOV) Δ -peptide (Δ -Fc) mutants, and control proteins Fc, severe acute respiratory syndrome coronavirus (SARS-CoV) RBD-Fc, human immunodeficiency virus type 1 (HIV-1) gp120-Fc or SEBOV Δ -Fc were incubated with filovirus-resistant human acute T-cell leukemia Jurkat E6-1 lymphocytes at a concentration of 100 nM, and analyzed by flow cytometry using an Fc-specific fluorescein isothiocyanate-conjugated secondary antibody. Bars indicate mean fluorescence intensity (M.F.I.) averages of two or more experiments. Error bars indicate standard deviations

The ability of mutated SEBOV Δ -Fc to inhibit entry of pseudotyped retrovirus particles was assayed as described above, using MARV/MLV (Chapter 7.1.4). Vero E6 cells were incubated with 200 nM of each mutant or control protein and pseudotyped gammaretrovirus particles (Figure 7-40). SR Δ -Fc, a chimeric Δ -peptide consisting of the N-terminal half of SEBOV Δ -peptide and the C-terminal half of REBOV Δ -peptide, inhibited cell transduction only minimally and at levels comparable to REBOV Δ -Fc. Conversely, RSA Δ -Fc, a chimeric Δ -peptide consisting of the N-terminal half of REBOV Δ -peptide and the C-terminal half of SEBOV Δ -peptide, strongly inhibited transduction at levels comparably to SEBOV Δ -Fc. This observation suggests that SEBOV Δ -Fc primarily exerts

its entry-inhibitory effect through amino-acid residues located in its C-terminus. This notion is supported by the observation that successive C-terminal truncation of SEBOV Δ -Fc decreased cell-surface binding (Figure 7-38), as well as transduction inhibition (Δ 1-39-Fc > Δ 1-33-Fc > Δ 1-28-Fc > 1-17-Fc). The N-terminal truncation variant Δ 28-48-Fc, which represents the C-terminal half of SEBOV Δ -Fc, still had minimal inhibitory function on MARV/MLV cell transduction. SEBOV Δ T9A-Fc, Δ S14A-Fc, Δ W18A-Fc, and Δ W26A-Fc were not impaired in their ability to inhibit MARV/MLV entry when compared to wild-type SEBOV Δ -Fc, whereas Δ R21A-Fc and Δ C29A,C38A-Fc lost some activity. Together, these results suggest 1) that SEBOV Δ -peptide requires its N-terminus for stability or folding of the protein, although the N-terminus is not involved in attaching to SEBOV Δ -peptide's cell-surface binding partner; 2) that the inhibitory function of SEBOV Δ -Fc is mediated by its C-terminus; 3) that T₉ of SEBOV Δ -Fc is *O*-glycosylated but that this glycosylation is not important for function; and 4) that residues S₁₄, R₂₁, W₁₈, W₂₆ (all located within the N-terminal half of the peptide) and C₂₉/C₃₈ (in the C-terminal half) do not play crucial roles in MARV/MLV inhibition.

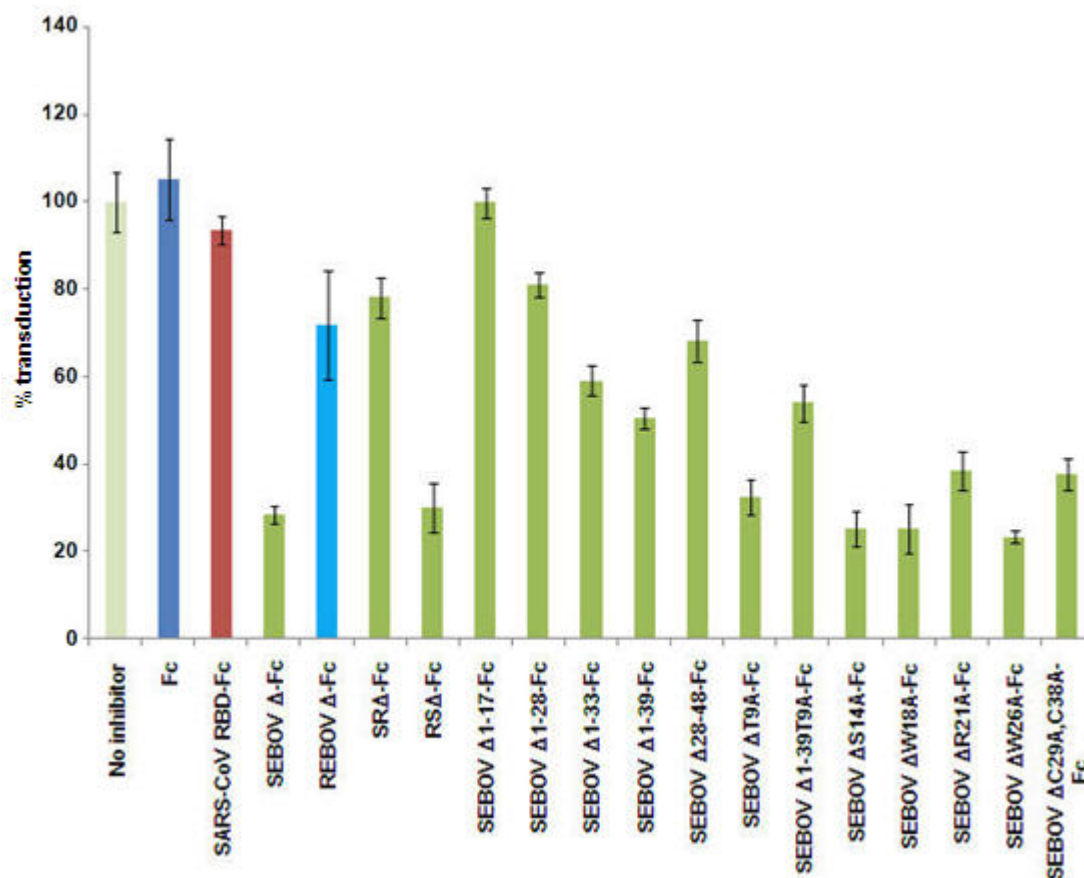


Figure 7-40. Analysis of the effect of Sudan ebolavirus Δ -peptide mutants on entry of gammaretrovirus particles pseudotyped with Lake Victoria marburgvirus isolate Musoke GP_{1,2}

Sudan ebolavirus (SEBOV) Δ -peptide (Δ -Fc) mutants, and control proteins Fc, severe acute respiratory syndrome coronavirus (SARS-CoV) RBD-Fc, SEBOV Δ -Fc or Reston ebolavirus (REBOV) Δ -Fc were incubated at 100 nM concentration with filovirus-permissive African green monkey kidney epithelial (Vero E6) cells and enhanced green fluorescent protein-expressing Moloney murine leukemia virus (MLV) pseudotyped with Lake Victoria marburgvirus isolate Musoke (MARV-Mus) GP_{1,2}. Entry of pseudotyped MLV was quantified by measuring green fluorescence using flow cytometry. Individual measure points show relative cell entry percentages compared to mock-inhibited control (defined as 100%) and indicate averages of two or more experiments. Error bars indicate standard deviations. SR, Sudan-Reston Δ -peptide chimera; RS, Reston-Sudan Δ -peptide chimera

7.2.7 Sudan ebolavirus Δ -Fc and Lake Victoria marburgvirus isolate Musoke 38-188-Fc may compete for the same cell-surface binding factor

It was shown that all filoviruses utilize at least one common cell-surface factor to achieve cell penetration (Chapter 7.1), and that CIEBOV, SEBOV, and ZEBOV Δ -Fc inhibit both MARV and ZEBOV cell entry with efficiencies equal to or greater than filoviral RBR-Fcs (Chapters 7.2.3 and 7.2.4). A cell-binding competition assay was developed to evaluate whether ebolaviral Δ -Fcs bind to the same factor as filoviral RBR-Fcs. Briefly, the human IgG₁ Fc region in SEBOV Δ -Fc was substituted by the Fc region of murine IgG_{2A} (SEBOV Δ -mFc, for expression gel see Figure 7-37). Vero E6 cells were incubated with 200 nM MARV-Mus 38-188-Fc or with 200 nM SEBOV Δ -mFc. Cells were washed, and the MARV samples incubated with 800 nM of SEBOV Δ -mFc or BSA and the SEBOV samples with 800 nM MARV-Mus 38-188-Fc or BSA. Cells were washed again and subsequently stained with FITC-conjugated anti-human Fc antibody (hAb) or FITC-conjugated anti-murine Fc antibody (mAb) and analyzed by flow cytometry (Figure 7-41). The presence of 800 nM SEBOV Δ -mFc reduced the cell-binding signal of 200 nM MARV-Mus 38-188-Fc roughly by 50%, and the presence of 800 nM MARV-Mus 38-188-Fc reduced the cell-binding signal of 200 nM SEBOV Δ -mFc roughly by 50% as well. These data suggest that at least SEBOV Δ -Fc might bind to the unknown filovirus receptor, and thereby modulate filovirus cell entry.

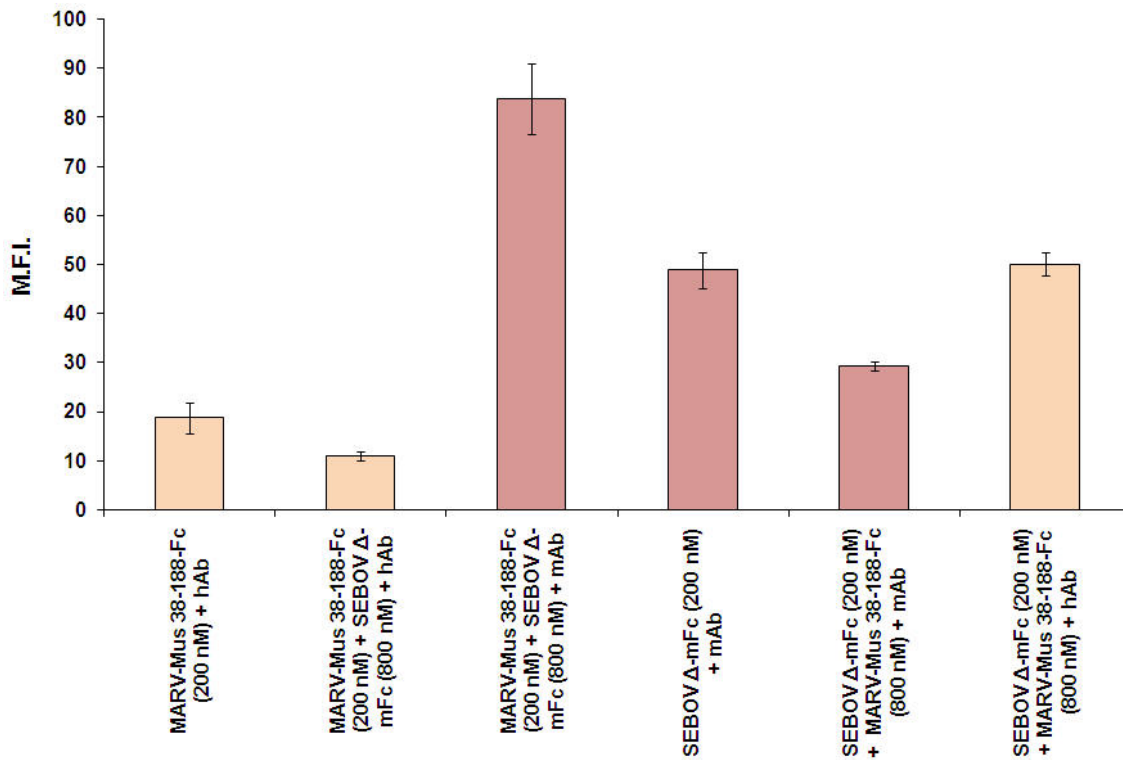


Figure 7-41. Sudan ebolavirus Δ -Fc and Lake Victoria marburgvirus isolate Musoke 38-188-Fc may compete for the same cell-surface binding factor

Filovirus-permissive African green monkey kidney epithelial (Vero E6) cells were incubated with 200 nM Lake Victoria marburgvirus isolate Musoke (MARV-Mus) 38-188-Fc and with or without 800 nM Sudan ebolavirus (SEBOV) Δ -mFc. Cell-surface binding was evaluated with either fluorescein isothiocyanate-conjugated anti-human Fc antibody (hAb; yellow columns) or fluorescein isothiocyanate-conjugated anti-murine Fc (mFc) antibody (mAb; red columns), and analyzed by flow cytometry. *Vice versa*, cells were incubated with 200 nM SEBOV Δ -mFc and with or without 800 nM MARV-Mus 38-188-Fc. Cell-surface binding was again evaluated with either fluorescein isothiocyanate-conjugated anti-human hAb or fluorescein isothiocyanate-conjugated anti-murine mAb. Bars indicate mean fluorescence intensity (M.F.I.) averages of two or more experiments. Error bars indicate standard deviations

7.2.8 Ebolaviral Δ -peptides do not inhibit cathepsin B activity

It is now known that ZEBOV cell entry is dependent on the presence of cathepsin B, and, to lesser extent, on cathepsin L (52, 130, 148, 232, 240). It is not known, however, whether cathepsins act prior to, during or after virus-receptor binding. The fact that ebolaviral Δ -Fc_s interfered with ebolaviral cell entry raised the possibility that they could interfere with cathepsin activity. To test this hypothesis, human cathepsin B was incubated with a concentration of ebolaviral Δ -Fc_s shown previously to inhibit ZEBOV GP_{1,2}-mediated entry (Figure 7-32) or with controls, and exposed to increasing concentrations of a cathepsin B substrate (Z-Arg-Arg-AMC) that fluoresces upon proteolytic cathepsin cleavage.

Figure 7-42 demonstrates that none of the four ebolaviral Δ -Fc_s had a significant effect on cathepsin B's ability to proteolytically cleave increasing amounts of substrate, whereas the known cathepsin B inhibitor CA074 inhibited the protease completely at very low concentrations. These data suggest that ebolaviral Δ -peptides probably do not interfere with cathepsin B during filovirus cell entry.

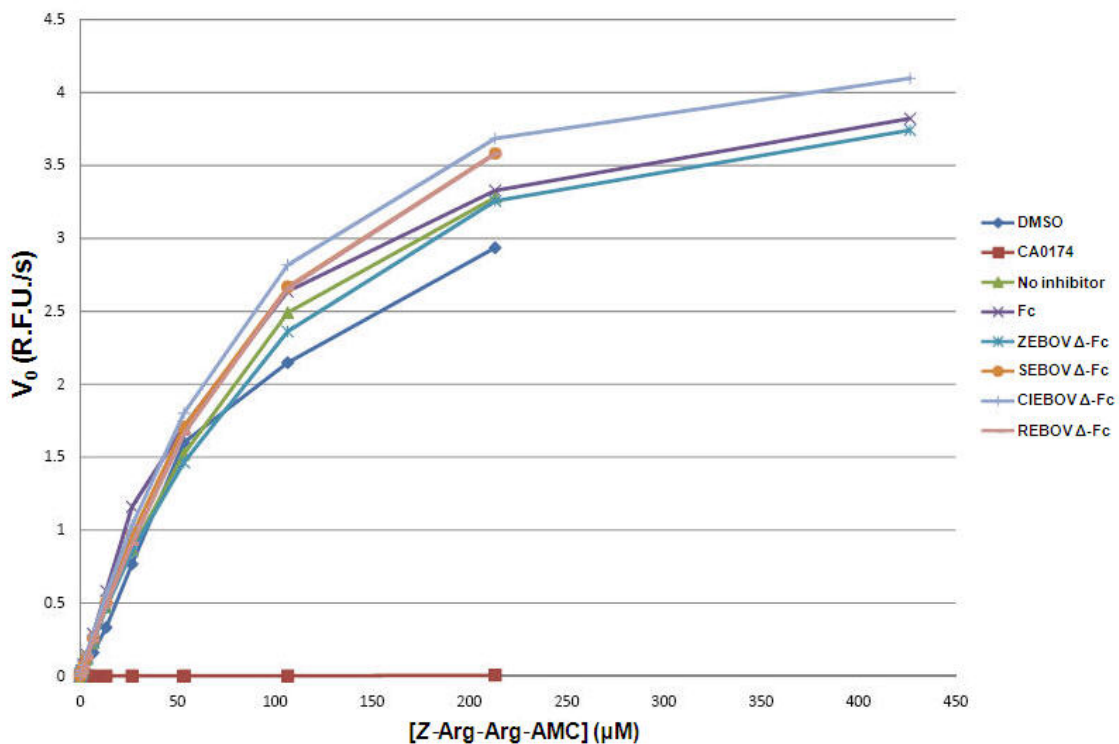


Figure 7-42. Ebolaviral Δ -peptides do not inhibit cathepsin B activity

30 nM of Côte d'Ivoire ebolavirus (CIEBOV), Reston ebolavirus (REBOV), Sudan ebolavirus (SEBOV) or Zaire ebolavirus (ZIEBOV) Δ -Fc or controls Fc, cathepsin B inhibitor CA0174 or dimethylsulfoxide (DMSO) were incubated with 1 $\mu\text{g}/\text{ml}$ human cathepsin B and increasing concentrations of Z-Arg-Arg-AMC fluorescent cathepsin B substrate. Fluorescence was measured as relative fluorescence units (R.F.U.) every three minutes for 1 h

7.3 Filoviral Fc-conjugated receptor-binding regions are strongly immunogenic filovirus candidate vaccines

7.3.1 C57/BL6 mice inoculated with Lake Victoria marburgvirus isolate Musoke 38-188-Fc or Zaire ebolavirus isolate Mayinga 54-201-Fc develop strong humeral and cytotoxic T-lymphocyte immune responses

The removal of the highly variable mucin-like domains (MLDs) and adjacent sequences resulted in increased binding of Lake Victoria marburgvirus isolate Musoke (MARV-Mus) and Zaire ebolavirus isolate Mayinga (ZEBOV-May) spike-protein fragments to filovirus-permissive cells (Chapter 7.1). These data suggested that the MLDs of filoviral spike proteins shield the rather conserved receptor-binding regions (RBRs), possibly to prevent the formation of cell entry-neutralizing antibodies by the filovirus-infected host. These “glycan shields” may also be the reason why, despite the fact that all filoviruses utilize a common receptor, there has so far been no success in developing a monovalent candidate vaccine that cross-protects against infection with heterologous filoviruses. If so, filoviral spike proteins devoid of the MLD could be valuable subunit candidate vaccines.

To evaluate whether purified protein preparations of filoviral RBRs could be used as subunit candidate vaccines, three groups of C57BL/6 house mice were immunized three times with purified preparations of MARV-Mus 38-188-Fc and RIBI adjuvant, ZEBOV-May 54-201-Fc and RIBI adjuvant or RIBI adjuvant alone, respectively (for immunization schedule, see Figure 7-43).

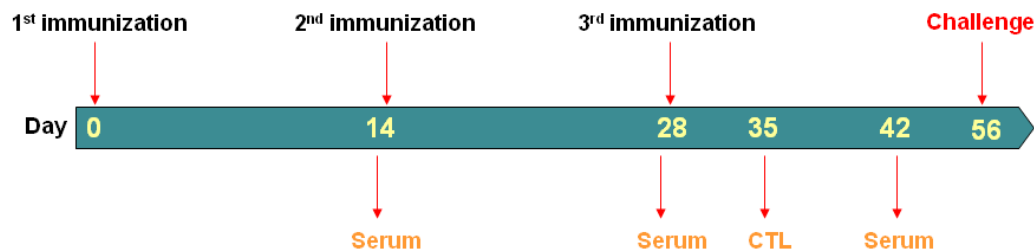


Figure 7-43. Immunization of mice with Lake Victoria marburgvirus isolate Musoke 38-188-Fc or Zaire ebolavirus isolate Mayinga 54-201-Fc

Three groups of 13 mice each were immunized intramuscularly on days 0, 14, and 28 with 20 µg per immunization of either Lake Victoria marburgvirus isolate Musoke (MARV-Mus) 38-188-Fc or Zaire ebolavirus isolate Mayinga (ZEBOV-May) 54-201-Fc in 200 µl RIBI adjuvant or with adjuvant alone. Sera were collected two weeks after each immunization for determination of antibody titers. On day 35, three mice of each group were euthanized and splenocytes were collected for analysis of cytotoxic T-lymphocyte (CTL) responses. On day 56, the remaining mice were challenged by intraperitoneal injection with 1,000 pfu (~30,000 LD₅₀) of mouse-adapted ZEBOV-May (33)

All tested mice (ten out of ten) immunized with ZEBOV-May 54-201-Fc developed high antibody titers ($\sim 10^4$) as measured by ELISA using γ -irradiated Zaire ebolavirus isolate Kikwit (ZEBOV-Kik) as antigen (123). Interestingly, and in support of the hypothesis, six out of ten mice immunized with MARV-Mus 38-188-Fc also developed comparable antibody titers against γ -irradiated ZEBOV-Kik, whereas four mice developed lower titers that were, however, clearly above background (Figure 7-44). These results suggest that immunization with MARV-Mus 38-188-Fc induced antibodies cross-reactive with ZEBOV-May GP₁.

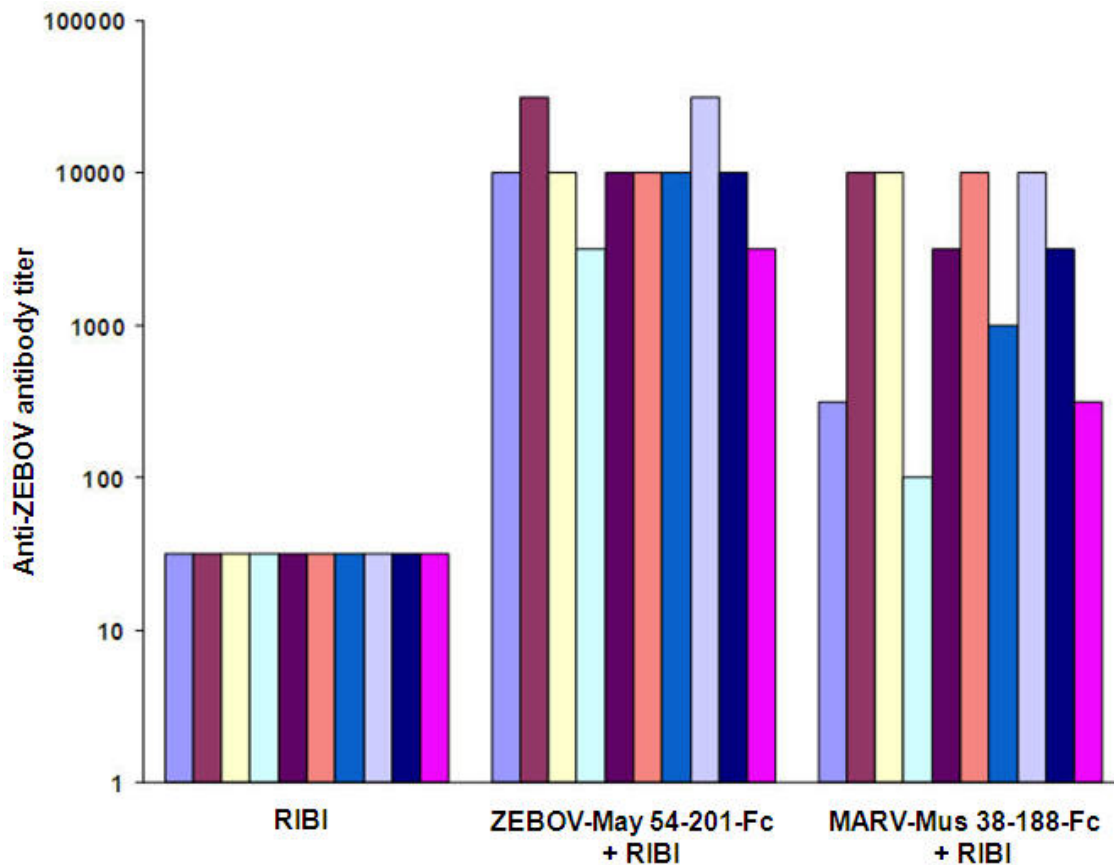


Figure 7-44. Mice immunized with Lake Victoria marburgvirus isolate Musoke 38-188-Fc or Zaire ebolavirus isolate Mayinga 54-201-Fc develop cross-reactive antibodies

Sera were collected from mice on days 14, 28, and 42. Antibody titers were determined by ELISA using γ -irradiated Zaire ebolavirus isolate Kikwit (ZEBOV-Kik) as antigen and a horseradish peroxidase-conjugated secondary antibody. Antibody titers were defined as the reciprocal of the highest dilution. Shown here are the antibody titers of sera collected on day 42. Each bar represents the antibody titer of one individual mouse. ZEBOV-May, Zaire ebolavirus isolate Mayinga; MARV-Mus, Lake Victoria marburgvirus isolate Musoke

To examine cytotoxic T-lymphocyte (CTL) responses induced by MARV-Mus 38-188-Fc and ZEBOV-May 54-201-Fc, pooled splenocytes harvested from three mice of each of the three immunized groups were incubated with a matrix of overlapping peptide pools derived from ZEBOV-May GP₁, stained for surface expression of CD8, CD44, and

intracellular IFN- γ , and analyzed by flow cytometry (Figure 7-45). Two pools contained peptides that stimulated splenocytes harvested from mice immunized with MARV-Mus 38-188-Fc and ZEBOV-May 54-201.

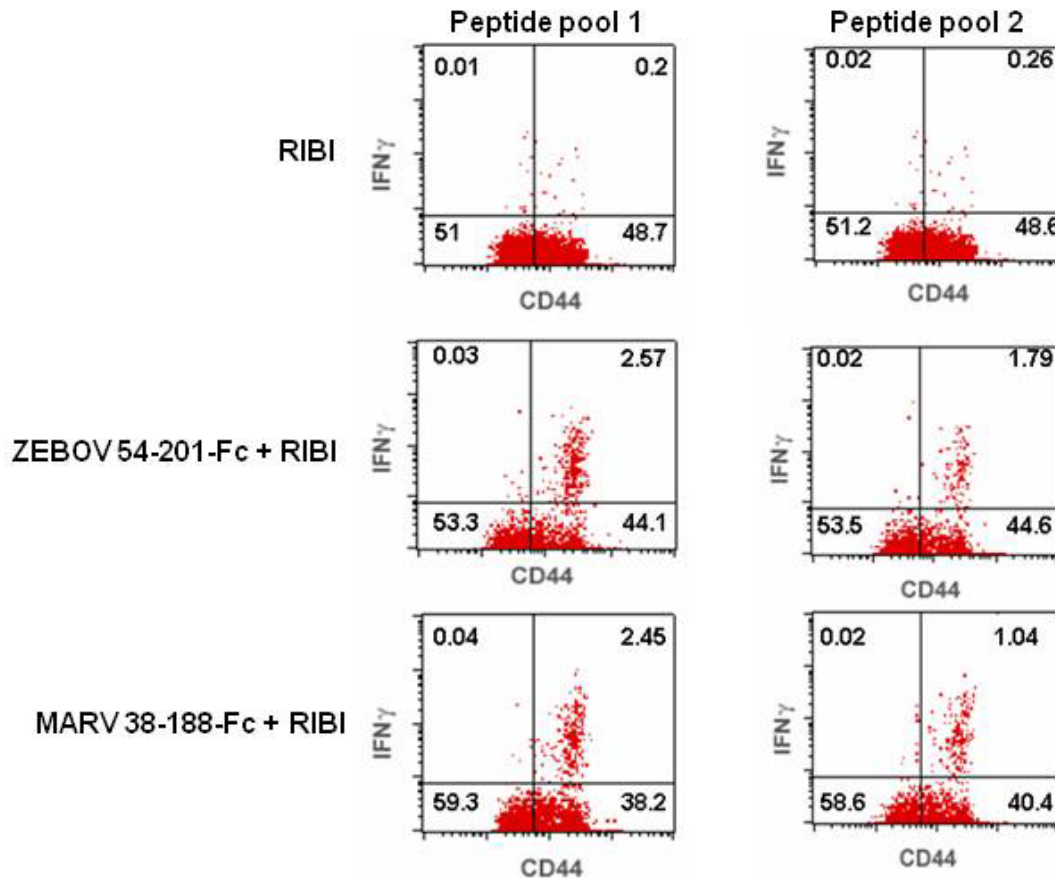


Figure 7-45. Mice immunized with Lake Victoria marburgvirus isolate Musoke 38-188-Fc or Zaire ebolavirus isolate Mayinga 54-201-Fc develop splenocytes reactive to Zaire ebolavirus isolate Mayinga GP₁ peptides

Splenocytes were collected from three euthanized mice of each immunized group on day 35. The cells were incubated with a matrix of overlapping peptide pools derived from Zaire ebolavirus isolate Mayinga (ZEBOV-May) GP₁, followed by staining for surface expression of CD8, CD44, and interferon γ (IFN- γ) and analysis by flow cytometry. Shown here are the results of this experiment gated on CD8⁺ cells. The numbers in each quadrant are the percentages of each cell population. The upper right quadrant of each panel represents the reactive splenocyte population

7.3.2 Sera from C57/BL6 mice inoculated with Lake Victoria marburgvirus 38-188-Fc or Zaire ebolavirus isolate Mayinga 54-201-Fc neutralize infectious Zaire ebolavirus *in vitro*

To determine if the induced cross-reactive antibodies also inhibit the replication of infectious filoviruses, filovirus-permissive African green monkey kidney epithelial (Vero E6) cells were incubated with infectious ZEBOV-May modified to express eGFP (270), at a multiplicity of infection (moi) of 1, together with sera harvested from mice immunized with RIBI adjuvant alone, with ZEBOV-May 54-201-Fc + RIBI or with MARV-Mus 38-188-Fc + RIBI. Interestingly, the sera from animals immunized with ZEBOV-May 54-201-Fc + RIBI or with MARV-Mus 38-188-Fc + RIBI, but not those from control animals, completely neutralized replication of infectious ZEBOV-May (Figure 7-46). These data indicate that MARV spike-protein fragments can induce the synthesis of ebolavirus-neutralizing antibodies in mice, and that such antibodies could be used as therapeutics, as they might also inhibit filovirus replication in nonhuman primates or humans.

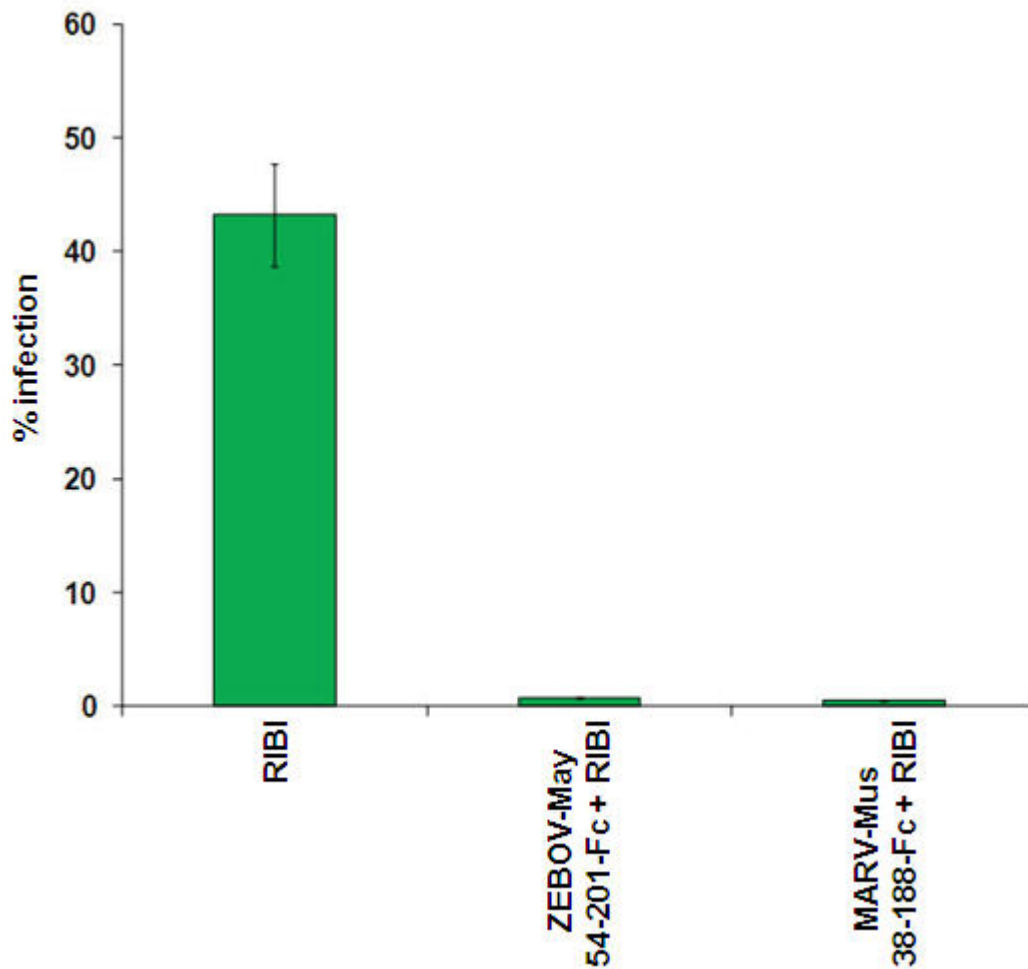


Figure 7-46. Sera from mice immunized with Lake Victoria marburgvirus isolate Musoke 38-188-Fc or Zaire ebolavirus isolate Mayinga 54-201-Fc inhibit replication of infectious Zaire ebolavirus

Filovirus-permissive African green monkey kidney epithelial (Vero E6) cells were infected with enhanced green fluorescent protein-expressing Zaire ebolavirus isolate Mayinga (ZEBOV-May) in the presence of sera harvested from mice immunized with RIBI adjuvant, ZEBOV-May 54-201-Fc + RIBI or with Lake Victoria marburgvirus isolate Musoke (MARV-Mus) 38-188-Fc + RIBI. Infection was quantified by measuring green fluorescence using Discovery-1 automated microscopy

7.3.3 C57/BL6 mice inoculated with Lake Victoria isolate Musoke 38-188-Fc or Zaire ebolavirus isolate Mayinga 54-201-Fc are partially and fully protected against challenge with infectious Zaire ebolavirus, respectively

To evaluate whether the induced antibodies and cytotoxic T-lymphocyte responses can protect against fatal disease caused by infectious filoviruses, the immunized mice were challenged with mouse-adapted ZEBOV-May (33) on day 56 post immunization and monitored continuously. All mice immunized with ZEBOV-May 54-201-Fc remained healthy. Most importantly, 50% of the mice immunized with MARV-Mus 38-188-Fc were similarly protected, whereas the other 50% developed symptoms of filovirus hemorrhagic fever and died. These promising data suggest that the development of a monovalent pan-filovirus vaccine may be possible, as they describe the first marburgvirus/ebolavirus cross-reactive candidate vaccine.

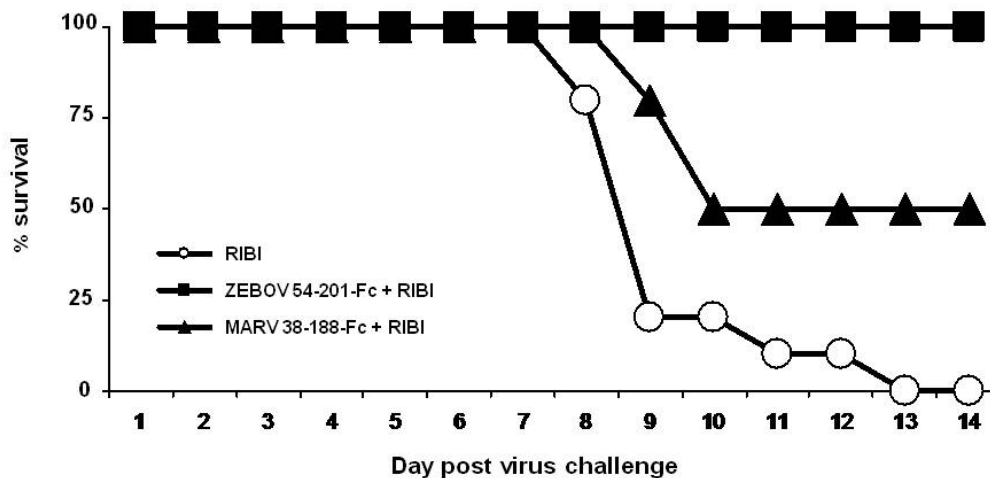


Figure 7-47. Mice immunized with Lake Victoria marburgvirus isolate Musoke 38-188-Fc or Zaire ebolavirus isolate Mayinga 54-201-Fc are partially and fully protected from infection with mouse-adapted Zaire ebolavirus isolate Mayinga, respectively

Mice were challenged with 1,000 pfu (~30,000 LD₅₀) of mouse-adapted Zaire ebolavirus isolate Mayinga (ZEBOV-May) (33) on day 56 after immunization with Lake Victoria marburgvirus isolate Musoke (MARV-Mus) 38-188-Fc + RIBI, ZEBOV-May 54-201-Fc + RIBI or RIBI alone. The survival rate of mice in the three different groups is shown in a Kaplan-Meier plot

8 DISCUSSION

Viral infections of animals are established by entry of viral particles into host cells using endocytic or nonendocytic pathways (63). The endocytic route is often pH-dependent and employs clathrin-coated pits, non-clathrin-coated pits, caveolae or macropinocytic vesicles, whereas the nonendocytic route generally results in direct penetration of the plasma membrane at neutral pH (244).

Enveloped viruses, such as filoviruses, use specific proteins (spike proteins or peplomers) on the virion surface that mediate host-cell attachment and fusion of the viral membrane with cellular membranes (63). This then results in the release of the viral genome into the host cell. According to their structural organization and their functional characteristics, spike proteins are currently grouped into three classes (116, 122, 150, 225, 226, 301). Viral class I fusion proteins, encoded, for instance, by coronaviruses (314), orthomyxoviruses (42), paramyxoviruses (317), and retroviruses (79), are typically glycosylated homotrimers that protrude vertically from the viral surface and contain mostly α -helical structures (63, 116, 150). Each monomer is comprised of two functionally distinct domains or subunits that are synthesized as one preprotein that is cleaved by a protease in the producer cell (63, 68). The N-terminal globular ectodomain mediates cell attachment and receptor association, whereas the C-terminal stalk-like fusion domain mediates the actual fusion process. Fusion domains of class I fusion proteins usually contain relatively hydrophobic and glycine-rich regions, commonly referred to as fusion peptides, at or close to their N-termini, and transmembrane regions, which anchor them to the viral membranes. After attachment of an ectodomain to a receptor, the fusion peptide becomes exposed and inserted into the target membrane. The fusion domain is then subjected to complex conformational changes, resulting in the formation of a hairpin-like structure formed by a trimeric coiled-coil stem at the fusion peptide's C-terminus and segments adjacent to the transmembrane domain (six-helix bundle). This rearrangement forces the viral and cellular membrane into close apposition, which results in fusion (63, 116, 122, 150).

Viral class II fusion proteins, encoded, for instance, by alphaviruses (166) and flaviviruses (186), are elongated homodimers that lie flat on the virion surface in icosahedral lattices, and are protected by a second glycoprotein (212). Each monomer consists of three globular domains composed mainly of β -sheets, and the fusion peptide is located within the peptide chain rather than at one of its termini. Receptor binding results in a switch from dimeric to trimeric conformations (319), the exposure of the fusion peptide and insertion into the target membrane, and subsequently to fusion (63, 116, 122, 150).

Viral class III fusion proteins, encoded, for instance, by rhabdoviruses and herpesviruses, are still rather uncharacterized and appear to be functional hybrids of class I and II proteins (122, 225, 226).

Two types of cell-surface structures facilitate virus entry. For one, viral spike proteins may attach to so-called attachment factors, such as glycosaminoglycans, C-type lectins or integrins. Binding to these factors frequently makes substantial contributions to the efficiency of viral entry by concentrating virions on the target-cell surface (13, 178, 204). More critically, most viruses require one or more cellular receptors, which can be glycans, lipids or proteins, to initiate cell penetration. Receptors are obligatory requirements for virus-cell entry, whereas attachment factors are not. The expression of true receptors in virus entry-resistant, but otherwise virus-susceptible, cells should therefore confer virus susceptibility. Also, cell types that express the receptor should generally not be resistant to virus entry. Conversely, a virus attachment factor can be present on a virus entry-resistant cell or be absent from a virus-permissive cell (63).

Receptor-binding regions (RBRs) of viral spike proteins are typically the most important antibody-neutralizing epitopes on virions, due to the functional importance of and limited variation in these regions (68). In some cases, such as murine and feline leukemia retroviruses and severe acute respiratory syndrome coronavirus (SARS-CoV), the RBRs are discrete, independently folded regions (receptor-binding domains, RBDs) that can efficiently bind cellular receptors and inhibit infection (14, 78, 304). These regions themselves also can be sufficient to elicit potent protective neutralizing antibodies that are

not produced during natural infection because of cloaking of the RBRs by adjacent spike-protein regions (68).

Filoviruses (marburgviruses and ebolaviruses) most likely enter target cells through pH-dependent receptor-mediated and clathrin-dependent endocytosis (12, 51, 103, 232, 262, 305, 318). This process is facilitated by the filoviral spike protein GP_{1,2}, which is a rather typical class I fusion protein (94). Its ectodomain, GP₁, mediates receptor binding, whereas its fusion domain, GP₂, facilitates membrane fusion (94, 162). GP₁ binds to numerous cell-surface attachment factors before binding to the receptor (6, 25, 48, 112, 178, 247, 261, 263), which has yet to be identified.

Here, small regions of the GP₁ proteins of two divergent filoviruses (Lake Victoria marburgvirus isolate Musoke (MARV-Mus) amino-acid residues 38-188 and Zaire ebolavirus isolate Mayinga (ZEBOV-May) amino-acid residues 54-201) were identified that bind filovirus-permissive cells more efficiently than the full-length ectodomains. Several lines of evidence suggest that these regions bind a cellular receptor rather than an attachment factor. First, these regions did not associate with cell lines refractory to filovirus infection, such as human acute T-cell leukemia Jurkat E6-1 lymphocytes (Figures 7-5 and 7-10). Second, they associated with filovirus-permissive cells, such as African green monkey kidney epithelial (Vero E6) cells, more efficiently than larger and more heavily glycosylated GP₁ variants (Figures 7-3 and 7-8). Indeed, ZEBOV-May GP₁ residues 54-201 do not contain sites that could be attached to *N*-glycans, which could associate with cell-surface lectin-like molecules (MARV-Mus GP₁ residues 38-188 include two potential *N*-glycosylation sites, at positions 94 and 171, but plasmids mutated to encode 38-188N94A-Fc, 38-188N171A-Fc or 38-188N94A,N171A-Fc did not express protein (data not shown)). Third, both regions 54-201 and 38-188, when fused to Fc, efficiently inhibited entry mediated by their respective GP_{1,2} at 50-200 nM, indicating that they associate with moderately high affinity and specifically with a factor critical to entry (Figures 7-13, 7-14, and 7-15). Finally, these regions include the most highly conserved region of filoviral GP₁ (172), which suggests that they play a crucial and conserved role in filovirus cell entry (Figure 8-1).

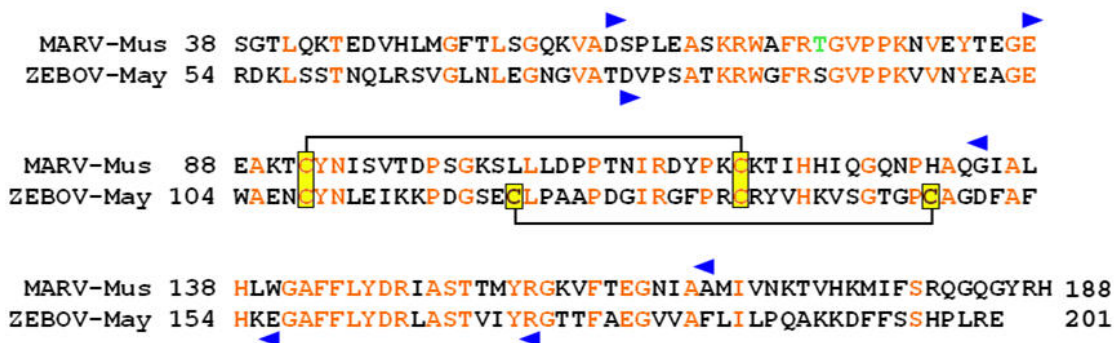


Figure 8-1. Sequence alignment of Lake Victoria marburgvirus isolate Musoke and Zaire ebolavirus isolate Mayinga receptor-binding regions

Sequence alignment of the filoviral receptor-binding regions (RBRs) Lake Victoria marburgvirus isolate Musoke (MARV-Mus) 38-188 and Zaire ebolavirus isolate Mayinga (ZEBOV-May) 54-201. Residues in orange indicate identical residues. A disulfide bond common to both receptor-binding regions is indicated with a bracket, as is a disulfide bond present only in ebolaviruses. Threonine 74 of MARV-Mus GP₁, which is an alanine in Lake Victoria marburgvirus isolate Angola (MARV-Ang) GP₁, is shown in green. Arrows indicate further truncations that reduced cell-surface binding and GP_{1,2}-mediated entry inhibition (see also Figures 7-1 and 7-6)

One rather surprising observation was that although MARV-Mus 38-188-Fc bound filovirus-permissive cells with much higher affinity than full-length GP₁-Fc (17-432-Fc), both fragments equally inhibited cell transduction by MARV-Mus GP_{1,2}-pseudotyped Moloney murine leukemia (MLV) virus particles (Figures 7-16). One possible explanation for this observation is that the mucin-like domain (MLD) of full-length GP₁ mediates a lower affinity interaction with an attachment factor on Vero E6 cells, which may contribute to inhibition of entry, but which may be more susceptible to the wash steps of the binding assay. Alternatively, partial misfolding of the longer truncation variants may impair cell surface association. It is important to note here that the created GP₁-Fc truncation variants were not evaluated in terms of folding. The goal of the truncation study was exclusively to identify a minimal receptor-binding GP₁ truncation variant, which was determined to consist of residues 54-201 in the case of ZEBOV-May and residues 38-188 in the case of

MARV-Mus. This, however, does not necessarily exclude the possibility that variants shorter than those could still be functional and that the smaller truncation variants evaluated here were simply misfolded. Alternatively, misfolding could also explain why some constructs, such as MARV-Mus 38-308-Fc, 61-308-Fc, and 87-308-Fc, were found to bind to filovirus-resistant cells (Figure 7-5), which did not bind any other filoviral glycoprotein-Fc construct tested. Further experiments are necessary to explain these findings. These could be performed in the near future after conformation-dependent antibodies to different regions of filoviral GP₁s have become available, as such antibodies could be used to evaluate the proper folding of GP₁ truncation variants that behave aberrantly.

Several mutational studies of ZEBOV GP_{1,2} are consistent with association of region 54-201 with a specific cellular receptor. For instance, Manicassamy *et al.* have shown that GP_{1,2} containing short deletions within the 54-201 region are nonfunctional. Furthermore, a thorough mutational scanning study demonstrated that residues D₅₅, L₅₇, L₆₃, R₆₄, F₈₈, K₉₅, and I₁₇₀ do not interfere with GP_{1,2} expression, processing or pseudotype incorporation, but rather interfered with GP_{1,2}-mediated infection (172). Brindley *et al.* conducted a similar study and identified residues G₈₇, F₈₈, K₁₁₄, K₁₁₅, K₁₄₀, G₁₄₃, P₁₄₆, C₁₄₇, F₁₅₃, H₁₅₄, F₁₅₉, F₁₆₀, and Y₁₆₂ as crucial for receptor binding (37). Finally, Mpanju *et al.* confirmed the important role of F₈₈ and F₁₅₉ during Zaire ebolavirus and Côte d'Ivoire ebolavirus entry (193).

Medina *et al.* have observed that a ZEBOV GP_{1,2} lacking GP₁ residues 241-496 nonetheless retained its ability to mediate entry of a pseudotyped retrovirus, whereas GP_{1Δ227-496} did not (183). Similar results were obtained for MARV during studies performed for this dissertation. In particular, MARV-Mus GP_{1,2} lacking GP₁ residues 266-432 could still mediate transduction of pseudotyped MLV particles as or more efficiently than full-length GP_{1,2} (residues 17-681). GP_{1,2} lacking GP₁ residues 231-432 had minimal, but detectable functionality, whereas GP_{1,2} lacking GP₁ residues 189-432 did not mediate entry (data not shown). Together, these data indicate that large parts of the filoviral GP₁ molecules, going even beyond the MLDs, are dispensable for cell-entry mediation, but that the identified receptor-binding regions (RBRs) of ZEBOV-May (54-201) and MARV-Mus

(38-188) fused to GP₂ are not sufficient to facilitate fusion. This observation is in accordance with the current understanding of fusion mediated by class I fusion proteins, during which a “clamp” downstream of the RBR keeps the protein in a “native” fusion-competent state and prevents premature initiation of the fusion process. This “clamp” is removed after receptor-binding or another trigger to convert the fusion-competent conformation to a membrane-embedded hairpin conformation, which is characterized by the insertion of GP₂'s fusion peptide into the host-cell membrane (301). The described results above suggest that the “clamp” is located upstream of residue 240 in the case of ZEBOV-May, and upstream of residue 230 in the case of MARV-Mus.

Numerous studies have demonstrated that digestion of ZEBOV GP_{1,2} with cathepsin B and/or L removes all but a 17-19 kD fragment of GP₁, which remains attached to undigested GP₂ through a disulfide bond. The resulting 17-19 kD-GP₂ complex can still mediate infection. These findings suggest that the 17-19 kD fragment may be identical to GP₁ residues 33-201 (54-201 plus the N-terminal amino-acid residues containing the cysteine that connects GP₁ to GP₂), although the exact cathepsin cleavage site(s) have yet to be determined (52, 130, 148, 232, 240). Interestingly, Kaletsky *et al.* demonstrated that the 17-19 kD fragment not only is sufficient for mediating cell entry, but also binds with increased affinity to filovirus-permissive cells compared to full-length GP₁ (148). This observation indirectly confirms results presented here, namely the increased cell-binding properties of ZEBOV-May 54-201-Fc compared to longer GP₁ fragments (Figure 7-8).

Last, Dube *et al.* recently confirmed that ZEBOV-May 54-201-Fc binds filovirus-permissive cells, whereas it does not bind filovirus-resistant cells. Interestingly, Dube *et al.* used human embryonic kidney (HEK) 293F and human monocyte THP-1 cells for experiments, both of which can be grown as either adherent or as suspension cultures. ZEBOV-May 54-201-Fc bound the cells in their adherent state, but not when they were grown in suspension (65). These findings could indicate that the filovirus receptor may be a cell-adhesion molecule.

Although the genomic organization of marburgviruses and ebolaviruses is similar, and although they cause similar diseases of comparable severity, it has not been clear

whether all filoviruses utilize a common receptor. Several observations in the literature raised the possibility that their receptors or entry mechanisms are distinct. For instance, MARV has been reported to be less susceptible than ZEBOV to treatment of target cells with proteases and glycosidases (51). Electron micrographs of the filoviruses entering cells have been used to suggest that MARV enters cells differently than ZEBOV (231), although earlier and more recent work suggested that both viruses enter by endocytosis (103, 232). Some variation in the relative efficiencies with which MARV and ZEBOV GP_{1,2} mediate entry into different cell lines also raised the possibility of distinct receptors (51). Here, data are presented that demonstrate that MARV-Mus 38-188-Fc efficiently inhibited cell transduction by MLV particles pseudotyped with MARV-Mus or ZEBOV-May spike proteins. Likewise, ZEBOV-May 54-201-Fc inhibited cell transduction by both MARV/MLV and ZEBOV/MLV (Figures 7-13 and 7-14). Both MARV-Mus 38-188-Fc and ZEBOV-May 54-201 inhibited replication of infectious ZEBOV-May, albeit at much higher concentrations (800 nM vs. 50-200 nM) (Figure 7-17). These higher concentrations may be necessary to interfere with the greater number of GP_{1,2} molecules present on the filamentous filoviruses, compared to the significantly smaller and spherical gammaretroviral particles.

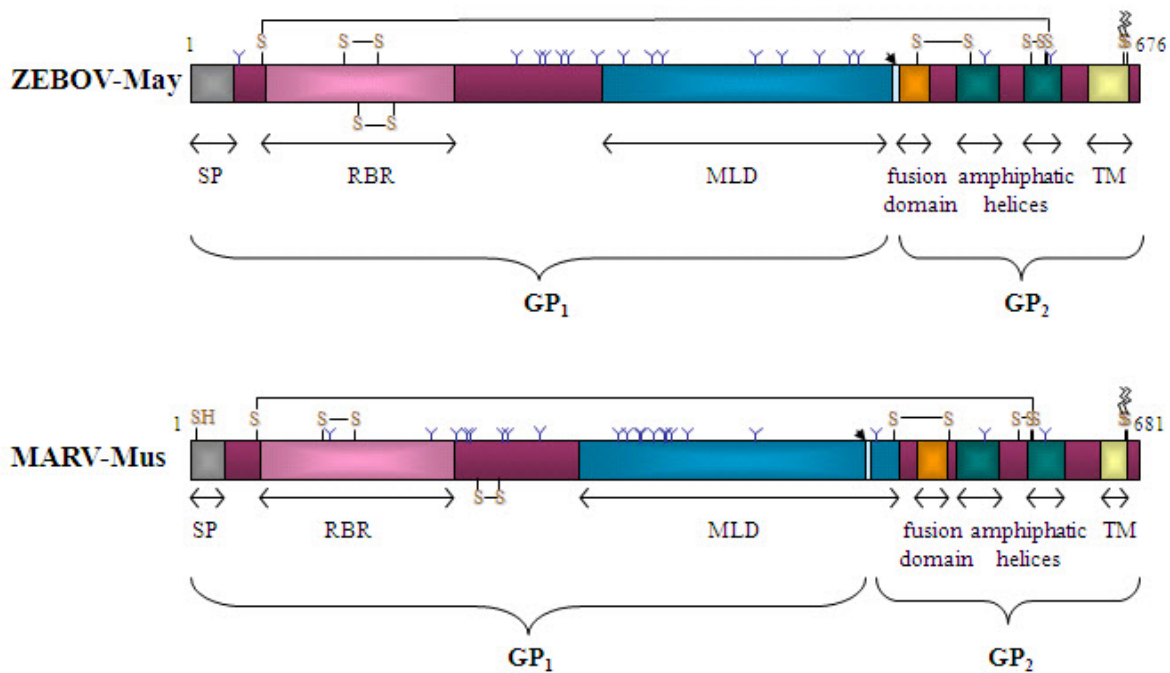


Figure 8-2. Location of the identified receptor-binding regions within filoviral full-length spike proteins

ZEBOV-May, Zaire ebolavirus isolate Mayinga; MARV-Mus, Lake Victoria marburgvirus isolate Musoke; SP, signal peptide; RBR, receptor-binding region (ZEBOV-May: residues 54-201; MARV-Mus: residues 38-188); MLD, mucin-like domain; TM, transmembrane domain (adapted from (157) with permission)

Sequence alignments of region 38-188 of all known MARV isolates (Figure 8-3) and of region 54-201 of all known ZEBOV isolates (Figure 8-4) clearly suggest that all these isolates would compete for the same entry factor.

MARV-Ang	SGT	LQKTEDVHLM	GFTLSGQKVA	DSPLEASKRW	AFRAGVPPKN	VEYTEGEEAK	TCYNISVTDP
MARV-Ci67	SGT	LQKTEDVHLM	GFTLSGQKVA	DSPLEASKRW	AFRTGVPPKN	VEYTEGEEAK	TCYNISVTDP
MARV-05DRC	SGT	LQKTEDVHLM	GFTLSGQKVA	DSPLEASKRW	AFRTGVPPKN	VEYTEGEEAK	TCYNISVTDP
MARV-07DRC	SGT	LQKTEDVHLM	GFTLSGQKVA	DSPLEASKRW	AFRTGVPPKN	VEYTEGEEAK	TCYNISVTDP
MARV-09DRC	SGT	LQKTEDVHLM	GFTLSGQKVA	DSPLEASKRW	AFRTGVPPKN	VEYTEGEEAK	TCYNISVTDP
MARV-Mus	SGT	LQKTEDVHLM	GFTLSGQKVA	DSPLEASKRW	AFRTGVPPKN	VEYTEGEEAK	TCYNISVTDP
MARV-"Mus-pp3"	SGT	LQKTEDVHLM	GFTLSGQKVA	DSPLEASKRW	AFRTGVPPKN	VEYTEGEEAK	TCYNISVTDP
MARV-"Mus-pp4"	SGT	LQKTEDVHLM	GFTLSGQKVA	DSPLEASKRW	AFRTGVPPKN	VEYTEGEEAK	TCYNISVTDP
MARV-Ozo	SGT	LQKTEDVHLM	GFTLSGQKVA	DSPLEASKRW	AFRTGVPPKN	VEYTEGEEAK	TCYNISVTDP
MARV-Pop	SGT	LQKTEDVHLM	GFTLSGQKVA	DSPLEASKRW	AFRTGVPPKN	VEYTEGEEAK	TCYNISVTDP
MARV-Ravn	SGT	LQKTEDVHLM	GFTLSGQKVA	DSPLEASKRW	AFRTGVPPKN	VEYTEGEEAK	TCYNISVTDP
MARV-Rat	SGT	LQKTEDVHLM	GFTLSGQKVA	DSPLEASKRW	AFRTGVPPKN	VEYTEGEEAK	TCYNISVTDP
MARV-Ang	SGKSLLLDPP	TNIRDYPKCK	TIHHIQGQNP	HAQGIALHLW	GAFFLYDRIA	STTMYRGKVF	
MARV-Ci67	SGKSLLLDPP	TNIRDYPKCK	TIHHIQGQNP	HAQGIALHLW	GAFFLYDRIA	STTMYGRGVF	
MARV-05DRC	SGKSLLLDPP	TNIRDYPKCK	TIHHIQGQNP	HAQGIALHLW	GAFFLYDRIA	STTMYRGKVF	
MARV-07DRC	SGKSLLLDPP	TNIRDYPKCK	TIHHIQGQNP	HAQGIALHLW	GAFFLYDRIA	STTMYRGKVF	
MARV-09DRC	SGKSLLLDPP	SNIRDYPKCK	TVHHIQGQNP	HAQGIALHLW	GAFFLYDRVA	STTMYRGKVF	
MARV-Mus	SGKSLLLDPP	TNIRDYPKCK	TIHHIQGQNP	HAQGIALHLW	GAFFLYDRIA	STTMYRGKVF	
MARV-"Mus-pp3"	SGKSLLLDPP	TNIRDYPKCK	TIHHIQGQNP	HAQGIALHLW	GAFFLYDRIA	STTMYRGKVF	
MARV-"Mus-pp4"	SGKSLLLDPP	TNIRDYPKCK	TIHHIQGQNP	HAQGIALHLW	GAFFLYDRIA	STTMYRGKVF	
MARV-Ozo	SGKSLLLDPP	TNIRDYPKCK	TIHHIQGQNP	HAQGIALHLW	GAFFLYDRIA	STTMYRGKVF	
MARV-Pop	SGKSLLLDPP	SNIRDYPKCK	TVHHIQGQNP	HAQGIALHLW	GAFFLYDRVA	STTMYRGKVF	
MARV-Ravn	SGKSLLLDPP	SNIRDYPKCK	TVHHIQGQNP	HAQGIALHLW	GAFFLYDRVA	STTMYRGKVF	
MARV-Rat	SGKSLLLDPP	TNIRDYPKCK	TIHHIQGQNP	HAQGIALHLW	GAFFLYDRIA	STTMYGRGVF	
MARV-Ang	TEGNIAAMIV	NKTVHKMIFS	RQGQGYRH				
MARV-Ci67	TEGNIAAMIV	NKTVHKMIFS	RQGQGYRH				
MARV-05DRC	TEGNIAAMIV	NKTVHKMIFS	RQGQGYRH				
MARV-07DRC	TEGNIAAMIV	NKTVHKMIFS	RQGQGYRH				
MARV-09DRC	TEGNIAAMIV	NKTVHRMIFS	RQGQGYRH				
MARV-Mus	TEGNIAAMIV	NKTVHKMIFS	RQGQGYRH				
MARV-"Mus-pp3"	TEGNIAAMIV	NKTVHKMIFS	RQGQGYRH				
MARV-"Mus-pp4"	TEGNIAAMIV	NKTVHKMIFS	RQGQGYRH				
MARV-Ozo	TEGNIAAMIV	NKTVHKMIFS	RQGQGYRH				
MARV-Pop	TEGNIAAMIV	NKTVHKMIFS	RQGQGYRH				
MARV-Ravn	TEGNIAAMIV	NKTVHRMIFS	RQGQGYRH				
MARV-Rat	TEGNIAAMIV	NKTVHKMIFS	RQGQGYRH				

Figure 8-3. Sequence alignment of Lake Victoria marburgvirus receptor-binding regions

Alignment of GP₁ residues 38-188 of all sequenced Lake Victoria marburgvirus (MARV) isolates. Variations are in red. Residue 74 of MARV-Ang GP₁, which is an alanine and not a threonine like in all other MARV isolates, is shown in green. Ci67, Cieplik isolate; DRC, Democratic Republic of the Congo isolate; Mus, Musoke isolate; Ozo, Ozolin isolate; Pop, Poppinga isolate; Rat, Ratayczak isolate.

ZEBOV-Boueé	RDKLSST	NQLRSVGLNL	EGNGVATDVP	SATKRWGFRS	GVPPKVVNYE	AGEWAENCYN
ZEBOV-Ecran	RDKLSST	NQLRSVGLNL	EGNGVATDVP	SATKRWGFRS	GVPPKVVNYE	AGEWAENCYN
ZEBOV-Entsiami	RDKLSST	NQLRSVGLNL	GGNGVATDVP	SATKRWGFRS	GVPPKVVNYE	AGEWAENCYN
ZEBOV-Etakangaye	RDKLSST	NQLRSVGLNL	GGNGVATDVP	SATKRWGFRS	GVPPKVVNYE	AGEWAENCYN
ZEBOV-Gabon94	RDKLSST	NQLRSVGLNL	EGNGVATDVP	SATKRWGFRS	GVPPKVVNYE	AGEWAENCYN
ZEBOV-Kik	RDKLSST	NQLRSVGLNL	EGNGVATDVP	SATKRWGFRS	GVPPKVVNYE	AGEWAENCYN
ZEBOV-Makokou	RDKLSST	NQLRSVGLNL	GGNGVATDVP	SATKRWGFRS	GVPPKVVNYE	AGEWAENCYN
ZEBOV-May	RDKLSST	NQLRSVGLNL	EGNGVATDVP	SATKRWGFRS	GVPPKVVNYE	AGEWAENCYN
ZEBOV-May8mc	RDKLSST	NQLRSVGLNL	EGNGVATDVP	SATKRWGFRS	GVPPKVVNYE	AGEWAENCYN
ZEBOV-Mendemba-A	RDKLSST	NQLRSVGLNL	GGNGVATDVP	SATKRWGFRS	GVPPKVVNYE	AGEWAENCYN
ZEBOV-Mendemba B	RDKLSST	NQLRSVGLNL	GGNGVATDVP	SATKRWGFRS	GVPPKVVNYE	AGEWAENCYN
ZEBOV-Mvoula	RDKLSST	NQLRSVGLNL	EGNGVATDVP	SATKRWGFRS	GVPPKVVNYE	AGEWAENCYN
ZEBOV-Olloba	RDKLSST	NQLRSVGLNL	GGNGVATDVP	SATKRWGFRS	GVPPKVVNYE	AGEWAENCYN
ZEBOV-Boueé	LEIKKPDGSE	CLPAAPDGIR	GFPRCRYVHK	VSGTGPCAGD	FAFHKEGAFF	LYDRLASTVI
ZEBOV-Ecran	LEIKKPDGSE	CLPAAPDGIR	GFPRCRYVHK	VSGTGPCAGD	FAFHKEGAFF	LYDRLASTVI
ZEBOV-Entsiami	LEIKKPDGSE	CLPAAPDGIR	GFPRCRYVHK	VSGTGPCAGD	FAFHKEGAFF	LYDRLASTVL
ZEBOV-Etakangaye	LEIKKPDGSE	CLPAAPDGIR	GFPRCRYVHK	VSGTGPCAGD	FAFHKEGAFF	LYDRLASTVF
ZEBOV-Gabon94	LEIKKPDGSE	CLPAAPDGIR	GFPRCRYVHK	VSGTGPCAGD	FAFHKEGAFF	LYDRLASTVI
ZEBOV-Kik	LEIKKPDGSE	CLPAAPDGIR	GFPRCRYVHK	VSGTGPCAGD	FAFHKEGAFF	LYDRLASTVI
ZEBOV-Makokou	LEIKKPDGSE	CLPAAPDGIR	GFPRCRYVHK	VSGTGPCAGD	FAFHKEGAFF	LYDRLASTVL
ZEBOV-May	LEIKKPDGSE	CLPAAPDGIR	GFPRCRYVHK	VSGTGPCAGD	FAFHKEGAFF	LYDRLASTVI
ZEBOV-May8mc	LEIKKPDGSE	CLPAAPDGIR	GFPRCRYVHK	VSGTGPCAGD	FAFHKEGAFF	LYDRLASTVI
ZEBOV-Mendemba-A	LEIKKPDGSE	CLPAAPDGIR	GFPRCRYVHK	VSGTGPCAGD	FAFHKEGAFF	LYDRLASTVL
ZEBOV-Mendemba B	LEIKKPDGSE	CLPAAPDGIR	GFPRCRYVHK	VSGTGPCAGD	FAFHKEGAFF	LYDRLASTVL
ZEBOV-Mvoula	LEIKKPDGSE	CLPAAPDGIR	GFPRCRYVHK	VSGTGPCAGD	FAFHKEGAFF	LYDRLASTVL
ZEBOV-Olloba	LEIKKPDGSE	CLPAAPDGIR	GFPRCRYVHK	VSGTGPCAGD	FAFHKEGAFF	LYDRLASTVL
ZEBOV-Boueé	YRGTTFAEV	VAFLLILPQAK	KDFFSSHPLR	E		
ZEBOV-Ecran	YRGTTFAEV	VAFLLILPQAK	KDFFSSHPLR	E		
ZEBOV-Entsiami	YRGTTFAEV	VAFLLILPQAK	KDFFSSHPLR	E		
ZEBOV-Etakangaye	YRGTTFAEV	VAFLLILPQAK	KDFFSSHPLR	E		
ZEBOV-Gabon94	YRGTTFAEV	VAFLLILPQAK	KDFFSSHPLR	E		
ZEBOV-Kik	YRGTTFAEV	VAFLLILPQAK	KDFFSSHPLR	E		
ZEBOV-Makokou	YRGTTFAEV	VAFLLILPQAK	KDFFSSHPLR	E		
ZEBOV-May	YRGTTFAEV	VAFLLILPQAK	KDFFSSHPLR	E		
ZEBOV-May8mc	YRGTTFAEV	VAFLLILPQAK	KDFFSSHPLR	E		
ZEBOV-Mendemba-A	YRGTTFAEV	VAFLLILPQAK	KDFFSSHPLR	E		
ZEBOV-Mendemba B	YRGTTFAEV	VAFLLILPQAK	KDFFSSHPLR	E		
ZEBOV-Mvoula	YRGTTFAEV	VAFLLILPQAK	KDFFSSHPLR	E		
ZEBOV-Olloba	YRGTTFAEV	VAFLLILPQAK	KDFFSSHPLR	E		

Figure 8-4. Sequence alignment of Zaire ebolavirus receptor-binding regions

Alignment of GP₁ residues 54-201 of all sequenced Zaire ebolavirus (ZEBOV) isolates. Variations are in red. Kik, Kikwit isolate; May, Mayinga isolate

Fc fusion proteins of other ebolaviruses analogous to ZEBOV-May 54-201-Fc, such as Côte d'Ivoire ebolavirus isolate Côte d'Ivoire (CIEBOV-CI) 54-201-Fc, Reston ebolavirus isolate Pennsylvania (REBOV-Pen) 55-202-Fc, or Sudan ebolavirus isolate Gulu (SEBOV-Gul) 54-201, inhibited cell transduction of MLV particles pseudotyped with MARV-Mus spike protein, albeit with varying efficiencies (Figure 7-22). For instance, while SEBOV-Gul 54-201-Fc still inhibited MARV/MLV cell transduction, it did so much

less efficiently than all other ebolaviral RBR-Fcs. It is noteworthy that expression of SEBOV-Gul 54-201-Fc resulted in two protein populations migrating as two separate bands during SDS-PAGE (Figure 7-18). While the identity of the second, unpredicted, band remains to be determined, this observation suggests that experiments performed with this protein preparation might have simply contained lower quantities of functional RBR compared to preparations of other ebolavirus RBRs. At the time of these experiments, the sequence of the fifth ebolavirus, ‘Uganda ebolavirus’ (‘UEBOV’), was not yet known. It was determined recently, and sequence alignment of its GP₁ residues 54-201 with the corresponding residues of all other ebolaviruses imply that this ‘UEBOV’ also uses the receptor used by the other ebolaviruses (Figure 8-5).

CIEBOV-CI	RD KLSST S QLK S VGLNL E NG V ATD V P T ATKR W G F RA G VPPK V VNYE A GEWA E NCYN
REBOV-Pen	RD KLSST S QLK S VGLNL E NG I ATD V P S ATKR W G F RS G VPPK V VS Y E A GEWA E NCYN
SEBOV-Gul	KD H L AST D QLK S VGLNL E GS G V S TD I P S ATKR W G F RS G VPPK V VS Y E A GEWA E NCYN
‘UEBOV-Bundibugyo’	RD KLSST S QLK S VGLNL E NG V ATD V P T ATKR W G F RA G VPPK V VNYE A GEWA E NCYN
ZEBOV-May	RD KLSST N QLR S VGLNL E NG V ATD V P S ATKR W G F RS G VPPK V VNYE A GEWA E NCYN
CIEBOV-CI	L A I KK V DGSE C L P E A P E G V R D F P RCRY V HK V S G T G P C P G G L A F H K E G A F F L Y D R L A S T I I
REBOV-Pen	L E I KK S DGSE C L P L P P D G V R G F P RCRY V HK V Q G T G P C P G D L A F H K N G A F F L Y D R L A S T V I
SEBOV-Gul	L E I KK P DGSE C L P P P P D G V R G F P RCRY V HK A G G T G P C P G D Y A F H K D G A F F L Y D R L A S T V I
‘UEBOV-Bundibugyo’	L D I KK A DGSE C L P E A P E G V R G F P RCRY V HK V S G T G P C P E G Y A F H K E G A F F L Y D R L A S T I I
ZEBOV-May	L E I KK P DGSE C L P A A P D G I R G F P RCRY V HK V S G T G P C A G D F A F H K E G A F F L Y D R L A S T V I
CIEBOV-CI	Y R G T T F A E G V I A F L I L P K A R K D F F Q S P P L H E
REBOV-Pen	Y R G T T F A E G V V A F L I L S E P K K H F W K A T P A H E
SEBOV-Gul	Y R G V N F A E G V I A F L I L A K P K E T F L G S P P I R E
‘UEBOV-Bundibugyo’	Y R S T T F S E G V V A F L I L P E T K K D F F Q S P P L H E
ZEBOV-May	Y R G T T F A E G V V A F L I L P Q A K K D F F S S H P L R E

Figure 8-5. Sequence alignment of ebolaviral receptor-binding regions

Alignment of GP₁ residues 54-201 of one isolate of each ebolavirus. Variations are in red. CIEBOV-CI, Côte d’Ivoire ebolavirus isolate Côte d’Ivoire; REBOV-Pen, Reston ebolavirus isolate Pennsylvania; SEBOV-Gul, Sudan ebolavirus isolate Gulu; ‘UEBOV,’ ‘Uganda ebolavirus;’ ZEBOV-May, Zaire ebolavirus isolate Mayinga

The CIEBOV, REBOV, SEBOV, and ‘UEBOV’ RBR-Fcs have yet to be tested for their inhibitory effect on infectious filoviruses. To do so, an assay similar to that described here for the evaluation of ZEBOV-May 54-201-Fc could be employed (Chapter 7.1.6).

Alternatively, quantitative RT-PCR could be used to evaluate the effect of the RBR-Fcs on

filovirus replication. In any case, the experiments should be expanded to include not only one but all available filoviruses to see whether the extent of replication inhibition exerted by the RBR-Fcs differs among the different viruses. Even without these experiments, however, the data described above clearly indicate that all filoviruses use at least one common cell-entry factor. Recently, another group came to the same conclusion. Manicassamy *et al.*, using a viral entry-interference assay, demonstrated that cells transfected with MARV spike protein became resistant to transduction with HIV-1-like particles pseudotyped with ZEBOV spike protein and *vice versa* (173). It is not unprecedented that several viruses bind to the same receptor. For instance, Radoshitzky *et al.* have recently demonstrated that the New World hemorrhagic fever arenaviruses Guanarito virus, Junín virus, Machupo virus, and Sabiá virus all utilize the same human cell-surface receptor, transferrin receptor 1 (TfR1) to enter their target cells (219). SARS-CoV and human coronavirus NL63 (HCoV-NL63) enter cells even by distinct mechanisms (with SARS-CoV being dependent on and HCoV-NL63 being independent of cathepsin L activity in the endosome) despite angiotensin-converting enzyme 2 (ACE2) being an obligate receptor for both (128, 130, 167). Further study will be necessary to clarify if the downstream entry processes of marburgviruses and ebolaviruses are similarly distinct. Of course, the data presented here do not exclude the possibility that either marburgviruses or ebolaviruses or both utilize additional entry factors. For example, it is striking that both MARV-Mus 38-188-Fc and ZEBOV-May 54-201-Fc inhibited cell transduction by MARV/MLV with comparable efficiencies at low concentrations in a typical dose-dependent manner (Figure 7-13), whereas the same two proteins inhibited ZEBOV/MLV in a more linear manner with different efficiencies at much higher concentrations (Figure 7-14). These data suggested to some that ZEBOV might enter cells by using the same receptor as MARV, while at the same time being able to utilize a second molecule that does not bind to MARV. If so, this would mean that ZEBOV GP₁ contains a second receptor-binding site missing in MARV GP₁. Theoretically, this is possible. For instance, ZEBOV GP₁ residues 54-201 contain two overlapping disulfide bonds, whereas only one disulfide bond exists within MARV GP₁ residues 38-188. Conversely, the remainder of ZEBOV GP₁

does not contain any disulfide bonds, whereas that of MARV contains one such connection (Figures 8-1 and 8-2). These differences in cystine arrangements could lead to rather different GP₁ tertiary structures and therefore to the exposure of residues able to bind to alternative receptors. However, there are currently no experimental data that support this hypothesis.

To date, monovalent filovirus candidate vaccines that protect simultaneously from both marburgvirus and ebolavirus infection have not been described. Also, spike-protein cross-reactive neutralizing antibodies are not available. The conservation of the filoviral receptor-binding regions and their binding to a common receptor suggested the possibility of creating such vaccines and antibodies or even small molecules that could inhibit cell entry of all filoviruses. The cell-binding data obtained with MARV-Mus and ZEBOV-May GP₁-Fc truncation variants described in Chapters 7.1.1 and 7.1.2 indicated that the RBRs, which bound filovirus-permissive cells with much higher affinity than the full-length ectodomains, are cloaked by surrounding amino-acid residues, such as the MLDs. This led to the hypothesis that the filoviral RBRs within native spike proteins are altogether inaccessible to host immune-system components, such as antibodies. A trigger, such as binding to an attachment factor on the surface of a filovirus-permissive cell, subtle pH changes, or proteolytic cleavage (by cathepsins or other proteases) could lead to conformational changes, thereby exposing the RBRs and allowing them to bind to the receptor. Alternatively, the filoviral spike proteins could fluctuate between two conformational states, one of which buries the RBRs and one that exposes them. If so, an equilibrium that strongly favors the “closed” conformation could explain the absence of RBR-neutralizing antibodies in infected animals and humans (Figure 8-8).

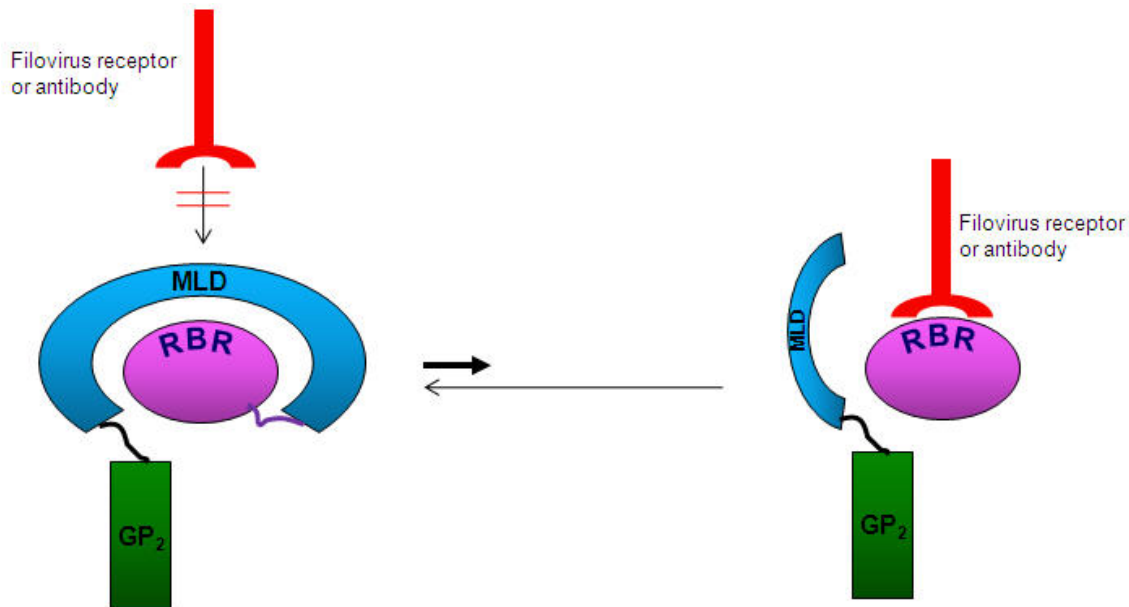


Figure 8-6. Hypothetical model for the role of filoviral-spike protein mucin-like domains

Filoviral GP₁'s mucin-like domain (MLD, blue) covers the receptor-binding region (RBR, purple) in the spike protein's native prefusion state, thereby making it inaccessible to the filovirus cell-surface receptor or antibodies (red). Conformational changes, either occurring naturally or after exposure to a trigger, remove the MLD, thereby exposing the RBR and permitting receptor binding. Since these conformational changes are either short-lived or occur directly in the vicinity of the receptor, antibodies do not develop against the RBR. However, such antibodies could be raised against the RBR if immunogens were created that consisted of the spike protein without the MLD

Shortly before the submission of this dissertation, Lee *et al.* published the crystal structure of a trimeric MLD-deleted ZEBOV-May GP_{1,2} without its transmembrane anchor in its prefusion state (162). The structural data are largely consistent with this hypothesis. They demonstrate that GP₁ is composed of a single domain. In the trimer, the three GP₁ subunits are arranged to form a chalice that is cradled by the GP₂ subunits. "Glycan caps," consisting of regions downstream of the RBRs, restrict access to the RBRs. The structural data also project the MLDs on top and to the side of these caps, thereby cloaking the RBRs even further (Figure 8-9).

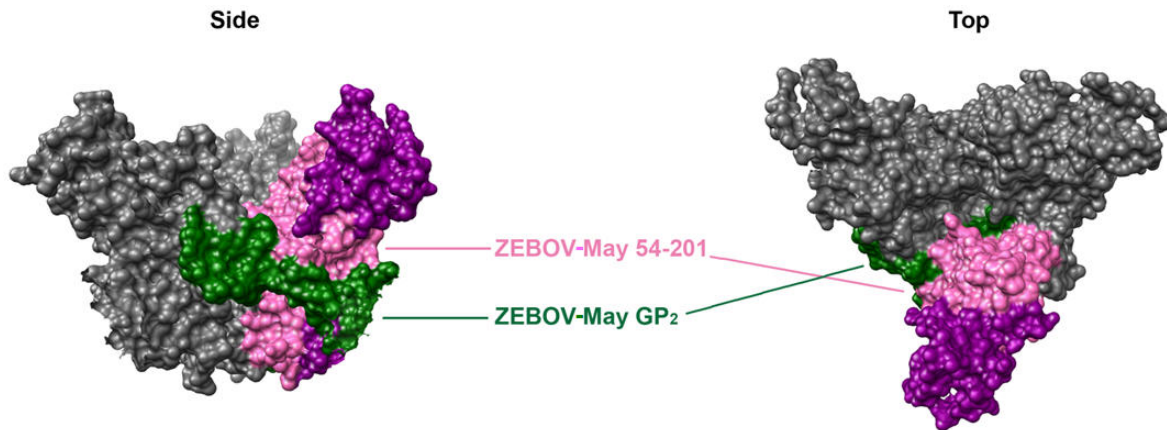


Figure 8-7. Crystal structure of trimeric mucin-like domain-deleted Zaire ebolavirus isolate Mayinga spike protein in its trimeric prefusion state (162)

The colored regions represent one monomer of trimeric mucin-like domain-deleted (MLD-deleted) spike protein (GP_{1,2}). Left: side-view of the protein (the viral membrane would be located on the bottom). Right: top (receptor's) view of the protein (the viral membrane would be located underneath). Pink and purple: GP₁. Pink: GP₁'s receptor-binding region (RBR); purple: RBR-flanking regions, including the “glycan cap” (left, on top of the RBR); dark green: GP₂. The MLDs are projected to sit on top and to the sides of the “glycan caps” (not shown)

The crystal structure also provides an explanation for the actions of cellular cathepsins during filovirus cell entry. A short loop at the very C-terminus of the ZEBOV-May RBR (residues 190-213) connects the receptor-binding site on the near-top of the chalice with the base of GP₁. This loop is exposed enough to suggest that cathepsins may cleave it, probably around residue 190. Consequently, the entire “glycan cap” and the MLD would be removed and expose the RBR further. This suggests that the observed increase in cell-surface affinity of the series of C-terminal GP₁ truncation variants up to residue 201 (Figure 7-8) mimics the actions of cathepsins, with each shorter truncation variant containing less of the sterically hindering RBR-flanking regions and therefore a more exposed RBR.

Together, the structural data emphasize the hypothesis that immunogens consisting of filoviral spike proteins devoid of the MLD and RBR-flanking sequences should be able to induce antibodies that may cross-react with the RBRs of heterologous filoviruses. Here,

it is shown that purified protein preparations of MARV-Mus 38-188-Fc or ZEBOV-May 54-201-Fc induced such cross-neutralizing antibodies in mice (Figure 7-44). Sera from mice immunized with either MARV-Mus 38-188-Fc or ZEBOV-May 54-201-Fc inhibited replication of infectious ZEBOV-May (Figure 7-46), clearly proving the efficacy of cross-neutralizing antibodies *in vitro*. Mice immunized with ZEBOV-May 54-201-Fc were completely protected from infection with mouse-adapted ZEBOV-May. More importantly, 50% of the mice immunized with MARV-Mus 38-188-Fc were protected from infection with mouse-adapted ZEBOV-May as well (Figure 7-47). This is the first report of a monovalent cross-protective filovirus candidate vaccine. Unfortunately, it could not be tested whether ZEBOV-May 54-201-Fc also cross-protects from infection with MARV. Whereas the mouse model for ZEBOV-May infection is well established (33), a mouse model for MARV did not exist at the time of the described experiments. Recently, however, Warfield *et al.* established such a model for three isolates of MARV in severe-combined immunodeficiency (SCID) mice (290), which will facilitate the evaluation of the RBR immunogens in the near future. Clearly, it is also necessary to evaluate whether the RBR immunogens also work in different types (for instance BALB/c) of immunocompetent mice. The level of conservation of the filovirus RBRs and the immunization results obtained thus far suggest that it should be possible to develop an efficacious pan-filovirus vaccine. Such a vaccine might be easy to produce in biofermenters, be advantageous for transport even in rural areas in the absence of a cold chain because it could be lyophilized, and it could be safer and more efficacious than other candidate vaccines because of the absence of replicating platforms (VSIV or HPIV-3 candidate vaccines) and the absence of background immunity against vector backbones (adenovirus candidate vaccines). More studies need to be performed to evaluate whether the overall extent of cross-protection can be increased from the currently observed 50% to 100% by, for instance, changing the intervals of booster immunizations, amount of immunogen or type of adjuvant. Also, it may be useful to evaluate the CIEBOV, REBOV, SEBOV, and 'UEBOV' RBR-Fcs for their availability to protect animals from infection with homologous or heterologous filoviruses as one may have superior immunogenic qualities over the others. Furthermore,

immunization results in mice do not necessarily predict success in guinea-pig or nonhuman primate models. Therefore, it won't be known whether the RBR subunit preparations are truly viable candidate vaccines for ape and human populations at risk of filovirus infection until challenge studies have been performed in different animal models. Unfortunately, it is not trivial to perform these experiments. This is because the filoviral RBR-Fc preparations described in this dissertation are extremely difficult to procure. For instance, functional MARV-Mus 38-188-Fc expresses in mammalian tissue culture (HEK 293T cells) only to levels of ~ 0.1 $\mu\text{g/ml}$ supernatant. This means that for the described mouse experiment with MARV-Mus 38-188-Fc, more than 520 175 cm^2 flasks of HEK 293T cells needed to be transfected with the appropriate expression plasmid to yield the necessary amount of protein needed for the immunization schedule described in Figure 7-43. Since guinea pigs, and especially nonhuman primates, are considerably larger than mice, much larger amounts of RBR-Fc would have to be produced for immunization, a task that is not viable both from workload and financial perspectives. Furthermore, the RBR-Fc preparations are sensitive to both speed and type of elution from protein A-sepharose Fast Flow beads used for purification. For example, while acid elution yielded functional proteins as long as neutralization occurred rapidly after elution, salt elution resulted in misfolded and/or aggregating preparations. Attempts to purify RBR-Fcs from suspension cells cultured in roller bottles or, with the help of a company, in bioreactors have so far not yielded functional proteins. One way of overcoming this problem may be to exchange the Fc tag for, for instance, an HA, myc or FLAG tag, which may change expression levels and purification conditions. However, thus far all attempts to purify RBRs not tagged with Fc regions have failed. Likewise, the production of His-tagged RBRs from bacteria or insect cells resulted only in dysfunctional proteins unable to inhibit cell transduction of MLV pseudotyped with filoviral spike proteins. Another possibility may be to subject the RBRs to alanine and glycine scanning to select for better expressing variants. This approach is currently pursued in the laboratory. Alternatively, the now available crystal structure of ZEBOV-May GP₁ (162) may aid in the design of improved (longer or shorter) RBR variants that could better accommodate the Fc or other tags and be expressed to higher

levels. Finally, it may be possible to fuse the RBRs to transmembrane anchors and express these proteins from recombinant vesiculoviruses or human parainfluenzaviruses. While some advantages of subunit vaccines would be lost this way, this strategy could still result in a pan-filovirus vaccine, whose creation is of utmost priority.

Another priority in filovirus research is the establishment of potent antivirals both for treatment of individuals with filoviral hemorrhagic fever, as well as for post-exposure prophylaxis for laboratory workers after accidental infection. The data presented here suggest that filovirus-neutralizing antibodies could be efficient antivirals *in vivo*, and that one particular antibody could possibly suffice to treat infections with or exposures to any of the known filoviruses. Experiments are currently ongoing in Sina Bavari's laboratory to identify and characterize the neutralizing antibodies raised during the mouse inoculations.

The identification of cellular receptors that mediate virus entry can contribute to the development of antiviral therapies and vaccines, and provide insight into the pathogenesis of viral diseases. Multiple approaches have been used to identify viral receptors, including library screens (28), virus-overlay protein-binding assays (VOPBAs) (44), anti-idiotypic antibodies (95), and logical inference from what is known about a given virus and its host (154). None of these approaches has led to identification of more than a few receptors, and all of them are labor-intensive and present difficulties when receptors are expressed ubiquitously or are part of multi-component complexes. One increasingly important methodology for characterizing protein-protein interaction uses coimmunoprecipitation and identification of binding partners via mass spectrometry. This approach has led to the rapid and unequivocal identification of the receptors for SARS-CoV (167), Hendra and Nipah viruses (199), and the New World hemorrhagic fever arenaviruses Guanarito, Junín, Machupo, and Sabiá (219). In brief, fusion proteins, consisting of the ectodomain of the spike protein of a given virus and the Fc domain of human IgG₁ are synthesized *in vitro* and used to immunoprecipitate candidate receptors from lysates of virus-permissive cells. Such binding partners are then separated on polyacrylamide gels, excised, trypsinized,

and their peptides sequenced using mass spectrometry (Figure 8-7). Identified proteins that localize to the cell surface and have a cell-expression pattern that overlaps with the known virus tissue tropism are subsequently cloned and expressed in virus-resistant cells. These cells are then challenged with retrovirus (MLV-, SIV- or HIV-1-based) particles pseudotyped with the full-length viral spike protein and expressing a marker gene, enhanced green fluorescent protein (eGFP), to test for successful transduction. Identification of viral receptors has led to 1) the development of candidate entry inhibitors, 2) the clarification of the tissue-tropism of the respective viruses and thereby to a better understanding of pathogenesis, and 3) insight into the varying efficiencies of viral replication in different animal species and thereby into zoonotic transmission (158, 220).

The filoviral RBR-Fc molecules described here are currently being used as bait proteins for the identification of the unknown common filovirus receptor. As described above, filovirus-permissive cells, such as Vero E6 cells, are incubated with ZEBOV-May 54-201-Fc or MARV-Mus 38-188-Fc, therefore allowing those fusion proteins to bind to the receptor. The cells are then lysed with various detergents to remove the receptor from the cell membrane, and the receptor-RBR-Fc complexes are isolated from the lysates using Fc-specific protein A-sepharose Fast Flow beads. Proteins bound to the RBRs are then analyzed using polyacrylamide gel electrophoresis (PAGE) and identified using mass spectrometry.

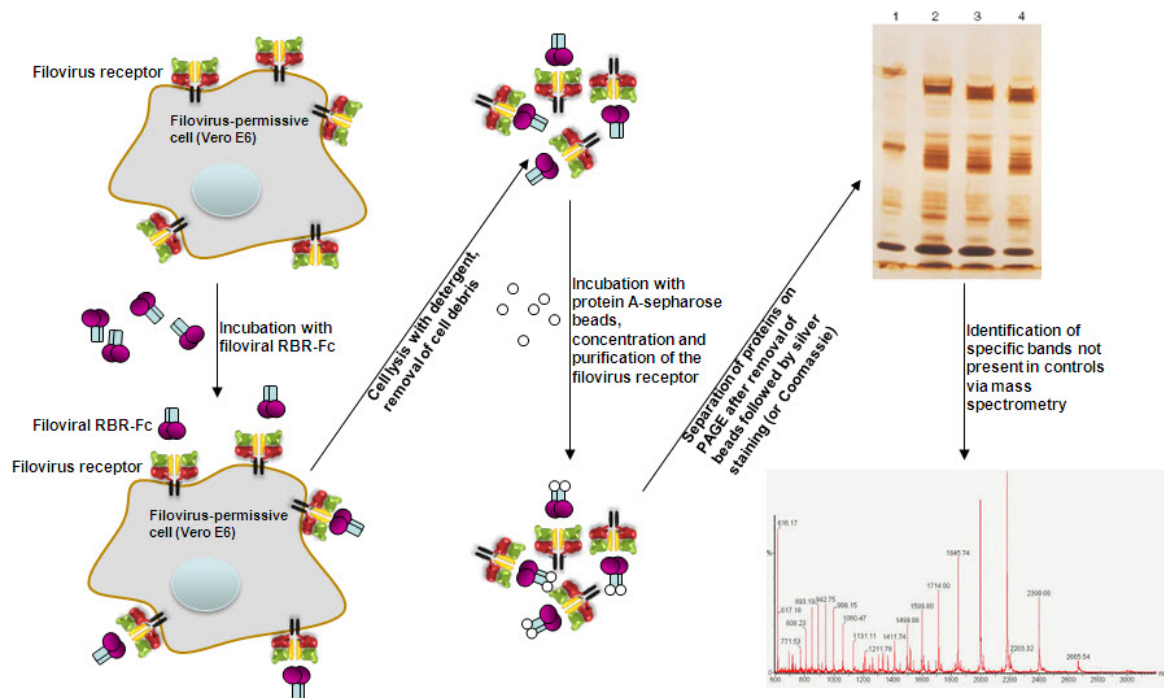


Figure 8-8. Principle of virus-receptor identification by coimmunoprecipitation

Filovirus-permissive cells are incubated with purified filoviral receptor-binding GP₁ fragments such as the receptor-binding region (RBR) C-terminally fused to the Fc region of an IgG or with control Fc fusion proteins. The filoviral, but not the control, fragments bind to the unknown filovirus receptor. The cells are lysed using detergent, and the lysate is cleared of cellular debris. The receptor-bait complexes are incubated with protein A-sepharose beads, which bind to the Fc region of the bait proteins. Beads are spun down and washed. The proteins are released from the beads by boiling, and subjected to 1D or 2D polyacrylamide gel electrophoresis (PAGE). Bands present in lysates of cells incubated with filoviral Fc bait proteins, but not present in lysates of cells incubated with control Fc bait proteins, are excised, sequenced, and identified by mass spectrometry

Thus far, the receptor has not been identified using this approach, although several receptor candidates were immunoprecipitated that later turned out to bind to the RBRs unspecifically (data not shown). For one, the experiments are hindered by the low expression levels of the filoviral RBR-Fcs and therefore the low availability of receptor-bait proteins, which do not allow screening of multiple cell types under a large variety of experimental conditions. Furthermore, both MARV-Mus 38-188-Fc and ZEBOV-May 54-201-Fc do not bind cell surfaces in a saturable manner, suggesting that parts of the RBRs

are in fact unnecessary for receptor binding and either mediate the additional binding to filovirus-nonspecific cell-surface factors (attachment factors) or destabilize the RBRs, thereby leading to their aggregation on the cell surface. The ZEBOV-May spike-protein crystal structure (162) suggests that RBRs shorter than 54-201 could be synthesized. In fact, truncation variants 76-201 and 76-172 (which could not be expressed as an Fc fusion protein) should still be functional. However, analysis of the GP₁ structural data clearly suggests that the large C-terminal Fc tag might occlude the receptor-binding site in constructs ending in residue 172. Such occlusion by the tag could also explain why some of the longer GP₁ truncation variants bound filovirus-permissive cells less efficiently than ZEBOV-May 54-201-Fc. As described above, substituting the Fc tag for other tags has so far not resulted in functional (MLV cell transduction-inhibiting) RBRs. Consequently, further mutational studies need to be performed to yield improved receptor-bait proteins. One alternative to further truncations is to increase the affinity of the RBRs through the introduction of point mutations. As mentioned above, residues D₅₅, L₅₇, L₆₃, R₆₄, G₈₇, F₈₈, K₉₅, K₁₁₄, K₁₁₅, K₁₄₀, G₁₄₃, P₁₄₆, C₁₄₇, F₁₅₃, H₁₅₄, F₁₅₉, F₁₆₀, Y₁₆₂, and I₁₇₀ were suggested to be crucial for ZEBOV-May GP₁ receptor binding (37, 172, 193). Mutation of residues F₈₈ and F₁₅₉ to alanine abolished cell transduction with retroviral pseudotypes (37, 193). Therefore, these mutations were introduced into ZEBOV-May 54-201-Fc (54-201F88A-Fc, 54-201F159A-Fc) by site-directed mutagenesis with the aim of creating nonfunctional bait proteins as ideal negative controls for receptor coimmunoprecipitation experiments. However, both 54-201F88A-Fc and 54-201F159A-Fc bound filovirus-permissive cells comparable to 54-201-Fc and inhibited cell transduction by MLV pseudotyped with filoviral spike proteins (data not shown). Supporting these results, three murine antibodies (1E1, 2D3, and 1F6), raised against the F₈₈ epitope and provided by Carolyn Wilson (Food and Drug Administration, Bethesda, MD, USA) within a collaboration, inhibited cell transduction by MLV pseudotyped with filoviral spike proteins, but did not interfere with cell-surface binding of 54-201-Fc (data not shown). Brindley *et al.* reported that simultaneous mutation of residues G₇₄ and V₇₅ or V₉₆ and V₉₇ to alanines resulted in spike proteins that mediated cell entry approximately four times more efficiently than wild-type

spike protein (37). Therefore, these mutations were introduced into ZEBOV-May 54-201-Fc (54-201G74A,V75A-Fc and 54-201V96A,V97A-Fc) by site-directed mutagenesis with the aim of creating an RBR with higher affinity to the filovirus receptor. Unfortunately, these constructs bound filovirus-permissive cells and inhibited transduction by pseudotypes to the same level as 54-201-Fc (data not shown). The crystal structure of ZEBOV-May spike protein, published after these experiments were performed, suggests that residues D₅₅, L₅₇, L₆₃, and R₆₄ are important for fusion-mediated conformational changes of GP_{1,2}. Residues F₁₅₉, F₁₆₀, Y₁₆₂, and I₁₇₀ are buried within GP₁ and stabilize the protein. Residues G₈₇, F₈₈, F₁₅₃, and H₁₅₄ pack against hydrophobic residues. Only six of the implicated residues above, K₁₁₄, K₁₁₅, K₁₄₀, G₁₄₃, P₁₄₆, and C₁₄₇, are surface-exposed and probably comprise the receptor-binding site (162) (Figure 8-9). These results explain why 54-201F88A-Fc and 54-201F159A-Fc are still functional RBRs – the exchanged residues do not partake in receptor binding. The crystal structure also reveals that residues G₇₄ and V₇₅ are located far away from the predicted receptor-binding site at the base of the GP₁ chalice close to GP₂, and that residues V₉₆ and V₉₇ are buried within the molecule (162). These locations suggest that spike proteins containing the G74A/V75A and V96A/V97A mutations mediate improved cell entry not through improved receptor binding but rather by easing conformational changes during the fusion process.

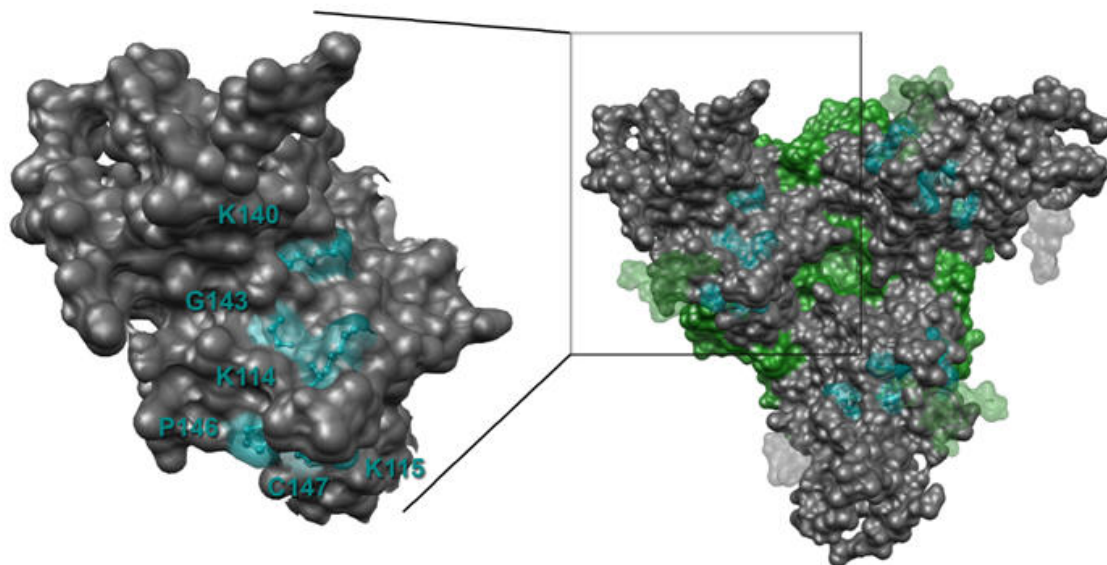


Figure 8-9. The receptor-binding sites of trimeric mucin-like domain-deleted Zaire ebolavirus isolate Mayinga spike protein in its trimeric prefusion state (162)

Left: Magnification of one GP₁ monomer. Right: top (receptor's) view of trimeric GP_{1,2} (the viral membrane would be located underneath). Grey: GP₁; green: GP₂; cyan: residues suggested to be of importance for receptor binding (K₁₁₄, K₁₁₅, K₁₄₀, G₁₄₃, P₁₄₆, and C₁₄₇) and located within the projected receptor-binding site

Clearly, additional mutational studies need to be performed to further define the filovirus RBRs, and to increase their expression properties, as well as their affinities to the filovirus receptor, if the coimmunoprecipitation approach is to be pursued.

The most intriguing result of this dissertation is the observation that ZEBOV-May secreted glycoprotein (sGP-Fc) and secondary secreted glycoprotein (ssGP-Fc), both of which contain ZEBOV-May spike protein's region 54-201, did not bind to filovirus-permissive cells (Figure 7-24) and barely inhibited GP_{1,2}-mediated entry (Figure 7-27), whereas sGP's C-terminal cleavage product Δ -peptide (Δ -Fc) did both very efficiently. That sGP-Fc and ssGP-Fc did not interact with the unknown filovirus receptor is not necessarily surprising, as their structures are most likely very different from that of the spike protein. For instance, ZEBOV spike protein is a trimer of GP₁-GP₂ heterodimers (162). On the other hand, ZEBOV sGP forms a parallel homodimer defined by two

intermolecular disulfide bonds at both the N- and C-termini of each monomer (16) (Figure 5-8). ssGP is most likely a monomer, or possibly a dimer, formed by a so far hypothetical single intermolecular disulfide bond (286) (Figure 5-11). These different quaternary arrangements probably lead to vastly different folding patterns, one result of which could be the loss of the receptor-binding function of the RBR within sGP and ssGP. Barrientos *et al.* recently characterized the structure of ZEBOV sGP using chemical methods. Their results support this hypothesis at least for sGP. Accordingly, sGP folds into a structure predominantly containing β -sheets that permits reversible folding under a wide range of conditions. Barrientos *et al.* speculate that the secreted sGP is some kind of a molecular switch in the sera of ebolavirus-infected animals that changes conformation depending on local changes in milieu (17). There is currently no information available on the structure of ssGP. However, ssGP consists of 295 N-terminal amino-acid residues identical to those of GP₁ fused to only two unique C-terminal residues. This sequence suggested that ZEBOV-May ssGP-Fc should display a cell-binding and transduction-inhibitory pattern similar to ZEBOV-May GP₁ truncation variant 33-308-Fc. Indeed, 33-308-Fc barely bound to filovirus-permissive cells (Figure 7-8). However, 33-308-Fc was not evaluated for correct folding. Additionally, since the functions of sGP and ssGP, if any, remain unknown, it was impossible to evaluate whether the expressed sGP- and ssGP-Fc fusion proteins were folded correctly. Specific, conformation-dependent antibodies against sGP or ssGP are not yet available, either. Also, the Fc tags could have interfered with the structure of the two proteins. Thus, the possibility remains that these two secreted glycoproteins do bind to the filovirus receptor after all and that this binding was not detected in the assays described. Much more interesting, however, is that the C-terminal cleavage product of ebolaviral sGP, Δ -peptide, behaved reminiscent of filoviral RBRs at least when fused to Fc. In fact, CIEBOV, SEBOV, and ZEBOV Δ -Fc bound exclusively to filovirus-permissive cells (Figure 7-29), inhibited the replication of infectious ZEBOV-May (Figure 7-33), and inhibited cell transduction by MLV pseudotyped with MARV-Mus spike protein (Figure 7-32). REBOV Δ -Fc on the other hand inhibited cell transduction only minimally (Figure 7-32) and infectious ZEBOV-May replication not at all (Figure 7-33) (the sequence of the

'UEBOV' Δ -peptide was not known at the time of the experiments). This is intriguing because REBOV is the only filovirus currently suspected to be apathogenic for humans, which suggests that filoviral Δ -peptides could be virulence factors. For instance, a guinea pig-adapted ZEBOV-May strain (ZEBOV-May-8mc), which is mutated in the *GP* gene editing site and therefore produces only minute amounts of sGP, was found to be more virulent than wild-type virus (3, 134, 280). Since Δ -peptides are produced by furin-mediated proteolytic cleavage of maturing sGP, it is possible that it is not the lack of expressed sGP, but the lack of expressed Δ -peptide that makes this virus more virulent. This hypothesis could be addressed by creating a Δ -peptide knock-out virus using the available reverse genetics system for ZEBOV (270). For instance, the furin-cleavage site within sGP could be mutated to prevent cleavage of sGP and therefore individual secretion of Δ -peptide during virus replication, or a stop codon could be introduced into the sequence prior to the one encoding the furin-cleavage site to prevent synthesis of Δ -peptide. Cell-culture and animal experiments could then be performed in which the replication and pathology induced by these various viruses is compared to wild-type virus, and Δ -peptide could be provided *in trans* to see whether changes in virulence of the mutated viruses could be reverted to wild-type levels.

At this moment, it remains difficult to speculate on the mode of action of Δ -peptides. A closer look at their sequences reveals 1) that the amino-acid sequences of the Δ -peptides of each individual ebolavirus (CIEBOV, REBOV, SEBOV, 'UEBOV,' and ZEBOV) are 100% conserved among all known and sequenced isolates of these viruses, but 2) that they vary greatly among each other (Figure 8-10).

CIEBOV	S	L	P	S	P	P	T	T	Q	A	K	T	T	K	N	W	F	Q	R	I	P	L	Q	W	E	R	K	T	S	R	E	R	T	Q	C	Q	P	Q									
REBOV	E	L	S	K	E	K	L	A	T	H	P	P	T	P	S	W	F	Q	R	I	P	L	Q	W	E	Q	S	L	Q	D	G	Q	R	K	C	R	E	K	V								
SEBOV	E	L	Q	R	E	E	S	P	T	G	P	P	G	S	I	R	T	W	F	Q	R	I	P	L	G	W	E	H	T	Y	Q	K	G	K	Q	H	C	R	L	R	I	R	Q	K	V	E	E
'UEBOV'	S	L	P	P	A	S	P	T	K	P	P	R	T	T	K	T	W	F	Q	R	I	P	L	Q	W	E	K	E	T	S	R	G	K	T	Q	C	R	F	H	P	Q	T	Q	S	P	Q	L
ZEBOV	E	L	P	T	Q	G	P	T	Q	Q	L	K	T	T	K	S	W	L	K	I	P	L	Q	W	E	K	T	V	K	E	G	K	L	Q	C	R	I										

Figure 8-10. Sequence alignment of ebolaviral Δ -peptides

Δ -peptides of each individual ebolavirus are 100% identical irrespective of the analyzed isolate, but they vary greatly among each other. Highlighted residues indicate residues identical in all five (brown), four (cyan) or at least three ebolaviral Δ -peptides (green). CIEBOV, Côte d'Ivoire ebolavirus; REBOV, Reston ebolavirus; SEBOV, Sudan ebolavirus; 'UEBOV,' 'Uganda ebolavirus;' ZEBOV, Zaire ebolavirus

Sequence comparisons revealed no similarities among ebolaviral Δ -peptides and filoviral RBRs or spike proteins. Furthermore, computational blast analyses did not reveal any protein or peptide sequence remotely related to Δ -peptides. The conserved amino-acid sequence in the center of the peptides (Figure 8-10) does not seem to play a crucial role for their function, as the mutation of several of these conserved residues in SEBOV Δ -Fc (Δ 1-48-Fc) to alanines (Δ W18A-Fc, Δ R21A-Fc, and Δ W26A-Fc) did not impair cell binding or transduction inhibition considerably (Figures 7-38 and 7-40). On the other hand, consecutive truncation of SEBOV Δ -Fc's C-terminus (Δ 1-39-Fc, Δ 1-33-Fc, Δ 1-28-Fc, and Δ 1-17-Fc) did result in progressive loss of function (Figure 7-40). A chimera consisting of the N-terminal half of SEBOV Δ -peptide and the C-terminal half of REBOV Δ -peptide (SR Δ -Fc) behaved like full-length REBOV Δ -Fc and inhibited cell transduction by MARV/MLV only minimally, whereas a chimera consisting of the N-terminal half of REBOV Δ -peptide and the C-terminal half of SEBOV Δ -peptide (RS Δ -Fc) mimicked SEBOV Δ -Fc and inhibited transduction efficiently (Figure 7-40). Together, these results suggest that ebolaviral Δ -peptides mediate their function through their C-termini. Mutant Δ 28-48-Fc, which consists only of SEBOV Δ -peptide's C-terminus inhibited cell transduction by MARV/MLV only minimally (Figure 7-40). This observation suggests that Δ -peptide's N-terminus is most likely important for its function (for instance, by mediating correct folding of the peptide), but not for binding to its cell-surface partner. This notion is

also supported by the observation that the introduction of mutations into the N-terminal half of the peptide (Δ T9A-Fc, Δ S14A-Fc) did not decrease the inhibitory effect on cell transduction by MARV/MLV, and by the fact that consecutive N-terminal truncation variants up to residue 28 did not express. A closer look at the C-termini of ebolaviral Δ -peptides (Figure 8-10) led to the conclusion that they must exert their inhibitory effects through charged interactions as no sequence similarity is obvious. Further mutational studies are currently ongoing in an attempt to convert REBOV Δ -Fc into an efficient filovirus cell-entry inhibitor by introducing additional positively charged residues and/or SEBOV Δ -peptide-like residues into its C-terminus.

The fact that ebolaviral Δ -peptides bind with high affinity to filovirus-permissive cells but not to filovirus-resistant cells, and that they inhibit replication of infectious ZEBOV and MARV spike protein-mediated cell entry suggests that these peptides might bind to the common filovirus receptor. If so, another approach to identify the filovirus receptor may be to use ebolaviral Δ -Fc as bait proteins in coimmunoprecipitation experiments. A closer look at the ZEBOV-May GP_{1,2} crystal structure (162) raises the possibility that the linear arrangement of certain residues in the C-termini of Δ -peptides might indeed mimic GP_{1,2}'s receptor-binding site, in which similar residues are arranged three-dimensionally in close proximity (Figure 8-11).

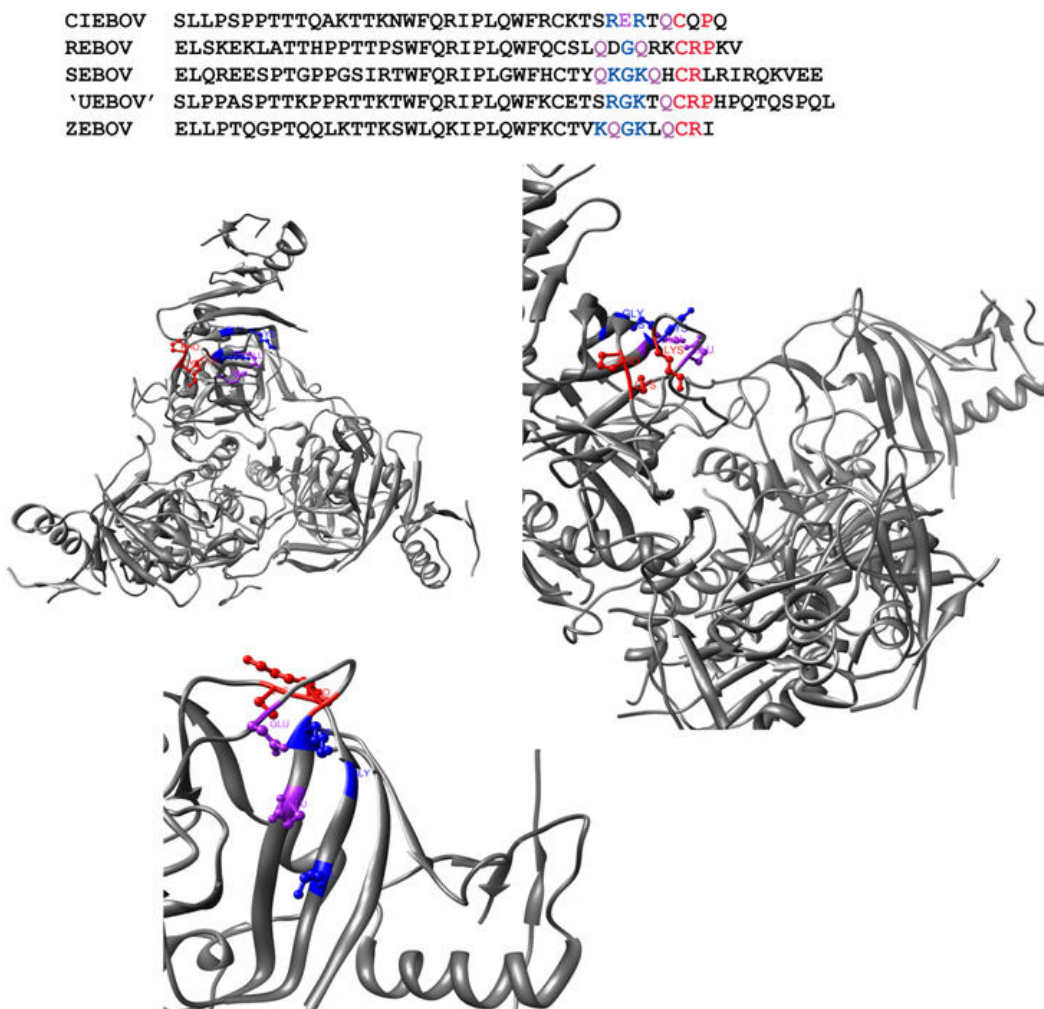


Figure 8-11. Comparison of the C-termini of ebolaviral Δ -peptides with the receptor-binding site suggested by the crystal structure of mucin-like domain-deleted Zaire ebolavirus isolate Mayinga GP_{1,2} (162)

Top: alignment of ebolaviral Δ -peptides. Highlighted in color are residues that may or may not imitate residues in the ebolaviral spike-proteins receptor-binding site (RBS) by either charge or structure. CIEBOV, Côte d'Ivoire ebolavirus; REBOV, Reston ebolavirus; SEBOV, Sudan ebolavirus; 'UEBOV,' 'Uganda ebolavirus;' ZEBOV, Zaire ebolavirus. Middle, left: ZEBOV-May GP_{1,2} (top view). Middle, right: ZEBOV-May GP_{1,2} (tilted side view). Bottom: ZEBOV-May GP_{1,2} (magnified tilted side view). Red (middle, bottom): ZEBOV-May GP_{1,2} amino-acid residues K₁₁₅, P₁₄₆, C₁₄₇. Purple (middle, bottom): ZEBOV-May GP_{1,2} amino-acid residues E₁₁₂, E₁₂₀. Blue (middle, bottom): ZEBOV-May GP_{1,2} amino-acid residues K₁₁₄, G₁₄₃, K₁₄₀.

However, the data presented here are ambiguous as to whether these peptides truly bind the receptor. In competition-binding experiments, 800 nM of SEBOV Δ -mFc reduced cell binding of 200 nM MARV-Mus 38-188-Fc by roughly 50%. *Vice versa*, 800 nM of MARV-Mus 38-188-Fc reduced cell binding of 200 nM of SEBOV Δ -mFc roughly by 50% (Figure 7-41). However, this experiment can only be taken as a hint for possible competition of ebolaviral Δ -peptides and RBRs for a common molecule because it was impossible to reach cell-surface saturation with either Δ -Fc or RBR-Fc independent of which concentration was used (up to 2 μ M, data not shown). Furthermore, this kind of experiment could at best demonstrate competition for the same or directly neighboring binding sites of the unknown filovirus receptor. Absent competition would not exclude the possibility that the peptides bind the receptor at a different location than the RBRs, thereby leading either to allosteric structural changes in the receptor that could lead to the occlusion of the spike protein-binding site or to the inhibition of events necessary for filovirus cell internalization that occur downstream of receptor-binding.

Another important point to keep in mind is that all experiments described here were performed with ebolaviral Δ -peptides fused C-terminally to Fc tags. It is quite possible that the large tags interfere with or modulate the peptides' functions and, for instance, change them from entry *facilitators* to entry inhibitors. Experiments to address this possibility have thus far failed because the exchange of the Fc tag for other, shorter, tags has resulted in peptides that were expressed at levels too low for follow-up experiments (data not shown). Chemically synthesized SEBOV Δ -peptide (Biomatik Corporation, Wilmington, DE, USA) did not have measurable effects on cell transduction with MARV/MLV or replication of infectious ZEBOV (data not shown). This result is not surprising, as it is not known at this point in time whether Δ -peptides are post-translationally modified and whether their conserved cysteine residues are used to form intermolecular or intramolecular disulfide bonds. It is feasible to assume that the Fc tag of Δ -Fc, which forms dimers, forces the Δ -peptide into a dimeric structure it would otherwise assume through the formation of intermolecular disulfide bonds. Since the chemically synthesized peptide was unmodified,

such a dimer would not have been present in the chemical preparation and the monomer could have been misfolded or nonfunctional.

The data presented here suggest that post-translational modifications of Δ -peptides could also control their function as filovirus cell-entry modifiers. For instance, mutating SEBOV Δ -peptide residue T₉ to alanine (SEBOV Δ T9A-Fc) did lead to a migration shift during PAGE analysis (data not shown), more efficient binding to filovirus-permissive cells (Figure 7-38), and an unaltered ability to inhibit MARV/MLV cell transduction (Figure 7-40). In this regard it is also interesting to remember that SEBOV Δ -Fc is the longest of the ebolaviral Δ -peptides, yet it migrated lower than the other peptides during SDS-PAGE (Figure 7-28). This observation suggests that CIEBOV, REBOV, and ZEBOV Δ -peptides contain additional glycosylation sites or other posttranslational modifications, which could be responsible for the differences observed among them in MLV cell transduction-inhibition assays.

At the moment, two hypotheses as to the role of Δ -peptides in ebolaviral hemorrhagic fever pathogenesis are under evaluation. First, it will be tested whether Δ -peptides are secreted from cells infected with ebolaviruses in amounts sufficient enough to modulate cell entry. If so, the peptides could be expressed by ebolaviruses to prevent the infection of cells already infected (superinfection). For instance, the peptides secreted from an ebolavirus-infected cell could bind to the filovirus receptor on the very same cell and thereby block it as a receptor for additional virus particles. Since marburgviruses do not express Δ -peptides, this would mean that these viruses either have developed alternative ways to prevent superinfection or simply do not prevent it all. Experiments to address these questions could be set up using recombinant filoviruses expressing reporter proteins that fluoresce in different colors. For instance, an eGFP-expressing Δ -peptide knock-out virus could be used to infect cells later challenged with a red-fluorescent protein-expressing virus in the presence or absence of Δ -peptide, and cells could then be analyzed for simultaneous expression of both fluorescent proteins. Similar experiments could then be performed with recombinant marburgviruses, used, for instance, as the superinfecting viruses of cells already infected with ebolaviruses. Of course, ebolaviral Δ -peptides also could interfere

with steps of the viral entry process other than receptor binding. Here, data are presented that exclude the modulation of cathepsin B by SEBOV Δ -Fc (Figure 7-42), which is but one factor playing an important role in filovirus cell entry. Further experiments are necessary to rule out an effect of Δ -peptides on cathepsin L as well, and to determine whether Δ -peptides penetrate cells either directly or by endocytosis as they could, for instance, act in the endosome rather than on the cell-surface in the absence of Fc tags.

Second, it can be imagined that the filovirus receptor is transported to the cell surface using the same route filoviruses use for egress. In such a case, Δ -peptides could prevent the binding and thereby trapping of budding virions to the receptor inside of the virus-producing cell. Currently, not enough data have been published on differences and similarities of marburgvirus and ebolavirus cell egress to support this hypothesis at least by seemingly circumstantial data. It is, however, possible that marburgviruses and ebolavirus viruses use different routes for budding and that these different routes explain why marburgviruses could exit cells efficiently in the absence of Δ -peptides, whereas ebolaviruses could not.

9 SUMMARY

The GP_{1,2} spike proteins of filoviruses (marburgviruses and ebolaviruses) mediate viral cell-surface attachment, membrane fusion, and entry into cells expressing the unknown filovirus receptor(s). Here, it is shown that a 151 amino-acid fragment of the Lake Victoria marburgvirus GP₁ subunit (residues 38-188), fused to the Fc region of human IgG₁, bound filovirus-permissive cell lines more efficiently than full-length GP₁. An analogous 148 amino-acid fragment of the Zaire ebolavirus GP₁ subunit (residues 54-201) similarly bound the same cell lines more efficiently than a series of longer GP₁-truncation variants. Neither the marburgvirus GP₁ fragment, nor that of ebolavirus, bound to filovirus-resistant lymphocyte cell lines thought not to express the filovirus receptor. Both Lake Victoria marburgvirus 38-188-Fc and Zaire ebolavirus 54-201-Fc specifically inhibited the replication of infectious Zaire ebolavirus, as well as transduction of filovirus-permissive cells by gammaretroviruses pseudotyped with either the Lake Victoria marburgvirus or the Zaire ebolavirus GP_{1,2} spike protein. Similarly, GP₁-Fc fusion fragments of Côte d'Ivoire ebolavirus, Reston ebolavirus, and Sudan ebolavirus, corresponding to Zaire ebolavirus GP₁ residues 54-201, inhibited gammaretroviruses pseudotyped with Lake Victoria marburgvirus GP_{1,2}. These studies identified the receptor-binding regions (RBRs) of marburgviruses and ebolaviruses, and demonstrated that all filoviruses utilize at least one common receptor.

In addition to the GP_{1,2} spike glycoprotein, ebolaviruses, but not marburgviruses, express two secreted glycoproteins, sGP and ssGP, from the *GP* gene by cotranscriptional editing. All three proteins have identical N-termini that include residues 54-201. However, it is shown that neither sGP-Fc nor ssGP-Fc binds to filovirus-permissive cells. Both proteins were unable to inhibit transduction of such cells by gammaretroviruses pseudotyped with the Lake Victoria marburgvirus GP_{1,2} spike protein, indicating that they do not bind to the filovirus receptor. Instead, it is shown that Fc-conjugated Δ -peptide, which is a short C-terminal cleavage product of sGP bearing no sequence similarity to the filoviral RBRs, inhibited pseudotyped gammaretroviruses and infectious Zaire ebolavirus

specifically and in a dose-dependent manner. Δ -Fc derived from Côte d'Ivoire, Sudan, and Zaire ebolavirus sGP inhibited Lake Victoria marburgvirus GP_{1,2} spike protein-mediated entry and replication of infectious Zaire ebolavirus comparably or better than Zaire ebolavirus 54-201-Fc. Interestingly, Δ -Fc derived from sGP of Reston ebolavirus, thought to be the only filovirus apathogenic for humans, had little or no effect. These data suggest that Δ -peptides modulate filovirus cell entry and may be important virulence factors.

Last, the immunogenic properties of filoviral RBR-Fcs were evaluated in a lethal ebolavirus mouse model. C57/BL6 mice were immunized on days 0, 21, and 35 with Zaire ebolavirus 54-201-Fc + RIBI adjuvant or Lake Victoria marburgvirus 38-188-Fc + RIBI adjuvant and challenged with mouse-adapted Zaire ebolavirus on day 62. All mice immunized with Zaire ebolavirus 54-201-Fc survived otherwise lethal challenge without showing any signs of disease. Half of the mice immunized with Lake Victoria marburgvirus 38-188-Fc also survived otherwise lethal Zaire ebolavirus infection. Sera collected from mice immunized with Zaire ebolavirus 54-201-Fc or Lake Victoria marburgvirus 38-188-Fc neutralized Zaire ebolavirus infection of Vero E6 cells, and strong cytotoxic T-lymphocyte responses were detected in mice immunized with either RBR-Fc. This is the first report of a cross-protective filovirus candidate vaccine.

GERMAN SUMMARY

Das Oberflächenprotein der Filoviren (Marburg- und Ebolaviren), GP_{1,2}, ist verantwortlich für die Oberflächenadsorption an, Membranfusion mit, und Penetration von Zellen, welche den noch unbekanntem Filovirusrezeptor exprimieren. Hier wird gezeigt, dass ein aus 151 Aminosäuren bestehendes und mit der Fc-Region von humanem IgG₁ fusioniertes Lake Victoria marburgvirus GP₁-Fragment (Aminosäuren 38-188; 38-188-Fc) mit höherer Affinität an filovirusempfindliche Zellen bindet als unverändertes GP₁. Das analoge Zaire ebolavirus GP₁-Fragment, bestehend aus 148 Aminosäuren (Aminosäuren 54-201) und der Fc-Region von humanem IgG₁ (54-201-Fc), band an die gleichen Zellen mit ebenfalls höherer Affinität als längere Fragmente. Weder das Marburgvirus, noch das Ebolavirus

GP₁-Fragment vermochte es, an filovirusresistente Lymphozyten zu binden, von welchen vermutet wird, dass sie den Filovirusrezeptor nicht exprimieren. Sowohl Lake Victoria marburgvirus 38-188-Fc, als auch Zaire ebolavirus 54-201-Fc, hemmten die Replikation von infektiösem Zaire ebolavirus und die Transduktion filovirusempfindlicher Zellen durch Gammaretroviren, die mit Lake Victoria marburgvirus oder Zaire ebolavirus GP_{1,2}-Oberflächenproteinen pseudotypisiert waren. Analoge Fc-Fusionskonstrukte, welche die zum 54-201-Fragment analogen Sequenzen der GP₁-Proteine von Côte d'Ivoire, Reston, oder Sudan ebolavirus enthielten, hemmten ebenfalls die Zelltransduktion durch Lake Victoria marburgvirus GP_{1,2} pseudotypisierte Gammaretroviren. Diese Experimente identifizierten die Rezeptorbinderegionen (RBR) der Marburg- und Ebolaviren und zeigen, dass all Filoviren mindestens einen gemeinsamen Rezeptor benutzen.

Mittels kotranskriptionalen Editings des *GP*-Gens exprimieren Ebolaviren, nicht aber Marburgviren, neben dem GP_{1,2}-Oberflächenprotein zwei sezernierte Glykoproteine (sGP, ssGP). Alle drei Proteine besitzen identische N-Termini, welche die Aminosäuren 54-201 beinhalten. Hier wird gezeigt, dass weder sGP-Fc, noch ssGP-Fc, an filovirusempfindliche Zellen binden konnte. Keines der beiden Proteine konnte die Zelltransduktion dieser Zellen mit Lake Victoria marburgvirus GP_{1,2} pseudotypisierten Gammaretroviren hemmen, was vermuten lässt, dass sie nicht an den Filovirus-Rezeptor banden. Stattdessen wird gezeigt, dass Fc-konjugiertes Δ -Peptid – ein kurzes, C-terminales Spaltprodukt von sGP ohne Sequenzähnlichkeit zu filoviralen Rezeptorbinderegionen (Δ -Fc) – sowohl die Zelltransduktion mit pseudotypisierten Gammaretroviren hemmte, als auch die Replikation von infektiösem Zaire ebolavirus. Côte d'Ivoire, Sudan und Zaire ebolavirus Δ -Fc hemmten den durch Lake Victoria marburgvirus GP_{1,2}-vermittelten Zelleintritt und die Replikation von infektiösem Zaire ebolavirus vergleichbar zu oder besser als Zaire ebolavirus 54-201-Fc. Interessanterweise hatte Δ -Fc des Reston ebolavirus, welches als einziges der Filoviren als humanapathogen gilt, geringen oder keinen Effekt. Diese Ergebnisse lassen vermuten, dass Δ -Peptide an der Zellpenetration durch Filoviren beteiligt sind und möglicherweise wichtige Virulenzfaktoren darstellen.

Zuletzt wurden die immunogenen Eigenschaften der filoviralen Fc-konjugierten Rezeptorbinderegionen in einem letalen Mausmodell untersucht. C57/BL6-Mäuse wurden nach 0, 21 und 35 Tagen mit Zaire ebolavirus 54-201-Fc + RIBI-Adjuvans oder Lake Victoria marburgvirus 38-188-Fc + RIBI-Adjuvans immunisiert und nach 62 Tagen mit mausadaptiertem Zaire ebolavirus infiziert. Alle mit Zaire ebolavirus 54-201-Fc-immunisierten Mäuse überlebten die ansonsten tödliche Infektion ohne sichtliche Krankheitssymptome. Die Hälfte der mit Lake Victoria marburgvirus 38-188-Fc-immunisierten Mäuse überlebten ebenfalls die ansonsten tödliche Infektion mit Zaire ebolavirus. Sera, die mit Zaire ebolavirus 54-201-Fc oder Lake Victoria marburgvirus 38-188-Fc immunisierten Mäusen entnommen wurden, hemmten die Infektion von Vero E6 Zellen mit Zaire ebolavirus. Darüber hinaus konnte eine starke zytotoxische T-Zellantwort in immunisierten Mäusen nachgewiesen werden. Hiermit wird erstmalig ein Filovirusimpfstoffkandidat beschrieben, der sowohl partiell vor Marburg-, als auch vollständig vor Ebolaviren schützt.

10 REFERENCES

1. 1978. EBOLA (EBO); Strain: ME. *Am. J. Trop. Med. Hyg.* **27**(2 suppl. part 2):383-384.
2. **Agafonov, A. P., G. M. Ignatyev, V. A. Kuzmin, Z. L. Akimenko, T. V. Kosareva, and Ye. A. Kashentseva.** 1992. The Immunogenic Properties of Marburg Virus Proteins. *Vopr. Virusol.* **37**:58-61 [Russian].
3. **Akinfeyeva, L. A., O. I. Aksyonova, I. V. Vasilyevich, Z. I. Ginko, K. A. Zarkov, N. M. Zubavichene, L. R. Katkova, O. P. Kuzovlev, V. I. Kuzubov, L. I. Lokteva, and Ye. I. Ryabchikova.** 2005. A case of Ebola hemorrhagic fever. *Infekt. Bolezn.* **3**:85-88 [Russian].
4. **Alazard-Dany, N., V. Volchkova, O. Reynard, C. Carbonnelle, O. Dolnik, M. Ottmann, A. Khromykh, and V. E. Volchkov.** 2006. Ebola virus glycoprotein GP is not cytotoxic when expressed constitutively at a moderate level. *J. Gen. Virol.* **87**:1247-1257.
5. **Alibek, K., and S. Handelman.** 1999. *Biohazard.* Random House, New York, NY, USA.
6. **Alvarez, C. P., F. Lasala, J. Carrillo, O. Muñiz, A. L. Corbí, and R. Delgado.** 2002. C-Type Lectins DC-SIGN and L-SIGN Mediate Cellular Entry by Ebola Virus in *cis* and in *trans*. *J. Virol.* **76**:6841-6844.
7. **Aman, M. J., C. M. Bosio, R. G. Panchal, J. C. Burnett, A. Schmaljohn, and S. Bavari.** 2003. Molecular mechanisms of filovirus cellular trafficking. *Microbes Infect.* **5**:639-649 [Epub Apr. 24, 2003], and **5**:1287 [Epub Sep. 18, 2003] [Erratum].
8. **Amblard, J., P. Obiang, S. Edzang, C. Prehaud, M. Bouloy, and B. le Guenno.** 1997. Identification of the Ebola virus in Gabon in 1994. *Lancet* **349**:181-182.
9. **Babiker Mohd el Tahir.** 1978. The Haemorrhagic Fever Outbreak in Maridi, Western Equatoria, Southern Sudan, p. 125-127. *In* S. R. Pattyn (ed.), *Ebola Virus Haemorrhagic Fever.* Elsevier/North-Holland Biomedical Press, Amsterdam, The Netherlands.
10. **Baltzer, G., W. Slenczka, L. Stöppler, H. A. Schmidt-Wilke, E. Hermann, R. Siegert, and G. A. Martini.** 1979. Marburg-Virus-Krankheit. Verlaufsbeobachtungen über 12 Jahre (1967-1979), p. 1203-1206. *In* B. Schlegel (ed.), *Verhandlungen der Deutschen Gesellschaft für Innere Medizin.* J. F. Bergmann Verlag, Munich, Germany [German].
11. **Bamberg, S., L. Kolesnikova, P. Möller, H.-D. Klenk, and S. Becker.** 2005. VP24 of Marburg Virus Influences Formation of Infectious Particles. *J. Virol.* **79**:13421-13433.
12. **Bär, S., A. Takada, Y. Kawaoka, and M. Alison.** 2006. Detection of Cell-Cell Fusion Mediated by Ebola Virus Glycoproteins. *J. Virol.* **80**:2815-2822.

13. **Baribaud, F., R. W. Doms, and S. Pöhlmann.** 2002. The role of DC-SIGN and DC-SIGNR in HIV and Ebola virus infection: can potential therapeutics block virus transmission and dissemination? *Expert Opin. Ther. Targets* **6**:423-431.
14. **Barnett, A. L., D. L. Wensel, W. Li, D. Fass, and J. M. Cunningham.** 2003. Structure and Mechanism of a Coreceptor for Infection by a Pathogenic Feline Retrovirus. *J. Virol.* **77**:2717-2729.
15. **Baron, R. C., J. B. McCormick, and O. A. Zubeir.** 1983. Ebola virus disease in southern Sudan: hospital dissemination and intrafamilial spread. *Bull. WHO* **61**:997-1003.
16. **Barrientos, L. G., A. M. Martin, P. E. Rollin, and A. Sanchez.** 2004. Disulfide bond assignment of the Ebola virus secreted glycoprotein sGP. *Biochem. Biophys. Res. Commun.* **323**:696-702 [Epub Sep. 9, 2004].
17. **Barrientos, L. G., A. M. Martin, R. M. Wohlhueter, and P. E. Rollin.** 2007. Secreted glycoprotein from live Zaire ebolavirus-infected cultures: preparation, structural and biophysical characterization, and thermodynamic stability. *J. Infect. Dis.* **196**(suppl. 2):S220-S231.
18. **Basler, C. F., X. Wang, E. Mühlberger, V. Volchkov, J. Paragas, H.-D. Klenk, A. García-Sastre, and P. Palese.** 2000. The Ebola virus VP35 protein functions as a type I IFN antagonist. *Proc. Natl. Acad. Sci. USA* **97**:12289-12294.
19. **Bausch, D. G., M. Borchert, T. Grein, C. Roth, R. Swanepoel, M. L. Libande, A. Talarmin, E. Bertherat, J.-J. Muyembe-Tamfum, B. Tugume, R. Colebunders, K. M. Kondé, P. Pirard, L. L. Olinda, G. R. Rodier, P. Campbell, O. Tomori, T. G. Ksiazek, and P. E. Rollin.** 2003. Risk Factors for Marburg Hemorrhagic Fever, Democratic Republic of the Congo. *Emerg. Infect. Dis.* **9**:1531-1537.
20. **Bausch, D. G., and T. W. Geisbert.** 2007. Development of vaccines for Marburg hemorrhagic fever. *Expert Rev. Vaccines* **6**:57-74.
21. **Bausch, D. G., S. T. Nichol, J. J. Muyembe-Tamfum, M. Borchert, P. E. Rollin, H. Sleurs, P. Campbell, F. K. Tshioko, C. Roth, R. Colebunders, P. Pirard, S. Mardel, L. A. Olinda, H. Zeller, A. Tshomba, A. Kulidri, M. L. Libande, S. Mulangu, P. Formenty, T. Grein, H. Leirs, L. Braack, T. Ksiazek, S. Zaki, M. D. Bowen, S. B. Smit, P. A. Leman, F. J. Burt, A. Kemp, and R. Swanepoel, for the International Scientific and Technical Committee for Marburg Hemorrhagic Fever Control in the Democratic Republic of the Congo.** 2006. Marburg Hemorrhagic Fever Associated with Multiple Genetic Lineages of Virus. *New England J. Med.* **355**:909-919.
22. **Bechtelsheimer, H., G. Korb, and P. Gedigk.** 1970. Die „Marburg-Virus“-Hepatitis - Untersuchungen bei Menschen und Meerschweinchen. *Virch. Arch. A Pathol. Patholog. Anat.* **351**:273-290 [German].
23. **Becker, S., S. Huppertz, H.-D. Klenk, and H. Feldmann.** 1994. The nucleoprotein of Marburg virus is phosphorylated. *J. Gen. Virol.* **75**:809-818.
24. **Becker, S., C. Rinne, U. Hofsäß, H.-D. Klenk, and E. Mühlberger.** 1998. Interactions of Marburg Virus Nucleocapsid Proteins. *Virology* **249**:406-417.

25. **Becker, S., M. Spiess, and H.-D. Klenk.** 1995. The asialoglycoprotein receptor is a potential liver-specific receptor for Marburg virus. *J. Gen. Virol.* **76**:393-399.
26. **Bitekerezo, M., C. Kyobutungi, R. Kizza, J. Mugeni, E. Munyarugero, F. Tirwomwe, E. Twongyeirwe, G. Muhindo, V. Nakibuuka, M. Nakate, L. John, A. Ruiz, K. Frame, G. Priotto, L. Pepper, J. Kabakyenga, S. Baingana, and D. Ledo.** 2002. The outbreak and control of Ebola viral haemorrhagic fever in a Ugandan medical school. *Trop. Doct.* **32**:10-15.
27. **Boehmann, Y., S. Enterlein, A. Randolph, and E. Mühlberger.** 2005. A reconstituted replication and transcription system for Ebola virus Reston and comparison with Ebola virus Zaire. *Virology* **332**:406-417 [Epub Dec. 15, 2004].
28. **Bonaparte, M. I., A. S. Dimitrov, K. N. Bossart, G. Crameri, B. A. Mungall, K. A. Bishop, V. Choudhry, D. S. Dimitrov, L.-F. Wang, B. T. Eaton, and C. C. Broder.** 2005. Ephrin-B2 ligand is a functional receptor for Hendra virus and Nipah virus. *Proc. Natl. Acad. Sci. USA* **102**:10652-10657.
29. **Borio, L., T. Ingelsby, C. J. Peters, A. L. Schmaljohn, J. M. Hughes, P. B. Jahrling, T. Ksiazek, K. M. Johnson, A. Meyerhoff, T. O'Toole, M. S. Ascher, J. Bartlett, J. G. Breman, E. M. Eitzen, Jr., M. Hamburg, J. Hauer, D. A. Henderson, R. T. Johnson, G. Kwik, M. Layton, S. Lillibridge, G. J. Nabel, M. T. Osterholm, T. M. Perl, P. Russell, and K. Tonat, for the Working Group on Civilian Biodefense.** 2002. Hemorrhagic Fever Viruses as Biological Weapons - Medical and Public Health Management. *J. Am. Med. Assoc.* **287**:2391-2405.
30. **Boumandouki, P., P. Formenty, A. Epelboin, P. Campbell, C. Atsangandoko, Y. Allarangar, É. M. Leroy, M. L. Kone, A. Molamou, O. Dinga-Longa, A. Salemo, R. Y. Kounkou, V. Mombouli, J. R. Ibara, P. Gaturuku, S. Nkunku, A. Lucht, and H. Feldmann.** 2005. Prise en charge des malades et des défunts lors de l'épidémie de fièvre hémorragique due au virus Ebola d'octobre à décembre 2003 au Congo. *Bull. Soc. Pathol. Exot.* **98**:218-223 [French].
31. **Bowen, E. T. W., G. Lloyd, W. J. Harris, G. S. Platt, A. Baskerville, and E. E. Vella.** 1977. Viral Haemorrhagic Fever in Southern Sudan and Northern Zaire. Preliminary Studies on the Aetiological Agent. *Lancet* **i**:571-573.
32. **Bray, M.** 2006. Therapy of Ebola and Marburg Virus Infections, p. 419 -452. *In* E. Bogner and A. Holzenburg (ed.), *New Concepts of Antiviral Therapy*. Springer-Verlag, Dordrecht, The Netherlands.
33. **Bray, M., K. Davis, T. Geisbert, C. Schmaljohn, and J. Huggins.** 1998. A Mouse Model for Evaluation of Prophylaxis and Therapy of Ebola Hemorrhagic Fever. *J. Infect. Dis.* **178**:651-661, and **178**:1553 [Erratum].
34. **Bray, M., S. Hatfill, L. Hensley, and J. W. Huggins.** 2001. Haematological, Biochemical and Coagulation Changes in Mice, Guinea-pigs and Monkeys Infected with a Mouse-adapted Variant of Ebola Zaire Virus. *J. Comp. Pathol.* **125**:243-253.
35. **Breman, J. G., K. M. Johnson, G. van der Groen, C. B. Robbins, M. V. Szczeniowski, K. Ruti, P. A. Webb, F. Meier, D. L. Heymann, T. A. Leonard, J. B. McCormick, G. Ndoli, E. Zannotto, L. W. Robbins, J.-F. Bergmann, E. S. Lloyd, R. Kamanu, J. M. Hackett, and J. W. Krebs.** 1999. A Search for Ebola

- Virus in Animals in the Democratic Republic of the Congo and Cameroon: Ecologic, Virologic, and Serologic Surveys, 1979-1980. *J. Infect. Dis.* **179(suppl. 1)**:S139-S147.
36. **Breman, J. G., P. Piot, K. M. Johnson, M. K. White, M. Mbuyi, P. Sureau, D. L. Heymann, S. van Nieuwenhove, J. B. McCormick, J. P. Ruppol, V. Kintoki, M. Isaäcson, G. van der Groen, P. A. Webb, and K. Ngvete.** 1978. The Epidemiology of Ebola Haemorrhagic Fever in Zaire, 1976, p. 103-124. *In* S. R. Pattyn (ed.), *Ebola Virus Haemorrhagic Fever*. Elsevier/North-Holland Biomedical Press, Amsterdam, The Netherlands.
 37. **Brindley, M. A., L. Hughes, A. Ruiz, P. B. McCray, Jr., A. Sanchez, D. A. Sanders, and W. Maury.** 2007. Ebola Virus Glycoprotein 1: Identification of Residues Important for Binding and Postbinding Events. *J. Virol.* **81**:7702-7709 [Epub May 2, 2007].
 38. **Bukreyev, A., P. E. Rollin, M. K. Tate, L. Yang, S. R. Zaki, W.-J. Shieh, B. R. Murphy, P. L. Collins, and A. Sanchez.** 2007. Successful Topical Respiratory Tract Immunization of Primates against Ebola Virus. *J. Virol.* **81**:6379-6388 [Epub Apr. 7, 2007].
 39. **Bukreyev, A. A., E. F. Belanov, V. M. Blinov, and S. V. Netesov.** 1995. Complete Nucleotide Sequences of Marburg Virus Genes 5 and 6 Encoding VP30 and VP24 Proteins. *Biochem. Mol. Biol. Int.* **35**:605-613.
 40. **Bukreyev, A. A., V. E. Volchkov, V. M. Blinov, and S. V. Netesov.** 1993. The GP-protein of Marburg virus contains the region similar to the 'immunosuppressive domain' of oncogenic retrovirus P15E proteins. *FEBS Lett.* **323**:183-187.
 41. **Bukreyev, A. A., V. E. Volchkov, V. M. Blinov, and S. V. Netesov.** 1993. The VP35 and VP40 proteins of filoviruses - Homology between Marburg and Ebola viruses. *FEBS Lett.* **322**:41-46.
 42. **Bullough, P. A., F. M. Hughson, J. J. Skehel, and D. C. Wiley.** 1994. Structure of influenza haemagglutinin at the pH of membrane fusion. *Nature* **371**:37-43.
 43. **Bwaka, M. A., M.-J. Bonnet, P. Calain, R. Colebunders, A. de Roo, Y. Guimard, K. R. Katwiki, K. Kibadi, M. A. Kipasa, K. J. Kuvula, B. B. Mapanda, M. Massamba, K. D. Mupapa, J.-J. Muyembe-Tamfum, E. Ndaberey, C. J. Peters, P. E. Rollin, and E. van den Enden.** 1999. Ebola Hemorrhagic Fever in Kikwit, Democratic Republic of the Congo: Clinical Observations in 103 Patients. *J. Infect. Dis.* **179(suppl. 1)**:S1-S7.
 44. **Cao, W., M. D. Henry, P. Borrow, H. Yamada, J. H. Elder, E. V. Ravkov, S. T. Nichol, R. W. Compans, K. P. Campbell, and M. B. Oldstone.** 1998. Identification of α -dystroglycan as a receptor for lymphocytic choriomeningitis virus and Lassa fever virus. *Science* **282**:2079-2081.
 45. **Cárdenas, W. B., Y.-M. Loo, M. Gale, Jr., A. L. Hartman, C. R. Kimberlin, L. Martínez-Sobrido, E. Ollmann Saphire, and C. F. Basler.** 2006. Ebola Virus VP35 Protein Binds Double-Stranded RNA and Inhibits Alpha/Beta Interferon Production Induced by RIG-I Signaling. *J. Virol.* **80**:5168-5178.

46. **Casals, J.** 1971. Absence of Serological Relationship Between the Marburg Virus and Some Arboviruses, p. 98-104. *In* G. A. Martini and R. Siegert (ed.), Marburg Virus Disease. Springer-Verlag, Berlin, Germany.
47. **Centers for Disease Control and Prevention.** 2008. Select Agent Program. <http://www.cdc.gov/od/sap/>.
48. **Chan, S. Y., C. J. Empig, F. J. Welte, R. F. Speck, A. Schmaljohn, J. F. Kreisberg, and M. A. Goldsmith.** 2001. Folate Receptor- α Is a Cofactor for Cellular Entry by Marburg and Ebola viruses. *Cell* **106**:117-126.
49. **Chan, S. Y., and M. A. Goldsmith.** 2004. Molecular Mechanisms of Filovirus Entry, p. 91-135. *In* H.-D. Klenk and H. Feldmann (ed.), Ebola and Marburg Viruses - Molecular and Cellular Biology. Horizon Bioscience, Wymondham, Norfolk, United Kingdom.
50. **Chan, S. Y., M. C. Ma, and M. A. Goldsmith.** 2000. Differential induction of cellular detachment by envelope glycoproteins of Marburg and Ebola (Zaire) viruses. *J. Gen. Virol.* **81**:2155-2159.
51. **Chan, S. Y., R. F. Speck, M. C. Ma, and M. A. Goldsmith.** 2000. Distinct Mechanisms of Entry by Envelope Glycoproteins of Marburg and Ebola (Zaire) Viruses. *J. Virol.* **74**:4933-4937.
52. **Chandran, K., N. J. Sullivan, U. Felbor, S. P. Whelan, and J. M. Cunningham.** 2005. Endosomal Proteolysis of the Ebola Virus Glycoprotein Is Necessary for Infection. *Science* **308**:1643-1645.
53. **Chepurnov, A. A., Yu. P. Chuyev, O. V. Pyankov, and I. V. Yefimova.** 1995. Effects of Some Physical and Chemical Factors on Inactivation of Ebola Virus. *Vopr. Virusol.* **40**:74-76 [Russian].
54. **Chepurnov, A. A., N. M. Zubavichene, and A. A. Dadaeva.** 2003. Elaboration of laboratory strains of Ebola virus and study of pathophysiological reactions of animals inoculated with these strains. *Acta Trop.* **87**:321-329 [Epub Jun. 19, 2003].
55. **Choe, H., W. Li, P. L. Wright, N. Vasilieva, M. Venturi, C. C. Huang, C. Grundner, T. Dorfman, M. B. Zwick, L. Wang, E. S. Rosenberg, P. D. Kwong, D. R. Burton, J. E. Robinson, J. G. Sodroski, and M. Farzan.** 2003. Tyrosine sulfation of human antibodies contributes to recognition of the CCR5 binding region of HIV-1 gp120. *Cell* **114**:161-170.
56. **Ciorba, A., G. Matteucci, L. Perini, M. E. Caristo, and D. Brown.** 1997. Infezione da Virus Ebola nella Scimmia: Reperti Clinici et Anatomopatologici Osservati nel Corso del Primo Episodio Verificatosi in Europa. *Veterinaria* **11**:109-112 [Italian].
57. **Conrad, J. L., M. Isaacson, E. B. Smith, H. Wulff, M. Crees, P. Geldenhuys, and J. Johnston.** 1978. Epidemiologic Investigation of Marburg Virus Disease, Southern Africa, 1975. *Am. J. Trop. Med. Hyg.* **27**:1210-1215.
58. **Cox, N., J. B. McCormick, K. M. Johnson, and M. P. Kiley.** 1983. Evidence for Two Subtypes of Ebola Virus Based on Oligonucleotide Mapping of RNA. *J. Infect. Dis.* **147**:272-275.

59. **Daddario-DiCaprio, K. M., T. W. Geisbert, J. B. Geisbert, U. Ströher, L. E. Hensley, A. Grolla, E. A. Fritz, F. Feldmann, H. Feldmann, and S. M. Jones.** 2006. Cross-Protection against Marburg Virus Strains by Using a Live, Attenuated Recombinant Vaccine. *J. Virol.* **80**:9659-9666.
60. **Daddario-DiCaprio, K. M., T. W. Geisbert, U. Ströher, J. B. Geisbert, A. Grolla, E. A. Fritz, L. Fernando, E. Kagan, P. B. Jahrling, L. E. Hensley, S. M. Jones, and H. Feldmann.** 2006. Postexposure protection against Marburg haemorrhagic fever with recombinant vesicular stomatitis virus vectors in non-human primates: an efficacy assessment. *Lancet* **367**:1399-1404 [Epub Apr. 27, 2006].
61. **Dalgleish, A. G., P. C. Beverley, P. R. Clapham, D. H. Crawford, M. F. Graves, and R. A. Weiss.** 1984. The CD4 (T4) antigen is an essential component of the receptor for the AIDS retrovirus. *Nature* **312**:763-767.
62. **Dietrich, M., H. H. Schumacher, D. Peters, and J. Knobloch.** 1978. Human Pathology of Ebola (Maridi) Virus Infection in The Sudan, p. 37-41. *In* S. R. Pattyn (ed.), *Ebola Virus Haemorrhagic Fever*. Elsevier/North-Holland Biomedical Press, Amsterdam, The Netherlands.
63. **Dimitrov, D. S.** 2004. Virus entry: molecular mechanisms and biomedical applications. *Nat. Rev. Microbiol.* **2**:109-122.
64. **Dorfman, T., M. J. Moore, A. C. Guth, H. Choe, and M. Farzan.** 2006. A tyrosine-sulfated peptide derived from the heavy-chain CDR3 region of an HIV-1-neutralizing antibody binds gp120 and inhibits HIV-1 infection. *J. Biol. Chem.* **281**:28529-28535 [Epub Jul. 18, 2006].
65. **Dube, D., K. L. Schornberg, T. S. Stantchev, M. I. Bonaparte, S. E. Delos, A. H. Bouton, C. C. Broder, and J. M. White.** 2008. Cell adhesion promotes Ebola virus envelope glycoprotein-mediated binding and infection. *J. Virol.* **82**:7238-7242 [Epub Apr. 30, 2008].
66. **DuBridg, R. B., P. Tang, H. C. Hsia, P. M. Leong, J. H. Miller, and M. P. Calos.** 1987. Analysis of mutation in human cells by using an Epstein-Barr virus shuttle system. *Mol. Cell. Bio.* **7**:379-387.
67. **Ebihara, H., A. Takada, D. Kobasa, S. Jones, G. Neumann, S. Theriault, M. Bray, H. Feldmann, and Y. Kawaoka.** 2006. Molecular Determinants of Ebola Virus Virulence in Mice. *PLoS Pathogens* **2**:705-711 (article e73) [Epub Jul. 21, 2006].
68. **Eckert, D. M., and P. S. Kim.** 2001. Mechanisms of viral membrane fusion and its inhibition. *Annu. Rev. Biochem.* **70**:777-810.
69. **Egbring, R., W. Slenczka, and G. Baltzer.** 1971. Clinical Manifestations and Mechanisms of the Haemorrhagic Diathesis in Marburg Virus Disease, p. 41-49. *In* G. A. Martini and R. Siebert (ed.), *Marburg Virus Disease*. Springer-Verlag, Berlin, Germany.
70. **el Mekki, A., G. van der Groen, and S. R. Pattyn.** 1978. Attempts to Classify Ungrouped Arboviruses by Electron Microscopy, p. 261-267. *In* S. R. Pattyn (ed.),

- Ebola Virus Haemorrhagic Fever. Elsevier/North-Holland Biomedical Press, Amsterdam, The Netherlands.
71. **el Mekki, A. A., and G. van der Groen.** 1981. A Comparison of Indirect Immunofluorescence and Electron Microscopy for the Diagnosis of Some Haemorrhagic Viruses in Cell Cultures. *J. Virol. Meth.* **3**:61-69.
 72. **Elliott, L. H., M. P. Kiley, and J. B. McCormick.** 1985. Descriptive Analysis of Ebola Virus Proteins. *Virology* **147**:169-176.
 73. **Elliott, L. H., A. Sanchez, B. P. Holloway, M. P. Kiley, and J. B. McCormick.** 1993. Ebola protein analyses for the determination of genetic organization. *Arch. Virol.* **133**:423-436.
 74. **Emond, R. T. D., B. Evans, E. T. W. Bowen, and G. Lloyd.** 1977. A case of Ebola infection. *Br. Med. J.* **2**:541-544.
 75. **Falzarano, D., O. Krokhin, G. van Domsallar, W. Kristin, J. Seebach, H.-J. Schnittler, and H. Feldmann.** 2007. Ebola sGP - The first viral glycoprotein shown to be C-mannosylated. *Virology* **368**:83-90 [Epub Jul. 20, 2007].
 76. **Falzarano, D., O. Krokhin, V. Wahl-Jensen, J. Seebach, K. Wolf, H.-J. Schnittler, and H. Feldmann.** 2006. Structure-Function Analysis of the Soluble Glycoprotein, sGP, of Ebola Virus. *ChemBioChem* **7**:1605-1611 [Epub Sep. 15, 2006].
 77. **Farzan, M., T. Mirzabekov, P. Kolchinsky, R. Wyatt, M. Cayabyab, N. P. Gerard, C. Gerard, J. Sodroski, and H. Choe.** 1999. Tyrosine Sulfation of the Amino Terminus of CCR5 Facilitates HIV-1 Entry. *Cell* **96**:667-676.
 78. **Fass, D., R. A. Davey, C. A. Hamson, P. S. Kim, J. M. Cunningham, and J. M. Berger.** 1997. Structure of a Murine Leukemia Virus Receptor-Binding Glycoprotein at 2.0 Angstrom Resolution. *Science* **277**:1662-1666.
 79. **Fass, D., S. C. Harrison, and P. S. Kim.** 1996. Retrovirus envelope domain at 1.7 Å resolution. *Nat. Struct. Biol.* **3**:465-469.
 80. **Feldmann, H., T. W. Geisbert, P. B. Jahrling, H.-D. Klenk, S. V. Netesov, C. J. Peters, A. Sanchez, R. Swanepoel, and V. E. Volchkov.** 2005. Family *Filoviridae*, p. 645-653. *In* C. M. Fauquet, M. A. Mayo, J. Maniloff, U. Desselberger, and L. A. Ball (ed.), *Virus Taxonomy - Eighth Report of the International Committee on Taxonomy of Viruses*. Elsevier/Academic Press, San Diego, CA, USA.
 81. **Feldmann, H., S. M. Jones, K. M. Daddario-DiCaprio, J. B. Geisbert, U. Ströher, A. Grolla, M. Bray, E. A. Fritz, L. Fernando, F. Feldmann, L. E. Hensley, and T. W. Geisbert.** 2007. Effective Post-Exposure Treatment of Ebola Infections. *PLoS Pathogens* **3**:54-61 (article e2) [Epub Jan. 19, 2007].
 82. **Feldmann, H., and H.-D. Klenk.** 1996. Marburg and Ebola Viruses, p. 1-53. *In* K. Maramorosch, F. A. Murphy, and A. J. Shatkin (ed.), *Advances in Virus Research*, vol. 47. Academic Press, San Diego, CA, USA.
 83. **Feldmann, H., E. Mühlberger, A. Randolph, C. Will, M. P. Kiley, A. Sanchez, and H.-D. Klenk.** 1992. Marburg virus, a filovirus: messenger RNAs, gene order, and regulatory elements of the replication cycle. *Virus Res.* **24**:1-19.

84. **Feldmann, H., E. Mühlberger, A. Randolph, H. Wunder, C. Will, W. Slenczka, and H.-D. Klenk.** 1991. Complete sequence analysis of the Marburg virus genome and relationship to other nonsegmented negative strand RNA viruses. *Tropenmed. Parasitol.* **42(suppl. IV):**447-448.
85. **Feldmann, H., S. T. Nichol, H.-D. Klenk, C. J. Peters, and A. Sanchez.** 1994. Characterization of Filoviruses Based on Differences in Structure and Antigenicity of the Virion Glycoprotein. *Virology* **199:**469-473.
86. **Feldmann, H., W. Slenczka, and H.-D. Klenk.** 1996. Emerging and reemerging of filoviruses, p. 77-100. *In* T. F. Schwarz and G. Siegl (ed.), *Imported Virus Infections*, Archives of Virology Supplement, vol. 11. Springer, Vienna, Austria.
87. **Feldmann, H., C. Will, M. Schikore, W. Slenczka, and H.-D. Klenk.** 1991. Glycosylation and Oligomerization of the Spike Protein of Marburg Virus. *Virology* **182:**353-356.
88. **Feng, Z., M. Cerveny, Z. Yan, and B. He.** 2007. The VP35 Protein of Ebola Virus Inhibits the Antiviral Effect Mediated by Double-Stranded RNA Dependent Protein Kinase PKR. *J. Virol.* **81:**182-192 [Epub Oct. 25, 2006].
89. **Formenty, P., C. Boesch, M. Wyers, C. Steiner, F. Donati, F. Dind, F. Walker, and B. le Guenno.** 1999. Ebola Virus Outbreak among Wild Chimpanzees Living in a Rain Forest of Côte d'Ivoire. *J. Infect. Dis.* **179(suppl. 1):**S120-S126.
90. **Formenty, P., A. Epelboin, Y. Allaranger, F. Libama, P. Boumandouki, L. Koné, A. Molamou, N. Gami, J. V. Mombouli, M. Guardo Martinez, and S. Ngampo.** 2005. Séminaire de formation des formateurs et d'analyse des épidémies de fièvre hémorragique due au virus Ebola en Afrique centrale de 2001 à 2004. Brazzaville, République du Congo, 6-8 avril 2004. *Bull. Soc. Pathol. Exot.* **98:**244-254 [French].
91. **Formenty, P., C. Hatz, B. le Guenno, A. Stoll, P. Rogenmoser, and A. Widmer.** 1999. Human Infection Due to Ebola Virus, Subtype Côte d'Ivoire: Clinical and Biologic Presentation. *J. Infect. Dis.* **179(suppl. 1):**S48-S53.
92. **Francesconi, P., Z. Yoti, S. Declich, P. A. Onek, M. Fabiani, J. Olango, R. Andraghetti, P. E. Rollin, C. Opira, D. Greco, and S. Salmaso.** 2003. Ebola Hemorrhagic Fever Transmission and Risk Factors of Contacts, Uganda. *Emerg. Infect. Dis.* **9:**1430-1437.
93. **Gajdusek, D. C.** 1962. Virus hemorrhagic fevers. Special reference to hemorrhagic fever with renal syndrome (epidemic hemorrhagic fever). *J. Pediatr.* **60:**841-857.
94. **Gallaher, W. R.** 1996. Similar Structural Models of the Transmembrane Proteins of Ebola and Avian Sarcoma Viruses. *Cell* **85:**477-478.
95. **Gaulton, G., M. S. Co, and M. I. Greene.** 1985. Anti-idiotypic antibody identifies the cellular receptor of reovirus type 3. *J. Cell Biochem.* **28:**69-78.
96. **Gear, J. H. S.** 1988. The Diagnosis of Hemorrhagic Fever, p. 231-239. *In* J. H. S. Gear (ed.), *CRC Handbook of Viral and Rickettsial Hemorrhagic Fevers*. CRC Press, Boca Raton, FL, USA.
97. **Gear, J. S. S., G. A. Cassel, A. J. Gear, B. Trappler, L. Clausen, A. M. Meyers, M. C. Kew, T. H. Bothwell, R. Sher, G. B. Miller, J. Schneider, H. J. Koornhof,**

- E. D. Gomperts, M. Isaäcson, and J. H. S. Gear.** 1975. Outbreak of Marburg virus disease in Johannesburg. *Br. Med. J.* **4**:489-493.
98. **Gedigk, P., H. Bechtelsheimer, and G. Korb.** 1968. Die pathologische Anatomie der „Marburg-Virus“-Krankheit (sog. „Marburger Affenkrankheit“). *Dtsch. Med. Wochenschr.* **93**:590-601 [German].
99. **Geisbert, T. W., K. M. Daddario-DiCaprio, J. B. Geisbert, H. A. Young, P. Formenty, E. A. Fritz, T. Larsen, and L. E. Hensley.** 2007. Marburg virus Angola infection of rhesus macaques: pathogenesis and treatment with recombinant nematode anticoagulant protein c2. *J. Infect. Dis.* **196(suppl. 2)**:S372-S381.
100. **Geisbert, T. W., K. M. Daddario-DiCaprio, K. J. Williams, J. B. Geisbert, A. Leung, F. Feldmann, L. E. Hensley, H. Feldmann, and S. M. Jones.** 2008. Recombinant vesicular stomatitis virus vector mediates postexposure protection against Sudan Ebola hemorrhagic fever in nonhuman primates. *J. Virol.* **82**:5664-5668 [Epub Apr. 2, 2008].
101. **Geisbert, T. W., and L. E. Hensley.** 2004. Ebola virus: new insights into disease aetiopathology and possible therapeutic interventions. *Expert Rev. Mol. Med.* **6**:1-24.
102. **Geisbert, T. W., L. E. Hensley, P. B. Jahrling, T. Larsen, J. B. Geisbert, J. Paragas, H. A. Young, T. M. Fredeking, W. E. Rote, and G. P. Vlasuk.** 2003. Treatment of Ebola virus infection with a recombinant inhibitor of factor VIIa/tissue factor: a study in rhesus monkeys. *Lancet* **362**:1953-1958 [Epub Dec. 12, 2003].
103. **Geisbert, T. W., and P. B. Jahrling.** 1995. Differentiation of filoviruses by electron microscopy. *Virus Res.* **39**:129-150.
104. **Geisbert, T. W., and P. B. Jahrling.** 2003. Towards a vaccine against Ebola virus. *Expert Rev. Vaccines* **2**:89-101.
105. **Geisbert, T. W., P. Pushko, K. Anderson, J. Smith, K. J. Davis, and P. B. Jahrling.** 2002. Evaluation in Nonhuman Primates of Vaccines against Ebola Virus. *Emerg. Infect. Dis.* **8**:503-507.
106. **Georges-Courbot, M. C., C. Y. Lu, J. Lansoud-Soukate, E. Leroy, and S. Baize.** 1997. Isolation and partial molecular characterisation of a strain of Ebola virus during a recent epidemic of viral haemorrhagic fever in Gabon. *Lancet* **349**:181.
107. **Georges, A.-J., E. M. Leroy, A. A. Renaut, C. T. Benissan, R. J. Nabias, M. T. Ngoc, P. I. Obiang, J. P. M. Lepage, E. J. Bertherat, D. D. Bénoni, E. J. Wickings, J. P. Amblard, J. M. Lansoud-Soukate, J. M. Milleliri, S. Baize, and M.-C. Georges-Courbot.** 1999. Ebola Hemorrhagic Fever Outbreaks in Gabon, 1994-1997: Epidemiologic and Health Control Issues. *J. Infect. Dis.* **179(suppl. 1)**:S65-S75.
108. **Gergonne, B., F. Belanger, and K. Leitmeyer.** 2001. Ebola Outbreak in Gulu - Uganda, October - December 2000. Epicentre - Médecins Sans Frontières, Paris, France.
109. **Germain, M.** 1978. Collection of Mammals and Arthropods During the Epidemic of Haemorrhagic Fever in Zaire, p. 185-189. *In* S. R. Pattyn (ed.), *Ebola Virus*

- Haemorrhagic Fever. Elsevier/North-Holland Biomedical Press, Amsterdam, The Netherlands.
110. **Gomis-Rüth, F. X., A. Dessen, J. Timmins, A. Bracher, L. Kolesnikowa, S. Becker, H.-D. Klenk, and W. Weissenhorn.** 2003. The Matrix Protein VP40 from Ebola Virus Octamerizes into Pore-like Structures with Specific RNA Binding Properties. *Structure* **11**:423-433.
 111. **Gonzalez, J.-P.** 1995. Ebola, une rivière tranquille au cœur de l'Afrique. *Cah. Santé* **5**:145-146 [French].
 112. **Gramberg, T., H. Hofmann, P. Möller, P. F. Lalor, A. Marzi, M. Geier, M. Krumbiegel, T. Winkler, F. Kirchhoff, D. H. Adams, S. Becker, J. Münch, and S. Pöhlmann.** 2005. LSECTin interacts with filovirus glycoproteins and the spike protein of SARS coronavirus. *Virology* **340**:224-236 [Epub Jul. 26, 2005].
 113. **Grolla, A., A. Lucht, D. Dick, J. E. Strong, and H. Feldmann.** 2005. Laboratory diagnosis of Ebola and Marburg hemorrhagic fever. *Bull. Soc. Pathol. Exot.* **98**:205-209.
 114. **Haasnoot, J., W. de Vries, E.-J. Geutjes, M. Prins, P. de Haan, and B. Berkhout.** 2007. The Ebola Virus VP35 Protein Is a Suppressor of RNA Silencing. *PLoS Pathogens* **3**:794-803 (article e86) [Epub Jun. 22, 2007].
 115. **Han, Z., H. Boshra, J. O. Sunyer, S. H. Zwiers, J. Paragas, and R. N. Harty.** 2003. Biochemical and Functional Characterization of the Ebola Virus VP24 Protein: Implications for a Role in Virus Assembly and Budding. *J. Virol.* **77**:1793-1800.
 116. **Harrison, S. C.** 2005. Mechanism of membrane fusion by viral envelope proteins. *Adv. Virus Res.* **64**:231-261.
 117. **Hart, M. K.** 2003. Vaccine research efforts for filoviruses. *Int. J. Parasitol.* **33**:583-595 [Epub Apr. 3, 2003].
 118. **Hartlieb, B., T. Muziol, W. Weissenhorn, and S. Becker.** 2007. Crystal structure of the C-terminal domain of Ebola virus VP30 reveals a role in transcription and nucleocapsid association. *Proc. Natl. Acad. Sci. USA* **104**:624-629 [Epub Jan. 3, 2007].
 119. **Hartman, A. L., J. E. Dover, J. S. Towner, and S. T. Nichol.** 2006. Reverse Genetic Generation of Recombinant Zaire Ebola Viruses Containing Disrupted IRF-3 Inhibitory Domains Results in Attenuated Virus Growth In Vitro and Higher Levels of IRF-3 Activation without Inhibiting Viral Transcription or Replication. *J. Virol.* **80**:6430-6440.
 120. **Harty, R. N., M. E. Brown, G. Wang, J. Huibregtse, and F. P. Hayes.** 2000. A PPxY motif within the VP40 protein of Ebola virus interacts physically and functionally with a ubiquitin ligase: Implications for filovirus budding. *Proc. Natl. Acad. Sci. USA* **97**:13871-13876.
 121. **Havemann, K., and H. A. Schmidt.** 1971. Haematological Findings in Marburg Virus Disease: Evidence for Involvement of the Immunological System, p. 34-40. *In* G. A. Martini and R. Siegert (ed.), *Marburg Virus Disease*. Springer-Verlag, Berlin, Germany.

122. **Heldwein, E. E., H. Lou, F. C. Bender, G. H. Cohen, R. J. Eisenberg, and S. C. Harrison.** 2006. Crystal structure of glycoprotein B from herpes simplex virus 1. *Science* **313**:217-220.
123. **Hevey, M., D. Negley, J. Geisbert, P. Jahrling, and A. Schmaljohn.** 1997. Antigenicity and Vaccine Potential of Marburg Virus Glycoprotein Expressed by Baculovirus Recombinants. *Virology* **239**:206-216.
124. **Hevey, M., D. Negley, P. Pushko, J. Smith, and A. Schmaljohn.** 1998. Marburg Virus Vaccines Based upon Alphavirus Replicons Protect Guinea Pigs and Nonhuman Primates. *Virology* **251**:28-37.
125. **Heymann, D. L., J. S. Weisfeld, P. A. Webb, K. M. Johnson, T. Cairns, and H. Bequist.** 1980. Ebola Hemorrhagic Fever: Tandala, Zaire, 1977-1978. *J. Infect. Dis.* **142**:372-376.
126. **Hoenen, T., A. Groseth, D. Falzarano, and H. Feldmann.** 2006. Ebola virus: unravelling pathogenesis to combat a deadly disease. *Trends Mol. Med.* **12**:206-215 [Epub Apr. 17, 2006].
127. **Hoenen, T., L. Kolesnikova, and S. Becker.** 2007. Recent advances in filovirus- and arenavirus-like particles. *Future Virol.* **2**:193-203.
128. **Hofmann, H., K. Pyrc, L. van der Hoek, M. Geier, B. Berkhout, and S. Pohlmann.** 2005. Human coronavirus NL63 employs the severe acute respiratory syndrome coronavirus receptor for cellular entry. *Proc. Natl. Acad. Sci. USA* **102**:7988-7993.
129. **Hovette, P.** 2005. Epidémie de Fièvre Hémorragique à Virus Marburg en Angola. *Méd. Trop.* **65**:127-128 [French].
130. **Huang, I.-C., B. J. Bosch, F. Li, W. Li, K. H. Lee, S. Ghiran, N. Vasilieva, T. S. Dermody, S. C. Harrison, P. R. Dormitzer, M. Farzan, R. P. J. M., and H. Choe.** 2006. SARS Coronavirus, but Not Human Coronavirus NL63, Utilizes Cathepsin L to Infect ACE2-expressing Cells. *J. Biol. Chem.* **281**:3198-3203 [Epub Dec. 8, 2005].
131. **Huang, I.-C., W. Li, J. Sui, W. Marasco, H. Choe, and M. Farzan.** 2008. Influenza A virus neuraminidase limits viral superinfection. *J. Virol.* **82**:4834-4843 [Epub Mar. 5, 2008].
132. **Huggins, J., Z.-X. Zhang, and M. Bray.** 1999. Antiviral Drug Therapy of Filovirus Infections: S-Adenosylhomocysteine Hydrolase Inhibitors Inhibit Ebola Virus In Vitro and in a Lethal Mouse Model. *J. Infect. Dis.* **179(suppl. 1)**:S240-S247.
133. **Huijbregts, B., P. de Wachter, L. S. Ndong Obiang, and M. E. Akou.** 2003. Ebola and the decline of gorilla *Gorilla gorilla* and chimpanzee *Pan troglodytes* populations in Minkebe Forest, north-eastern Gabon. *Oryx* **37**:437-443.
134. **Ignatiev, G. M., A. A. Dadaeva, S. V. Luchko, and A. Chepurnov.** 2000. Immune and pathophysiological processes in baboons experimentally infected with Ebola virus adapted to guinea pigs. *Immunol. Lett.* **71**:131-140 [Epub Feb. 14, 2000].

135. **International Society for Infectious Diseases.** 2008. ProMED-mail. <http://www.promedmail.org>.
136. **Ito, H., S. Watanabe, A. Takada, and Y. Kawaoka.** 2001. Ebola Virus Glycoprotein: Proteolytic Processing, Acylation, Cell Tropism, and Detection of Neutralizing Antibodies. *J. Virol.* **75**:1576-1580.
137. **Jacob, H.** 1971. The Neuropathology of the Marburg Disease, p. 54-61. *In* G. A. Martini and R. Siebert (ed.), *Marburg Virus Disease*. Springer-Verlag, Berlin, Germany.
138. **Jahrling, P. B., T. W. Geisbert, D. W. Dalgard, E. D. Johnson, T. G. Ksiazek, W. C. Hall, and C. J. Peters.** 1990. Preliminary report: isolation of Ebola virus from monkeys imported to USA. *Lancet* **335**:502-505.
139. **Jahrling, P. B., T. W. Geisbert, J. B. Geisbert, J. R. Swearingen, M. Bray, N. K. Jaax, J. W. Huggins, J. W. LeDuc, and C. J. Peters.** 1999. Evaluation of Immune Globulin and Recombinant Interferon- α 2b for Treatment of Experimental Ebola Virus Infections. *J. Infect. Dis.* **179**(suppl. 1):S224-S234.
140. **Jasenosky, L. D., G. Neumann, I. Lukashevich, and Y. Kawaoka.** 2001. Ebola Virus VP40-Induced Particle Formation and Association with the Lipid Bilayer. *J. Virol.* **75**:5205-5214.
141. **Jeffers, S. A., D. A. Sanders, and A. Sanchez.** 2002. Covalent Modifications of the Ebola Virus Glycoprotein. *J. Virol.* **76**:12463-12472.
142. **Jensen, V.** 2004. Biosynthesis, characterization and role of Ebola virus secreted glycoproteins in target cell activation. Ph.D. Dissertation. The University of Manitoba, Winnipeg, Manitoba, Canada.
143. **John, S. P., T. Wang, S. Steffen, S. Longhi, C. S. Schmaljohn, and C. B. Jonsson.** 2007. The Ebola Virus VP30 is an RNA Binding Protein. *J. Virol.* **81**:8967-8976 [Epub Jun. 13, 2007].
144. **Johnson, E. D., B. K. Johnson, D. Silverstein, P. Tukei, T. W. Geisbert, A. Sanchez, and P. B. Jahrling.** 1996. Characterization of a new Marburg virus isolate from a 1987 fatal case in Kenya, p. 101-114. *In* T. F. Schwarz and G. Siegl (ed.), *Imported Virus Infections, Archives of Virology Supplement*, vol. 11. Springer-Verlag, Vienna, Austria.
145. **Johnson, K. M., P. A. Webb, J. V. Lange, and F. A. Murphy.** 1977. Isolation and Partial Characterisation of a New Virus Causing Acute Haemorrhagic Fever in Zaire. *Lancet* **i**:569-571.
146. **Johnson, R. F., S. E. McCarthy, P. J. Godlewski, and R. N. Harty.** 2006. Ebola Virus VP35-VP40 Interaction Is Sufficient for Packaging 3E-5E Minigenome RNA into Virus-Like Particles. *J. Virol.* **80**:5135-5144.
147. **Jones, S. M., H. Feldmann, U. Ströher, J. B. Geisbert, L. Fernando, A. Grolla, H.-D. Klenk, N. J. Sullivan, V. E. Volchkov, E. A. Fritz, K. M. Daddario, L. E. Hensley, P. B. Jahrling, and T. W. Geisbert.** 2005. Live attenuated recombinant vaccine protects nonhuman primates against Ebola and Marburg viruses. *Nat. Med.* **11**:786-790 [Epub Jun. 5, 2005].

148. **Kaletsky, R. L., G. Simmons, and P. Bates.** 2007. Proteolysis of the Ebola virus glycoproteins enhances virus binding and infectivity. *J. Virol.* **81**:13378-13384 [Epub Oct. 10, 2007].
149. **Karesh, W., and P. Reed.** 2005. Ebola and great apes in Central Africa: current status and future needs. *Bull. Soc. Pathol. Exot.* **98**:237-238.
150. **Kielian, M., and F. A. Rey.** 2006. Virus membrane-fusion proteins: more than one way to make a hairpin. *Nat. Rev. Microbiol.* **4**:67-76.
151. **Kiley, M. P., E. T. W. Bowen, G. A. Eddy, M. Isaäcson, K. M. Johnson, J. B. McCormick, F. A. Murphy, S. R. Pattyn, D. Peters, O. W. Prozesky, R. L. Regnery, D. I. H. Simpson, W. Slenczka, P. Sureau, G. van der Groen, P. A. Webb, and H. Wulff.** 1982. Filoviridae: a Taxonomic Home for Marburg and Ebola Viruses. *Intervirology* **18**:24-32.
152. **Kiley, M. P., N. J. Cox, L. H. Elliott, A. Sanchez, R. DeFries, M. J. Buchmeier, D. D. Richman, and J. B. McCormick.** 1988. Physicochemical Properties of Marburg Virus: Evidence for Three Distinct Virus Strains and Their Relationship to Ebola Virus. *J. Gen. Virol.* **69**:1957-1967.
153. **Kiley, M. P., R. L. Regnery, and K. M. Johnson.** 1980. Ebola Virus: Identification of Virion Structural Proteins. *J. Gen. Virol.* **49**:333-341.
154. **Klatzmann, D., E. Champagne, S. Chamaret, J. Gruet, D. Guetard, T. Hercend, J.-C. Gluckman, and L. Montagnier.** 1984. T-lymphocyte T4 molecule behaves as the receptor for human retrovirus LAV. *Nature* **312**:767-768.
155. **Knobloch, J., M. Dietrich, D. Peters, G. Nielsen, and H.-H. Schumacher.** 1977. Maridi-hämorrhagisches Fieber - eine neue Viruserkrankung. *Dtsch. Med. Wochenschr.* **102**:1575-1581 [German].
156. **Kolesnikova, L., H. Bugany, H.-D. Klenk, and S. Becker.** 2002. VP40, the Matrix Protein of Marburg Virus, Is Associated with Membranes of the Late Endosomal Compartment. *J. Virol.* **76**:1825-1838.
157. **Kuhn, J. H.** 2008. Filoviruses - A Compendium of 40 Years of Epidemiological, Clinical, and Laboratory Studies. *Archives of Virology Supplement*, vol. 20. Springer, Vienna, Austria.
158. **Kuhn, J. H., W. Li, S. R. Radoshitzky, H. Choe, and M. Farzan.** 2007. Severe acute respiratory syndrome coronavirus entry as a target of antiviral therapies. *Antivir. Ther.* **12**:639-650.
159. **Lahm, S. A.** 2000. The Impact of Gold Panning and Associated Human Activities on Wildlife and the Environment in the Minkebe Forest, North-eastern Gabon. Report to the CARPE Project. United States Agency for International Development, Washington, DC, USA.
160. **Lamb, R. A.** 2007. *Mononegavirales*, p. 1357-1361. In D. M. Knipe and P. M. Howley (ed.), *Fields Virology*, 5th ed, vol. 1. Lippincott Williams & Wilkins, Philadelphia, PA, USA.
161. **Latiff, K., J. Meanger, J. Mills, and R. Ghildyal.** 2004. Sequence and structure relatedness of matrix protein of human respiratory syncytial virus with matrix proteins of other negative-sense RNA viruses. *Clin. Microbiol. Infect.* **10**:945-948.

162. **Lee, J. E., M. L. Fusco, A. J. Hessel, W. B. Oswald, D. R. Burton, and E. Ollmann Saphire.** 2008. Structure of the Ebola virus glycoprotein bound to an antibody from a human survivor. *Nature* **454**:177-182.
163. **Leirs, H., J. N. Mills, J. W. Krebs, J. E. Childs, D. Akaibe, N. Woollen, G. Ludwig, C. J. Peters, T. G. Ksiazek, D. S. Bressler, M. Curtis, M. L. Martin, L. Morgan, K. D. Wagoner, A. J. Williams, J. A. Comer, J. Liz, G. O. Maupin, J. G. Olson, M. Colyn, F. de Vree, J. Hulselmans, V. van Cakenberghe, E. van der Straeten, W. Verheyen, W. Wendelen, M. Loutte, D. Meirte, R. Hutterer, B. Ilenga, J.-B. Katshunga, A. Lubini, M. A. Mandango, K. Kargbo, J. Koniga, and C. Merriman.** 1999. Search for the Ebola Virus Reservoir in Kikwit, Democratic Republic of the Congo: Reflections on a Vertebrate Collection. *J. Infect. Dis.* **179**(suppl. 1):S155-S163.
164. **Leroy, E. M., B. Kumulungui, X. Pourrut, P. Rouquet, A. Hassanin, P. Yaba, A. Délicat, J. T. Paweska, J.-P. Gonzalez, and R. Swanepoel.** 2005. Fruit bats as reservoirs of Ebola virus. *Nature* **438**:575-576.
165. **Leroy, E. M., S. Souquière, P. Rouquet, and D. Drevet.** 2002. Re-emergence of ebola haemorrhagic fever in Gabon. *Lancet* **359**:712.
166. **Lescar, J., A. Roussel, M. W. Wien, J. Navaza, S. D. Fuller, G. Wengler, and F. A. Rey.** 2001. The fusion glycoprotein shell of Semliki Forest virus: an icosahedral assembly primed for fusogenic activation at endosomal pH. *Cell* **105**:137-148.
167. **Li, W., M. J. Moore, N. Vasilieva, J. Sui, S. K. Wong, M. A. Berne, M. Somasundaran, J. L. Sullivan, K. Luzuriaga, T. C. Greenough, H. Choe, and M. Farzan.** 2003. Angiotensin-converting enzyme 2 is a functional receptor for the SARS coronavirus. *Nature* **426**:450-454.
168. **Licata, J. M., M. Simpson-Holley, N. T. Wright, Z. Han, J. Paragas, and R. N. Harty.** 2003. Overlapping Motifs (PTAP and PPEY) within the Ebola Virus VP40 Protein Function Independently as Late Budding Domains: Involvement of Host Proteins TSG101 and VPS-4. *J. Virol.* **77**:1812-1819.
169. **Lötfering, B., E. Mühlberger, T. Tamura, H.-D. Klenk, and S. Becker.** 1999. The Nucleoprotein of Marburg Virus Is Target for Multiple Cellular Kinases. *Virology* **255**:50-62.
170. **Lupton, H. W.** 1981. Inactivation of Ebola Virus with ⁶⁰Co Irradiation. *J. Infect. Dis.* **143**:291.
171. **Malashkevich, V. N., B. J. Schneider, M. L. McNally, M. A. Milhollen, J. X. Pang, and P. S. Kim.** 1999. Core structure of the envelope glycoprotein GP2 from Ebola virus at 1.9-Å resolution. *Proc. Natl. Acad. Sci. USA* **96**:2662-2667.
172. **Manicassamy, B., J. Wang, H. Jiang, and L. Rong.** 2005. Comprehensive Analysis of Ebola Virus GP1 in Viral Entry. *J. Virol.* **79**:4793-4805.
173. **Manicassamy, B., J. Wang, E. Rumschlag, S. Tymen, V. Volchkova, V. Volchkov, and L. Rong.** 2007. Characterization of Marburg virus glycoprotein in viral entry. *Virology* **358**:79-88 [Epub Sep.19, 2006].

174. **Martin-Serrano, J., D. Perez-Caballero, and P. D. Bieniasz.** 2004. Context-Dependent Effects of L Domains and Ubiquitination on Viral Budding. *J. Virol.* **78**:5554-5563.
175. **Martin-Serrano, J., T. Zang, and P. D. Bieniasz.** 2001. HIV-1 and Ebola virus encode small peptide motifs that recruit Tsg101 to sites of particle assembly to facilitate egress. *Nat. Med.* **7**:1313-1319.
176. **Martini, G. A., H. G. Knauff, G. Baltzer, H. A. Schmidt, and F. H. Kreutz.** 1968. Das klinische Bild der Marburg-Virus-Krankheit, genannt „Marburger Affenkrankheit“. *Dtsch. Ärztebl.* **65**:1675-1680 [German].
177. **Maruyama, T., L. L. Rodriguez, P. B. Jahrling, A. Sanchez, A. S. Khan, S. T. Nichol, C. J. Peters, P. W. H. I. Parren, and D. R. Burton.** 1999. Ebola Virus Can Be Effectively Neutralized by Antibody Produced in Natural Human Infection. *J. Virol.* **73**:6024-6030.
178. **Marzi, A., T. Gramberg, G. Simmons, P. Möller, A. J. Rennekamp, M. Krumbiegel, M. Geier, J. Eisemann, N. Turza, B. Saunier, A. Steinkasserer, S. Becker, P. Bates, H. Hofmann, and S. Pöhlmann.** 2004. DC-SIGN and DC-SIGNR Interact with the Glycoprotein of Marburg Virus and the S Protein of Severe Acute Respiratory Syndrome Coronavirus. *J. Virol.* **78**:12090-12095.
179. **Mason, C.** 2008. The strains of Ebola. *Can. Med. J.* **178**:1266-1267.
180. **McCauley, S., and J. Hein.** 2006. Using hidden Markov models and observed evolution to annotate viral genomes. *Bioinformatics* **22**:1308-1316.
181. **McCormick, J. B., S. P. Bauer, L. H. Elliott, P. A. Webb, and K. M. Johnson.** 1983. Biologic Differences Between Strains of Ebola Virus from Zaire and Sudan. *J. Infect. Dis.* **147**:264-267.
182. **Means, R. E., T. Greenough, and R. C. Desrosiers.** 1997. Neutralization Sensitivity of Cell Culture-Passaged Simian Immunodeficiency Virus. *J. Virol.* **71**:7895-7902.
183. **Medina, M. F., G. P. Kobinger, J. Rux, M. Gasmi, D. J. Looney, P. Bates, and J. M. Wilson.** 2003. Lentiviral vectors pseudotyped with minimal filovirus envelopes increased gene transfer in murine lung. *Mol. Ther.* **8**:777-789 [Epub Sep. 13, 2003].
184. **Mikhailov, V. V., I. V. Borisevich, N. K. Chernikova, N. V. Potryvayeva, and V. P. Krasnyanskii.** 1994. The Evaluation in Hamadryas Baboons of the Possibility for the Specific Prevention of Ebola Fever. *Vopr. Virusol.* **39**:82-84 [Russian].
185. **Milleliri, J.-M., C. Tévi-Benissan, S. Baize, E. Leroy, and M.-C. Georges-Courbot.** 2004. Les épidémies de fièvre hémorragique due au virus Ebola au Gabon (1994 - 2002): Aspects épidémiologiques et réflexions sur les mesures de contrôle. *Bull. Soc. Pathol. Exot.* **97**:199-205 [French].
186. **Modis, Y., S. Ogata, D. Clements, and S. C. Harrison.** 2004. Structure of the dengue virus envelope protein after membrane fusion. *Nature* **427**:313-319.
187. **Modrof, J., S. Becker, and E. Mühlberger.** 2003. Ebola Virus Transcription Activator VP30 Is a Zinc-Binding Protein. *J. Virol.* **77**:3334-3338.

188. **Modrof, J., C. Möritz, L. Kolesnikova, T. Konakova, B. Hartlieb, A. Randolph, E. Mühlberger, and S. Becker.** 2001. Phosphorylation of Marburg Virus VP30 at Serines 40 and 42 Is Critical for Its Interaction with NP Inclusions. *Virology* **287**:171-182.
189. **Modrof, J., E. Mühlberger, H.-D. Klenk, and S. Becker.** 2002. Phosphorylation of VP30 impairs Ebola virus transcription. *J. Biol. Chem.* **277**:33099-33104 [Epub Jun. 6, 2002].
190. **Möller, P., N. Pariente, H.-D. Klenk, and S. Becker.** 2005. Homo-Oligomerization of Marburgvirus VP35 Is Essential for Its Function in Replication and Transcription. *J. Virol.* **79**:14876-14886.
191. **Monath, T. P.** 1999. Ecology of Marburg and Ebola Viruses: Speculations and Directions for Future Research. *J. Infect. Dis.* **179**(suppl. 1):S127-S138.
192. **Moore, M. J., T. Dorfman, W. Li, S. K. Wong, Y. Li, J. H. Kuhn, J. Coderre, N. Vasilieva, Z. Han, T. C. Greenough, M. Farzan, and H. Choe.** 2004. Retroviruses pseudotyped with the severe acute respiratory syndrome coronavirus spike protein efficiently infect cells expressing angiotensin-converting enzyme 2. *J. Virol.* **78**:10628-10635.
193. **Mpanju, O. M., J. S. Towner, J. E. Dover, S. T. Nichol, and C. A. Wilson.** 2006. Identification of two amino acid residues on Ebola virus glycoprotein 1 critical for cell entry. *Virus Res.* **121**:205-214 [Epub Jul. 12, 2006].
194. **Mühlberger, E., A. Sanchez, A. Randolph, C. Will, M. P. Kiley, H.-D. Klenk, and H. Feldmann.** 1992. The Nucleotide Sequence of the L Gene of Marburg Virus, a Filovirus: Homologies with Paramyxoviruses and Rhabdoviruses. *Virology* **187**:534-547.
195. **Mühlberger, E., M. Weik, V. E. Volchkov, H.-D. Klenk, and S. Becker.** 1999. Comparison of the Transcription and Replication Strategies of Marburg and Ebola Virus by Using Artificial Replication Systems. *J. Virol.* **73**:2333-2342.
196. **Murphy, F. A.** 1978. Pathology of Ebola Virus Infection, p. 43-59. *In* S. R. Pattyn (ed.), *Ebola Virus Haemorrhagic Fever*. Elsevier/North-Holland Biomedical Press, Amsterdam, The Netherlands.
197. **Nabeth, P., and Médecins Sans Frontières/Epicentre.** 1995. Intervention sur un cas de Fièvre Virale Hémorragique à Virus Ebola - Tabou, Côte d'Ivoire, Décembre 1995. Paris, France [French].
198. **National Institute of Allergy and Infectious Diseases.** 2008. NIAID Category A, B & C Priority Pathogens. http://www3.niaid.nih.gov/Biodefense/bandc_priority.htm.
199. **Negrete, O. A., E. L. Levroney, H. C. Aguilar, A. Bertolotti-Ciarlet, R. Nazarian, S. Tajyar, and B. Lee.** 2005. EphrinB2 is the entry receptor for Nipah virus, an emergent deadly paramyxovirus. *Nature* **436**:401-405.
200. **Neumann, G., H. Feldmann, S. Watanabe, I. Lukashevich, and Y. Kawaoka.** 2002. Reverse Genetics Demonstrates that Proteolytic Processing of the Ebola Virus Glycoprotein Is Not Essential for Replication in Cell Culture. *J. Virol.* **76**:406-410.

201. **Nikiforov, V. V., Yu. I. Turovskii, P. P. Kalinin, L. A. Akinfeyeva, L. R. Katkova, V. S. Barmin, Ye. I. Ryabchikova, N. I. Popkova, A. M. Shestopalov, V. P. Nazarov, S. V. Vedishchev, and S. V. Netyosov.** 1994. A case of Marburg virus laboratory infection. *Zh. Mikrobiol. Epidemiol. Immunobiol.* (3):104-106 [Russian].
202. **Nkoghe, D., P. Formenty, É. M. Leroy, S. Nnegue, S. Y. Obame Edou, J. Iba Ba, Y. Allarangar, J. Cabore, C. Bachy, R. Andraghetti, A. C. de Benoist, E. Galanis, A. Rose, D. Bausch, M. Reynolds, P. Rollin, C. Choueibou, R. Shongo, B. Gergonne, L. M. Koné, A. Yada, C. Roth, and M. Toung Mve.** 2005. Plusieurs épidémies de fièvre hémorragique à virus Ebola au Gabon, octobre 2001 à avril 2002. *Bull. Soc. Pathol. Exot.* 98:224-229 [French].
203. **Noda, T., H. Sagara, E. Suzuki, A. Takada, H. Kida, and Y. Kawaoka.** 2002. Ebola Virus VP40 Drives the Formation of Virus-Like Filamentous Particles Along with GP. *J. Virol.* 76:4855-4865.
204. **Ohshiro, Y., T. Murakami, K. Matsuda, K. Nishioka, K. Yoshida, and N. Yamamoto.** 1996. Role of Cell Surface Glycosaminoglycans of Human T Cells in Human Immunodeficiency Virus Type-1 (HIV-1) Infection. *Microbiol. Immunol.* 40:827-835.
205. **Okware, S. I., F. G. Omaswa, S. Zaramba, A. Opio, J. J. Lutwama, J. Kamugisha, E. B. Rwaguma, P. Kagwa, and M. Lamunu.** 2002. An outbreak of Ebola in Uganda. *Trop. Med. Int. Health* 7:1068-1075.
206. **Oswald, W. B., T. W. Geisbert, K. J. Davis, J. Geisbert, N. J. Sullivan, P. B. Jahrling, P. W. H. I. Parren, and D. R. Burton.** 2007. Neutralizing Antibody Fails to Impact the Course of Ebola Virus Infection in Monkeys. *PLoS Pathogens* 3:62-66 (article e9) [Epub Jan. 19, 2007].
207. **Panchal, R. G., G. Ruthel, T. A. Kenny, G. H. Kallstrom, D. Lane, S. S. Badie, L. Li, S. Bavari, and M. J. Aman.** 2003. *In vivo* oligomerization and raft localization of Ebola virus protein VP40 during vesicular budding. *Proc. Natl. Acad. Sci. USA* 100:15936-15941.
208. **Parren, P. W. H. I., T. W. Geisbert, T. Maruyama, P. B. Jahrling, and D. R. Burton.** 2002. Pre- and Postexposure Prophylaxis of Ebola Virus Infection in an Animal Model by Passive Transfer of a Neutralizing Human Antibody. *J. Virol.* 76:6408-6412.
209. **Pattyn, S. R., E. T. W. Bowen, and P. A. Webb.** 1985. Ebola, p. 379-380. *In* N. Karabatsos (ed.), *International Catalogue of Arboviruses 1985 Including Certain Other Viruses of Vertebrates*, 3rd ed. The American Society of Tropical Medicine and Hygiene, San Antonio, TX, USA.
210. **Peters, C. J., P. B. Jahrling, T. G. Ksiazek, E. D. Johnson, and H. Lupton.** 1992. Filovirus Contamination of Cell Cultures, p. 267-274, *Continues Cell Lines - An International Workshop on Current Issues*, Bethesda, MD, USA, 1991, vol. 76. S. Karger, Basel, Switzerland.
211. **Piot, P., P. Sureau, G. Breman, D. Heymann, V. Kintoki, M. Masamba, M. Mbuyi, M. Miatudila, F. Ruppel, S. van Nieuwenhove, M. K. White, G. van der**

- Groen, P. Webb, H. Wulff, and K. M. Johnson.** 1978. Clinical Aspects of Ebola Virus Infection in Yambuku Area, Zaire, 1976, p. 7-14. *In* S. R. Pattyn (ed.), Ebola Virus Haemorrhagic Fever. Elsevier/North-Holland Biomedical Press, Amsterdam, The Netherlands.
212. **Pletnev, S. V., W. Zhang, S. Mukhopadhyay, B. R. Fisher, R. Hernandez, D. T. Brown, T. S. Baker, M. G. Rossmann, and R. J. Kuhn.** 2001. Locations of carbohydrate sites on alphavirus glycoproteins show that E1 forms an icosahedral scaffold. *Cell* **105**:127-136.
213. **Pourrut, X., B. Kumulungui, T. Wittmann, G. Moussavou, A. Délicat, P. Yaba, D. Nkoghe, J.-P. Gonzalez, and E. M. Leroy.** 2005. The natural history of Ebola virus in Africa. *Microbes Infect.* **7**:1005-1014 [Epub May 16, 2005].
214. **Pringle, C. R.** 1997. The Order *Mononegavirales* - current status. *Arch. Virol.* **142**:2321-2326.
215. **Pringle, C. R., D. J. Alexander, M. A. Billeter, P. L. Collins, D. W. Kingsbury, M. A. Lipkind, Y. Nagai, C. Orvell, B. Rima, R. Rott, and V. ter Meulen.** 1991. The order *Mononegavirales*. *Arch. Virol.* **117**:137-140.
216. **Pringle, C. R., and A. J. Easton.** 1997. Monopartite Negative Strand RNA Genomes. *Semin. Virol.* **8**:49-57.
217. **Prinz, A.** 2005. Contributions to Visual Anthropology - Ethnomedical Background of the Ebola Epidemic 2004 in Yambio, South Sudan. *Viennese Ethnomed. Newsl.* **VII**:16-19.
218. **Prodromou, C., and L. H. Pearl.** 1992. Recursive PCR: a novel technique for total gene synthesis. *Protein Eng.* **5**:827-829.
219. **Radoshitzky, S. R., J. Abraham, C. F. Spiropoulou, J. H. Kuhn, D. Nguyen, W. Li, J. Nagel, P. J. Schmidt, J. H. Nunberg, N. C. Andrews, M. Farzan, and H. Choe.** 2007. Transferrin receptor 1 is a cellular receptor for New World haemorrhagic fever arenaviruses. *Nature* **446**:92-96 [Epub Feb. 7, 2007].
220. **Radoshitzky, S. R., J. H. Kuhn, C. F. Spiropoulou, C. G. Albarino, D. P. Nguyen, J. Salazar-Bravo, T. Dorfman, A. S. Lee, E. Wang, S. R. Ross, H. Choe, and M. Farzan.** 2008. Receptor determinants of zoonotic transmission of New World hemorrhagic fever arenaviruses. *Proc. Natl. Acad. Sci. USA* **105**:2664-2669 [Epub Feb. 11, 2008].
221. **Regnery, R. L., K. M. Johnson, and M. P. Kiley.** 1980. Virion Nucleic Acid of Ebola Virus. *J. Virol.* **36**:465-469.
222. **Reid, S. P., C. Valmas, O. Martinez, F. M. Sanchez, and C. F. Basler.** 2007. Ebola virus VP24 proteins inhibit the interaction of NPI-1 subfamily karyopherin α proteins with activated STAT1. *J. Virol.* **81**:13469-13477 [Epub Oct. 10, 2007].
223. **Reiter, P., M. Turell, R. Coleman, B. Miller, G. Maupin, J. Liz, A. Kuehne, J. Barth, J. Geisbert, D. Dohm, J. Glick, J. Pecor, R. Robbins, P. Jahrling, C. Peters, and T. Ksiazek.** 1999. Field Investigations of an Outbreak of Ebola Hemorrhagic Fever, Kikwit, Democratic Republic of the Congo, 1995: Arthropod Studies. *J. Infect. Dis.* **179**(suppl. 1):S148-S154.

224. **Richman, D. D., P. H. Cleveland, J. B. McCormick, and K. M. Johnson.** 1983. Antigenic Analysis of Strains of Ebola Virus: Identification of Two Ebola Virus Subtypes. *J. Infect. Dis.* **147**:268-271.
225. **Roche, S., S. Bressanelli, F. A. Rey, and Y. Gaudin.** 2006. Crystal structure of the low-pH form of the vesicular stomatitis virus glycoprotein G. *Science* **313**:187-191.
226. **Roche, S., F. A. Rey, Y. Gaudin, and S. Bressanelli.** 2007. Structure of the prefusion form of the vesicular stomatitis virus glycoprotein G. *Science* **315**:843-848.
227. **Rollin, P. E., R. J. Williams, D. L. Bressler, S. Pearson, M. Cottingham, G. Pucak, A. Sanchez, S. G. Trappier, R. L. Peters, P. W. Greer, S. Zaki, T. Demarcus, K. Hendricks, M. Kelley, D. Simpson, T. W. Geisbert, P. B. Jahrling, C. J. Peters, and T. G. Ksiazek.** 1999. Ebola (Subtype Reston) Virus among Quarantined Nonhuman Primates Recently Imported from the Philippines to the United States. *J. Infect. Dis.* **179(suppl. 1)**:S108-S114.
228. **Ruigrok, R. W. H., G. Schoehn, A. Dessen, E. Forest, V. Volchkov, O. Dolnik, H.-D. Klenk, and W. Weissenhorn.** 2000. Structural Characterization and Membrane Binding Properties of the Matrix Protein VP40 of Ebola virus. *J. Mol. Biol.* **300**:103-112.
229. **Ryabchikova, E., L. Kolesnikova, M. Smolina, V. Tkachev, L. Pereboeva, S. Baranova, A. Grazhdantseva, and Y. Rassadkin.** 1996. Ebola virus infection in guinea pigs: presumable role of granulomatous inflammation in pathogenesis. *Arch. Virol.* **141**:909-921.
230. **Ryabchikova, E. I., L. V. Kolesnikova, and S. V. Netesov.** 1999. Animal Pathology of Filovirus Infections, p. 145-173. *In* H.-D. Klenk (ed.), *Marburg and Ebola Viruses*, vol. 235. Springer-Verlag, Berlin, Germany.
231. **Ryabchikova, E. I., and B. B. S. Price.** 2004. Ebola and Marburg Viruses - A View of Infection Using Electron Microscopy. Battelle Press, Columbus, OH, USA.
232. **Sanchez, A.** 2007. Analysis of filovirus entry into vero e6 cells, using inhibitors of endocytosis, endosomal acidification, structural integrity, and cathepsin (B and L) activity. *J. Infect. Dis.* **196(suppl. 2)**:S251-S258.
233. **Sanchez, A., and M. P. Kiley.** 1987. Identification and Analysis of Ebola Virus Messenger RNA. *Virology* **157**:414-420.
234. **Sanchez, A., M. P. Kiley, B. P. Holloway, and D. D. Auperin.** 1993. Sequence analysis of the Ebola virus genome: organization, genetic elements, and comparison with the genome of Marburg virus. *Virus Res.* **29**:215-240.
235. **Sanchez, A., M. P. Kiley, B. P. Holloway, J. B. McCormick, and D. D. Auperin.** 1989. The Nucleoprotein Gene of Ebola Virus: Cloning, Sequencing, and *in Vitro* Expression. *Virology* **170**:81-91.
236. **Sanchez, A., M. P. Kiley, H.-D. Klenk, and H. Feldmann.** 1992. Sequence analysis of the Marburg virus nucleoprotein gene: comparison to Ebola virus and other non-segmented negative-stranded RNA viruses. *J. Gen. Virol.* **73**:347-357.
237. **Sanchez, A., S. G. Trappier, B. W. J. Mahy, C. J. Peters, and S. T. Nichol.** 1996. The virion glycoproteins of Ebola viruses are encoded in two reading frames

- and are expressed through transcriptional editing. *Proc. Natl. Acad. Sci. USA* **93**:3602-3607.
238. **Sanchez, A., S. G. Trappier, U. Ströher, S. T. Nichol, M. D. Bowen, and H. Feldmann.** 1998. Variation in the Glycoprotein and VP35 Genes of Marburg Virus Strains. *Virology* **240**:138-146.
239. **Sänger, C., E. Mühlberger, B. Lötfering, H.-D. Klenk, and S. Becker.** 2002. The Marburg Virus Surface Protein GP Is Phosphorylated at Its Ectodomain. *Virology* **295**:20-29.
240. **Schorner, K., S. Matsuyama, K. Kabsch, S. Delos, A. Bouton, and J. White.** 2006. Role of Endosomal Cathepsins in Entry Mediated by the Ebola Virus Glycoprotein. *J. Virol.* **80**:4174-4178.
241. **Scianimanico, S., G. Schoehn, J. Timmins, R. H. W. Ruigrok, H.-D. Klenk, and W. Weissenhorn.** 2000. Membrane association induces a conformational change in the Ebola virus matrix protein. *EMBO J.* **19**:6732-6741.
242. **Shimojima, M., Y. Ikeda, and Y. Kawaoka.** 2007. The mechanism of Axl-mediated Ebola virus infection. *J. Infect. Dis.* **196(suppl. 2)**:S259-S263.
243. **Shimojima, M., A. Takada, H. Ebihara, G. Neumann, K. Fujioka, T. Irimura, S. Jones, H. Feldmann, and Y. Kawaoka.** 2006. Tyro3 Family-Mediated Cell Entry of Ebola and Marburg Viruses. *J. Virol.* **80**:10109-10116.
244. **Sieczkarski, S. B., and G. R. Whittaker.** 2002. Dissecting virus entry via endocytosis. *J. Gen. Virol.* **83**:1535-1545.
245. **Siegert, R., H.-L. Shu, W. Slenczka, D. Peters, and G. Müller.** 1967. Zur Ätiologie einer unbekanntenen, von Affen ausgegangenen menschlichen Infektionskrankheit. *Dtsch. Med. Wochenschr.* **92**:2341-2343 [German].
246. **Siegert, R., and D. I. H. Simpson.** 1985. Marburg, p. 659-660. *In* N. Karabatsos (ed.), *International Catalogue of Arboviruses 1985 Including Certain Other Viruses of Vertebrates*, 3rd ed. The American Society of Tropical Medicine and Hygiene, San Antonio, TX, USA.
247. **Simmons, G., J. D. Reeves, C. C. Grogan, L. H. Vandenberg, F. Baribaud, J. C. Whitbeck, E. Burke, M. J. Buchmeier, E. J. Soilleux, J. L. Riley, R. W. Doms, P. Bates, and S. Pöhlmann.** 2003. DC-SIGN and DC-SIGNR Bind Ebola Glycoproteins and Enhance Infection of Macrophages and Endothelial Cells. *Virology* **305**:115-123 [Epub Dec. 19, 2002].
248. **Simmons, G., A. J. Rennekamp, N. Chai, L. H. Vandenberg, J. L. Riley, and P. Bates.** 2003. Folate Receptor Alpha and Caveolae Are Not Required for Ebola Virus Glycoprotein-Mediated Viral Infection. *J. Virol.* **77**:13433-13438.
249. **Sinn, P. L., M. A. Hickey, P. D. Staber, D. E. Dylla, S. A. Jeffers, B. L. Davidson, D. A. Sanders, and P. B. McCray, Jr.** 2003. Lentivirus Vectors Pseudotyped with Filoviral Envelope Glycoproteins Transduce Airway Epithelia from the Apical Surface Independently of Folate Receptor Alpha. *J. Virol.* **77**:5902-5910.
250. **Slenczka, W., and D. Peters.** 1977. Ebola-Virus, ein neuer Vertreter der Marburg-Virus-Gruppe. *Tropenmed. Parasitol.* **28**:260 [German].

251. **Smith, D. H., B. K. Johnson, M. Isaacson, R. Swanepoel, K. M. Johnson, M. Killey, A. Bagshawe, Tarap Siongok, and W. Koinange Keruga.** 1982. Marburg-Virus Disease in Kenya. *Lancet* **i**:816-820.
252. **Smorodintsev, A. A., L. I. Kazbintsev, and V. G. Chudakov.** 1963. Virus Hemorrhagic Fevers. Gosudarstvennoe Izdatelstvo Meditsinskoi Literatury, Leningrad, Leningrad Region, USSR [Russian].
253. **Sokol, D. K.** 2002. From Anonymity to Notoriety. Historical Problems Associated With Outbreaks of Emerging Infectious Diseases; A Case Study: Ebola Haemorrhagic Fever. Master of Science Thesis in Social and Economic History. Open University, Walton Hall, Milton Keynes, United Kingdom.
254. **Stille, W., E. Böhle, E. Helm, W. van Rey, and W. Siede.** 1968. Über eine durch Cercopithecus aethiops übertragene Infektionskrankheit („Grüne-Meerkatzen-Krankheit“, „Green Monkey Disease“). *Dtsch. Med. Wochenschr.* **93**:572-582 [German].
255. **Ströher, U., and H. Feldmann.** 2006. Progress towards the treatment of Ebola haemorrhagic fever. *Expert Opin. Invest. Drugs* **15**:1523-1535.
256. **Sullivan, N. J., T. W. Geisbert, J. B. Geisbert, L. Xu, Z.-Y. Yang, M. Roederer, R. A. Koup, P. B. Jahrling, and G. J. Nabel.** 2003. Accelerated vaccination for Ebola virus haemorrhagic fever in non-human primates. *Nature* **424**:681-684.
257. **Sullivan, N. J., A. Sanchez, P. E. Rollin, Z.-Y. Yang, and G. J. Nabel.** 2000. Development of a preventive vaccine for Ebola virus infection in primates. *Nature* **408**:605-609.
258. **Sureau, P. H.** 1989. Firsthand Clinical Observations of Hemorrhagic Manifestations in Ebola Hemorrhagic Fever in Zaire. *Rev. Infect. Dis.* **11(suppl. 4)**:S790-S793.
259. **Swanepoel, R., P. A. Leman, F. J. Burt, N. A. Zachariades, L. E. O. Braack, T. G. Ksiazek, P. E. Rollin, S. R. Zaki, and C. J. Peters.** 1996. Experimental Inoculation of Plants and Animals with Ebola Virus. *Emerg. Infect. Dis.* **2**:321-325.
260. **Swenson, D. L., K. L. Warfield, K. Kuehl, T. Larsen, M. C. Hevey, A. Schmaljohn, S. Bavari, and M. J. Aman.** 2004. Generation of Marburg virus-like particles by co-expression of glycoprotein and matrix protein. *FEMS Immunol. Med. Microbiol.* **40**:27-31 [Epub Oct. 3, 2003].
261. **Takada, A., K. Fujioka, M. Tsuiji, A. Morikawa, N. Higashi, H. Ebihara, D. Kobasa, H. Feldmann, T. Irimura, and Y. Kawaoka.** 2004. Human Macrophage C-Type Lectin Specific for Galactose and N-Acetylgalactosamine Promotes Filovirus Entry. *J. Virol.* **78**:2943-2947.
262. **Takada, A., C. Robison, H. Goto, A. Sanchez, K. G. Murti, M. A. Whitt, and Y. Kawaoka.** 1997. A system for functional analysis of Ebola virus glycoprotein. *Proc. Natl. Acad. Sci. USA* **94**:14764-14769.
263. **Takada, A., S. Watanabe, H. Ito, K. Okazaki, H. Kida, and Y. Kawaoka.** 2000. Downregulation of β 1 Integrins by Ebola Virus Glycoprotein: Implication for Virus Entry. *Virology* **278**:20-26.

264. **Thill, M., and H. Tolou.** 2004. Fièvre Hémorragique à Virus Ebola : Nouvel Opus Meurtrier au Soudan. *Méd. Trop.* **64**:331-333 [French].
265. **Timmins, J., G. Schoehn, C. Kohlhaas, H.-D. Klenk, R. W. H. Ruigrok, and W. Weissenhorn.** 2003. Oligomerization and polymerization of the filovirus matrix protein VP40. *Virology* **312**:359-368 [Epub Jun. 20, 2003].
266. **Timmins, J., G. Schoehn, S. Ricard-Blum, S. Scianimanico, T. Vernet, R. W. H. Ruigrok, and W. Weissenhorn.** 2003. Ebola Virus Matrix Protein VP40 Interaction with Human Cellular Factors Tsg101 and Nedd4. *J. Mol. Biol.* **326**:493-502 [Epub Jan. 23, 2003].
267. **Titenko, A. M., Ye. I. Andayev, and T. I. Borisova.** 2001. Dynamics of Marburg and Ebola virus antigen expression in infected Vero cells. *Vopr. Virusol.* **46**:43-45 [Russian].
268. **Todorović, K., M. Mocić, R. Klačnja, L. Stojković, M. Bordjoški, A. Gligić, and Ž. Stefanović.** 1969. An Unknown Virus Disease Transmitted From Infected Green-Monkeys to Men. *Glas Srp. Akad. Nauka Umetn. Odelj. Med. Nauka CCLXXV*:91-101 [Serbo-Croatian].
269. **Towner, J. S., M. L. Khristova, T. K. Sealy, M. J. Vincent, B. R. Erickson, D. A. Bawiec, A. L. Hartman, J. A. Comer, S. R. Zaki, U. Ströher, F. Gomes da Silva, F. del Castillo, P. E. Rollin, T. G. Ksiazek, and S. N. Nichol.** 2006. Marburgvirus Genomics and Association with a Large Hemorrhagic Fever Outbreak in Angola. *J. Virol.* **80**:6497-6516.
270. **Towner, J. S., J. Paragas, J. E. Dover, M. Gupta, C. S. Goldsmith, J. W. Huggins, and S. T. Nichol.** 2005. Generation of eGFP expressing recombinant Zaire ebolavirus for analysis of early pathogenesis events and high-throughput antiviral drug screening. *Virology* **332**:20-27 [Epub Dec. 9, 2004].
271. **Towner, J. S., X. Pourrut, C. G. Albariño, C. N. Nkogue, B. H. Bird, G. Grard, T. G. Ksiazek, J.-P. Gonzalez, S. T. Nichol, and E. M. Leroy.** 2007. Marburg Virus Infection Detected in a Common African Bat. *PLoS One* **2**:article e764 [Epub Aug. 22, 2007] <http://www.plosone.org>.
272. **Towner, J. S., P. E. Rollin, D. G. Bausch, A. Sanchez, S. M. Crary, M. Vincent, W. F. Lee, C. F. Spiropoulou, T. G. Ksiazek, M. Lukwiya, F. Kaducu, R. Downing, and S. N. Nichol.** 2004. Rapid Diagnosis of Ebola Hemorrhagic Fever by Reverse Transcription-PCR in an Outbreak Setting and Assessment of Patient Viral Load as a Predictor of Outcome. *J. Virol.* **78**:4330-4341.
273. **Tshomba Oloma, A.** 2005. Prédiction clinique de fièvre hémorragique de Marburg dans l'épidémie de Watsa. Master's of Science thesis. Prins Leopold Instituut voor Tropische Geneeskunde, Antwerp, Belgium [French].
274. **Urata, S., T. Noda, Y. Kawaoka, S. Morikawa, H. Yokosawa, and J. Yasuda.** 2007. Tsg101 interacts with Marburg VP40 depending on the PPPY motif, but not the PT/SAP motif as for Ebola virus, and plays a critical role in the budding of Marburg virus-like particles induced by VP40, NP, and GP. *J. Virol.* **81**:4895-4899 [Epub Feb. 14, 2007].

275. **US Department of Health and Human Services, Centers for Disease Control and Prevention, and National Institutes of Health.** 2007. Biosafety in Microbiological and Biomedical Laboratories (BMBL), 5th ed. HHS Publication No. (CDC) 93-8395, US Government Printing Office, Washington, DC, USA.
276. **van der Groen, G.** 1978. Growth of Lassa and Ebola Viruses in Different Cell Lines, p. 255-260. *In* S. R. Pattyn (ed.), Ebola Virus Haemorrhagic Fever. Elsevier/North-Holland Biomedical Press, Amsterdam, The Netherlands.
277. **van der Groen, G., and L. H. Elliot [sic].** 1982. Lack of Cross Reactivity of Rhabdovirus Antibodies With Marburg and Ebola Antigens in The Indirect Immunofluorescent Antibody Test. *Ann. Soc. Belge Méd. Trop.* **62**:67-68.
278. **Volchkov, V., V. Volchkova, O. Dolnik, H. Feldmann, and H.-D. Klenk.** 2004. Structural and Functional Polymorphism of the Glycoproteins of Filoviruses, p. 59-89. *In* H.-D. Klenk and H. Feldmann (ed.), Ebola and Marburg Viruses - Molecular and Cellular Biology. Horizon Bioscience, Wymondham, Norfolk, United Kingdom.
279. **Volchkov, V. E., S. Becker, V. A. Volchkova, V. A. Ternovoj, A. N. Kotov, S. V. Netesov, and H.-D. Klenk.** 1995. GP mRNA of Ebola Virus is Edited by the Ebola Virus Polymerase and by T7 and Vaccinia Virus Polymerase. *Virology* **214**:421-430.
280. **Volchkov, V. E., A. A. Chepurinov, V. A. Volchkova, V. A. Ternovoj, and H.-D. Klenk.** 2000. Molecular Characterization of Guinea Pig-Adapted Variants of Ebola Virus. *Virology* **277**:147-155.
281. **Volchkov, V. E., and H. Feldmann.** 2002. Expression Strategy and Functions of the Filoviral Glycoproteins, p. 225-252. *In* A. Holzenburg and E. Bogner (ed.), Structure-Function Relationships of Human Pathogenic Viruses. Kluwer Academic/Plenum Publishers, London, United Kingdom.
282. **Volchkov, V. E., H. Feldmann, V. E. Volchkova, and H.-D. Klenk.** 1998. Processing of the Ebola virus glycoprotein by the proprotein convertase furin. *Proc. Natl. Acad. Sci. USA* **95**:5762-5767.
283. **Volchkov, V. E., V. A. Volchkova, A. A. Chepurinov, V. M. Blinov, O. Dolnik, S. V. Netesov, and H. Feldmann.** 1999. Characterization of the L gene and 5' trailer region of Ebola virus. *J. Gen. Virol.* **80**:355-362.
284. **Volchkov, V. E., V. A. Volchkova, E. Mühlberger, L. V. Kolesnikova, M. Weik, O. Dolnik, and H.-D. Klenk.** 2001. Recovery of Infectious Ebola Virus from Complementary DNA: RNA Editing of the GP Gene and Viral Cytotoxicity. *Science* **291**:1965-1969.
285. **Volchkov, V. E., V. A. Volchkova, U. Ströher, S. Becker, O. Dolnik, M. Cieplik, W. Garten, H.-D. Klenk, and H. Feldmann.** 2000. Proteolytic Processing of Marburg Virus Glycoprotein. *Virology* **268**:1-6.
286. **Volchkova, V. A., H. Feldmann, H.-D. Klenk, and V. E. Volchkov.** 1998. The Nonstructural Small Glycoprotein sGP of Ebola Virus is Secreted as an Antiparallel-Oriented Homodimer. *Virology* **250**:408-414.

287. **Volchkova, V. A., H.-D. Klenk, and V. E. Volchkov.** 1999. Delta-Peptide Is the Carboxy-Terminal Cleavage Fragment of the Nonstructural Small Glycoprotein sGP of Ebola Virus. *Virology* **265**:164-171.
288. **Wahl-Jensen, V., T. A. Afanasieva, J. Seebach, U. Ströher, H. Feldmann, and H.-J. Schnittler.** 2005. Effects of Ebola Virus Glycoproteins on Endothelial Cell Activation and Barrier Function. *J. Virol.* **79**:10442-10450.
289. **Wahl-Jensen, V., S. K. Kurz, P. R. Hazelton, H.-J. Schnittler, U. Ströher, D. R. Burton, and H. Feldmann.** 2005. Role of Ebola Virus Secreted Glycoproteins and Virus-Like Particles in Activation of Human Macrophages. *J. Virol.* **79**:2413-2419.
290. **Warfield, K. L., D. A. Alves, S. B. Bradfute, D. K. Reed, S. VanTongeren, W. V. Kalina, G. G. Olinger, and S. Bavari.** 2007. Development of a model for marburgvirus based on severe-combined immunodeficiency mice. *Viol. J.* **4**:article 108 [Epub Oct. 27, 2007] <http://www.virologyj.com>.
291. **Warfield, K. L., C. M. Bosio, B. C. Welcher, E. M. Deal, M. Mohamadzadeh, A. Schmaljohn, M. J. Aman, and S. Bavari.** 2003. Ebola virus-like particles protect from lethal Ebola virus infection. *Proc. Natl. Acad. Sci. USA* **100**:15889-15894.
292. **Warfield, K. L., G. Olinger, E. M. Deal, D. L. Swenson, M. Bailey, D. L. Negley, M. K. Hart, and S. Bavari.** 2005. Induction of Humoral and CD8⁺ T Cell Responses Are Required for Protection against Lethal Ebola Virus Infection. *J. Immunol.* **175**:1184-1191.
293. **Warfield, K. L., D. L. Swenson, G. Demmin, and S. Bavari.** 2005. Filovirus-like particles as vaccines and discovery tools. *Expert Rev. Vaccines* **4**:429-440.
294. **Warfield, K. L., D. L. Swenson, D. L. Negley, A. Schmaljohn, M. J. Aman, and S. Bavari.** 2004. Marburg virus-like particles protect guinea pigs from lethal Marburg virus infection. *Vaccine* **22**:3495-3502 [Epub Mar. 4, 2004].
295. **Warfield, K. L., D. L. Swenson, G. G. Olinger, W. V. Kalina, M. J. Aman, and S. Bavari.** 2007. Ebola virus-like particle-based vaccine protects nonhuman primates against lethal Ebola virus challenge. *J. Infect. Dis.* **196(suppl. 2)**:S430-S437.
296. **Warfield, K. L., D. L. Swenson, G. G. Olinger, D. K. Nichols, W. D. Pratt, R. Blouch, D. A. Stein, M. J. Aman, P. L. Iversen, and S. Bavari.** 2006. Gene-Specific Countermeasures Against Ebola Virus Based on Antisense Phosphorodiamidate Morpholino Oligomers *PLoS Pathogens* **2**:5-13 (article e1) [Epub Jan. 13, 2006].
297. **Weik, M., J. Modrof, H.-D. Klenk, S. Becker, and E. Mühlberger.** 2002. Ebola Virus VP30-Mediated Transcription Is Regulated by RNA Secondary Structure Formation. *J. Virol.* **76**:8532-8539.
298. **Weissenhorn, W.** 2004. Structure of Viral Proteins, p. 27- 57. *In* H.-D. Klenk and H. Feldmann (ed.), *Ebola and Marburg Viruses - Molecular and Cellular Biology*. Horizon Bioscience, Wymondham, Norfolk, United Kingdom.
299. **Weissenhorn, W., L. J. Calder, S. A. Wharton, J. J. Skehel, and D. C. Wiley.** 1998. The central structural feature of the membrane fusion protein subunit from the

- Ebola virus glycoprotein is a long triple-stranded coiled coil. *Proc. Natl. Acad. Sci. USA* **95**:6032-6036.
300. **Weissenhorn, W., A. Carfi, K.-H. Lee, J. J. Skehel, and D. C. Wiley.** 1998. Crystal Structure of the Ebola Virus Membrane Fusion Subunit, GP2, from the Envelope Glycoprotein Ectodomain. *Mol. Cell* **2**:605-616.
301. **White, J. M., S. E. Delos, M. Brecher, and K. L. Schornberg.** 2008. Structures and Mechanisms of Viral Membrane Fusion Proteins: Multiple Variations on a Common Theme. *Crit. Rev. Biochem. Mol. Biol.* **43**:189-219.
302. **Wilson, J. A., M. Bray, R. Bakken, and M. K. Hart.** 2001. Vaccine Potential of Ebola Virus VP24, VP30, VP35, and VP40 Proteins. *Virology* **286**:384-390.
303. **Wilson, J. A., M. Hevey, R. Bakken, S. Guest, M. Bray, A. L. Schmaljohn, and M. K. Hart.** 2000. Epitopes Involved in Antibody-Mediated Protection from Ebola Virus. *Science* **287**:1664-1666.
304. **Wong, S. K., W. Li, M. J. Moore, H. Choe, and M. Farzan.** 2004. A 193-amino acid fragment of the SARS coronavirus S protein efficiently binds angiotensin-converting enzyme 2. *J. Biol. Chem.* **279**:3197-3201.
305. **Wool-Lewis, R. J., and P. Bates.** 1998. Characterization of Ebola Virus Entry by Using Pseudotyped Viruses: Identification of Receptor-Deficient Cell-Lines. *J. Virol.* **72**:3155-3160.
306. **Wool-Lewis, R. J., and P. Bates.** 1999. Endoproteolytic Processing of the Ebola Virus Envelope Glycoprotein: Cleavage is Not Required for Function. *J. Virol.* **73**:1419-1426.
307. **World Health Organization - Regional Office for Africa.** 1996. Ebola Viral Haemorrhagic Fever Epidemic (VHF). Final Report. Kikwit (Bandundu), Zaire, 1995. Brazzaville, Congo (Brazzaville).
308. **World Health Organization.** 1978. Ebola haemorrhagic fever in Sudan, 1976. Report of a WHO/International Study Team. *Bull. WHO* **56**:247-270.
309. **World Health Organization.** 1978. Ebola haemorrhagic fever in Zaire, 1976. Report of an International Commission. *Bull. WHO* **56**:271-293.
310. **World Health Organization.** 2005. Ebola haemorrhagic fever, Congo. *Wkly. Epidemiol. Rec.* **80**:178.
311. **World Health Organization.** 2005. Marburg haemorrhagic fever, Angola - update. *Wkly. Epidemiol. Rec.* **80**:298.
312. **World Health Organization.** 2007. Marburg haemorrhagic fever, Uganda. *Wkly. Epidemiol. Rec.* **82**:297-298.
313. **World Health Organization.** 2005. Marburg virus disease, Angola. *Wkly. Epidemiol. Rec.* **80**:115-117.
314. **Xu, Y., Z. Lou, Y. Liu, H. Pang, P. Tien, G. F. Gao, and Z. Rao.** 2004. Crystal structure of severe acute respiratory syndrome coronavirus spike protein fusion core. *J. Biol. Chem.* **279**:49414-49419.
315. **Yang, Z.-Y., H. J. Duckers, N. J. Sullivan, A. Sanchez, E. G. Nabel, and G. J. Nabel.** 2000. Identification of the Ebola virus glycoprotein as the main viral determinant of vascular cell cytotoxicity and injury. *Nat. Med.* **6**:886-889.

316. **Yasuda, J., M. Nakao, Y. Kawaoka, and H. Shida.** 2003. Nedd4 Regulates Egress of Ebola Virus-Like Particles from Host Cells. *J. Virol.* **77**:9987-9992.
317. **Yin, H. S., R. G. Paterson, X. Wen, R. A. Lamb, and T. S. Jardetzky.** 2005. Structure of the uncleaved ectodomain of the paramyxovirus (hPIV3) fusion protein. *Proc. Natl. Acad. Sci. USA* **102**:9288-9293.
318. **Yonezawa, A., M. Cavrois, and W. C. Greene.** 2005. Studies of Ebola Virus Glycoprotein-Mediated Entry and Fusion by Using Pseudotyped Human Immunodeficiency Virus Type 1 Virions: Involvement of Cytoskeletal Proteins and Enhancement by Tumor Necrosis Factor Alpha. *J. Virol.* **79**:918-926.
319. **Zhang, Y., W. Zhang, S. Ogata, D. Clements, J. H. Strauss, T. S. Baker, R. J. Kuhn, and M. G. Rossmann.** 2004. Conformational changes of the flavivirus E glycoprotein. *Structure* **12**:1607-1618.

11 PUBLICATIONS AND PRESENTATIONS

The following publications and presentations were either directly connected to the research described in this dissertation (filovirus-related studies) or were supported by the dissertation's author by methods, tools, and insights stemming from this research.

First author publications

- 1) **Kuhn, Jens H., Kelly L. Warfield, Sheli R. Radoshitzky, Dana Swenson, Gene G. Olinger, Sina Bavari, Michael Farzan, and M. Javad Aman.** Both Lake Victoria Marburgvirus and Zaire ebolavirus GP₁ Receptor-binding Domains Cross-Protect Against Challenge with Homologous and Heterologous Filoviruses in a Lethal Mouse Model. In preparation.
- 2) **Kuhn, Jens H., Sheli R. Radoshitzky, Kelly L. Warfield, John Misasi, Marc A. Hogenbirk, Phil Kranzusch, Sina Bavari, James M. Cunningham, M. Javad Aman, and Michael Farzan.** Modulation of Filovirus Cell Entry by Ebolaviral Δ -Peptides. In preparation.
- 3) **Kuhn, Jens H., Sheli R. Radoshitzky, Alexander C. Guth, Kelly L. Warfield, Wenhui Li, Martin J. Vincent, Jonathan S. Towner, Stuart T. Nichol, Sina Bavari, Hyeryun Choe, M. Javad Aman, and Michael Farzan.** 2006. Conserved Receptor-binding Domains of Lake Victoria Marburgvirus and Zaire Ebolavirus Bind a Common Receptor. *The Journal of Biological Chemistry* **281(23)**:15951-15959 [Epub April 4, 2006].

Coauthored publications

- 1) **Dube, Derek, Matthew Brecher, Sean Rose, Kathryn L. Schornberg, Edward Park, Jens H. Kuhn, Sue Delos, and Judith M. White.** The Primed ('19kDa') Ebola Virus Glycoprotein: Identification of Sequence and Residues Critical for Host Cell Binding. Submitted.

- 2) **Radoshitzky, Sheli R., Jens H. Kuhn, Christina F. Spiropoulou, César G. Albariño, Dan P. Nguyen, Jorge Salazar-Bravo, Tatyana Dorfman, Amy S. Lee, Enxiu Wang, Susan R. Ross, Hyeryun Choe, and Michael Farzan.** 2008. Receptor determinants of zoonotic transmission of New World hemorrhagic fever arenaviruses. *PNAS – Proceedings of the National Academy of Sciences of the United States of America* **105(7)**:2664-2669 [Epub February 11, 2008].
- 3) **Li, Wenhui, Jianhua Sui, I-Chueh Huang, Jens H. Kuhn, Sheli R. Radoshitzky, Wayne A. Marasco, Hyeryun Choe, and Michael Farzan.** 2007. The S proteins of human coronavirus NL63 and severe acute respiratory syndrome coronavirus bind overlapping regions of ACE2. *Virology* **367(2)**:367-374 [Epub July 12, 2007].
- 4) **Radoshitzky, Sheli R., Jonathan Abraham, Christina F. Spiropoulou, Jens H. Kuhn, Dan Nguyen, Wenhui Li, Jane Nagel, Paul J. Schmidt, Jack H. Nunberg, Nancy C. Andrews, Michael Farzan, and Hyeryun Choe.** 2007. Transferrin receptor 1 is a cellular receptor for New World haemorrhagic fever arenaviruses. *Nature* **446(7131)**:92-96 [Epub February 7, 2007].
- 5) **Li, Wenhui, Chengsheng Zhang, Jianhua Sui, Jens H. Kuhn, Michael J. Moore, Shiwen Luo, Swee-Kee Wong, I-Chueh Huang, Keming Xu, Natalya Vasilieva, Akikazu Murakami, Yaqing He, Wayne A. Marasco, Yi Guan, Hyeryun Choe, and Michael Farzan.** 2005. Receptor and viral determinants of SARS-coronavirus adaptation to human ACE2. *The EMBO Journal* **24(8)**:1634-1643 [Epub March 24, 2005].
- 6) **Moore, Michael J., Tatyana Dorfman, Wenhui Li, Swee Kee Wong, Yanhan Li, Jens H. Kuhn, James Coderre, Natalya Vasilieva, Zhongchao Han, Thomas C. Greenough, Michael Farzan, and Hyeryun Choe.** 2004. Retroviruses Pseudotyped with the Severe Acute Respiratory Syndrome Coronavirus Spike Protein Efficiently Infect Cells Expressing Angiotensin-Converting Enzyme 2. *Journal of Virology* **78(19)**:10628-10635.

Reviews

- 1) **Kuhn, Jens H., Wenhui Li, Sheli R. Radoshitzky, Hyeryun Choe, and Michael Farzan.** 2007. Severe acute respiratory syndrome coronavirus entry as a target of antiviral therapies. *Antiviral Therapy* **12(4 Pt. B)**: 639-650.
- 2) **Li, Wenhui, Swee-Kee Wong, Fang Li, Jens H. Kuhn, I-Chueh Huang, Hyeryun Choe, and Michael Farzan.** 2006. Animal Origins of the Severe Acute Respiratory Syndrome Coronavirus: Insight from ACE2-S-Protein Interactions. *Journal of Virology* **80(9)**: 4211-4219.
- 3) **Kuhn, J. H., S. R. Radoshitzky, W. Li, S. Kee Wong, H. Choe, and M. Farzan.** 2006. The SARS Coronavirus Receptor ACE2 – A Potential Target for Antiviral Therapy, pp. 397-418 (chapter 3.1). *In* Bogner, Elke, and Andreas Holzenburg (eds.), *New Concepts of Antiviral Therapy*, Springer, Dordrecht, The Netherlands.
- 4) **Kuhn, J. H., W. Li, H. Choe, and M. Farzan.** 2004. Angiotensin-converting enzyme 2: a functional receptor for SARS coronavirus. *CMLS – Cellular and Molecular Life Sciences* **61(11)**:2738-2743.

Patents

- 1) **Kuhn, Jens H., Sheli R. Radoshitzky, and Michael R. Farzan.** 2006. Broad-Spectrum Filovirus Vaccine and Related Proteins, Nucleic Acids, Compositions, and Methods. Provisional patent, applied for.

Conference abstracts

- 1) **Kuhn, Jens H., Kelly L. Warfield, Sheli R. Radoshitzky, Dana Swenson, Gene G. Olinger, Sina Bavari, Michael Farzan, and M. Javad Aman.** 2008. Filoviral Receptor-Binding Domains are Promising Subunit Vaccine Candidates, p. 254 (abstract VP-129). *In* Abstracts Book of the XIV. International Congress of Virology, August 10-15, Istanbul, Turkey.

- 2) **Radoshitzky, Sheli R., Jens H. Kuhn, Christina F. Spiropoulou, César Albariño, Jorge Salazar-Bravo, Tatyana Dorfman, Amy S. Lee, Enxiu Wang, Susan R. Ross, Hyeryun Choe, and Michael Farzan.** 2008. RECEPTOR Determinants of Zoonotic Transmission of New World Hemorrhagic Fever Arenaviruses, p. 86 (abstract VOP-136). *In* Abstracts Book of the XIV. International Congress of Virology, August 10-15, Istanbul, Turkey.
- 3) **Kuhn, Jens H., Kelly L. Warfield, Sheli R. Radoshitzky, Dana Swenson, Gene G. Olinger, Sina Bavari, Michael Farzan, and M. Javad Aman.** 2008. Filoviral Receptor-Binding Domains are Promising Subunit Vaccine Candidates, p. 280 (abstract P21-1). *In* Scientific Program & Abstracts of the 27th Annual Meeting of the American Society for Virology, July 12-16, Ithaca, NY, USA.
- 4) **Radoshitzky, Sheli R., Jens H. Kuhn, Christina F. Spiropoulou, César Albariño, Jorge Salazar-Bravo, Tatyana Dorfman, Amy S. Lee, Enxiu Wang, Susan R. Ross, Hyeryun Choe, and Michael Farzan.** 2008. Receptor Determinants of Zoonotic Transmission of New World Hemorrhagic Fever Arenaviruses, p. 86 (abstract W7-2). *In* Scientific Program & Abstracts of the 27th Annual Meeting of the American Society for Virology, July 12-16, Ithaca, NY, USA.
- 5) **Radoshitzky, Sheli R., Jens H. Kuhn, Christina F. Spiropoulou, César Albariño, Jorge Salazar-Bravo, Tatyana Dorfman, Amy S. Lee, Enxiu Wang, Susan R. Ross, Hyeryun Choe, and Michael Farzan.** 2008. Receptor Determinants of Zoonotic Transmission of New World Hemorrhagic Fever Arenaviruses, p. 77 (abstract 307). *In* Abstract Book of the Keystone Symposia on Molecular and Cellular Biology “Cell Biology of Virus Entry, Replication and Pathogenesis”, April 14-18, Victoria, British Columbia, Canada.
- 6) **Kuhn, Jens H., Kelly L. Warfield, Sheli R. Radoshitzky, Dana Swenson, Gene G. Olinger, Sina Bavari, Michael Farzan, and M. Javad Aman.** 2007. Filoviral Receptor-Binding Domains are Promising Subunit Vaccine Candidates, p. 41 (abstract V4). *In* Abstracts of the NERCE/BEID [New England Regional Center of

Excellence/Biodefense and Emerging Infectious Diseases] Fourth Annual Retreat, November 11-12, Bretton Woods, NH, USA.

- 7) **Radoshitzky, Sheli R., Jens H. Kuhn, Christina F. Spiropoulou, César Albariño, Jorge Salazar-Bravo, Tatyana Dorfman, Amy S. Lee, Enxiu Wang, Susan R. Ross, Hyeryun Choe, and Michael Farzan.** 2007. Receptor Determinants of Zoonotic Transmission of New World Hemorrhagic Fever Arenaviruses, p. 22. *In* Abstracts of the NERCE/BEID [New England Regional Center of Excellence/Biodefense and Emerging Infectious Diseases] Fourth Annual Retreat, November 11-12, Bretton Woods, NH, USA.
- 8) **Kuhn, Jens H., Kelly L. Warfield, Sheli R. Radoshitzky, Dana Swenson, Gene G. Olinger, Sina Bavari, Michael Farzan, and M. Javad Aman.** 2007. Filoviral Receptor-Binding Domains are Promising Subunit Vaccine Candidates, p. 38. *In* Third European Congress of Virology – Programme and Abstracts, September 1-5, CCN CongressCenter Nürnberg, Nuremberg, Germany.
- 9) **Radoshitzky, Sheli R., Jonathan Abraham, Christina F. Spiropoulou, Jens H. Kuhn, Dan Nguyen, Jane Nagel, Paul J. Schmidt, Jack H. Nunberg, Nancy C. Andrews, Michael Farzan, and Hyeryun Choe.** 2007. Transferrin receptor 1 is a cellular receptor for New World haemorrhagic fever arenaviruses, p. 7. *In* Third European Congress of Virology – Programme and Abstracts, September 1-5, CCN CongressCenter Nürnberg, Nuremberg, Germany.
- 10) **Kuhn, Jens H., Kelly L. Warfield, Sheli R. Radoshitzky, Dana Swenson, Gene G. Olinger, Sina Bavari, Michael Farzan, and M. Javad Aman.** 2007. Filoviral Receptor-Binding Domains are Promising Subunit Vaccine Candidates, p. 201. *In* Abstracts of the 4th Annual NIAID [National Institute of Allergy and Infectious Diseases] RCE [Regional Centers of Excellence for Biodefense and Emerging Infectious Diseases] Research Meeting, April 15-17, St. Louis, MO, USA.
- 11) **Radoshitzky, Sheli R., Jonathan Abraham, Christina F. Spiropoulou, Jens H. Kuhn, Dan Nguyen, Jane Nagel, Paul J. Schmidt, Jack H. Nunberg, Nancy C. Andrews, Michael Farzan, and Hyeryun Choe.** 2007. Transferrin Receptor 1 is a

Cellular Receptor for New World Hemorrhagic Fever Arenaviruses, p. 63. *In* Abstracts of the 4th Annual NIAID [National Institute of Allergy and Infectious Diseases] RCE [Regional Centers of Excellence for Biodefense and Emerging Infectious Diseases] Research Meeting, April 15-17, St. Louis, MO, USA.

- 12) Radoshitzky, Sheli R., Jonathan Abraham, Christina F. Spiropoulou, Jens H. Kuhn, Dan P. Nguyen, Jane Nagel, Jack H. Nunberg, Stefan Kunz, Michael Farzan, and Hyeryun Choe.** 2006. Identification of the Cellular Receptor for New World Hemorrhagic Fever Arenaviruses, p. 38 (abstract 2). *In* NERCE/BEID [New England Regional Center of Excellence/Biodefense and Emerging Infectious Diseases] and NBC [Northeast Biodefense Center] Third Annual Retreat, October 29-31, Bolton Landing, NY, USA.
- 13) Kuhn, Jens H., Sheli R. Radoshitzky, Kelly L. Warfield, Alexander C. Guth, Jonathan S. Towner, Martin J. Vincent, Stuart T. Nichol, Sina Bavari, Wenhui Li, Hyeryun Choe, M. Javad Aman, and Michael Farzan.** 2006. Determination and Evaluation of Filoviral Receptor-Binding Domains (RBDs) And RBD-Containing Soluble Glycoproteins as Possible Inhibitors of Infection and Vaccine Candidates, p. 9 (abstract 5). *In* Abstracts of the NERCE/BEID [New England Regional Center of Excellence/Biodefense and Emerging Infectious Diseases] and NBC [Northeast Biodefense Center] Third Annual Retreat, October 29-31, Bolton Landing, NY, USA.
- 14) Warfield, Kelly L., Jens H. Kuhn, Sheli R. Radoshitzky, Dana L. Swenson, Gene G. Olinger, Sina Bavari, Michael Farzan, and M. Javad Aman.** 2006. Evaluation of the Vaccine Potential of Recombinant Receptor-Binding Domains of Filovirus Glycoproteins. *In* Abstracts of “Filoviruses: Recent Advances and Future Challenges - An ICID Global Symposium”, September 17-19, Winnipeg, Manitoba, Canada.
- 15) Kuhn, Jens H., Sheli R. Radoshitzky, Alexander X. Guth, Wenhui Li, Stuart T. Nichol, Sina Bavari, Hyeryun Choe, M. Javad Aman, and Michael Farzan.** 2006. Lake Victoria Marburgvirus and Zaire Ebolavirus Attach to a Common Cell-Entry Factor, p. 133 (abstract W23-7). *In* American Society for Virology 25th Annual Meeting – Scientific Program & Abstracts, July 15-19, Madison, WI, USA.

- 16) **Kuhn, Jens H., Sheli R. Radoshitzky, Alexander X. Guth, Wenhui Li, Stuart T. Nichol, Hyeryun Choe, and Michael Farzan.** 2006. Lake Victoria marburgviruses and Zaire ebolaviruses attach to a common cell-entry factor. *In* Abstracts of the Regional Centers for Biodefense and Emerging Infectious Diseases Research Third Annual Meeting, March 26-28, New York, NY, USA.
- 17) **Kuhn, Jens H., Sheli R. Radoshitzky, Alexander X. Guth, Stuart T. Nichol, Wenhui Li, Hyeryun Choe, and Michael Farzan.** 2005. Lake Victoria marburgvirus and Zaire ebolavirus attach to a common cell-entry factor, p. 38. *In* Abstracts of the Medizinische B-Schutz-Tagung 2005 – Biological Medical Defense Conference 2005, October 26-27, Munich, Germany.
- 18) **Kuhn, Jens H., Sheli R. Radoshitzky, Alex Guth, Wenhui Li, Hyeryun Choe, and Michael Farzan.** 2005. Lake Victoria Marburgvirus and Zaire Ebolavirus Attach to a Common Receptor, p. 26 (abstract V5). *In* Abstracts of the 2nd Annual Retreat of the New England Regional Center of Excellence in Biodefense/Emerging Infectious Diseases (NERCE/BEID), September 25-26, Durham, NH, USA.

Posters

- 1) **Kuhn, Jens H., Kelly L. Warfield, Sheli R. Radoshitzky, Dana Swenson, Gene G. Olinger, Sina Bavari, Michael Farzan, and M. Javad Aman.** 2008. Filoviral Receptor-Binding Domains are Promising Subunit Vaccine Candidates. Presented at the XIV. International Congress of Virology, August 10-15, Istanbul, Turkey.
- 2) **Kuhn, Jens H., Kelly L. Warfield, Sheli R. Radoshitzky, Dana Swenson, Gene G. Olinger, Sina Bavari, Michael Farzan, and M. Javad Aman.** 2008. Filoviral Receptor-Binding Domains are Promising Subunit Vaccine Candidates. Presented at the 27th Annual Meeting of the American Society for Virology, July 12-16, Ithaca, NY, USA.
- 3) **Kuhn, Jens H., Kelly L. Warfield, Sheli R. Radoshitzky, Dana Swenson, Gene G. Olinger, Sina Bavari, Michael Farzan, and M. Javad Aman.** 2008. Filoviral

Receptor-Binding Domains are Promising Subunit Vaccine Candidates. Presented at the IVth International Symposium on Filoviruses, March 26-28, Libreville, Gabon.

- 4) **Kuhn, Jens H., Kelly L. Warfield, Sheli R. Radoshitzky, Dana Swenson, Gene G. Olinger, Sina Bavari, Michael Farzan, and M. Javad Aman.** 2007. Filoviral Receptor-Binding Domains are Promising Subunit Vaccine Candidates. Presented at the NERCE/BEID [New England Regional Center of Excellence/Biodefense and Emerging Infectious Diseases] Fourth Annual Retreat, November 11-12, Bretton Woods, NH, USA.
- 5) **Radoshitzky, Sheli R., Jonathan Abraham, Christina F. Spiropoulou, Jens H. Kuhn, Dan Nguyen, Jane Nagel, Paul J. Schmidt, Jack H. Nunberg, Stefan Kunz, Nancy C. Andrews, Michael Farzan, and Hyeryun Choe.** 2006. Transferrin Receptor 1 is a Receptor for New World Hemorrhagic Fever Arenaviruses. Presented at the NERCE/BEID [New England Regional Center of Excellence/Biodefense and Emerging Infectious Diseases] and NBC [Northeast Biodefense Center] Third Annual Retreat, October 29-31, Bolton Landing, NY, USA.
- 6) **Kuhn, Jens H., Sheli R. Radoshitzky, Kelly L. Warfield, Sina Bavari, Hyeryun Choe, M. Javad Aman, and Michael Farzan.** 2006. Molecular Characterization and Evaluation of the Cell-Binding and Virus Entry-Inhibitory Properties of Marburg- and Ebolaviral Receptor-Binding Domains and Secreted Glycoproteins, poster N° 14. Presented at “Filoviruses: Recent Advances and Future Challenges - An ICID Global Symposium”, September 17-19, Winnipeg, Manitoba, Canada.
- 7) **Kuhn, Jens H., Sheli R. Radoshitzky, Alexander X. Guth, Stuart T. Nichol, Wenhui Li, Hyeryun Choe, and Michael Farzan.** 2005. Marburgviruses and Zaire Ebolaviruses attach to a common cell-entry factor. Presented at the Medizinische B-Schutz-Tagung 2005 – Biological Medical Defense Conference 2005, October 26-27, Munich, Germany.
- 8) **Kuhn, Jens H., Sheli R. Radoshitzky, Alexander X. Guth, Wenhui Li, Stuart T. Nichol, Hyeryun Choe, and Michael Farzan.** 2005. Lake Victoria marburgvirus and Zaire ebolavirus use a common cell-entry factor. Presented at the 2nd Annual Retreat of

the New England Regional Center of Excellence/Biodefense and Emerging Infectious Diseases (NERCE/BEID), September 25-26, Durham, NH, USA.

- 9) **Kuhn, Jens H., Sheli R. Radoshitzky, Alexander X. Guth, Wenhui Li, Hyeryun Choe, and Michael Farzan.** 2005. Lake Victoria marburgvirus and Zaire ebolavirus attach to a common cell-entry factor. Presented at the 6th Harvard DMS Virology Program Retreat “Major League Science”, September 15-16, Provincetown, MA, USA.

Oral presentations

- 1) **07/12/2008:** Receptor determinants of zoonotic transmission of New World hemorrhagic fever arenaviruses. 27th Annual Meeting of the American Society for Virology, July 12-16, Ithaca, New York, USA (15 min.).
- 2) **09/05/2007:** Filoviral Receptor-Binding Domains are Promising Subunit Vaccine Candidates. Third European Congress of Virology, September 1-5, CCN CongressCenter Nürnberg, Nuremberg, Germany (15 min.).
- 3) **04/17/2007:** Filoviral Receptor-Binding Domains are Promising Subunit Vaccine Candidates. 4th Annual NIAID [National Institute of Allergy and Infectious Diseases] RCE [Regional Centers of Excellence for Biodefense and Emerging Infectious Diseases] Research Meeting, April 15-17, St. Louis, MO, USA (15 min.).
- 4) **02/12/2007:** Entry-inhibitory effects of filoviral receptor-binding domains and soluble glycoproteins. United States Army Medical Research Institute of Infectious Diseases (USAMRIID), Fort Detrick, Frederick, MD, USA (60 min.).
- 5) **10/30/2006:** Determination and Evaluation of Filoviral Receptor-binding Domains (RBDs) and RBD-containing Soluble Glycoproteins as Possible Inhibitors of Infection and Vaccine Candidates. NERCE/BEID [New England Regional Center of Excellence/Biodefense and Emerging Infectious Diseases] and NBC [Northeast Biodefense Center] Third Annual Retreat, October 29-31, Bolton Landing, NY, USA (15 min.).

- 6) **07/16/2006:** Lake Victoria marburgvirus and Zaire ebolavirus attach to a common cell-entry factor. American Society for Virology 25th Annual Meeting – Scientific Program & Abstracts, July 15-19, Madison, WI, USA (15 min.).
- 7) **03/27/2006:** Conserved Receptor-Binding Domains of Filoviruses Bind a Common Receptor. Regional Centers for Biodefense and Emerging Infectious Diseases Research Third Annual Meeting, March 26-28, New York, NY, USA (15 min.).
- 8) **11/07/2005:** Lake Victoria marburgviruses and Zaire Ebolaviruses attach to a common cell-entry factor. Harvard Medical School Department of Microbiology and Molecular Genetics Monday Talk, Boston, MA, USA (20 min.).
- 12) **10/26/2005:** Lake Victoria marburgviruses and Zaire Ebolaviruses attach to a common cell-entry factor. Medizinische B-Schutz-Tagung 2005 – Biological Medical Defense Conference 2005, October 26-27, Munich, Germany (20 min.)

12 DECLARATION

I, Jens H. Kuhn, hereby confirm that I have prepared this dissertation myself. I assure that I have only used the cited references, sources, and support, and that I have not submitted this dissertation at another department or university. I declare that I am aware of the rules and regulations for dissertations and defenses at my university. The advisors for this dissertation were Assoc. Prof. Michael R. Farzan, PhD, and Prof. Volker Haucke, PhD.

GERMAN DECLARATION

Hiermit bestätige ich, Jens H. Kuhn, dass ich die vorliegende Arbeit selbstständig angefertigt habe. Ich versichere, dass ich ausschließlich die angegebenen Quellen und Hilfsmittel in Anspruch genommen habe und dass ich diese Dissertation keiner anderen Fakultät oder Universität zur Prüfung vorgelegt habe. Die Bestimmungen der Promotionsordnung sind mir bekannt. Die von mir vorgelegte Dissertation ist von Herrn Assoc. Prof. Michael R. Farzan, PhD, und Herrn Prof. Dr. rer. nat. Volker Haucke betreut worden.

Frederick, MD, USA, November 2008

(Jens H. Kuhn)

13 CURRICULUM VITAE

The curriculum vitae (pages 253-255) has been removed from the online version of this dissertation due to data-privacy requirements.

Der Lebenslauf (Seiten 253-255) ist in der Online-Version dieser Dissertation aus Gründen des Datenschutzes nicht enthalten.